UNIVERSITY OF LONDON THESIS

Degree phD Year 2007 Name of Author ZHICHAO GUO

UNIVERSITY COLLEGE LONDON
Department of Chemical Engineering

ULTRASONIC EFFECTS ON CRYSTALLIZATION PROCESSES

ZHICHAO GUO

A Thesis Submitted to University of London for the Degree of Doctor of Philosophy

JANUARY 2007

Supervisor: Professor A.G. Jones

University Of London

ProQuest LLC
789 East Eisenhower Parkway
P.O. Box 1346
Ann Arbor, MI 48106-1346

ABSTRACT

This thesis reports a study of the effects of ultrasound on crystal nucleation from solution and particle breakage.

Firstly, the effect of ultrasound on reactive crystallization when nucleation is consistent with a predominantly homogeneous model is studied by measuring the induction time. Barium sulphate is used as the working substance precipitated by mixing aqueous $BaCl_2$ and Na_2SO_4 solutions. The relationship between amplitude of ultrasonic processor and power input was determined. The experiments were carried with various ultrasonic power inputs. It is observed that increasing ultrasound has a significant effect on reducing the induction time. At a given supersaturation level, the induction time decreases with increasing ultrasonic energy. The relationship between power input (E) and the activation energy of nucleation (E_N) is discussed. And the equation between total power input (E) and the nucleation coefficient (k_N) is obtained.

A cluster coagulation model, which brings together the current nucleation models and the theories describing the behavior of colloidal suspensions, was applied to estimate the induction time under various power inputs. A comparison between the predictions of the model and the results of experiments shows that the number of monomers in dominating clusters ($\bar{g}$) in the solution remains constant with increasing power input.

The mechanism of the ultrasonic effect on homogeneous nucleation is analyzed. It is found that when temperature is kept constant, the main effect of ultrasound is to increase the diffusion coefficient (D_{AB}). Other parameters change only slightly or remain constant within the ultrasonic field. This suggests that diffusion acceleration is the main reason for the reduction of the induction time. The relationship of D_{AB} and power input is also discussed. A mathematical model of power input and diffusion coefficient is presented, from which it is predicted that diffusivity enhancement (D_{AB}- D_{AB0}) has an exponential relationship with power input. The above relationship is consistent with the

results of the experiments.

Induction times have also been measured with and without ultrasound to investigate its effect on induction time of spectinomycin hydrochloride, roxithromycin and sucrose during anti-solvent crystallization. The relationship between ultrasonic power input and diffusion coefficient is also investigated. It is found that at the same power input, the ultrasonic effect on D_{AB} decreases with increased solution viscosity.

The effect of ultrasound on $BaSO_4$ nucleation is also studied by measuring the induction time when nucleation is consistent with a predominantly heterogeneous model. In these experiments, barium sulphate is used as the working substance precipitated by mixing aqueous $BaCl_2$ and Na_2SO_4 solutions with relatively low concentrations compared to the experiments of homogeneous nucleation. It is observed that at a given supersaturation level, the induction time significantly decreases with increasing ultrasonic energy during heterogeneous nucleation.

The mechanism of the ultrasonic effect on heterogeneous nucleation is analyzed. The effect of ultrasound is to increase the diffusion coefficient (D_{AB}) while reducing the contact angle (θ) and geometric factor (f). This gives rise to an increase in the heterogeneous nucleation rate and shorter induction time. The ultrasonic effect on critical supersaturation ratio (S_{crit}) is also investigated to determine the mechanism of ultrasonic effect on f and θ. It is proposed that both the force from the cavitational bubble implosion and the nucleation process occurring at bubble/solution/foreign solid interface are the predominant reasons why contact angle (θ) decreases with the increase of power input. In addition, the effects of ultrasound on nucleation order (n) and the nucleation coefficient (k_N) are also investigated, and compared with the corresponding effects during homogeneous nucleation.

A cluster coagulation model is used to calculate the induction time at different levels of supersaturation when nucleation is consistent with a predominantly heterogeneous model. It is found that the dominant cluster size increases with increasing supersaturation and increasing ultrasonic energy.

The effect of ultrasound on nucleation of $BaSO_4$ is studied by a Kodak Ektapro Hs motion analyzer. Firstly, the dispersion processes of ink with ultrasound and stirring are used to compare difference of the mixing processes and hydraulic flows. The vessel is divided into several sections to investigate the local mixing process by recording the movement of small silicon carbide crystals. Velocity variance is used to indicate the difference of turbulence when ultrasound is applied and when stirring is applied respectively. The cavitation distribution in different sections is also obtained. $BaSO_4$ is precipitated by mixing aqueous solutions of $BaCl_2$ and Na_2SO_4. The nucleation processes are observed by Kodak motion analyzer in different sections. The mechanism of nucleation by ultrasound is analyzed. Then, the induction times at different temperatures are measured with different power inputs at a given supersaturation level. The relationship between the cavitation distribution and temperature is established. Ethanol and acetone are used to verify this relationship.

The Kodak motion analyzer is also applied to observe the ultrasonic effect to breakage process of agglomerated crystals where ethanol is used as the suspending liquid. The cavitational effects on the particles with different sizes are investigated. The mixing processes with stirring and with ultrasound are investigated by the dispersion of ink in the ethanol. Small sugar crystals are used as indicators for the movement of hydraulic flows. The vessel is also divided into several sections to investigate the local mixing process. Velocity variance is used to indicate the difference of turbulence when ultrasound is applied and when stirring is applied respectively. The cavitation distribution in different sections is also recorded. The agglomerated sugar crystals are used as working substance to observe the breakage processes in different sections. The main mechanisms of breakage in different sections are analyzed. The crystal product with 5 minutes ultrasonic treatment is compared with the products with 5 minutes stirring treatment and the sugar crystals after mechanical grinding as well. It is found that compared to grinding process, ultrasound has a selective effect on solid bonds between crystals.

Finally, the thesis details a commercial evaluation to apply sonocrystallization technology industrially. In essence, the drafts of two possible new crystallizer designs are presented. One is using sonocrystallization technology to control crystallization processes in traditional crystallizers (normally of volume more than 2000L). Another technique is using ultrasound to initiate a new technology, namely scale-out of crystallization processes, which can be used to substitute industrial scale-up of crystallization processes from laboratory-scale. Here, instead of using one traditional crystallizer with large volume, new unit is composed of many small sonocrystallizers (1 or 2 L) linked by parallel connection method to provide enough productive capacity. The business opportunity is analyzed and the plans to approach this business market are also evaluated.

Finally, possible future work on sonocrystallization is also proposed and difficulties are evaluated as well.

ACKNOWLEDGEMENTS

The author wishes to express his gratitude to the following:

Professor Alan Jones for providing the author this opportunity to study at UCL and carry out this exciting research; for his excellent supervision and support throughout the project; and for his help to the author during the difficulties in both this research and my life in London.

Dr Panagiota Angeli for the loan of a Kodak Ektapro Hs motion analyser to the experiments. Dr. T. Al-Wahaibi and Ms. K. Ioannu to introduce how to operate the analyser. And Ms. S. Germana to take photographs of experimental samples.

Ms. Sarah Bailey, Mr. Julian Perfect, Mr. Martin Town, Mr. Martyn Vale and Mr. Mike Gorecki for their invaluable help on managing the technical and computational side of the project.

MSc students Mr. Nan Li, Ms. Bhavini Patel and Dr Hongxun Hao for their support during the experiments of ultrasonic effects on nucleation and breakage.

My friends and colleagues in the department and other friends in UK, who shared in my joy and despair.

The UK government for the provision of an ORS.

UCL for the provision of the job of vice-warden and my colleagues in Ifor Evans Hall. Especially, I want to thank my colleagues for all of their help during my work in Ifor.

The Centre For Scientific Enterprise Limited for the provision of 5 MBA courses in LBS and the scholarship to support the commercial evaluation of my PhD project. These courses brought me new knowledge benefiting all the rest of my life.

The Chinese Embassy, the members in Chinese Students and Scholars Association, UCL and Professor David Norse, the pro-provost at UCL. You gave me the chance to make so many good friends and widen my thought.

My family for their constant support and encouragement throughout my studies, without which this work would not have been possible. Especially, the author wants to express the cherish memory of his two grandfathers. Although you cannot see the achievement in my study, I cannot make it without your encouragement beforehand. I will remember your edification forever.

TABLE OF CONTENTS

LIST OF FIGURES AND TABLES

LIST OF FIGURES

LIST OF TABLES

CHAPTER 1

INTRODUCTION

1.1 Introduction

Crystallization is a technique which involves the formation of an ordered solid phase from a homogeneous gas, liquid or amorphous phase. The main advantages of crystallization over other separation processes are as follows:

1. High purity. The rigid structure of the crystalline material results in a low tendency to incorporate foreign substances or solvent molecules. Hence high purity substances can be produced in crystallization.
2. Low level of energy consumption. The main advantage of crystallization over distillation is the production of substances at a low level of energy consumption.
3. Relatively mild process conditions. Crystallization is a favorable unit operation for temperature sensitive or even temperature labile substances, since many crystallization processes, such as anti-solvent crystallization, reactive crystallization and so on, can be operated at very low temperature.
4. Efficiency of separation. Crystallization can be used to separate the mixtures, such as, mixture of isomer, azeotropic mixture, temperature sensitive mixture, which cannot be separated by other separation processes.
5. Less environmental pollution. Normally, crystallization processes will not generate any exhaust gas, which causes environmental pollution after emission without treatment.
6. A safe and low cost process. Crystallization processes can be operated at low temperature, so the material requirement of a crystallizer is lower than that of a distillation column and the operating environment is safer.

Crystallization processes can be used in not only mass production with the output over 1 million tons per year, such as sugar and salt crystallization, but small-scale production such as manufacture of single crystals. In addition to purity and yield, the quality requirements of crystal products include crystalline form, crystal mean size and

size distribution etc. Some special quality standards even include the color and the degree of hardness of chemical crystal product.

Normally, crystallization processes are divided into 4 categories: solution crystallization, melting crystallization, sublimation crystallization, and precipitation crystallization. The solid-liquid separation technique is the essential and most important of them. The crystallizer can be operated as continuous or batch processes. The advantages of continuous crystallization are: low operational cost; low labor cost; stable process; high throughput. However, it also has some disadvantages. Generally, scale is easily to form on the wall of crystallizer and crystal size is normally small compared to batch crystallization. The throughput and solution volume is used to determine what kind of crystallizers will be adopted. Normally, if the flow rate of solution is higher than $20m^3/h$, continuous crystallization will be adopted. Batch crystallization is used widely in some processes with long precipitation time, and in some processes to treat poisonous materials or expensive but low yield substances. The advantages of batch crystallization make it used as commonly as continuous crystallization in the chemical industry.

1.2 Pharmaceutical crystallization

Solution crystallization is widely used for manufacturing bioactive drug substances and formulation of excipients during final and intermediate stages of purification and separation. This process defines drug chemical purity and physical properties: particle habit and size, crystal structure polymorphism and degree of crystal imperfection. Consequently, crystalline variations are responsible for a wide range of pharmaceutical formulation problems, such as bio-inequivalence, as well as chemical and physical instability of the solid drugs in their final dosage forms. Over 90% of all pharmaceutical products, such as tablets, aerosols, capsules, suspensions and suppositories contain drugs in particulate, generally crystalline, form (Shekunov and York, 2000). The role of crystallization processes in pharmaceutical science and technology can be associated

both with its influence on the solid-state properties of the drug substances and with an effect on drug product stability and performance. The concept of crystal and particle engineering applied to pharmaceutical substances requires, first of all, reproducibility and consistency of the solid-state properties. These problems are related to such fundamental issues as formation of disordered and amorphous states, kinetics of polymorphism and chiral separation, solid-state reactions, surface energies and relationship of these phenomena to molecular and crystallographic structure. Progress with advanced drug delivery systems includes: nano- and micro-particles and controlled release formulations, reduction of manufacturing cost and complexity, necessary development of continuous, one-step crystallization techniques which allow a precise control over the particle size, shape and crystallinity.

As one of the most important process in pharmaceutical industry, crystallization determines not only the production cost of pharmaceuticals but also the curative effects. The pharmaceuticals with similar components and similar molecule formula, even at very high purity, may have different effects, if the physical properties of solids, such as crystal habit, crystalline form and crystal size distribution etc, are different, viz. the quality standard of pharmaceuticals includes not only purity but also the configuration of crystals, which is important for biological effects of pharmaceuticals. Except for some simple compounds (inorganic salts), the majority of pharmaceuticals with large molecules, particularly, biological pharmaceuticals, are polymorphous compounds. The crystalline forms depend on the operational conditions during the crystallization process. The change of operational conditions may change the crystalline form of the product. As a result, the pharmaceuticals may have less effect or even become non-effective. So crystallization is not only a method for separation, purification and solidification, but also a procedure to conform bio-activity and curative effect of the solid pharmaceuticals after chemical synthesis.

In the global pharmaceutical market, the similar pharmaceuticals from different countries or different companies frequently have different curative effects. The main

reasons are (Guo, 2003):

1. Crystal habits are different. For example, chlormycetin has three forms, but only the metastable form has curative effect. Rifamicin, a polymorphous compound, can only be absorbed by muscle after re-crystallization from acetone or butanol. Sulfanilamide has α, β and γ forms, but, however, crystals with α and β forms have very high side-effects and are not suitable for use as medicine.
2. Crystal size distributions (CSD) are different. The CSD includes two parameters, viz. mean particle size and size distribution. Specific volumes of pharmaceuticals are determined by above two parameters. The change of crystal habit and crystalline form may also change CSD. The human body also has different absorbability to crystal products with different CSD. For example, the CSD requirement of procaine penicillin is that more than 65% crystals should have sizes between 1 and 15 μ m, and crystals with the size larger than 50 μ m should not exist in the product.
3. Impurity contents are different. The poor operational conditions during crystallization process can make mother liquid or impurities, which may have passive influence on curative effect of pharmaceuticals, present in crystal product. For example, trace amounts of butanol can cause lincomycin crystals to become non-effective.

Controls of polymorphism and powder properties are often the most important issues in crystallization process development of active pharmaceutical ingredients. The quality standard of pharmaceuticals is much stricter than normal chemical products. The control of pharmaceutical quality requires advanced crystallization technology. After the crystallization process is determined, it is also very important to design an operable crystallizer and choose suitable control units. To achieve the requirements of pharmaceutical crystal products, some crystallization techniques such as, reactive

crystallization, extractive crystallization, rectifying crystallization, supercritical crystallization, membrane crystallization and some coupled crystallization technologies, have already been used in crystal production.

Crystallizers and the control units are vital factors for crystallization processes. The choice and design of crystallization processes are established on the basis of the phase diagrams, crystallization kinetics and fluid dynamics. The phase diagrams and crystallization kinetics are very rarely published in the open literature. So it is necessary to measure the above parameters for process design.

The composition of crystallization mother solution is always very complex (normally, it is not possible to obtain the components using normal analytical methods), and the composition, the density and viscosity of mother liquid may fluctuate during the crystallization processes. Both the mother liquid and crystal product may decompose and lose biological activity. All of these factors not only require better controls of mass transfer and heat transfer, but make pharmaceutical crystallization more susceptible than other crystallization processes. Any changes of operational parameters may breach the crystallization process, worsen quality of product and decrease the yield of production.

Because the pharmaceutical industry is always with high profit and low output, any quality and yield improvements of product may bring significant benefit to the producer.

The production of particles from solution is a very complex process, which involves mass, energy, momentum and population transfer. Kinetic parameters are used to describe the events of growth (growth rate), birth and death (nucleation rate, agglomeration rate and disruption rate) of a precipitation process. The interplaies of these parameters and their dependence on supersaturation, hydrodynamics and mixing determine the crystal size distribution.

1.3 Supersaturation

Crystallization is a result of three main consequent stages: establishment of

supersaturation, nucleation and crystal growth. Supersaturation is also the impetus for nucleation and growth during crystallization process. In chemistry, the term supersaturation refers to a solution that contains more of the dissolved material than could be dissolved by the solvent under existing conditions. Supersaturated solutions are prepared or resulted when some conditions of a saturated solution are changed, for example temperature, volume (by evaporation), pressure or reactions.

The state of supersaturation is an essential requirement for all crystallization operations. In solution, when the condition is changed and the concentration of solute exceeds the equilibrium (saturation) solution concentration, the crystal will not be precipitated until the concentration is improved to a certain value. This value is called supersolubility. Supersaturated solutions are metastable. Every solution has a maximum amount that it can be supersaturated before it becomes unstable. The zone between the saturation curve and this unstable boundary is called the metastable zone and is where all crystallization operations occur. The work of Miers and Isaac (See Mullin 2000) on the relationship between supersaturation and spontaneous crystallization led to a diagrammatic representation of the metastable zone on a solubility-supersolubility diagram as shown in Figure 1.1. The lower continuous solubility curve can be located with precision with appropriate techniques. The upper broken supersolubility curve, which represents temperatures and concentrations where uncontrolled spontaneous crystallization occurs, is not as well defined as that of the solubility curve. Its position in the diagram is considerably affected by, amongst other things, the rate at which supersaturation is generated and the intensity of agitation.

Despite the fact that the supersasolubility curve is ill-defined, there is no doubt that a region of metastability exists in the supersaturated region above the solubility curve. The diagram is therefore divided into three zones, one well-defined and the other two variable to some degree:

1. The stable (unsaturated) zone where crystallization is impossible.
2. The meststable (supersaturated) zone, between the solubility and supersolubility curves, where spontaneous crystallization is improbable. However, if crystal seeds were placed in such a metastable solution, growth would occur on it.

3. The unstable or labile (supersaturated) zone, where spontaneous crystallization is probable, but not inevitable.

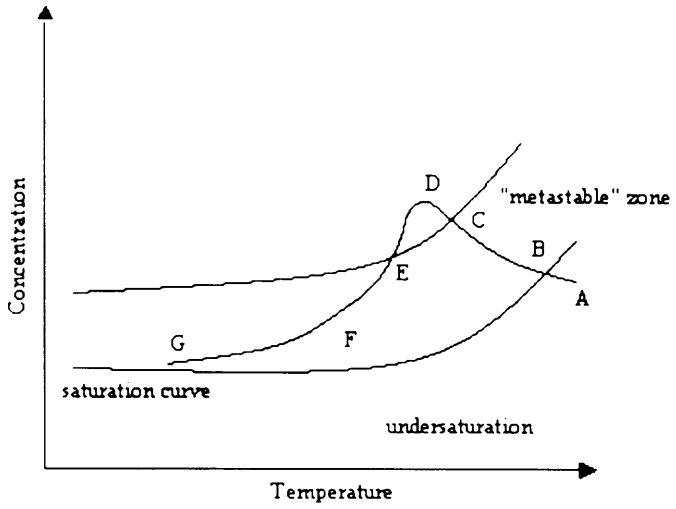

Figure 1.1 The progression of cooling crystallization (Mullin 2000)

A. Feed location, undersaturated
B. Solution cools to saturation
C. Enter "metastable" zone, nucleation begins
D. Rapid nucleation
E. Concentration decreases with crystal growth
F. Crystal growth during main cooling cycle
G. Exit location, supersaturated

On an industrial scale, a large supersaturation driving force is necessary to initiate primary nucleation. In continuous crystallization, once primary nucleation has begun, the crystal size distribution begins to take shape. Figure 1.1 describes the progression of cooling crystallization. For cooling crystallization process, if a solution represented by point *A* in Figure 1.1 is cooled without loss of solvent. Spontaneous crystallization cannot occur in metastable zone from *B*, where solution cools to saturation, to *C*, where solution leaves metastable zone and nucleation begins. At point *C*, crystallization may be spontaneous or may be induced by seeding, agitation or mechanical shock. Further cooling to point *D* can induce rapid nucleation, which may be necessary before crystallization can be induced, especially with very soluble substances. After the

nucleation process, solution comes back with the metastable zone, where nuclei continue growing with high growth rate from E to F. With the increase of crystal size, the supsaturation level decreases and the crystal growth rate becomes lower. At last, when solution reach point G, the crystallization process stops. Control of supersaturation is the key to successful crystallizer operation. The local and global supersaturation ratios that are experienced over the course of a crystallization operation are critical because they determine the balance between nucleation and growth not only at the onset of crystallization but throughout the course of a batch or semi-batch operation. This balance, in turn, determines the resulting physical properties and, in many cases, the distribution of chemical impurities between the crystals and the liquors (Paul et al., 2005).

1.4 Precipitation kinetics

1.4.1 Nucleation

The mechanism nucleation can be divided into primary nucleation and secondary nucleation.

1.4.1.1 Primary Nucleation

Primary nucleation involves the formation of a new solid phase from a clear solvent. This type of nucleation is further sub-divided into homogeneous and heterogeneous nucleation. In heterogeneous nucleation, nucleation starts on foreign substrates of mostly microscopic particles. If such substrates are absent, new phase formation takes place by statistical fluctuations of solute entities clustering together, a mechanism known as homogeneous nucleation.

In the absence of control of supersaturation, nucleation usually predominates. When nucleation does predominate, the outcome is dependent on the number of crystals formed. As discussed below, this control may be exceedingly difficult to achieve at any

scale, and particularly difficult to reproduce upon scale-up, often because of mixing problems.

A specific crystallization can be dominated by either nucleation or growth, depending on how the critical variables are controlled, the amount of seed, the size distribution and surface qualities of the seed, and the environment in which supersaturation is created. Both nucleation and growth virtually always proceed simultaneously. In general, nucleation dominates when supersaturation, either local or global, is near to or greater than the upper limit of the metastable region (Figure 1.1). Growth can dominate at low supersaturation and in the presence of sufficient crystal surface area. Both inherent nucleation rate and growth rate of the specific compound also play a major role in determining the dominant mechanism.

In some cases, a process that is dominated by nucleation can result in an acceptable process outcome. The process may appear satisfactory in laboratory scale operation. However, there are several potential problems with a nucleation-driven process upon scale-up, including:

1. Fine crystals and/or wide particle size distribution (PSD);
2. High surface area;
3. Low bulk density;
4. The risk of large batch-to-batch variation;
5. Occlusion of solvent and impurities;
6. Agglomeration/aggregation;
7. Lack of control of hydrates, solvates, and polymorphs.

In addition, scale-up of a nucleation-dominated process is difficult to predict unless the generation of supersaturation is well controlled. In the case of extremely high nucleation rate, the degree of control required to prevent formation of the large number of nuclei may not be achievable in a stirred vessel, in part because of the inherent

properties of the compound and/or because of mixing scale-up problems. Extreme examples of this are found in ionic reactions to precipitate inorganic salts. Organic acid base reactions can also generate nuclei at high rates. An in-line type crystallization may be required for anti-solvent and/or reactive crystallization both of which may be dominated by nucleation in the absence of strategies to promote growth.

Nucleation must also be minimized by tight control of supersaturation in processes involving resolution of optical isomers and, in some cases, of polymorph formation depending on the zone of stability of the operation.

The nucleation rate is both species specific and a function of supersaturation ratio. The relation between nucleation rate, growth rate, and particle size is a function of supersaturation ratio. The actual rate and supersaturation properties are system specific and can vary over exceedingly wide ranges.

In addition, for a specific compound, the nucleation rate is also dependent on the solvent(s) system, impurity levels, and mixing. These factors combine to cause the extreme difficulties that are often encountered in controlling a nucleation based on crystallization process, especially scale-up.

1.4.1.2 Secondary nucleation

Crystals already present in the solution induce secondary nucleation. Nucleation takes place at a low supersaturation level and is mainly influenced by the prevailing hydrodynamic conditions and the suspension density. In the recent literature, it is acknowledged that secondary nucleation in solution crystallization can be divided into two major mechanisms: Firstly, a mechanical process where by secondary nuclei are formed by attrition due to contacts between crystals themselves and crystals and parts of the crystallizer. This can occur at very low supersaturation levels. Secondly, an activated process known as surface nucleation, which needs a certain supersaturation to happen. This phenomenon can be violent and is difficult to control since it has

non-linear kinetics (Verdurand et al., 2005).

1.4.2 Crystal growth

Control of supersaturation is the key to successful crystallizer operation. The factors, which can influence the crystal growth rate of a certain compound, are discussed by Myerson (2002). In addition to molecular structure and the solvent system, the growth rate can be greatly modified by the presence of dissolved impurities that may either compete for growth sites or block these sites. As with nucleation rate, these differences can be so extreme as to make growth impracticably slow, or in the opposite extreme, the rate may be sufficient to achieve an essentially all growth process with careful control of supersaturation and growth area.

Supersaturation has an important effect on growth rate. However, if an essentially all growth process is desired, the increased growth rate that can be achieved at higher supersaturation may come at the expense of increased nucleation, leading to broader PSD and possibly bimodal distribution. And the mechanism of the controlling surface integration process may cause the growth rate dispersion during crystallization processes as well (Ristic et al., 1996; Finnie et al., 1999). Therefore, in many cases, it is quite difficult to obtain the crystal product with narrow size distribution.

In design of a crystallization process, therefore, the balance that is achieved between nucleation and growth rates is critical to particle size. Supersaturation ratio can be controlled to limit nucleation in order for growth to predominate. This becomes increasingly difficult at lower inherent growth rates.

Impurities can have a large effect on growth and can dominate the course of a crystallization process in the following ways:

1. They can retard nucleation rate leading to high supersaturation before "oiling out" and/or "crashing out".

2. They can retard or stop growth.
3. They can co-crystallize and/or form solid solutions.

Experimentation is required to evaluate these affects. One useful technique is to spike with known impurities when they can be isolated for this purpose. However, as is often the case, the number and possibly low concentration of impurities often make this impractical. An experimentally simpler method is to re-crystallize the compound with and without spiking of the mother liquors obtained from the process isolation.

Differences in nucleation and growth may be observed by such techniques as in-line particle size/particle count and concentration measurement, but if these are not available, much can be deduced by comparing photomicrographs of the resulting crystals. Both size and shape can be affected. If no significant differences are observed, the impurities from the process may not cause any nucleation or growth changes and the inherent properties of the compound may be assumed to prevail.

1.4.3 Nucleation versus growth

Control of crystallization processes requires control of either nucleation or growth, or, as is most often the case, both modes of crystal development simultaneously. Each operation must be evaluated to determine which of the process objectives is the most critical, to determine whether nucleation or growth should be the dominant phase. Many of the literatures are focused on nucleation, for the obvious reason that the number and size of nuclei initially formed can dominate the remainder of the operation. However, it is generally agreed that nucleation can be difficult to control, since there are several factors that can play a role in the conditions for nucleation onset, nucleation rate, and number of crystals generated before growth predominates (Paul et al., 2005). And the hydrodynamic conditions in impeller-driven stirred vessels can cause the shear rate difference inside the vessel. Shear rate can change nucleation rate, crystal growth rate,

polymerisation and multiphase mass transfer etc. significantly. This will influence the crystallization processes consequently (Chew et al., 2004).

1.4.4 Agglomeration

1.4.4.1 Mechanism of agglomeration

One mechanism for agglomerate growth is attributed to growing nuclei colliding and becoming "cemented" together by continuing growth between two or more crystals. Although simultaneous collision of more than two particles is not statistically important, the addition of a large number of nuclei to an original two-crystal agglomerate can readily occur by ongoing collisions leading to very large agglomerates.

Several investigators have developed models for the effectiveness of collisions that lead to agglomeration. This complex interaction of hydrodynamics and surface chemistry is difficult to predict or describe but can be critical to the successful operation and scale-up of a crystallization process. In particular, for reactive crystallization in which high supersaturation levels are inherently present, agglomeration is very likely to occur as the precipitate forms. Careful control may be necessary to avoid extensive agglomeration.

The difficulties that can result from agglomeration include:

1. Entrapment of solvent and/or impurities in the crystal mass;
2. Reduced effective surface area for true growth;
3. Subsequent break-up of agglomerates into small crystals that were captured during nucleation without opportunity for growth;
4. Difficulties in downstream processing because of these;
5. Small crystals;
6. Friability during dry processing (drying, solids transfer);

7. Leading to changes in PSD.

For these reasons, agglomeration is generally to be avoided. The use of additives (Myerson, 2002) may be considered for suppressing agglomeration. However, the use of additives in the pharmaceutical industry particularly for final products is generally not considered for regulatory reasons, barring extreme need.

1.4.4.2 Minimization of agglomeration

The primary process variables that can be manipulated to minimize agglomeration include:

1. Operation within the metastable region;
2. Controlled rate of supersaturation generation;
3. Removal of crystallization inhibitors from the feed stream;
4. Appropriately high seed levels;
5. Solvent selection;
6. Mixing conditions.

Both the formation and disruption of agglomerates are functions of mixing conditions and local shear. Attrition and disruption are both functions of mixing. Disruption refers to break-up of agglomerates that formed under conditions of low supersaturation that can be broken because the binding forces are small. Agglomerates that are formed under conditions of high supersaturation are much stronger and not as subject to disruption by typical mixing conditions. Attrition refers to break-up of large primary crystals that are formed by growth at low supersaturation and is a function of local shear and crystal shape (Paul et al., 2005).

1.4.5 Attrition and breakage

Attrition refers to the process by which asperities and fines are removed from the surface of parent particles suspended in solution, such that there is only a gradual change in their size. Breakage (or fragmentation) is the process by which the parent particles are broken down into smaller entities of significant size, resulting in a rapid disappearance of the original particles.

Several mechanisms exist for the attrition process. The most important are the result of crystal collisions with other crystals or with parts (impeller, wall) of the crystallizer (Biscans, 2004; Gahn and Mersmann, 1999(1); Gahn and Mersmann, 1999(2)). The production rate of the attrition fragments depends on the fluid dynamics of the suspension, on the mechanical properties of the solid material and on the physico-chemical properties of the liquid. Fracture may occur at the point of contact, but hydrodynamic forces can also operate over the surfaces in the vicinity of the point of contact and plastic and elastic deformation in the parent crystal can be generated. The fragment broken off from the crystal could be in a considerably disordered state (formation of dislocations) with many irregular surfaces. It is why these small crystalline fragments often grow more slowly than macro-crystals. Cases have even been reported where they do not grow at all. The probability of a fragment being non-growing increases with decreasing size. As the solubility of a particle increases with decreasing size (Ostwald ripening) for a given solution concentration, the supersaturation experienced by a crystal decreases with decreasing crystal size.

Attrition of a particle can lead to the formation of two particles, which have the similar size (particle splitting) leading to a uniform breakage function, or two particles of different size (attrition) leading to a parabolic breakage function or a number of particles leading to a multiple breakage function (Zauner and Jones, 2000).

1.5 Conclusion

Crystallization is an important operation unit in chemical industry. The requirement for its quality includes not only the purity, but the properties of crystals such as, crystal habit, mean size and size distribution. Successful control of crystallization processes in the laboratory and on scale-up requires understanding of the key properties of the molecule in question with regard to several system specific properties including nucleation and growth rates, induction time, width of metastable region, and morphology. These system properties are in turn dependent on operating variables including impurities, mixing, solvent systems, and supersaturation.

A crystallization process can be dominated by nucleation or growth. The choice can, to some extent, be directed by manipulation of the key variables—supersaturation, seeding, and crystal surface area depending on the desired outcome in terms of particle size, PSD, chemical purity, etc. This choice can determine the preferred crystallization equipment, method of crystallization, and procedure.

Understanding and control of these interdependent factors are key to successful development and scale-up to achieve the desired chemical and physical attributes of the product.

1.6 Research objectives

This research aims to investigate the effect of ultrasound on the primary nucleation and crystal breakage of precipitation processes. Ultrasound has the effect of increasing mass transfer, accelerating crystal growth, reducing agglomeration and disrupting particles. Barium sulphate is used as the working substance precipitated by mixing aqueous $BaCl_2$ and Na_2SO_4 solutions. And experiments are planned to investigate the effect of the ultrasonic power on primary nucleation and breakage. Mathematical models are developed to describe crystallization kinetic phenomena, which can be used

in the scale-up of sonocrystallization processes.

The effect of ultrasound on the induction time is investigated enabling the diffusion coefficient (D_{AB}) to be evaluated when nucleation is consistent with a predominantly homogeneous model. A novel physical model is developed to describe the relationship between ultrasonic power input and D_{AB}. To validate the model, the relationship between the ultrasonic power and diffusion coefficient (D_{AB}) is obtained using a non-linear regression analytical technique and compared with prediction results of the model. However, when nucleation is consistent with a predominantly heterogeneous model, the effect of ultrasound on the contact angle (θ) and geometric correction factor (f) is investigated. The importance of this research is to introduce ultrasound as a novel process technology in industrial crystallization processes. Through these experiments and analysis, the mechanism of ultrasonic effect on both homogeneous nucleation and heterogeneous nucleation can be determined.

The ultrasonic effect on microscopic process to form nuclei during both homogeneous nucleation and heterogeneous nucleation are also investigated. The influence of ultrasonic input on the clusters in solution is analyzed by a cluster coagulation model.

A Kodak Ektapro Hs motion analyzer is applied to observe the ultrasonic effect on the nucleation process directly to test the conclusions of the experiments.

The Kodak motion analyzer is also applied to observe the ultrasonic effect on breakage process of agglomerated crystals. This experiment can help to understand the breakage process in ultrasonic field and contribute the designing of the sonocrystallization technology which can control the agglomeration without breaking crystals.

The mathematic models and mechanism developed in the experiments can aid commercial development:

1. The directions to laboratory-scale development of sonocrystallization technology.

With the aid of the results from our research, the experimental cost can be reduced efficiently and the possibility of success can be increased significantly.

2. The directions to industrial scale-out of sonocrystallization processes. The operational conditions can be transferred directly to production unit whose theoretical foundation has been finished in this research.
3. The design and optimization of crystallizers with ultrasonic control of crystallization process. Especially, when ultrasound is used to reconstruct traditional crystallizers, using the theory and knowledge obtained from this research, it will be very easy to determine the number of ultrasound generators and their positions on crystallizers.

1.7 Thesis structure

The main focus of this research is the investigation of ultrasonic effect on nucleation and crystal breakage during crystallization processes.

In chapter 2, the mechanism of ultrasound on solution and an important phenomenon known as "cavitation" in ultrasonic field are highlighted. The reason why ultrasound can bring significant influence to fluid and fluid-solid systems is discussed. And the ultrasonic effects and its benefits to crystallization processes in existing work are also covered in this chapter.

In chapter 3, the mechanism of ultrasonic effect on nucleation is discussed when nucleation is consistent with a predominantly homogeneous model. The relationship between power input and other nucleation parameters such as, the apparent nucleation order (n) and nucleation rate coefficient (k_N) are obtained.

In chapter 4, the ultrasonic effect on microscopic process to form nuclei during homogeneous nucleation is investigated. The dominant cluster sizes at various power inputs in solution are obtained from a cluster coagulation model.

In chapter 5, the new model to describe the relationship between power input and

diffusion coefficient is established and validated by experimental work. The influence of viscosity on diffusion coefficient is also investigated.

In chapter 6, the nucleation process is captured by a Kodak Ektapro Hs motion analyzer. The diffusion and mixing processes in ultrasonic field are investigated. The relationship between cavitation and solution viscosity is established.

In chapter 7, the mechanism of ultrasonic effect on nucleation is investigated when nucleation is consistent with a predominantly heterogeneous model. The relationship between power input and the contact angle (θ) and geometric correction factor (f) are obtained. And the ultrasonic effects on apparent nucleation order (n) and nucleation rate coefficient (k_N) are discussed.

In chapter 8, the ultrasonic effect on microscopic processes to form nuclei during heterogeneous nucleation is investigated. The relationship between the dominant cluster sizes and power input is obtained from a cluster coagulation model.

In chapter 9, the Kodak Ektapro Hs motion analyzer is applied to observe the ultrasonic effect on breakage process of agglomerated crystals. Sugar crystals are used as the working substance. The cavitation effect on breakage is studied and the product with ultrasonic treatment is compared with the product after grinding and stirring.

In chapter 10, the commercial evaluation of sonocrystallization technology is presented.

CHAPTER 2

PRINCIPLES OF ULTRASOUND

2.1 Introduction

In general terms, ultrasound can be used both as an analytical technique and as a tool to assist processing in the chemical industry. At low power and high frequencies, it can be used to determine emulsions (Hibberd et al., 1997), to monitor particle-size distributions (Takeda and Goetz, 1998; Mougin et al., 2003; Povey et al., 1999), to investigate biological properties (Preston, 1986), and to supervise the real-time analysis of chemical reactions (Priego-Capote and Luque de Castro, 2004). At high power and low frequencies, ultrasound can be used for the processes of cleaning, which is the most industrially developed application (Monnier et al., 2000), emulsification (Freitas et al., 2004; Chemat et al., 2004; Behrend and Schubert, 2001), precipitation (Povey, 1997; Kapustin, 1963; Povey and Mason, 1998), extraction (Peña et al., 2005; Veličković et al., 2005; Liu et al., 2005), waste water treatment (Pétrier and Francony, 1997) and chemical reactions (Ince et al., 2001, Dirnstorfer et al., 2000; Contamine et al., 1994; Portenlänger and Heusinger, 1992).

When ultrasound propagates through a liquid medium, its power not only is a driving force for mass transfer, but also initiates an important phenomenon known as cavitation. Cavitational bubbles form during the negative-pressure period of the sound wave. When a cavitational bubble implodes, a localized hot spot is formed with a high temperature and high pressure with the release of a powerful shock wave. The reason for the above phenomena is that the collapse process is very rapid. The collapse time of a cavitational bubble is normally very short compared to its birth time. The power of ultrasound and cavitation phenomena influence primary nucleation during crystallization processes (Repacholi and Grandolifo, 1987; Li and Lin, 1995; Cains et al., 1998). When ultrasound is applied to crystallization system, it may bring influence to nucleation, crystal growth rate, agglomeration and breakage. The change of above parameters may bring significant influence on crystal product.

2.2 The physical properties of ultrasound

2.2.1 Ultrasonic wave

Ultrasonic energy consists of mechanical vibrations occurring above the upper frequency limit of human audibility (generally accepted as about 20 kHz). The frequency ranges of sound are shown in Figure 2.1. And the comparison between the features of ultrasound and normal sound are listed in Table 2.1.

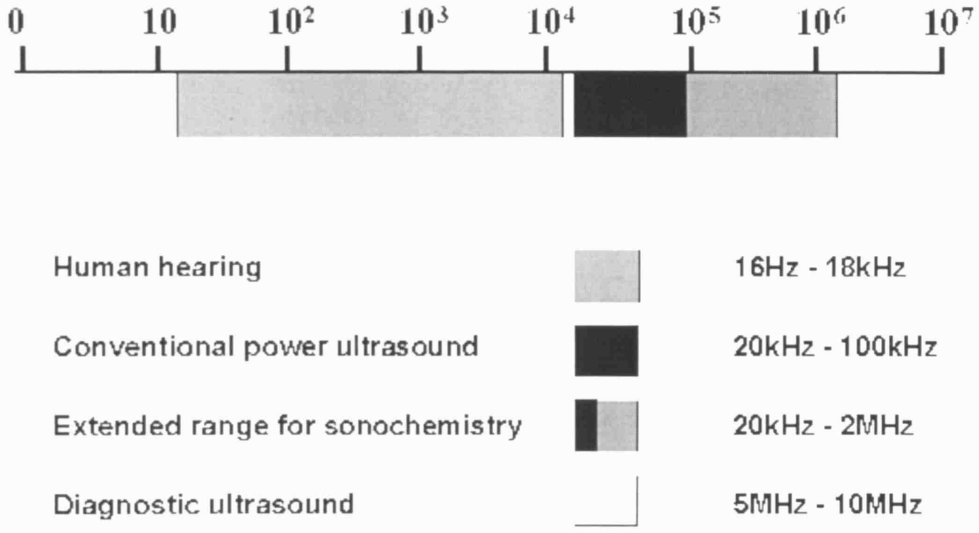

Figure 2.1 Frequency ranges of sound (Mason, 1991)

Table 2.1 Features of ultrasound which distinguish it from sound in water

Ultrasound	Normal sound
Transmitted by means of waves	Transmitted by means of waves
Beyond the range of human hearing	A periodic disturbance stimulating the ear
Wavelength between cm and μm	Wavelength between m and cm
Frequency between 20 000 and 10^{13} Hz	Frequency between 20 to 20 000Hz
With high sound pressure	With low sound pressure
With cavitation phenomenon	Without cavitation phenomenon

Ultrasound consists of a propagating disturbance in a medium, which causes subunits (particles) of the medium to vibrate. The vibratory motion of the particles characterizes ultrasonic (acoustic) energy propagation. Unlike electromagnetic radiation, acoustic energy cannot be transmitted through a vacuum. The transmission through the medium depends to a great extent on the ultrasound frequency and the state of the medium, i.e., gas, liquid, or solid, mainly in the form of longitudinal or compressional waves formed by alternate regions of compression and rarefaction of the particles of the medium, which vibrate in the direction of energy propagation. The distance between two consecutive points of maximum compression or rarefaction is called the wavelength. The compression and expansion cycle of ultrasound is shown in Figure 2.2.

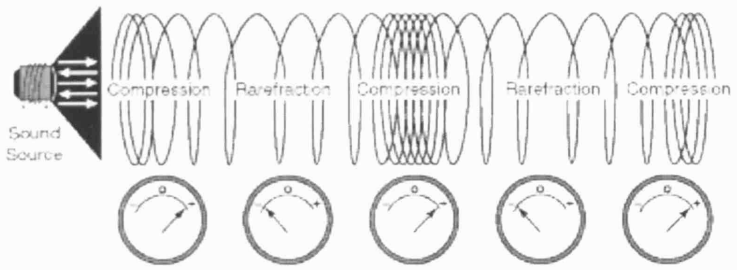

Figure 2.2 The compression and expansion cycle of ultrasound

(http://users.ox.ac.uk/~masondr/Sonochemistry/index2.htm)

The ultrasonic wave includes continuous wave, gated (amplitude-modulated), and acoustic-burst pulsed waves. A continuous wave at a single frequency is a simple sinusoidal wave having constant amplitude. The pressure of amplitude-modulated wave changes with distance at a fixed instant in time, or as a function of time at a fixed point in space. For the pulsed wave, the pressure amplitude is not constant and is zero for part of the time. No acoustic energy is being emitted between pulses and the ultrasound propagates through the medium as small packages of acoustic energy.

The ultrasonic field produced by a transducer obeys all the physical laws of wave phenomena. It can be thought of as being produced by many small point sources making up the transducer face and thus producing a characteristic interference pattern at any point in the field. As ultrasound is propagated from the transducer, there is a zone where the overall beam size remains relatively constant (the near field), though there are many variations of intensity within the zone itself, both across and along the beam axis. This zone is followed by a zone where the beam diverges and becomes more uniform (the far field).

In the far field of any transducer, the acoustic intensity is proportional to the square of the acoustic pressure. The directivity of the beam in the far field is determined by diffraction, in the same way that a light wave is affected by a small aperture; the higher the frequency of ultrasound produced for a given transducer size, the more directional is the beam. Furthermore, if the frequency is held constant but the diameter is reduced, the beam divergence increases (Repacholi and Grandolifo, 1987; Li and Lin, 1995; Cains et al., 1998).

2.2.2 Ultrasonic intensity

As ultrasound is propagated from the transducer, there is a zone where the overall beam size remains relatively constant (the near field), though there are many variations of intensity within the zone itself, both across and along the beam axis. This zone is followed by a zone where the beam diverges and becomes more uniform (the far field).

In the far field of any transducer, the acoustic intensity is proportional to the square of the acoustic pressure. The directivity of the beam in the far field is determined by diffraction, in the same way that a light wave is affected by a small aperture; the higher the frequency of ultrasound produced for a given transducer size, the more directional is the beam. The intensity distribution in the ultrasonic field and the flows caused by ultrasound are shown in Figure 2.3.

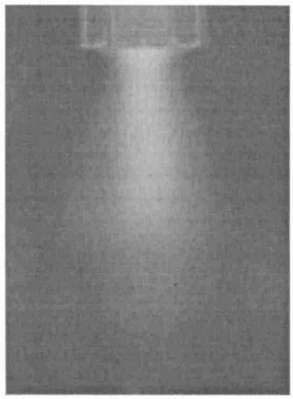

Figure 2.3 The intensity distribution in the ultrasonic field and the flows caused by ultrasound

(http://www.chemsoc.org/ExemplarChem/entries/2004/bristol_eaimkhong/sonochemistry.htm)

The intensity distribution along the axis of a transducer is such that an axial intensity peak occurs at some distance from the transducer. This peak is a common feature of both focused and non-focused fields, and its existence is an important factor in characterizing ultrasound fields.

The intensity of the ultrasonic field produced by the transducer also varies with time, if the ultrasound is pulsed, intensity averaging can be carried out in the time domain and it is therefore necessary to distinguish between time average (such as the average over the total time or over the pulse duration) and temporal peak intensities.

2.2.3 Speed of sound

The speed at which ultrasonic vibrations are transmitted through a medium is inversely proportional to the square root of the product of the density and the adiabatic compressibility of the material. The speed together with the frequency of ultrasound determines the wavelength of the waves that are propagated.

2.2.4 Refraction and reflection

When an ultrasound wave encounters an interface between two media and the dimensions of which are largely compared with the wavelength, part of the wave will be reflected back into the first medium with the same speed. The rest of the wave will be transmitted or refracted into the medium beyond the interface and will travel with the velocity of propagation in that medium. When the ultrasonic wavelength is equal to or greater than the dimensions of the reflecting object, the incident beam is scattered in all directions.

The ratio of the characteristic impedances of any two media on either side of an interface determines the degree of reflection and refraction or transmission of the incident wave. The characteristic acoustic impedance of a medium is the product of the density and the speed of sound in that medium. The extent to which ultrasonic energy is transmitted or reflected at an interface separating two continuous isotropic media is determined by the ratio of the characteristic acoustic impedances of the media (Li and Lin, 1995).

2.2.5 Attenuation and absorption

As an ultrasound beam is transmitted through a heterogeneous medium such as crystal suspension solution, its intensity is reduced or attenuated through a number of mechanisms, including beam divergence, scattering, absorption, reflection, diffraction, and refraction.

Beam divergence refers to the spreading of the beam in the far field through diffraction effects. For a given transducer radius, this phenomenon is greater at lower frequencies. As the beam area becomes larger, the intensity is reduced.

Scattering refers to the reflection of the incident ultrasound from interfaces (i.e., surfaces separating media of different characteristic acoustic impedances) with

dimensions close to or less than the ultrasound wavelength. In this case, the incident beam is scattered in all directions. Ultrasound impinging on solution with crystal nuclei, for example, would be scattered. When scattering occurs, it is greater at higher ultrasonic frequencies.

Absorption of ultrasound occurs when the ordered vibrational energy of the wave is dissipated into internal molecular motion, i.e., into heat. There are many mechanisms by which ultrasound absorption occurs in a medium, including viscous loss, hysteresis loss, and relaxation processes (Li and Lin, 1995).

2.2.6 Cavitation

Acoustically induced cavitation is one of the primary effects of power ultrasound to a continuum fluid. Ultrasound can impose an oscillatory pressure on the fluid. At low intensity, this pressure wave will induce motion and mixing within the fluid, a process known as acoustic streaming. Mixing can be increased by above process. At higher intensity, in addition to acoustic streaming and mixing effects, the local pressure in the expansion phase of the cycle falls below the vapor pressure of the fluid, which causes any minute bubbles or cavities to grow. If the ultrasonic intensity is increase further, the negative transient pressures will be produced in the fluid medium. This pressure cannot only enhance the bubble growth process, but produce new cavities by the tensioning effect on the fluid (Repacholi and Grandolifo, 1987; Li and Lin, 1995; Cains et al., 1998). These latter processes form cavitation phenomenon. In the expansion phase of the pressure wave, a void or bubble is created by the local fluid tension, or is expanded due to the decrease in pressure. In the compression phase, the increase in pressure either contracts the void or bubble to a smaller size, or eliminates it by implosion. Generally, these processes are non-linear, in that the changes in the radius of the void are not proportional to the variations in acoustic pressure. The generation of a cavitation bubble is shown in Figure 2.4.

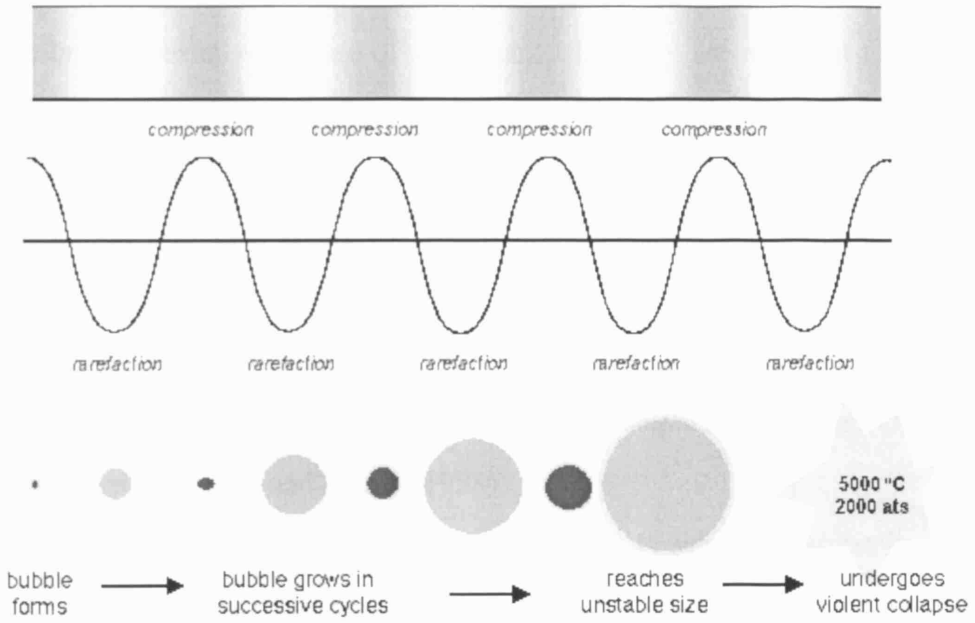

Figure 2.4 Generation of an acoustic bubble

(http://users.ox.ac.uk/~masondr/Sonochemistry/index2.htm)

There are two types of cavitation existing in the fluid - stable or transient. The stable cavitation bubble can exist over a timescale of a number of sonic pressure cycles, and oscillate nonlinearly around a certain equilibrium size. Transient cavitation bubble is unstable and can exist for only a single cycle. It may expand to many times of its original size during the expansion phase, then, collapses violently during the compression phase. The implosion of a gas-filled bubble will result in a number of smaller bubbles, while a vapor-filled bubble will collapse with considerable violence, since there is no residual compressible gas present to cushion the mechanical effect (McCausland et al., 2005).

Both cavitation bubbles are important mechanisms for ultrasonic effects on chemical and physical processes, the former being especially relevant at lower intensity levels (e.g., 300 mW/cm^2 or less in water) and the latter at higher levels. In many

experiments, both types of cavitation occur simultaneously, but in certain situations only stable cavitation occurs.

Stable bubbles exist which are of such a size that they are resonant in the sound field and oscillate with large amplitude. When a bubble expands and contracts during the ultrasound pressure cycle, the surrounding medium flows inwards and outwards with a higher velocity than if the gas bubbles were absent. As a rough guide, the resonant diameter of a cavitation bubble in water at 1 MHz is about 3.5 μm. Alternatively, gaseous nuclei may exist in the medium which are initially smaller than resonance size but which grow to that size in an applied sound field through the process of rectified diffusion (Povey and Mason, 1998).

When a gas bubble pulsates, its motion is not usually spherical, either because of distortion by an adjoining boundary or because of surface waves set up by the ultrasound field. Asymmetric or non-uniform oscillation of the air-liquid interface, at the surface of an air pocket or bubble, causes a steady eddying motion to be generated in the immediately adjoining liquid, often called micro-streaming, in which the velocity gradients may be high.

In contrast to stable cavitation, transient (or collapse) cavitation is more violent and occurs at higher ultrasound intensity levels. When a gas bubble or nucleus within the medium is acted on by an ultrasound field having a high-pressure amplitude, it may expand to a radius of twice the original value or more, then collapse violently. In the final stages of collapse, kinetic energy given to a relatively large volume of liquid has to be dissipated in an extremely small volume, and high temperatures and pressures result. Chemical changes are commonly produced by cavitation. The combination of high pressures and temperatures can generate aqueous free radicals and hydrated electrons (highly reactive chemical species) within the exposed medium by the dissociation of water vapour in the bubble during its contraction.

Studies show that transient cavitation does not occur unless the intensity exceeds some threshold value which is very dependent on experimental conditions. It has also

been found that the threshold for cavitation decreases with increasing temperature and with increasing volume of the irradiated liquid.

The number and size distribution of gas nuclei are particularly important for the occurrence of cavitation in the medium. Unfortunately, these quantities are not easily measured. The number of available nuclei within a fluid medium greatly increases when the medium is stirred or mechanically disturbed.

2.2.7 Stress and acoustic streaming

Stresses or forces resulting from an ultrasonic field acting on heterogeneous regions within a medium can be categorized as follows (Dunn and Pond, 1978):

1. Buoyancy forces that are oscillatory, have a time-average equal to zero, and produce a radiation pressure on bodies having a density different from the surrounding medium;
2. Displacement or radiation forces that have a non-zero time average and can cause an appreciable relative velocity between the inhomogeneity and the surrounding medium;
3. Viscosity-variation forces or viscous stresses that result in acoustic streaming because of variations in viscosity over the cycle of the applied ultrasound;
4. The Oseen force, another time-averaged force, which is due to the dependence of drag on the second power of relative velocity.

When an ultrasonic field is propagated within a liquid, the particles of the liquid take part in an oscillatory flow. Consider a particle oscillating in a direction parallel to a boundary, at the boundary itself, the velocity of the liquid flow will be zero provided the boundary is a fixed, rigid solid, and "non-slip" conditions apply. Conditions may then exist for establishing acoustic streaming, a time-independent circulatory motion of the liquid. As part of this motion, a thin boundary layer may exist between the surface and

the streaming liquid itself, within which the velocity gradient is large. Such streaming has been observed as circulatory flow in the vacuoles of plant cells (Nyborg, 1978). However, there must be non-uniformity or some kind of asymmetry for this streaming to be established. For an ultrasonic field propagating in a suspension of particles, relative motion occurs between the particles and the fluid, where boundary layers are established around each particle and give rise to an acoustic streaming field.

2.3 Power ultrasound: generation and equipment

Normally, there are 3 main types of transducers are used to convert mechanical or electrical energy to sound energy.

1. Liquid-driven transducers. Liquid is forced across a thin blade which causes the blade to vibrate. For each vibrational movement the leading face of the blade produces a pressure wave and the blade works as a powerful source of ultrasound.
2. Magnetostrictive transducers. Magnetostrictive transducers are electromechanical devices, which use magnetostriction, an effect found in some ferromagnetic materials, as core. Repeated rapid switching on and off of the current generates the mechanical vibrations on the core, which works as the source of ultrasound.
3. Piezoelectric transducers. Piezoelectric transducers are the most common devices employed for generation of ultrasound and utilized ceramics containing piezoelectric materials such as barium titanate or lead metaniobate. Piezoelectric transducers are better than 95% electrically efficient and can operated over the whole ultrasonic range.

There are numerous different pieces of ultrasonic equipment available for use as

sonochemical reactors. The differences between them are in the design of the power generator, the ultrasonic device used and the reactor or cell used in conjunction with the source of ultrasound.

"Ultrasonic bath" are of rather low power in order to avoid cavitaiton damage to the tank walls and the power density is low because the volumes of liquid in the tanks are generally large. And in order to amplify the acoustic energy generated from a transducer. It is normal practice to attach to the transducer a "horn" into the system. The horns are generally a half wavelength in length. The amplitude gain generated by the system depends on the shape of the final horn, for a uniform cylinder there is no gain in the amplitude but the horn acts as an extender for the tansference of the acoustic energy. In practical term, the highest energy transferable from the source depends on two factors:

1. The characteristics of the materials used to construct the transducer assembly and the horn.
2. The area of the emitting face.

The third type of sonochemical reactor involves parallel vibrating plates. This design is probably the best option for on-line use, the product being treated homogeneously during its transfer through the reactor whose walls are vibrating. When the plates are close, the attenuation of the sound by the liquid is minimal and standing waves patterns are not present.

The forth type of reactor is radial vibrating system. An ideal way of introducing ultrasound into a liquid flowing in a pipe would be to use the pipe itself as a bivrating source. Such systems are capable of handing high flow rates and viscous material. The cross-sectional geometry is an important factor in such devices. A cylindrical resonating pipe can provide a focus of ultrasonic energy in the center of the tube as a hexagonal pipe. Thus relatively low power at the perimeter inner surface gives high energy in the

center.

2.4 Ultrasonic effect on mixing

Mixing is a very common operation in the chemical industry. Mixing is accomplished by the movement of material between various parts of the bulk liquid mass due to the generated flow and diffusion. In many cases, the interactions between mixing and crystallization can affect every aspect of a crystallization operation including nucleation, growth, and maintenance of a crystal slurry. Mixing requirements for crystallizers involving the complete range of issues in blending and solid–liquid mixing includes (Paul et al., 2005):

1. Blending of solution and anti-solvent components to the molecular level to achieve supersaturation;
2. Blending of reagents to the molecular level to achieve reactive crystallization/precipitation;
3. Maintenance of a crystal slurry of the required solid/liquid ratio;
4. Avoidance of entrainment of gas/vapor from the head space;
5. Avoidance of encrustation—solid scale on walls and baffles;
6. Rate of heat transfer;
7. Minimization of secondary nucleation through impact;
8. Avoidance of shear damage to crystals;
9. Effect on agglomerate formation/break-up;
10. Maintenance of crystal slurry for satisfactory discharge of the slurry without excess retention of product crystals;
11. Possible operation over a wide volume range.

The initial blending of components to the molecular level while avoiding regions

of high supersaturation requires consideration of the mesomixing and micromixing environments of the contactor. Other requirements involve the macromixing capabilities of the crystallizer.

Mixing is accomplished by the movement of material between various parts of the bulk liquid mass due to the generated flow and diffusion.

Factors that improve with greater mixing intensity are (1) heat transfer, (2) bulk turnover, (3) dispersion of an additive such as an anti-solvent or reagent, (4) uniformity of crystal suspension, (5) avoidance of settling and minimization of wall scale, and (6) minimization of impurity concentration at the crystallizing surface. Since small-scale experiments inevitably operate with reduced turnover time and thus more passes by the impeller, these runs can sometimes achieve better results than would be expected on scale-up. An effort should be made in small scale to establish mixing sensitivity of the crystallization process.

However, these needs must be balanced against the possibly negative results of over-mixing that can result in crystal breakage and/or shedding of nuclei as well as increased secondary nucleation and growth rate dispersion as discussed above.

These concerns lead to the conclusion referred to above, that it is often necessary to choose a mixing condition (impeller speed, type, etc.) that may not be optimal for every aspect of the crystallization and may actually not be optimal for any of them. In many cases, however, one end result (i.e. PSD, bulk density, uniformity of suspension, approach to equilibrium solubility (yield)) may dictate the choice of mixing conditions. In this case, it becomes essential to determine if the negative effects can be tolerated.

Two basic principles are followed to induce mixing at the micro-scale. First, power input from the exterior is used, termed active mixing. These external energy sources are ultrasound (Yang et al., 2001), acoustic, bubble-induced vibrations (Liu et al., 2003, 2002), electrokinetic instabilities (Oddy et al., 2001), periodic variation of flow rate (Glasgow and Aubry, 2003; Niu and Lee, 2003; Qian and Bau, 2002), electrowetting-induced merging of droplets (Palk et al., 2003), piezoelectric vibrating

membranes (Woias et al., 2000), magneto-hydrodynamic action (West et al., 2002), small impellers (Lu et al., 2001), integrated micro-valves/pumps (Voldman et al., 1998), and others (Scheme 2). As a second means, the flow energy, e.g. due to pumping action or hydrostatic potential, is used to restructure a flow in a way which results in faster mixing. This is known as passive mixing.

In the case of mechanically agitated contactors, mixing depends upon the type of impeller, speed of impeller, dimensions of vessel and physico-chemical properties of the system. In the case of ultrasonic reactor (crystallizer), energy is dissipated in the system by the vibrating horn surface. Acoustic cavitation involves cavitation due to the passage of ultrasound. Mechanical effects of ultrasound are responsible for mixing during the homogeneous liquid phase reactions.

In the case of acoustic cavitation, absorption of the ultrasonic wave during its propagation in the cavitating liquid is responsible for an energy gradient that induces a macroscopic liquid flow called acoustic streaming. Acoustic streaming causes the mixing effects experienced in the liquid, and therefore, it is important in the design of sono-chemical reactors (crystallizer).

Ultrasound is a pressure wave which propagates through a liquid, with an energy (per unit volume) of

$$E = \frac{1}{2}\rho_0 u_0^2 \tag{2.1}$$

where E is acoustic energy density, ρ_0 is liquid density and u_0 is local fluctuating velocity (Monnier et al., 1999).

As mentioned above, ultrasound can impose an oscillatory pressure on the fluid and induce motion and mixing within the fluid at various intensities. Nevertheless, ultrasound also has mechanical effects on crystallization system. Three different phenomena are responsible for the mechanical effects (Dahlem et al., 1998). The first phenomenon is shock wave. The shock wave is produced by the implosion of cavitation bubbles. At the around area of implosion, the pressure can reach as high as 300MP. This shock wave is, according to Doktycz and Suslick (1990), responsible for the effects of

ultrasound on particles in suspension. And it can promote mixing process as well. If the implosion of cavitation bubble is near an interface, besides shock wave, it will generate a liquid jet. In heterogeneous solid-liquid systems, the interface produces a perturbation in the sonic field, which induces an asymmetric collapse of the cavitational bubbles. At extended interfaces several times larger than the resonance cavitation size, the result is a micro-jet of liquid passing through the cavitation which impinges with the solid surface at velocities estimated around 100 $m \cdot s^{-1}$ (Cains et al., 1998). The third important phenomenon is acoustic streaming, which causes mixing effects of ultrasound. An energy gradient will be formed during the absorption of the ultrasonic wave when it propagates through liquid medium. This energy gradient may induce a macroscopic liquid flow called acoustic streaming. It generates vigorous circulation around the ultrasound beam but the vorticity decreases when moving from the acoustic source. In the case of cavitating water, this absorption consists of both the attenuation by the liquid itself and the absorption of the sound wave by heterogeneous phase, such as cavitation bubbles, in liquid (Dahlem et al., 1998).

The mixing processes in a reactor take place on different scales, ranging from the macroscopic scale (macromixing) to the microscopic scale (micromixing). The term macromixing refers to the overall mixing performance in a reactor and is usually described by the residence time distribution (RTD). This concept was originally introduced by Danckwerts (1958) and is based on a macroscopic lumped population balance. A fluid element is followed from the time at which it enters the reactor (Lagrangian viewpoint). The probability that the fluid element will leave the reactor after a residence time τ is expressed as the residence time distribution (RTD) function. This function characterises the scale of mixing in a reactor.

The term mesomixing as introduced by Baldyga and Bourne (1992) describes the interaction by mixing between the feed plumes and the bulk. The reactant entering the reactor is eroded from the plumes and its scale is reduced to that of large eddies. In the literature, the terms macromixing and mesomixing are not always considered separately,

which has led to confusion when reactions were stated to be macromixing-controlled. In terms of the notation above, these processes are mesomixing-limited, as real macromixing limitation is very rare in precipitation reactors because of the well-mixing on the macro-scale and the relatively long residence times of the process. Mesomixing describes the very first moments of a fluid element entering the vessel, whereas macromixing considers the whole lifetime, *i.e.* the age, of an element in the reactor. In terms of space, mesomixing occurs only in the reaction zone.

Micromixing is regarded as turbulent mixing on the molecular level. It comprises the viscous-convective deformation of fluid elements, followed by molecular diffusion (Baldyga and Poherecki, 1995). A characteristic timescale for micromixing is usually based on Kolmogoroff's micro-scale of eddy lifetime (Baldyga et al., 1995 and Baldyga et al., 1997).

$$t_{micro} = 17.3 \times \left(\frac{\nu}{\varepsilon_{loc}} \right)^{1/2} \qquad (2.2).$$

where t_{micro} is micromixing time, ν is velocity and ε_{loc} is local power input. The inverse of the time constant t_{micro} (micromixing) can be interpreted as a transfer coefficient for mass transfer by diffusion. In a crystallizer for reactive crystallization, the crystal size distribution is influenced by micromixing, mesomixing and macromixing (Torbacke and Rasmuson, 2001).

The ultrasonic effect on mixing has been investigated in many studies. Monnier et al. (2000) found ultrasound does not bring significant influence on macromixing, but increasing ultrasonic power could improve micromixing efficiency. Vichare et al. (2001) discussed the flows in ultrasonic field in sonochemical reactor. The different dimensions of ultrasonic sources and source position were investigated. It was found that the average liquid circulation velocity increases with an increase in the diameter of the horn when the horn at different position. When the horn is at the same position and the ratio of the horn to the vessel cross-sectional area is constant, the average liquid circulation velocity is high with larger horn tip. When the horn is near the bottom of the

vessel, the mixing time is higher than the time when the horn is near the surface. But for a large size of the horn tip, the variation of mixing time with the horn position is less significant. It is found that mixing time is a strong function of the horn position, horn tip dimensions and geometry of the vessel.

Monnier et al. (1999) also compared the difference of mixing effect between impeller and ultrasound. The critical feed times with classic impellers are lower than those measured with ultrasound: ultrasound generates less mesomixing than a classic impeller. Their research also confirmed that power ultrasound generates micromixing. But the micromixing phenomenon achieved with ultrasound cannot be related to the dissipated power per unit mass, as in standard mechanical agitated reactors. The ultrasound technique is more local, yielding effects in a cylinder below the horn. And micromixing time is not improved by a lower reacting volume, revealing that the characteristic parameter is no more the energy dissipated per unit mass as with a classic impeller but the energy dissipated by the emitter. As a consequence, it seems better to use large volumes, the injection being located always near the emitter where the cavitation is the most intense. Nevertheless, the ultrasound technique consumes still too much energy to be efficient. Therefore, it must be used either locally in large volumes or in smaller volumes but with a careful confinement of the acoustic energy in the reactor. Their experiments show that viscous media have proved a good behavior of the ultrasound technique as well (Monnier et al., 1999). In addition to ultrasound with low frequency, high-frequency ultrasound also has significant influence on mixing process (Ito et al., 2002).

Above phenomena and conclusion are confirmed with other experiments (Yang et al., 2001) and new substances, such as in melt mixing (Kim and Lee, 2002), in the experiment of degradation of trichloroacetonitrile, chloropicrin and bromobenzene (Zhang and Hua, 2000), in electrochemical process (Javier et al., 1999), in the system with solid particles (Chen and Yu, 2004), in liquid-liquid homogeneous reaction (Entezari and Keshavarzi, 2001). And the ultrasonic effect on mixing is also compared

with other mixer, such as stirred tanks, jet mixers and ultrasound mixers (Patwardhan et al., 2003). Although the mixing effect of ultrasound is promising, its mixing efficiency is not so good.

2.5 Ultrasonic effect on mass transfer

Mass transfer is the net movement of a component in a mixture from one location to another location where the component exists at a different concentration. Often, the transfer takes place between two phases across an interface. Mass transfer occurs by two mechanisms (1) Molecular diffusion by random and spontaneous microscopic movement of individual molecules in a gas liquid or solid as a result of thermal motion; and (2) Eddy (turbulent) diffusion by random macroscopic fluid motion. Molecular and/or eddy diffusion frequently involves the movement of different species in opposing directions. When a net flow occurs in one of these directions, the total rate of mass transfer of individual species is increased or decreased by this bulk flow or convection effect, which is a third mechanism of mass transfer.

In a binary mixture, molecular diffusion occurs because of one or more different potentials or driving forces, including differences (gradients) of concentration (ordinary diffusion), pressure (pressure diffusion), temperature (thermal diffusion), and external force fields (forced diffusion) that act unequally on the different chemical species present. Molecular diffusion caused by concentration gradients is the most common type of molecular diffusion in commercial separation. It occurs in solids and in fluids that are stagnant or in laminar or turbulent motion. Eddy diffusion occurs in turbulent motion. When both molecular diffusion and eddy diffusion occur, they take place in parallel and are additive. Furthermore, they take place because of the same concentration difference (gradient). When mass transfer occurs under turbulent flow conditions, but across an interface or to a solid surface, Thus, even though eddy diffusion may be the dominant mechanism in the bulk of the fluid, the overall rate of

mass transfer is controlled by molecular diffusion because the eddy diffusion mechanism is damped or even eliminated as the interface or solid surface is approached (Seader and Henley, 1998).

Ultrasound waves cause a series of rapid and successive compressions and rarefactions, with rates depending on their frequency. This mechanism is of great relevance to the drying and dewatering of foods. The mechanical and physical effects of sound can be used to enhance many processes where diffusion takes place (Floros and Liang, 1994). Acoustic streaming can affect the thickness of the boundary layer, which exists between stirred fluid and solid. Cavitation can explosively collapse and generate localized pressure fluctuations. This effect increases diffusion during osmotic processes and accelerates degassing of the tissue (Floros and Liang, 1994). Diffusion across the boundary between the suspended solid and liquid is substantially accelerated in an ultrasonic field. Pressure and the frequency are the two main factors to take into consideration. No increase in diffusion rates was reported when the maximum value of intensity is achieved due to violent cavitation that produces an extreme turbulence or vapour locks at the interface. Lenart and Auslander (1980) showed that solute diffusion rates increase with higher acoustic intensities once the threshold value is crossed. Sajas and Gorbatow (1978) reported slight improvement in the diffusion rates at higher frequencies. The mechanism of effect of ultrasonic frequency on diffusion has not been elucidated. Simal, et al. (1998) reported the applicability of sonication to osmotic dehydration of porous fruit such as apple cubes and showed that the rates of mass transfer increase with the use of ultrasound in comparison with the osmotic process carried out under dynamic conditions.

To the mixing process of different flows, in addition to diffusion process, ultrasonic irradiation can also enhance the turbulent mass transport rate (convection). The solute is transferred at both large and small scales, so that the area of interface between fluids is enlarged. As a result, mass transfer rate is strongly enhanced by ultrasonic irradiation. In turbulence with mean fluid shear, the turbulent mixing is

enhanced by mean fluid shear mainly at large scales, and therefore the use of high-frequency ultrasound is a more promising technique for promoting turbulent mixing than the use of mean fluid shear or agitation (Ito et al., 2002).

In recent years, ultrasonic effect on mass transfer has been investigated in many literatures. Many previous studies have reported that mass transfer in liquids is promoted by ultrasonic irradiation in static fluids (Monnier et al., 1999; Kawahara et al., 2000; Vichare et al., 2001; Mitome et al., 1996). The first reason for above phenomenon is that ultrasound can increase diffusion coefficient significantly, which enhances mass transfer consequently. Trabelsi et al. (1996) reported that mass transfer rate under ultrasound has revealed an important enhancement effected by high frequency ultrasound (70 fold the diffusional mass transfer rate) and the still higher effect of a low frequency sonication (120 fold) for the oxidation of phenol (Trabelsi et al., 1996). The phenomenon, that ultrasound enhances mass transfer and oxidation rate, is also observed by Pollet et al. (2002). Moholkar, et al. (2003) (2004) reported that ultrasound increases mass transfer rate in a textile fabric and the intensity of cavitation can influence the mass transfer rate. And Javier Del Campo et al., (1999) reported the ultrasound enhances the mass transfer during sonoelectrochemical processes at low temperature.

Ultrasound can also make fluids become turbulent, which will induce convection for mass transfer. Ito et al. (2002) also found that ultrasound can enhance the turbulent mass transfer rate in a reacting liquid flow. Wadhawan, et al. (2001) found that the application of ultrasound drastically increases the convective flux toward the electrode in an insonated homogeneous solution which will increase the mass transfer rate.

Ultrasound can also be used to increase mass transfer rate for drug delivery. Zhang et al. (1996) reported that ultrasonic coupling media based on a methyl cellulose hydrogel or viscous sol can markedly lower overall permeation of human skin in vitro during application of low-frequency sonophoresis, because diffusive boundary layer can be eliminated or reduced by ultrasound. Some other researches also found that

ultrasound can increase mass transfer during drug delivery (Mitragotri, 2001).

In addition to the systems with solid-liquid or liquid-liquid, ultrasound can also be used to optimize the reaction with the mass transfer of gas and liquid in the liquid system (Schlafer et al., 2000).

Mass transfer rate control both nucleation rate and crystal growth rate during crystallization. Its enhancement accelerates crystallization processes and increases production rate of the crystallization unit.

2.6 Ultrasonic effect on crystallization processes

Sonocrystallization is the use of power ultrasound to control the course of a crystallization process (AEA Technol., 2001). The effect of ultrasound on crystallization was first observed in 1927 (Patrick et al., 2004). In the last decade, sonocrystallization has received much attention. The ultrasonic effect on crystallization has been reported to accelerate crystal precipitation (Nishida, 2004; Ichitsubo et al., 2004), retard precipitation (Dalas, 2001), change the crystal size distribution and crystal habit (Lee et al., 2001; Amara et al., 2001; Li et al., 2003; Guo et al., 2005;), change crystal property (Enomoto et al., 1996), increase nucleation rate (Teipel et al., 2002; Lyczko et al., 2002; Chow et al., 2003; Chow et al., 2004), depress agglomeration (Kim et al., 2002; Guo et al., 2005) and agglomerate particles (Kusters et al., 1993; Enomoto et al., 1997).

The application of power ultrasound to crystallizing systems appears to offer significant potential for modifying and improving both processes and products.

Crystallization is one of the oldest unit operations in the pharmaceutical industry, but crystallization processes frequently exhibit design and operational problems. These problems are related to product quality requirements such as filterability, caking behaviour, purity and tablet behaviour of pharmaceuticals on the one hand, and process requirements, such as capacity. Pharmaceutical crystallizations frequently produce crystals, which do not satisfy the defined quality and crystal size distribution

requirements. Another problem is the inclusion of mother liquor during subsequent re-crystallization may cause particulate agglomerate formation; a process referred to caking of particles. Operational problems also constitute a large portion of the problems encountered in crystallization processes. But, however, crystallization involves very few control parameters that can be adjusted to drive the processes of nucleation and growth towards the desired yield and product properties.

Power ultrasound offers an additional and highly flexible method of control. Particularly, ultrasound can be used to solve some problems during crystallization processes, which cannot be solved by other methods. Generally, after ultrasound is applied to crystallization system properly, it may bring following advantages to operation process (AEA Technol, 2005):

1. Narrowing of the metastable zone width.
2. Controlling initiation of nucleation.
3. Improving crystal shape and habit.
4. Reducing polymorphs.
5. Reducing processing time.
6. Improving filtration characteristics.
7. Improving product properties including, handling, bulk density and appearance.
8. Reducing agglomeration crystals with fewer imperfections.
9. Increasing process reproducibility.
10. Often the product produced is already within a tight specification and the need for extra milling or micronisation can be removed.
11. Improving product handling.
12. Rapid mixing of immiscible liquids.
13. Homogenisation and the production of stable microemulsions.
14. Accelerating catalytic reactions and solid/liquid separations.
15. Ultrasonic nucleation process can also eliminate the need to add seed crystals,

which can be advantageous in contained, sterile operations.

The main reason why ultrasound can bring such a significant influence to crystallization process is on account of its effects on crystallization kinetics. Ultrasound can influence nucleation, crystal growth, agglomeration and breakage during crystallization process.

2.6.1 Ultrasonic effect on primary nucleation

Initiation of crystallization is often difficult since problems may occur due to incorrect external factors such as temperature and pressure settings. Sonication is thought to enhance both the nucleation rate and crystal growth rate by producing fresh and/or more nuclei in the medium. In addition to increase nucleation rate, ultrasound can reduces metastable zone width, which controls nucleation rate at the initial stage of crystallization. Another effect of ultrasound on nucleation is to reduce the induction time between the establishment of supersaturation and the onset of nucleation and crystallization (McCausland et al., 2005).

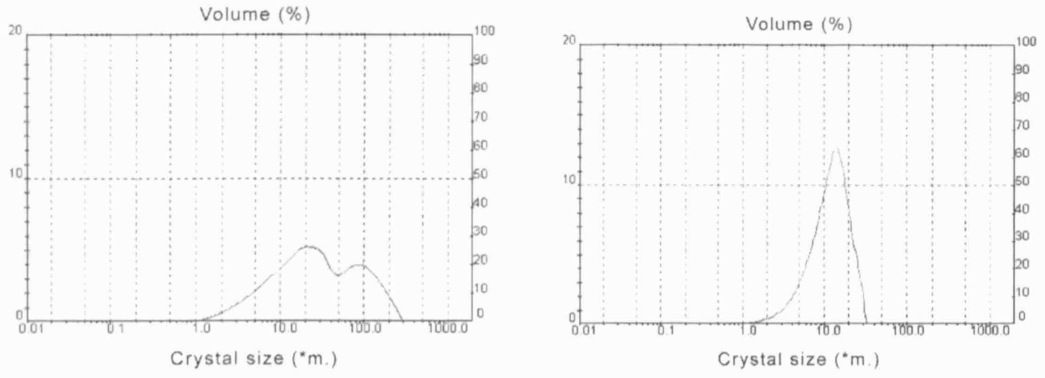

a **b**

Figure 2.5 CSD curve of roxithromycin seeds (Guo et al., 2005)
a: seeds by grinding
b: seeds by ultrasound

Guo et al. (2005) observed that ultrasound has a significant effect on reducing the induction time. After applying ultrasound to the system, the change in the apparent nucleation order is small, however the nucleation rate constant (k_N) increases significantly. And the quality of nuclei is also improved significantly compared to seeds by grinding. The size distribution of nuclei is shown in Figure 2.5.

Kim et al. (2002) observed that during the crystallization process of NTO, in a batch cooling crystallizer using conventional mechanical stirrer, the enhancement of nucleation is negligible while the nucleation rate is significantly increased by more than 10 times under ultrasound irradiation.

Lyczko et al. (2002) reported that when potassium sulphate is used as the working substance, ultrasound reduces the induction time especially for low absolute supersaturation. The metastable zone width can also be reduced by the application of ultrasound. The apparent orders of nucleation or growth are decreased by ultrasound. Amara et al. (2001) observed the similar phenomenon by using potash alum as substance.

From the study of Ueno et al. (2003), ultrasound can enhance the nucleation rate during triacylglycerols crystallization process. Ueno et al. (2003) also reported that ultrasound can decrease the induction times for crystallization and increase the nucleation rate of both tripalmitin and trilaurin. Ksaka et al. (2006) reported that the ultrasonic surface treatment can enhance nucleation and stimulate precipitation of desired crystal at a glass surface. Zhao et al. (2006) reported that ultrasonic oscillation can produce local shear at melts so as to promote the nucleation intensity in PPCN-100. The induction period of PPCN-100 is shortened. However, Miyasaka et al. (2006) reported that in ASA crystallization process, at a high level of ultrasonic energy, ultrasound irradiation increase the nucleation rate, but at a low level of ultrasonic energy, ultrasound irradiation may decrease the nucleation rate. Miyasaka et al. (2006) also reported that ultrasound dramatically increases the primary nucleation probability. And the induction time is reduced with an increase in the ultrasonic output in

$Na_2HPO_4 \cdot 12H_2O$ melt crystallization process. And Louhi-Kultanen et al. (2006) reported in his research in glycine crystallization that ultrasound can reduce the metastable zone width and increase the nucleation rate. From Li et al. (2006), ultrasound also reduces the metastable zone width and increases the nucleation rate in 7-ACDA crystallization process.

Chow et al. (2004) (2005) reported that increasing both the ultrasonic output level and the duty cycle can increase nucleation temperature in sucrose solution. But the precise mechanism for the enhanced nucleation temperatures at higher output and duty cycle settings is not clear. Ultrasound can also increase secondary nucleation rate. Ultrasound can break crystals and the crystal breakup forms new smaller crystal nucleating sites (secondary nucleation). Chow et al. (2004) also observed that during the fragmentation process, cavitation melts the ice and causes the weakening and fragmentation of the ice structures. The fragmentation event leads to an increase in the number of crystal nuclei in the solution. And flow patterns have been observed in sucrose solutions and the fragmentation of dendritic ice crystals could be related to the high shear forces created during bubble collapse, or to the asymmetric collapse of a cavitation bubble and formation of a jet. The compression of the ice phase may also cause secondary nucleation.

And ultrasound can even induce nuclei in some systems when nucleation processes are extremely difficult to occur. The nuclei of solid helium inside the wave can exist above a certain threshold in amplitude, after focusing a high intensity acoustic wave in liquid helium (Chavanne et al., 2001).

Ultrasound is used popularly in sugar industry to form nuclei at the initial stage of sugar crystallization. Sugar solution always has high viscosity and the nuclei are difficult to form. Ultrasound can increase nucleation rate at low supersaturation and the dispersion of nuclei is much easier than sugar seeds produced by grinding (Feng et al., 1997; Wang et al., 2005).

2.6.2 Ultrasonic effect on crystal growth and crystal habit

The controlled application of ultrasound at various stages of a crystallization process may be used to modify and tailor product properties to meet specified requirements. Rapid and efficient mixing can be used in precipitation, reaction and anti-solvent crystallizations, to bring about high product yields. Reduced metastable zone width is associated with better product quality in terms of size and habit and a lesser propensity for the solute to "crash out" with the extensive formation of fines. And continuing insonation can cause reduction in crystal size and less perfect crystals.

The specification of crystal habit is usually determined by the physical properties required of the product, both in terms of further processing and of end-use. Two reasons may cause the change of crystal habit by ultrasound. For one thing, crystal growth does not occur isotropically, and the faces that are exhibited by a crystal are those that grow more slowly. Extreme crystal habits form when the growth rate at a particular crystal face (or faces) occurs significantly more rapidly than the growth at other faces. These anisotropic effects are most marked when the driving force for growth, i.e. the supersaturation, is high. Crystals produced with ultrasound usually exhibit moderate and regular habits, because the process operates under conditions of low or moderate supersaturation. And Amara et al. (2001) mentioned that ultrasound can increase or decrease the growth rate of certain crystal faces and hot spots may influence the crystal lattice, while, abrasion may have some effects on the crystal habit change (Amara et al., 2001).

Ultrasound can be used to control crystal growth process, during crystallization of NTO in cooling crystallization, the effect of mixing can be ignored in the conventional batch crystallization of NTO by using mechanical stirrer if the optimal mixing condition (minimum impeller speed required to suspend all the crystals) was provided. Consequently, for the sake of controlling NTO crystals, higher nucleation rate associated with lower metastable zone width, and smaller and uniform crystal size could

be achieved by using ultrasound device (Kim et al. 2002). But, however, Balibar et al. (2003) reported that crystals grow and melt in a surprising way at velocities close to the sound velocity during He crystallization.

Nishida (2003) reported that ultrasonic irradiation was observed to accelerate the precipitation rate of calcium carbonate. The physical effect of mixing, which largely depends on the horn immersion depth, intensity and diameter of horn tip were found to affect the precipitation rate of calcium carbonate. Effects of cavitation, on the other hand, do not result in any improvements. Therefore precipitation of calcium carbonate is mostly affected by the physical effect of ultrasonic irradiation, especially macro-streaming rather than the chemical effects or micro-streaming. However, the morphology of the crystals formed is unaffected by ultrasonic irradiation.

But in the other cases, ultrasound may change crystal habits. Manish et al. (2005) reported that after the treatment of ultrasound, the agglomerates of ibuprofen comprised of crystals have different crystal habits such as needles, plates, and some hollow tubes. And the solubility, specific surface area and intrinsic dissolution rate increase with the treatment of ultrasonic energy. SEM and XRPD confirm crystal habit changes. Improvement in compressional properties and reduction in sticking was observed due to the change in crystal habit. Miao et al. (2005) also reported that ultrasound may change crystal morphology during the synthesis of CeO_2 nanotubes. Fini et al. (2002) observed that the ultrasound may change the morphology of particle in Indomethacin/Polyvinylpyrrolidone system. And Zhao et al. (2006) reported that during polypropylene/montmorillonite nanocomposites crystallization, ultrasonic oscillation can decrease the whole crystallization time of PP chains and change crystalline morphology. Louhi-Kultanen et al. (2006) also reported that in glycine crystallization process, ultrasound can both change the polymorph and reduce the size of crystal product. From Li et al. (2006), in 7-ACDA crystallization process, the ultrasound can mix reactants rapidly and uniformly, produce crystals with improved habit and enhance the controllability of the crystallization process. By adjusting the power density and

ultrasonic duration accompanied with proper precursor concentration, the size and size distribution of precipitated crystals can be effectively controlled.

From the study of Lee et al. (2003), ultrasound may change the microstructures of crystals.

Ultrasound can also be used to precipitate nano-sized crystals, after the treatment of ultrasound, spherical γ-MnO_2 crystals are obtained, while the MnO_2 crystals without ultrasonic treatment have needle shape (Li et al., 2005).

From the study of Ueno et al. (2003), ultrasound can accelerate the crystal growth rate and enhance the percentage of most stable polymorph for triacylglycerols in the product. Ueno et al. (2003) also reported that ultrasound irradiation can be used as an efficient tool for controlling the polymorphic crystallization of fats in his study.

But however, Dalas (2001) reported that the mechanism, the nature, the morphology and the size of the crystals are not influenced by the applied ultrasonic field, moreover, the crystal growth rate is retarded during carbonate scale formation.

Miyasaka et al. (2006) reported that during ASA crystallization, ultrasonic energy may control the perfection of the crystal shape.

2.6.3 Ultrasonic effect on agglomeration and breakage

Ultrasound may also be applied in the final stages of crystallization to break up agglomerates.

Ultrasound has a significant effect on reduction of the agglomeration. Three ultrasonic effects may contribute to this phenomenon. Firstly, the shock wave, which is caused by cavitation, can shorten the contact time between crystals. The crystals do not have enough time to bond together after contact. Secondly, agglomeration always occurs at the nucleation stage. The nuclei have a high ratio of surface area to volume, which causes high surface tension (Samsonov et al., 2003; Rusanov, 1999). Nuclei are prone to adhere together to decrease the surface tension. The surface tension decreases

as the crystals grow larger and therefore the crystals become stable and do not easily agglomerate. In anti-solvent crystallization, when the anti-solvent is added into the solution, it does not disperse immediately and produces a high localized supersaturation region. Poor mixing conditions increase the nucleation rate locally. This increases the possibility for nuclei to agglomerate (Gao and Zhao, 1998). However when the anti-solvent crystallization process only uses mechanical agitation, poor-mixed conditions are unavoidable. Compared with mechanical agitation, ultrasound has a great advantage as the mixing is improved. After introducing ultrasound into the crystallization process, the mixing is improved and the local nuclei population is controlled. The nucleation rate and the probability of contact between nuclei are decreased. The agglomeration is also significantly depressed. And Zhao et al. (2006) reported that ultrasonic oscillation can obviously prevent the agglomeration and improve the dispersion of clay in polymer matrix in polypropylene/montmorillonite nanocomposites crystallization process. From Li et al. (2006), in 7-ACDA crystallization process, the ultrasound can reduce the agglomeration significantly. Kakinouchi et al. (2006) found that brief irradiation promotes HEWL crystallization. However, the crystal clusters are damaged by the application of ultrasonic power. These results indicate that ultrasonic irradiation influences protein crystallization and changes the cluster formation in the solution. Furthermore, protein crystal growth under ultrasonic irradiation is strongly dependent on the irradiation duration and point.

The ultrasound also has breakage effect to crystals. Ciftcioglu and Aoki (See Kusters et al., 1993) believed that agglomerate breakage results from the interaction with cavitation bubbles formed in the liquid. Another mechanism for breakage is on account of the velocity increase and the collision between particles after ultrasound is applied to the system. The mechanical effects (shock wave, liquid jet and acoustic streaming) of ultrasound can increase the collision. Moreover, liquid jet acoustic streaming can erode crystal surface directly, which will increase both secondary nucleation rate and breakage rate during crystallization.

Guo et al. (2005) reported that ultrasound has a significant effect on depressing agglomeration and breaking crystals as shown in Figure 2.6.

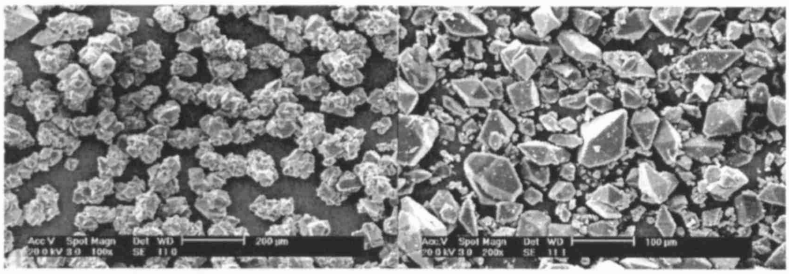

a b

Figure 2.6 SEM photos of roxithromycin crystals (Guo et al., 2005)
a: without ultrasound
b: with ultrasound

Kusters et al. (1993) reported that imploding cavitation bubbles rupture the agglomerates of silica and titania powders suspended in water. In their study, a sectional model for fragmentation is also used to simulate the evolution of the particle size distribution of silica and titania powders. Amara et al. (2001) observed that in addition to the change of crystal habit and size distribution during potash alum crystallization, ultrasound also depresses agglomeration and break crystals.

But Enomoto et al. (1997) mentioned that in addition to the effect of dispersion of agglomerated powders in solution. Ultrasound can also cause agglomeration. In the experiment of silica particle agglomeration behavior, the particle size and Si component in liquid phase are closely concerned with the agglomeration behaviour.

2.7 Conclusion

Ultrasonic energy consists of mechanical vibrations occurring above the upper

frequency limit of human audibility (generally accepted as about 20 kHz). Ultrasound consists of a propagating disturbance in a medium, which causes subunits (particles) of the medium to vibrate. When ultrasound propagates through a liquid medium, it can be refracted, reflected, absorbed and attenuated.

Ultrasonic power not only is a driving force for mass transfer, but also initiates an important phenomenon known as cavitation. The cavitation can cause the phenomenon of stress and acoustic streaming in fluids.

Ultrasound can impose an oscillatory pressure on the fluid and induce motion and mixing within the fluid at various intensities. Nevertheless, ultrasound also has mechanical effects on crystallization system. Three different phenomena are responsible for the mechanical effects: shock wave, micro-jet, and acoustic streaming. After ultrasound is applied to a system, the mass transfer rate can be accelerated significantly in both diffusion process and convection process.

Because of above effects, ultrasound may bring a significant influence on crystallization processes. The application of power ultrasound to crystallization systems appears to offer significant potential for modifying and improving both processes and products. The main reason why ultrasound can bring such a significant influence to crystallization processes is on account of its effects on crystallization kinetics. Ultrasound can influence nucleation, crystal growth, agglomeration and breakage during crystallization processes.

CHAPTER 3

THE EFFECT OF ULTRASOUND ON HOMOGENEOUS NUCLEATION

3.1 Introduction

In homogeneous nucleation, new phase formation takes place by statistical fluctuations of solute entities clustering together in a solution where foreign microscopic particles are absent (Mullin, 2000).

The driving force for primary nucleation is the supersaturation of the crystallization system, which is defined as the difference in the chemical potential of the substance in the liquid and in the solid phase. The rate coefficient or resistance for primary nucleation is a function of the cluster-liquid interfacial tension and diffusion coefficient. The internal states at the time of nuclei formation such as size, lattice structure and purity, are also a function of the supersaturation. Ultrasound can bring influence to some parameters. Thus, nuclei can form in the solution with low supersaturation. Associated with above phenomenon, the metastable zone width and induction time will be reduced. At similar supersaturation ratio, nucleation rate will be increased after ultrasound is applied to the system.

In this chapter, barium sulphate is used as the working substance precipitated by mixing aqueous solutions of $BaCl_2$ and Na_2SO_4. Induction time, which has an inversely proportional relationship with nucleation rate, is studied to determine the ultrasonic effect on primary nucleation in a reactive crystallization process. From this, the mechanism of the ultrasonic effect on nucleation is also investigated.

3.2 Theory

The nucleation rate (B) can be expressed in terms of an empirical relationship with concentration driving force (ΔC) as follows (Myerson, 2002, Mullin, 2000),

$$B = k_N \Delta C^n \tag{3.1}$$

The nucleation coefficient (k_N) is usually described by an Arrhenius-type equation (Jones, Budz and Mullin, 1986)

$$k_N = k_{N,o} \exp\left(\frac{-E_N}{RT}\right) \tag{3.2}$$

The activation energy of nucleation, E_N, has been found to be either positive or negative for different substances (Jones, Budz and Mullin, 1986).

The induction time can be assumed to be a function of the nucleation rate and expressed as follows:

$$B = K \cdot t_{ind}^{-1} \tag{3.3}$$

Combining equation (3.1) and equation (3.3), the induction time is expressed as follows,

$$t_{ind} = K k_N^{-1} (\sigma C_s)^{-n} \tag{3.4}$$

Finally, taking the natural logarithm on both sides of equation (3.4) produces the following equation,

$$\ln(t_{ind}) = \ln\left(\frac{K}{k_N C_s^n}\right) - n\ln(\sigma) \tag{3.5}$$

From the relationship between $\ln(t_{ind})$ and $\ln(\sigma)$, the apparent nucleation order can be determined. If the nuclei are visible immediately after they are formed, the true nucleation order and the apparent order are equal. In all other cases, the true nucleation order can be found by knowing the exponent for crystal growth (g). It can be expressed as (Myerson, 2002)

$$n=(3g+n'+4)/4 \tag{3.6}$$

Normally, the value of n' is approximate and also the value of n (Nyvlt, 1985).

From classical primary nucleation theory, the rate of homogeneous nucleation can be obtained from the number of critical clusters that cross the nucleation barrier. So the nucleation rate (B_{hom}) can be expressed as (Mersmann, 2001; Mersmann and Braun, 2002):

$$B_{\text{hom}} = k' n_c Z \tag{3.7}$$

where B_{hom} is homogeneous nucleation rate, k' is the rate which clusters cross the

barrier, n_c is the number concentration of critical clusters, and Z is the imbalance factor, which relates the number of critical nuclei in the equilibrium distribution to the number in the steady-state distribution.

The critical cluster (n_c) can be described by a Boltzmann distribution.

$$n_c = n_0 \exp(-\frac{\Delta G_c}{kT}) \tag{3.8}$$

where n_0 is the number concentration of molecules in the supersaturated solution, ΔG_c is the free energy of critical cluster, k is Bolzmann constant, and T is absolute temperature.

The free energy ΔG_c can be expressed by the following equation (Mersmann, 2001).

$$\Delta G_c = \frac{16\pi\gamma_{CL}^3 V_m^2}{3(kT\ln S)^2} \tag{3.9}$$

where γ_{CL} is the surface tension, V_m is the molecular volume, and S is supersaturation ratio.

The molecular volume (V_m) is given by:

$$V_m = \frac{1}{C_C N_A} \tag{3.10}$$

where N_A is Avogadro's number, and C_C is molecular density of solid. So

$$n_c = n_0 \exp\left[-\frac{16}{3}\pi(\frac{\gamma_{CL}}{kT})^3(\frac{1}{C_C N_A})^2 \frac{1}{(\nu\ln S)^2}\right] \tag{3.11}$$

where ν is the number of moles of ions formed from one mole of electrolyte. The coefficient k' can be derived from (Mersmann, 2001):

$$k' = \frac{3}{4} n_0^{\frac{4}{3}} D_{AB} A_c \tag{3.12}$$

where D_{AB} is the diffusion coefficient, and A_c is the surface area of cluster.

The imbalance factor (Z) is given by (Mersmann, 2001):

$$Z = \sqrt{\frac{Q}{2\pi kT}} = \sqrt{\frac{\Delta G_c}{3\pi kTi_c^2}} = \frac{2}{\pi C_c N_A L_c^2}\sqrt{\frac{\gamma_{CL}}{kT}} \tag{3.13}$$

where Q is quantity of heat, i_c is the critical cluster number, and L_c is the cluster diameter.

Inserting equations (3.11), (3.12) and (3.13) into equation (3.7), the homogeneous nucleation rate can be obtained from the following equation:

$$B_{hom} = 1.5 D_{AB} (CN_A)^{7/3} \sqrt{\frac{\gamma_{CL}}{kT}} \frac{1}{C_c N_A} \exp\left[-\frac{16}{3}\pi \left(\frac{\gamma_{CL}}{kT}\right)^3 \left(\frac{1}{C_c N_A}\right)^2 \frac{1}{(\nu \ln S)^2} \right] \tag{3.14}$$

Assuming the growth time to visible size after nuclei are formed can be ignored, the induction time is normally found to have an inverse ratio relationship with nucleation rate. It can be expressed by (Mullin, 2000; Myerson, 2002):

$$t_{ind}^{-1} = KB \tag{3.15}$$

where K is a coefficient of proportionality. Combining equations (3.14) and (3.15), the following equation is obtained.

$$t_{ind}^{-1} = 1.5K\ D_{AB} (CN_A)^{7/3} \sqrt{\frac{\gamma_{CL}}{kT}} \frac{1}{C_c N_A} \times \exp\left[-\frac{16}{3}\pi \left(\frac{\gamma_{CL}}{kT}\right)^3 \left(\frac{1}{C_c N_A}\right)^2 \frac{1}{(\nu \ln S)^2} \right] \tag{3.16}$$

Taking the natural logarithm on each side of equation (3.16):

$$\ln t_{ind} = A_1 + B_1 \ln^{-2} S \tag{3.17}$$

where

$$A_1 = -\ln 1.5K\ D_{AB} (CN_A)^{7/3} \sqrt{\frac{\gamma_{CL}}{kT}} \frac{1}{C_c N_A} \tag{3.18}$$

$$B_1 = \frac{16}{3}\pi \left(\frac{\gamma_{CL}}{kT}\right)^3 \left(\frac{1}{C_c N_A \nu}\right)^2 \tag{3.19}$$

The interfacial tension (γ_{CL}) can also be determined from the following equation (Mersmann, 1990).

$$\frac{\gamma_{CL}}{kT} = K_1 (C_c N_A)^{2/3} \ln\left(\frac{C_c}{C^*}\right) \tag{3.20}$$

3.3 Experimental

Induction time experiments were carried out at 25℃. Barium sulphate, precipitated by mixing aqueous $BaCl_2$ and Na_2SO_4 solutions, was used as the working substance to study the ultrasonic effect on homogenous nucleation during reactive crystallization processes.

A 750 W ultrasonic processor with the frequency of 20 kHz was used (Cole-Parmer Instruments, Illinois, USA), which functions by emitting vibration waves and inducing cavitational voids throughout a defined volume of liquid in each experiment. The ultrasound is produced by a transducer made up of a piezoelectric sandwich and is delivered from a titanium probe with a tip of 8mm in diameter. During insonation, the probe is immersed in the liquid, resulting in the wave traveling downwards and reflecting from the base. 5 amplitudes of ultrasonic processor (21%, 31%, 41%, 51% and 61% of the maximum power) are selected to research the influence of energy value to nucleation.

An isolated vessel is employed to determine the real power input to the system by applying ultrasound with a certain amplitude value to 200ml water continuously (Kim and Lee, 2002). When the change of temperature on heat capacity is ignored, the power input of ultrasonic processor can be obtained from:

$$E = n_{water} C_p \left(\frac{dT}{dt} \right) \tag{3.21}$$

where the specific heat capacity (C_p) of water is 75.327 J mol^{-1} K^{-1} at 25°C (National Institute of Standards and Technology, 2001). Thus, from the rate of temperature increase and the heat capacity of water, the relationship between the power input and amplitude can be obtained (Figure 3.1).

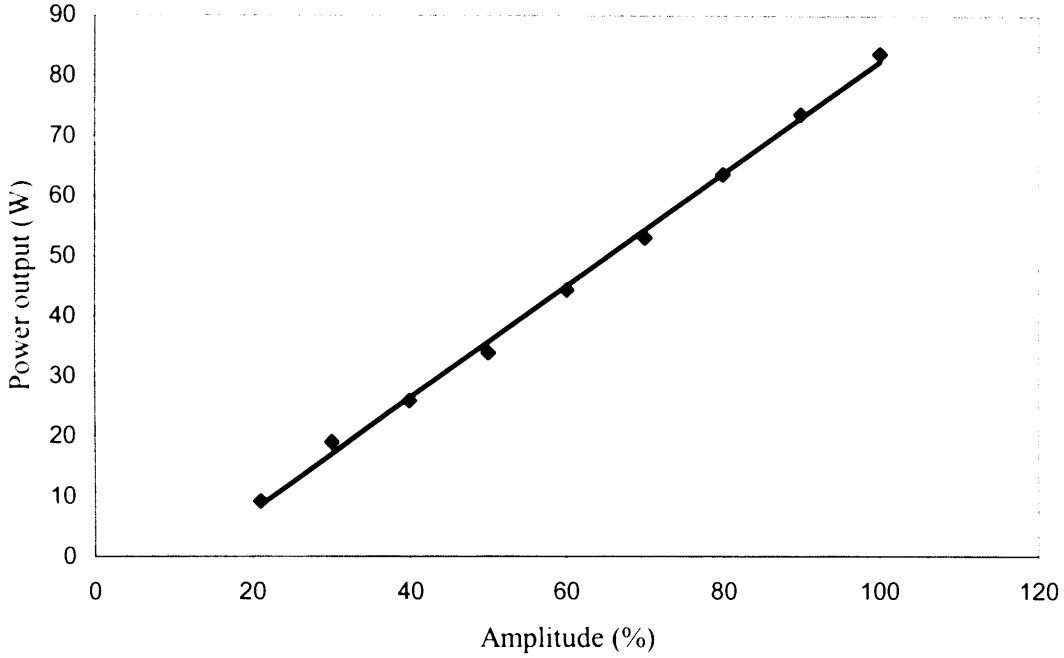

Figure 3.1 Variation of power input to the system vs amplitude

The experiments were performed in a jacketed vessel of diameter 55mm. The water-bath temperature is accurate to ±0.01K. Mixing was achieved with the use of a pitch blade impeller with an agitation rate of 400rpm. Three methods were tested to determine the induction time. They are: observing directly by the naked eye (Granberg and Ducreux, 2001), detecting the induction time by a conductivity meter (Tai and Chien, 2003) and detecting the induction time by a nephelometer (He and Oddo, 1995). A computer is connected to the instruments. The change of conductivity and turbidity, which is recorded as the change of input voltage, is collected automatically by software (SP 1300- PD from Data Translation Ltd). From the experiments, it is found that since the electrolyte solution is very dilute, it is impossible to get a stable signal from conductivity meter. It seems very unlikely that the induction time could be obtained from this method. When the induction time is observed directly by the naked eye, the

nuclei are always observed about 3 seconds later than by nephelometer. When the supersaturation is low, this delay is even more marked since it will take longer time for nuclei to grow to an observable size. So detecting the induction time by a nephelometer is considered as the more feasible method to determine induction time. Since the induction time can be obtained from change of voltage, there is no need to calibrate voltage and turbidity. The experimental apparatus is shown in Figure 3.2.

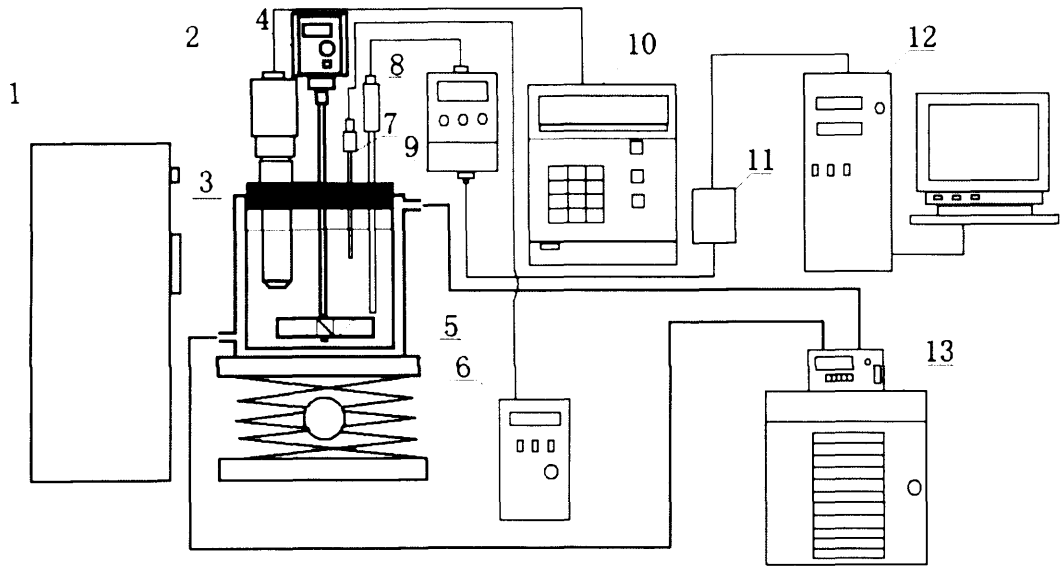

Figure 3.2 Sketch of the apparatus for measuring induction time

1. Focus lamp	**2. Ultrasonic probe**	**3. Jacketed vessel**
4. Agitation engine	**5. Iron shelf**	**6. Temperature meter**
7. The probe of temperature meter	**8. The probe of nephelometer**	**9. Nephelometer**
10. Ultrasonic processor	**11. Cable hub**	**12.Computer**
13. Water-bath		

To study the induction time, a precision electric analytical balance accurate to 1×10^{-4} g is used to measure required amounts of $BaCl_2$ and Na_2SO_4. Two 5000ml volumetric flasks are used to make 0.01M aqueous $BaCl_2$ and Na_2SO_4 solutions. In each

experiment, required amounts of $BaCl_2$ and Na_2SO_4 solutions are precisely measured and transferred by Finnpipettes to smaller volumetric flasks to make the solutions with required concentrations. After the above $BaCl_2$ solution is transferred into the vessel, the impeller and the nephelometer are switched on. After the signal of voltage becomes stable, Na_2SO_4 solution is immediately injected into the vessel. Simultaneously, the power ultrasound is run until the computer shows the induction time. During the process, the temperature is kept at 25℃ and the agitation rate is maintained at 400 rpm. The time between the initial mixing and the first observed change of voltage is defined as the induction time. The process is shown in Figure 3.3.

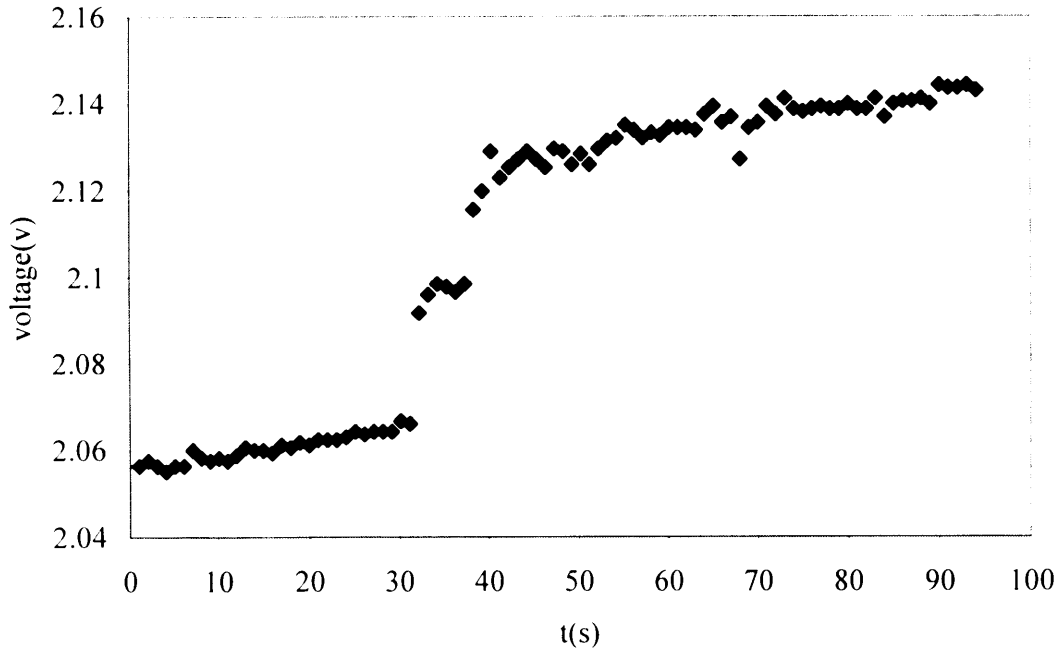

Figure 3.3 Variation of output voltage (reflecting turbidity) vs time

3.4 Results and discussion

The supersaturation level of barium sulphate can be determined from (Mullin, 2000):

$$S=(IP/K_a)^{1/\nu} \tag{3.22}$$

$$IP= C_{Ba}*C_{SO4}*(\gamma_{\pm})^2 \tag{3.23}$$

where $\gamma_{\pm}$ is the activity coefficient and K_{sp}=1.08*10^{-10}. The activity coefficient of $BaSO_4$ can be obtained from Bromley correlation (Söhnel and Garside, 1992).

$$\frac{1}{|z_+z_-|}\log\gamma_{\pm} = -0.511\frac{\sqrt{I}}{1+\sqrt{I}} + \frac{(0.06+0.6B_1)I}{(1+1.5I/|z_+z_-|)^2} + \frac{B_1 I}{|z_+z_-|} \tag{3.24}$$

For each compound, the constant B_1 is composed of ionic contributions.

$$B_1 = B_+ + B_- + \delta_+\delta_- \tag{3.25}$$

where B_+= 0.0022, B-=0, δ_+ =0.098 and δ_- =-0.40. So $K_a=K_{sp}\gamma_{\pm}$=1.040919*10^{-10}. From the above equations, the supersaturation ratio (S) can be calculated.

Generally, three measurements were made for each induction time and the average value is used. It is found that the highest deviation of different experiments is less than 3%. The results without ultrasound are compared with results from literature (He and Oddo, 1995) in Figure 3.4, which shows they are consistent. The data in Figure 3.4 shows two distinct regions. The linear portion with a lower slope at high $\ln^{-2} S$ values is due to the dominance of heterogeneous nucleation in the low supersaturation range, while the linear portion at low $\ln^{-2} S$ values is due to dominance of homogeneous nucleation in the high supersaturation range (Mullin, 2000).

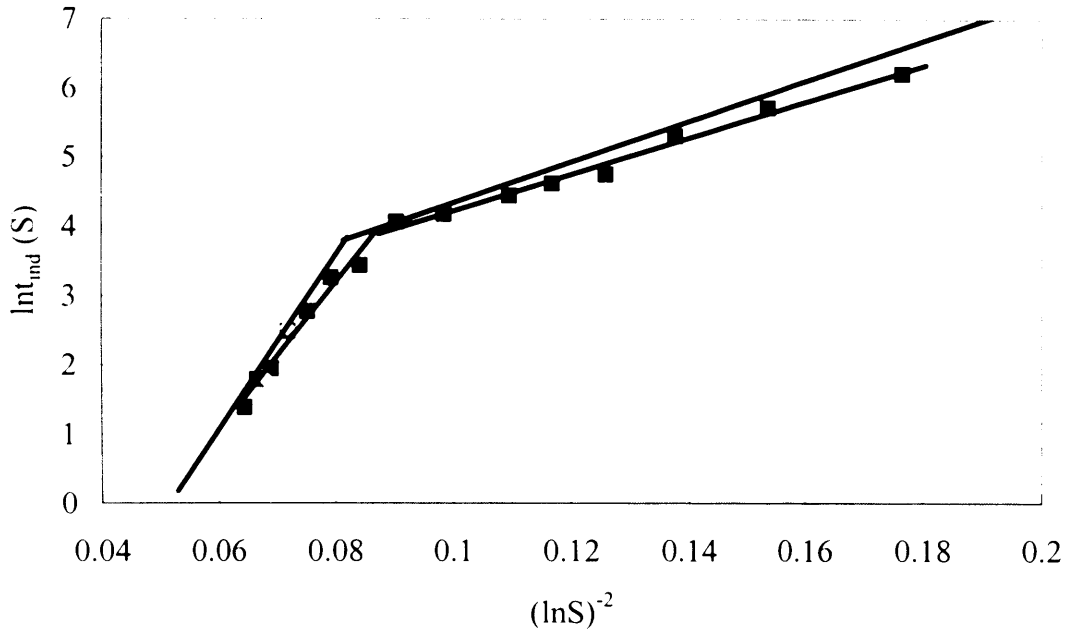

Figure 3.4 The comparison between the induction times without ultrasound from the experiments and the values from reference
(-) The value of induction time from reference
(■) The value of induction time from experiments

The result of induction time experiments with and without ultrasound is shown in Figure 3.5. The induction time decreases when supersaturation increases with and without ultrasound. From the experiments, however, it is observed that ultrasound has a significant effect in reducing the induction time, when nucleation is consistent with a predominantly homogeneous model. At the same supersaturation level, the induction time reduces with increasing ultrasonic energy.

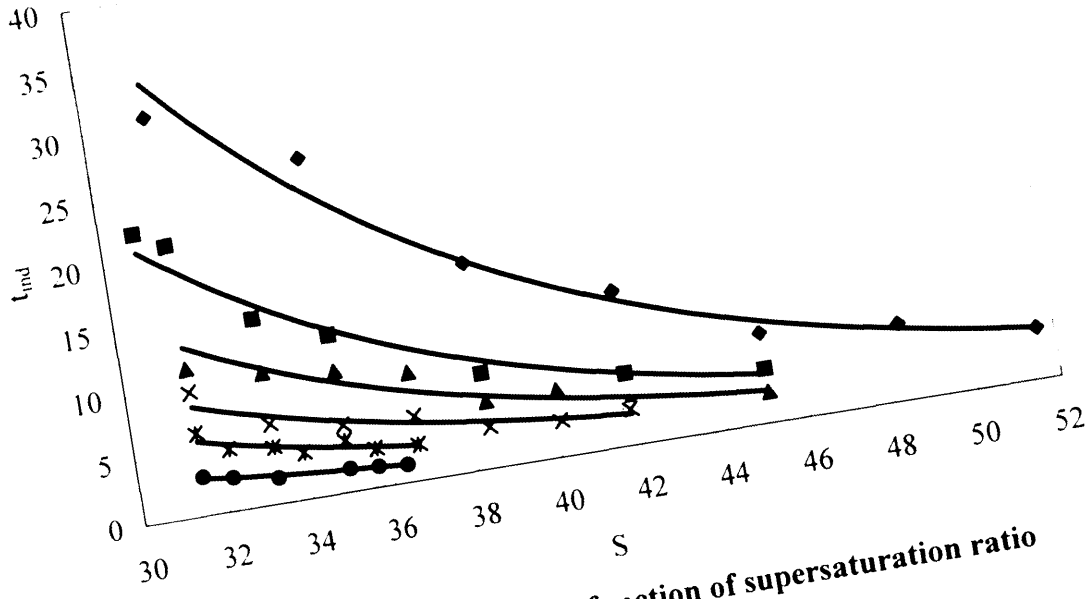

Figure 3.5 Induction time as a function of supersaturation ratio
(◆) Without ultrasound
(■) The amplitude is 21%
(▲) The amplitude is 31%
(×) The amplitude is 41%
(*) The amplitude is 51%
(●) The amplitude is 61%

The plots of $\ln(t_{ind})$ versus $\ln(\sigma)$ for experiments are shown in Figure 3.6. The slope and intercept of the straight line without ultrasound are -4.18 and 17.89 respectively. When ultrasound is applied to the system, the corresponding values for the straight line with 21% amplitude are –4.33 and 17.77; for the straight line with 31% amplitude are –4.40 and 17.66; for the straight line with 41% amplitude are –4.28 and 16.8; for the straight line with 51% amplitude are –4.71 and 17.86; for the straight line with 61% amplitude are –4.75 and 17.29. The apparent nucleation orders (n) are 4.18 without ultrasound, 4.33 with 21% amplitude, 4.40 with 31% amplitude, 4.28 with 41% amplitude, 4.71 with 51% amplitude, 4.75 with 61% amplitude. The values are very

close to each other. It can be concluded that when homogenous nucleation is predominant nucleation, ultrasound will not increase the apparent nucleation orders (n) significantly.

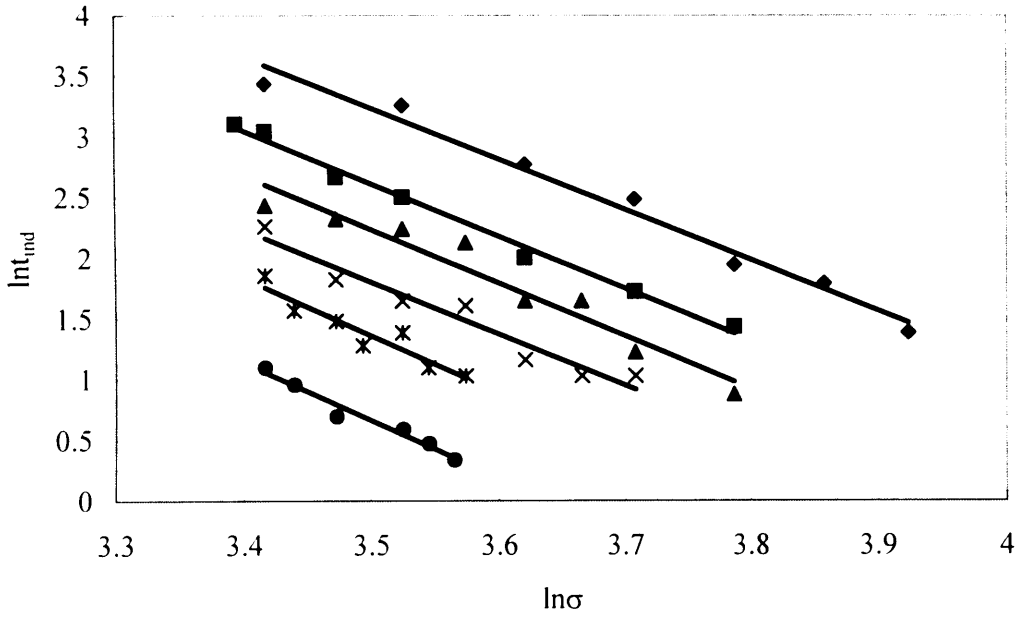

Figure 3.6 Induction time as a function of relative supersolubility
(◆) without ultrasound
(■) The amplitude is 21%
(▲) The amplitude is 31%
(╳) The amplitude is 41%
(*) The amplitude is 51%
(●) The amplitude is 61%

Since the error of experiments is unavoidable, the small deviation of slopes between experimental value and real value will cause a big difference of intercepts between experimental value and real value. To avoid this deviation, the distance between straight lines at lnσ=3.5, which is near to the middle point of all straight lines, is used to determine the ultrasonic effect on the nucleation coefficient (k_N). Comparing to k_N without power input, the k_N with 21% amplitude is increased by1.86 fold; the k_N with 31% amplitude is increased by 2.72 fold; the k_N with 41% amplitude is increased

by 4.19 fold; the k_N with 51% amplitude is increased by 6.51 fold; the k_N with 61% amplitude is increased by 13.14 fold.

Compared to the increase of apparent nucleation order (n) by ultrasound, the ultrasonic effect on nucleation coefficient (k_N) is much more significant. The increase of k_N is the main reason for the increase of nucleation rate in ultrasonic field.

To study the influence of power input on induction time, the corresponding power input at certain amplitude to the system can be obtained from Figure 3.1. When the amplitude is 21%, the power input value is 8.62W; 31%: 18.0W; 41%: 27.3W; 51%: 36.6W; 61%: 46.0W. When the temperature is fixed, the power input can work as a crystallization impetus, which is converse to the activation energy of nucleation (E_N). The activation energy of nucleation, E_N can be considered as energy barrier of crystallization. In this case, the exponent of equation (3.2) can be considered as the composition of above impetus and energy barrier. Thus, when ultrasound is applied to the system, when the temperature is kept constant, equation (3.2) can be expressed as

$$k_N = k_{N0} e^{-(E_N - E_0)/RT} \tag{3.26}$$

where k_{N0} is the value of k_N without power input, which can be expressed as

$$k_N = \left(k_{N0} / e^{E_N/RT}\right) e^{E_0/RT} \tag{3.27}$$

It is not possible to determine the real energy value, which is obtained by barium sulphate molecules from ultrasound, since water molecules will also absorb energy from ultrasound. But the energy to barium sulphate should have a direct proportion relationship with total power input, so equation (3.27) can be written as

$$k_N = ae^{bE} \tag{3.28}$$

Relationship of nucleation coefficient (k_N) and power input is shown in Figure 3.7. In Figure 3.7, Y axis is the ratio of k_N with different power input to k_N without power input. The equation from regression is:

$$k_N = 1.052e^{0.0528E} \tag{3.29}$$

From above observation, k_N has an exponential relationship with power input. The

phenomenon fits equation (3.28) well.

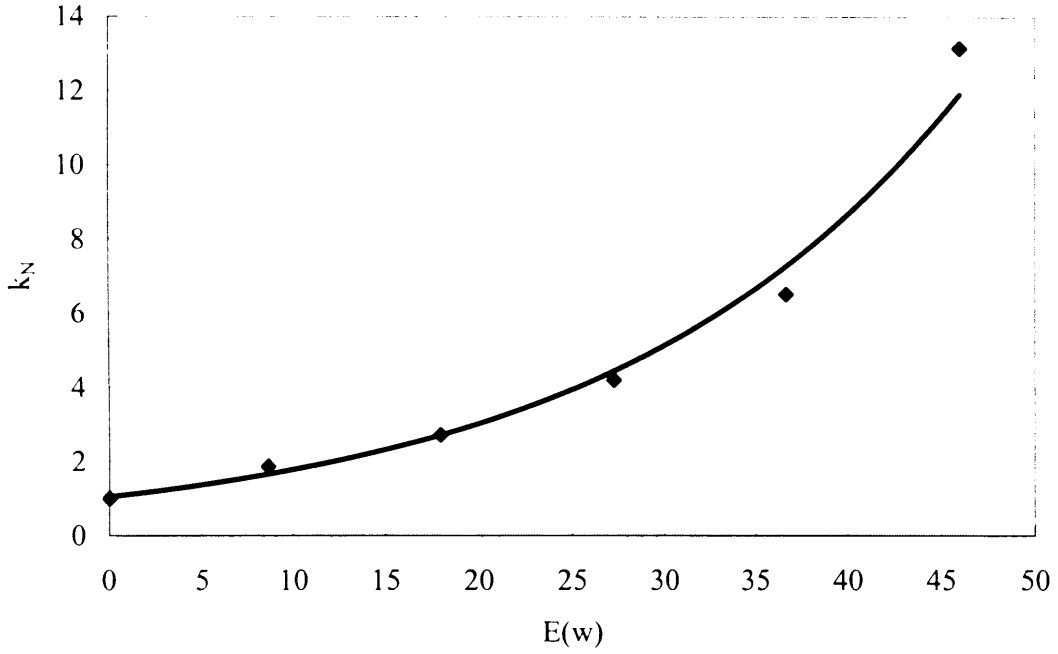

Figure 3.7 Nucleation coefficient (k_N) vs. power input

The plots of $\ln(t_{ind})$ versus $\ln^{-2}(S)$ are shown in Figure 3.8. The values of slope and intercept of the straight line without ultrasound are 106.85 and –5.34 respectively. When ultrasound is applied to the system, the corresponding values for the straight line with 21% amplitude are 104.63 and –5.80; 31%: 106.47 and –6.31; 41%: 102.06 and 6.39; 51%: 106.46 and 7.18; 61%: 106.93 and –7.92. The slopes of straight lines with different power inputs are very close to each other, but the intercepts are different. Within experimental error, it can be concluded that the straight lines of $\ln(t_{ind})$ versus $\ln^{-2}(S)$ with different power inputs are parallel with each other, but the intercepts differ.

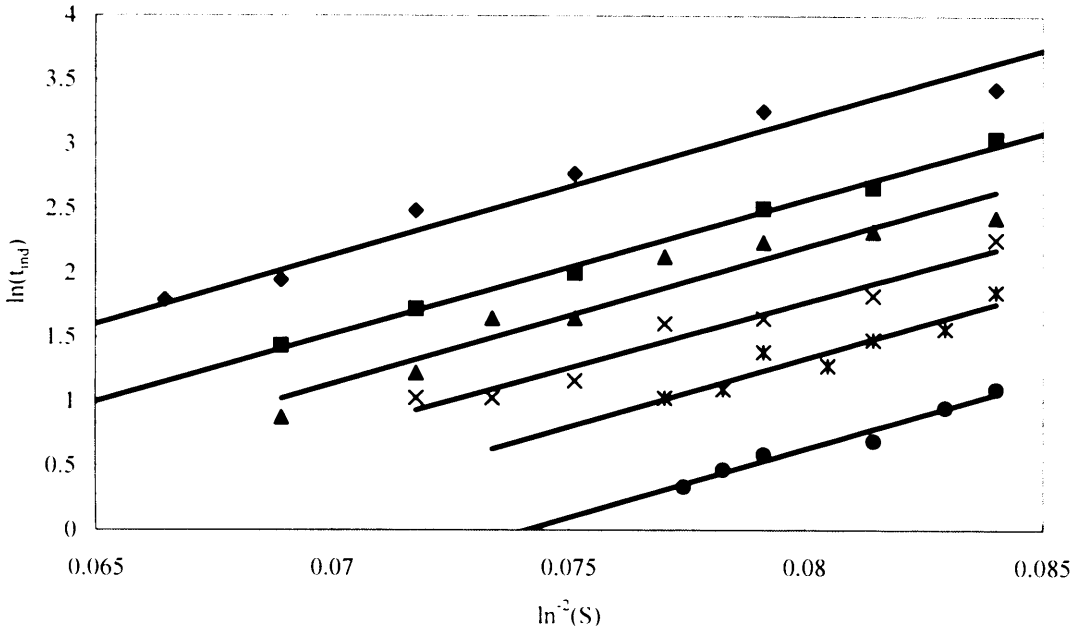

Figure 3.8 The plots of $\ln(t_{ind})$ versus $\ln^{-2}(S)$
(◆) Without ultrasound
(■) The amplitude is 21%
(▲) The amplitude is 31%
(×) The amplitude is 41%
(*) The amplitude is 51%
(●) The amplitude is 61%

The mechanism of ultrasonic radiation on homogeneous nucleation can be analyzed from equation (3.17). When ultrasound is applied to the system, the ultrasonic power will accelerate diffusion and increase D_{AB}. Ultrasound may also influence the solubility, which will influence the supersolubility as well (Thompson and Doraiswamy, 2000). If the heat cannot be removed immediately, the hot points may influence the local temperature. But if the heat dissipation is quick enough, the local temperature will remain constant and the induction time will not be influenced significantly. Some references (Tai-Quin, 1993; Lyczko and Espitalier, 2002) mention that ultrasound may influence the surface tension (γ_{CL}) when the mechanism of nucleation is predominantly

heterogeneous. In this work, we test the possibility that γ_{CL} may also be influenced when the nucleation mechanism is predominantly homogeneous.

A temperature meter is used to determine the temperature change which is caused by ultrasound. The longest time for the ultrasound to be applied to the system is 21 seconds, so this time and ultrasound with the power input as 46.0W is used to investigate the temperature change after ultrasound is applied to the system. It is found that the highest temperature change is only 0.2K. The power input and the insonation time in the experimental condition is much lower than above values, so it can be concluded that the temperature is kept approximately constant during the experiment. That is the influence of temperature on induction time can be ignored.

From equation (3.17), because the straight lines of $\ln(t_{ind})$ versus $\ln^{-2}(S)$ with different power inputs have approximately similar slopes (B_1), it can be concluded that the ultrasound has no or little influence on γ_{CL}. From equation (3.20), γ_{CL} is mainly influenced by temperature and will not be influenced by ultrasound. If the heat can be removed immediately and the temperature is constant, γ_{CL} will remain constant in ultrasonic field. In this experiment, the majority of heat released at the hot point can be removed almost immediately. The slight difference in the gradient of slopes may be the result of a small temperature increase at the hot point.

From equation (3.19), the main influence of ultrasound will be on D_{AB}. Thus the intercepts of straight lines with different ultrasonic amplitudes are different from each other. From the above observations, it can be inferred that ultrasound can accelerate diffusion and significantly shorten induction time. There are two steps in the model of the mass deposition process which is described in Figure 3.9, viz. a diffusion process, whereby solute molecules are transported from the bulk of the fluid phase through a stagnant film to the solid surface, followed by a first-order 'reaction' when the solute molecules arrange themselves into the crystal lattice (Mullin, 2000). Ultrasound has a significant effect on accelerating the diffusion process, which will increase mass

deposition rate and make more clusters cross the size barrier and then become crystal nuclei.

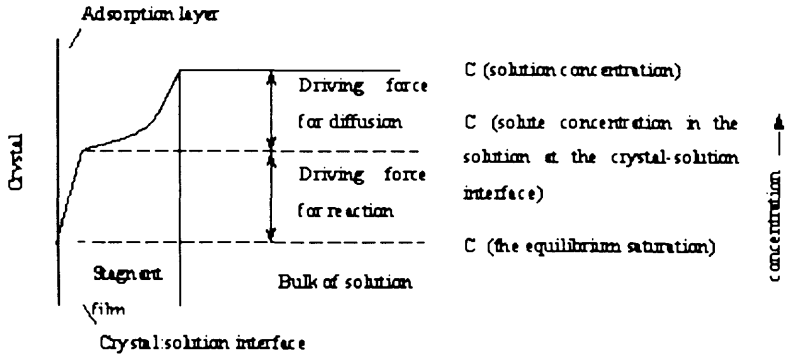

Figure 3.9 Concentration driving forces in crystallization from solution (Mullin, 2000)

From the change of intercepts, the magnitude of enhancement of D_{AB} with ultrasonic power input can be obtained. Since some experimental error is unavoidable, the small deviation of slopes between experimental value and real value will cause a large difference of intercepts between experimental value and real value. To avoid this deviation, the distance between straight lines at $\ln^{-2}(S)$=0.08, which is near to the middle point of all straight lines, is used to determine the ultrasonic effect on the D_{AB}. Since the straight lines are parallel, the distances, when $\ln^{-2}(S)$=0.08, should be equal to differences of the intercepts. Compared to D_{AB} without ultrasound, when power input is 8.62W, D_{AB} is increased by 1.89 fold; 18.0W: 2.72 fold; 27.3W: 4.19 fold; 36.6W: 6.50 fold; 46.0W: 13.12 fold.

3.5 Conclusion

The effect of ultrasound on reactive crystallization when nucleation is consistent with predominantly homogeneous model is studied by measuring the induction time. Barium sulphate is used as the working substance precipitated by mixing aqueous $BaCl_2$ and Na_2SO_4 solutions. The relationship between amplitude of ultrasonic processor and power input was determined. The experiments were carried with ultrasonic power input at 0, 8.62, 18.0, 27.3, 36.6 and 46.0W. It is observed that ultrasound has a significant effect in reducing the induction time. At a given supersaturation level, the induction time decreases with increasing ultrasonic energy.

The relationship with power input (E) and the activation energy of nucleation (E_N) is discussed. And the equation between total power input and k_N is obtained. When applying ultrasound to the system, the change in the apparent nucleation order (n) is small, however, the nucleation rate coefficient (k_N) increases significantly. From the experiments, it is observed that k_N has an exponential relationship with total power input. The above relationship fits the equation between total power input and k_N well.

The mechanism of the ultrasonic effect on homogeneous nucleation is analyzed. It is found that when temperature is kept constant, the main effect of ultrasound is to increase the diffusion coefficient (D_{AB}). Other parameters change only slightly or remain constant within the ultrasonic field. This suggests that diffusion acceleration is the main reason for the reduction of the induction time.

CHAPTER 4

THE EFFECT OF ULTRASOUND ON CLUSTER COAGULATION DURING HOMOGENEOUS NUCLEATION

4.1 Introduction

The kinetic and dynamic parameters of ultrasonic fields are such that they can cause effects at the level of atoms and molecules, quite apart from macroscopic effects. Thus, ultrasound can enable significant control of crystallization processes.

The induction time (t_{ind}) is defined as the time interval between the establishment of supersaturation and the formation of critical nuclei. Conventionally, two ways are used to interpret the experimental t_{ind}-S data. One of them is prediction of a linear relationship between $\ln(t_{ind})$ and $\ln\sigma$ (Pokrovsky, 1998). According to this method, the empirical nucleation rate constant and nucleation order can be estimated from the intercept and slope of a straight line, respectively. The second one is the prediction of a linear relationship between $\ln(t_{ind})$ and $\ln^{-2}(S)$. Qian (1997) and Tai (2003) applied a cluster coagulation model to calculate the induction time at different levels of supersaturation. From this model, the ultrasonic effect on the clusters in the solution can be investigated.

4.2 Theory

The nucleation processes are often initiated by the formation of a critical molecular cluster that is agglomerate in equilibrium with the original phase under the prevailing conditions. It can grow to a new nucleus as well as decay back into the old phase (Ford, 1996). At constant temperature, the dependence of the nucleation rate on supersaturation is related to the number of molecules in the critical cluster. While, at constant supersaturation, the dependence of the nucleation rate on temperature is related to the excess internal energy of the critical cluster (Ford, 1997).

The classical theory of homogeneous nucleation indicates that when the solution is supersaturated the monomers in solution start to coagulate and form clusters. If the size of a cluster exceeds a critical size, a nucleus forms and the subsequent growth of nucleus leads to a crystal. According to this theory, a stable nucleus is unlikely to result from the simultaneous collision of the required number of monomers since this would constitute an

extremely rare event. More likely, it could arise from sequence of bimolecular additions according to the scheme (Mullin, 2000):

$$\begin{aligned} A + A &\Leftrightarrow A_2 \\ A_2 + A &\Leftrightarrow A_3 \\ A_{g-1} + A &\Leftrightarrow A_g \text{(critical cluster)} \end{aligned} \tag{4.1}$$

The steady-state distribution of these molecular clusters can be calculated using the thermodynamic equation (Mullin, 2000):

$$n_g = n_1 \left(\frac{-\Delta G_g}{kT} \right) \tag{4.2}$$

g=2, 3, ……, g_c, where ΔG_g is overall excess free energy of formation of a g-mer; n_g and n_1 are the number concentrations of g-mers and monomers (molecules) respectively; k is the Boltzmann constant; and T is the absolute temperature.

The overall excess free energy (ΔG_g) is the sum of the surface excess free energy (ΔG_s) and the volume excess free energy (ΔG_v). ΔG_s is a positive quantity and ΔG_v is a negative quantity. ΔG_g is normally considered to be zero when nucleus radius is zero (Qian and Botsaris, 1997, Tai, Chien, 2003, Mullin, 2000, Mersmann, 2001). When it is used for equation (4.2), however, the result of n_g will be anomalous when calculating the distribution of single monomers in the bulk solution. And when it is used to calculate the distribution of clusters with other radius, the result cannot fit the experimental result well. In this work, we consider that in the bulk solution a single monomer has the smallest radius and is the fundamental composition of nuclei, so its excess free energy can be considered as zero (Mersmann, 2001). The model for overall excess free energy (ΔG_g) can then be calculated from following equation.

$$\Delta G_g = (4\pi)^{1/3} \gamma_{CL} (3gV_m)^{2/3} - (4\pi)^{1/3} \gamma_{CL} (3V_m)^{2/3} - (g-1)kT \ln S \tag{4.3}$$

where V_m is the monomer volume, γ_{CL} is the interfacial energy of the crystal, S is the supersaturation ratio of the solution, and g_c is the number of monomers in a critical cluster. After a cluster reaches the critical size, it will grow spontaneously. Clusters whose sizes are

below the critical size are termed embryos whereas those above are called nuclei.

The temporal variation of cluster size distribution can be described by the classical theory of coagulation due to Smoluchowski (1916). But, because both the rate constants for the coagulation between clusters of various sizes and the corresponding mechanism are unknown, it is not possible to evaluate the cluster size distribution directly. This problem can be circumvented by considering the mean or averaged behavior of the system. Homogeneous nucleation theories neglect cluster-cluster interactions on the assumption of a 'dilute solution theory', since it is believed that the cluster (embryo) concentrations are too low to give any appreciable coagulation rate and thus the rate to form the clusters with the size of the critical nucleus g_c (nucleation rate). It can be assumed that only the g-mers are present initially, and they coagulate to form $2g$-mers. Then the $2g$-mers coagulate to give $4g$-mers, and so on, until the critical nuclei-g_c-mers, are formed. According to this simplified model, the induction time t_{ind} can be evaluated by the following equation (Qian and Botsaris, 1997):

$$t_{ind} = \left(\frac{1}{8\pi D_{AB} r_{\bar{g}}}\right)\left(\frac{1}{n_{\bar{g}}}\right)\left(\frac{g_c}{\bar{g}} - 1\right) \tag{4.4}$$

In above equation, D_{AB} is the diffusion coefficient of clusters, $\bar{g}$ is the number of monomers in dominating clusters, r_g is the radius of $\bar{g}$-mer and $n_{\bar{g}}$ is the number concentrations of dominating clusters.

The thermodynamically stable nucleus exists when the total enthalpy ΔG_g does not change when elementary units are added or removed, that is:

$$\frac{\partial \Delta G_g}{\partial g} = 0 \tag{4.5}$$

So the critical cluster size can be derived from the classical nucleation theory by differentiating equation (4.3).

$$g_c = \frac{32\pi V_m^2 \gamma_{CL}^3}{3(kT \ln S)^3} \tag{4.6}$$

And $n_{\bar{g}}$ can be obtained by equation (4.2) and ΔG_g can be obtained from equation (4.3).

n_1 can be evaluated by the following equation:

$$n_1 = \frac{n_0}{\sum_{g=1}^{g_c} g(n_g / n_1)} \tag{4.7}$$

where n_0 is the initial number concentration of monomers, which is the initial concentration of barium sulphate in the solution after mixing reagent solutions.

Substituting equations (4.2), (4.3), (4.6), and (4.7) into equation (4.4) gives:

$$t_{ind} = \left(\frac{1}{8\pi D_{AB} r_{\bar{g}}}\right)\left\{n_1^{-1} \exp\left[-\bar{g}\ln S + \frac{\gamma_{CL}}{kT}(4\pi)^{1/3}(3\bar{g}V_m)^{2/3}\right]\right\}\left[\frac{32\pi V_m^2 \gamma_{CL}^3}{3\bar{g}(kT\ln S)^3} - 1\right] \tag{4.8}$$

From equation (4.8) the induction time (t_{ind}) can be evaluated by the contributions from diffusion, coagulation concentration, and critical nuclei size.

From equation (3.17), a plot of $\ln t_{ind}$ versus $\ln^{-2} S$ should yield a straight line, the slope of which should allow a value of the interfacial tension (γ_{CL}) to be calculated (He, Oddo, and Tomson,1995):

$$\gamma_{CL} = kT\left(\frac{3\pi a}{16V_m^2}\right)^{1/3} \tag{4.9}$$

where a is the slope of the straight line.

The Stokes-Einstein model is used to predict the diffusion coefficient (D_{AB}) in the solution.

$$D_{AB} = \frac{kT}{6\pi\mu_B r_A} \tag{4.10}$$

where T is the temperature; k is the Boltzmann constant; μ_B is the viscosity of the solvent, and r_A is radius of the diffusing magnitude. Although there are many arguments against this model, its vindication lies in its use as a model that predicts, in a number of cases, diffusion coefficients with the correct order of magnitudes (Hines and Maddox, 1985).

4.3 Results and discussion

The ultrasonic effect on diffusion coefficient (D_{AB}) is studied in the last chapter.

Compared to D_{AB} without ultrasound, when power input is 8.62W, D_{AB} is increased by 1.89 fold; 18.0W: 2.72 fold; 27.3W: 4.19 fold; 36.6W: 6.50 fold; 46.0W: 13.12 fold.

The majority of equations for prediction of the diffusion coefficient (D_{AB}) have been derived using the Stokes-Einstein equation as basic model (Bennett and Myers, 1983; Skelland, 1974). Their average errors can be up to 200-250% for non-electrolytes, and for electrolytes the errors can be even much higher (Skelland, 1974). Thus the Stokes-Einstein model can only be used to determine the order of magnitude of D_{AB}. The following data values are used: μ= 0.89cp (Hines and Maddox, 1985), k=1.38 × 10^{-23}J/K, and V_{water}=18cm^3/molecule, V_{BaSO4}=51.86 cm^3/molecule, which is calculated from $M_w/\rho N_A$, using M_w=233.3906g/mol, ρ=4.5g/cm^3, and N_A=6.02×10^{23} (Tai and Chien, 2003). Thus D_{AB} presently is 6.20×10^{-10}m^2/s. The experimental value of D_{AB} is determined from the result of the experiment without ultrasound at lowest superasturation ratio, which has longest induction time, so the experimental error is minimal. The second term (coagulation concentration) and third term (critical nuclei size) can be obtained through simulation, while t_{ind} is determined from experiment. It is found that with the assumption that there are 3 monomers in the dominating clusters in the bulk of solution, D_{AB} is 3.65×10^{-10}m^2/s, which is of comparable order of magnitude of D_{AB} derived from Stokes-Einstein model. When the dominating clusters are assumed to have more or fewer monomers, such as 1, 2, 4, 5, 6, ……, the order of magnitude of D_{AB} deviates from the prediction of the Stokes-Einstein model. Thus 3.65×10^{-10}m^2/s is used in other simulations and D_{AB} with different power inputs can be obtained. They are 6.90 × 10^{-10}m^2/s with 8.62W, 9.93×10^{-10}m^2/s with 18.0W, 1.52×10^{-9}m^2/s with 27.3W, 2.37×10^{-9}m^2/s with 36.6W, and 4.19×10^{-9} m^2/s with 46.0W.

From equation (4.9), the interfacial tension (γ_{CL}) can be evaluated. The estimated value of γ_{CL} is 62.13mJ/m^2 without ultrasound; when power input is 8.62W, γ_{CL} is 61.70 mJ/m^2; when power input is 18.0W, γ_{CL} is 62.06 mJ/m^2; when power input is 27.3W, γ_{CL} is 61.20 mJ/m^2; when power input is 36.6W, γ_{CL} is 62.06 mJ/m^2; when power input is 46.0W, γ_{CL} is 62.15 mJ/m^2. The slight difference of γ_{CL} with different power inputs may be the result of the experimental error of different experiments. Because

this deviation is unavoidable in each experiment, the average value of interfacial tension (γ_{CL}), which is 61.89 mJ/m^2, will be used in the following calculation. It is found that the highest deviation of different γ_{CL} is 1.1%. In the study of He (He, Oddo and Tomson, 1995), γ_{CL} is 93.4 mJ/m^2 when NaCl is lower than 0.003M and 79.2 mJ/m^2 when NaCl is higher than 1.0M. Other literature values of interfacial tension range from 38 mJ/m^2 to 150 mJ/m^2 (He, Oddo and Tomson, 1995; Carosso and Pelizzetti, 1984). It is found that the interfacial tension depends on the supersaturation range investigated and the concentration of sodium chloride. The quality of water may also bring a marked influence to the result of experiments. γ_{CL} obtained in this study are in fair agreement with the reported literature values.

The change of overall excess free energy (ΔG_g) with the number of monomers in clusters (g) in solution is shown in Figure 4.1. The change in ΔG_g with respect to g passes through a maximum value where $d\Delta G / dg = 0$. This maximum value, ΔG_{crit} corresponds to the critical nucleus. The behavior of a newly created crystalline lattice structures in a supersaturated solution depends on its size; it can either grow or redissolve. But the process which it undergoes should result in the decrease in the free energy of the particle. The critical nucleus represents the minimum size of a stable nucleus. Particles smaller than it will dissolve and particle larger than it will continue to grow (Mullin, 2000). From Figure 4.1, it is found that at the same value of g, ΔG_g decreases with the increase of supersaturation ratio. Thus it will be easier for clusters with multiple monomers to exist in the solution with high supersaturation. The number of monomers in critical nucleus also decreases with supersaturation ratio. This is one of the reasons why nucleation rate increases with supersaturation.

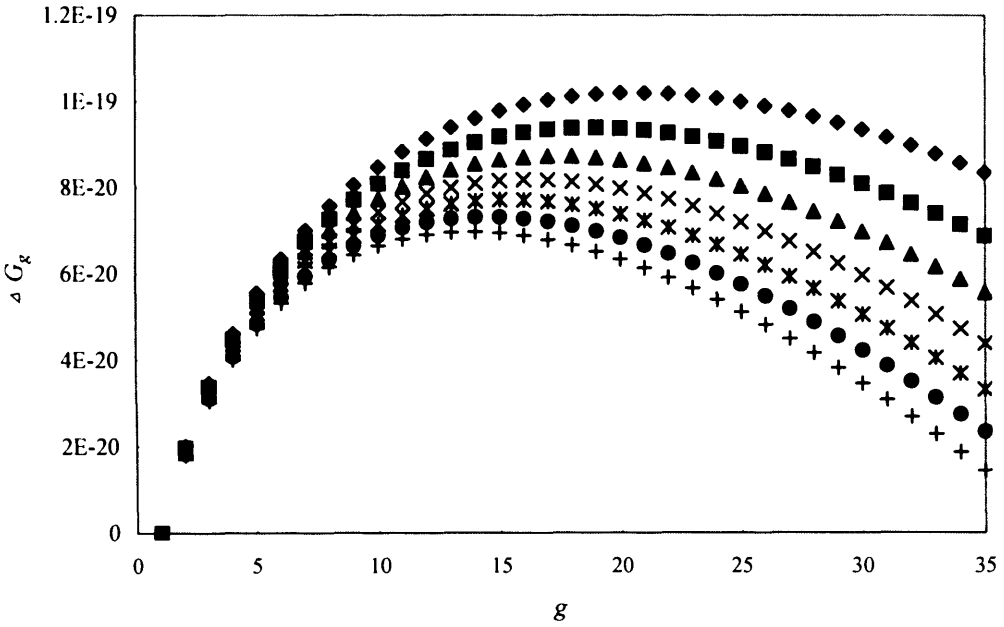

Figure 4.1 ΔG_g versus g in the solution
(◆) with the supersaturation ratio of 31.49
(■) with the supersaturation ratio of 34.99
(▲) with the supersaturation ratio of 38.42
(×) with the supersaturation ratio of 41.79
(*) with the supersaturation ratio of 45.11
(●) with the supersaturation ratio of 48.37
(+) with the supersaturation ratio of 51.59

Figure 4.2 illustrates the experimental data of induction time obtained from experiments and the theoretical curves calculated from equation (4.8) using assumed values of parameter $\bar{g}$. Both the experimental and theoretical results show that the induction time decreases with increasing supersaturation ratio at constant temperature. The total absolute deviation between the theoretical and experimental induction times (ε) is used to choose the best values for $\bar{g}$. ε can be obtained from equation (4.11) (Tai and Chien, 2003).

$$\varepsilon = \sum \left| t_{ind,\exp} - t_{ind,the} \right| / t_{ind,\exp} \tag{4.11}$$

The values of calculated ε for various $\bar{g}$ without ultrasound are listed in Table 4.1. It is found that $\bar{g} = 3$ gives the smallest value of ε . The experimental data with theoretical curves of induction time are also shown in Figure 4.2. The theoretical curve plotted by the parameter $\bar{g} = 3$ are closest to the experimental points. According to equation (4.8), the increase in induction time at higher supersaturation is mainly caused by the higher coagulation concentration of clusters and the smaller critical nuclei size.

After ultrasound is applied to the system, the experimental results show that the induction times decrease with energy increase at constant supersaturation. The predicted value and the total absolute deviation (ε) at various power inputs are listed in Tables 4.2, 4.3, 4.4, 4.5, 4.6.

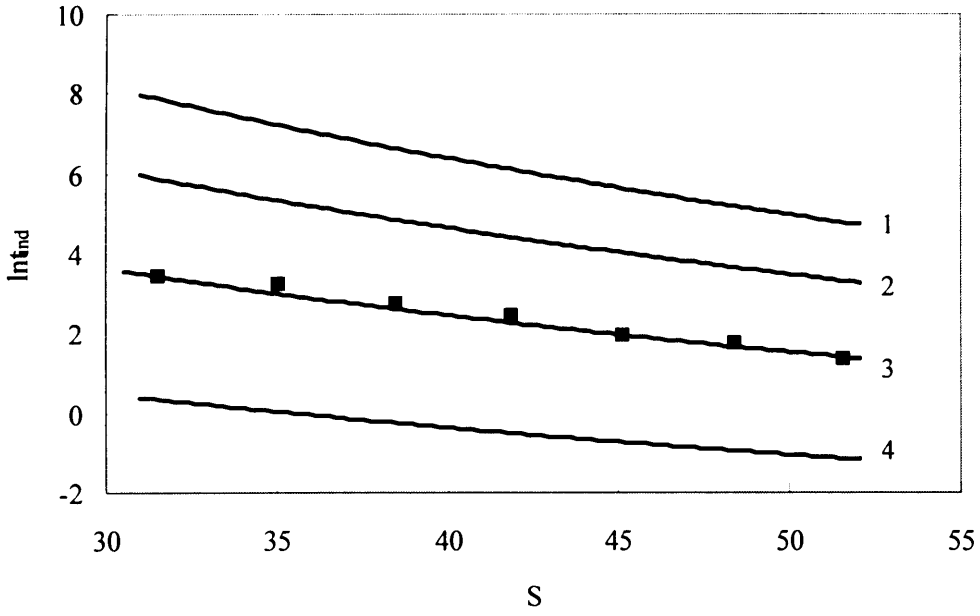

Figure 4.2 Induction time as a function of supersaturation without ultrasound

(■) The experimental data

(curve1) theoretical curve by using $\bar{g}$ =5

(curve2) theoretical curve by using $\bar{g}$ =4

(curve3) theoretical curve by using $\bar{g}$ =3

(curve4) theoretical curve by using $\bar{g}$ =2

Table 4.1 A comparison of the calculated ε for various $\bar{g}$ without ultrasound

S	Calculated induction time(s)						
	$t_{ind,\exp}(s)$	$\bar{g}$=1	$\bar{g}$=2	$\bar{g}$=3	$\bar{g}$=4	$\bar{g}$=5	$\bar{g}$=6
31.49	31	0.023	1.43	31	356.21	2626.17	13838.27
34.99	26	0.018	1.03	20.11	206.62	1360.66	6397.13
38.42	16	0.015	0.78	13.70	127.32	757.79	3215.91
41.79	12	0.013	0.60	9.70	82.36	447.25	1729.29
45.11	7	0.011	0.48	7.09	55.44	276.83	982.68
48.37	6	0.0098	0.39	5.33	38.58	178.30	584.75
51.59	4	0.0086	0.32	4.09	27.62	118.76	361.80
ε	0	6.99	6.60	0.71	48.51	313.64	1358.83

Table 4.2 A comparison of the calculated ε for various $\bar{g}$ with the power input of 8.62W

S		Calculated induction time(s)					
	$t_{ind,\exp}(s)$	$\bar{g}$=1	$\bar{g}$=2	$\bar{g}$=3	$\bar{g}$=4	$\bar{g}$=5	$\bar{g}$=6
30.79	22.3	0.013	0.81	18.01	211.98	1601.22	8646.32
31.49	21	0.012	0.76	16.40	188.47	1389.51	7321.83
33.25	14.4	0.011	0.64	13.12	142.33	990.10	4920.08
34.99	12.2	0.0097	0.55	10.64	109.32	719.92	3384.73
38.42	7.4	0.0081	0.41	7.25	67.37	400.95	1701.54
41.79	5.6	0.0069	0.32	5.13	43.58	236.64	914.97
45.11	4.2	0.0059	0.25	3.75	29.34	146.47	519.94
ε	0	6.99	6.66	0.84	54.20	390.05	1865.61

Table 4.3 A comparison of the calculated ε for various $\bar{g}$ with the power input of 18.0W

S	Calculated induction time(s)						
	$t_{ind,\exp}(s)$	$\bar{g}$ =1	$\bar{g}$ =2	$\bar{g}$ =3	$\bar{g}$ =4	$\bar{g}$ =5	$\bar{g}$ =6
31.49	11.4	0.0084	0.52	11.40	130.96	965.50	5087.60
33.25	10.2	0.0075	0.44	9.12	98.90	687.98	3418.73
34.99	9.4	0.0068	0.38	7.39	75.96	500.24	2351.89
36.71	8.4	0.0062	0.33	6.07	59.23	370.33	1652.06
38.42	5.2	0.0056	0.29	5.04	46.81	278.60	1182.32
40.11	5.2	0.0052	0.25	4.22	37.44	212.64	860.45
41.79	3.4	0.0048	0.22	3.57	30.28	164.43	635.77
45.11	2.4	0.0041	0.18	2.61	20.38	101.78	361.28
ε	0	7.99	7.59	0.95	61.92	426.68	1950.69

Table 4.4 A comparison of the calculated ε for various $\bar{g}$ with the power input of 27.3W

S	Calculated induction time(s)						
	$t_{ind,\exp}(s)$	$\bar{g}$ =1	$\bar{g}$ =2	$\bar{g}$ =3	$\bar{g}$ =4	$\bar{g}$ =5	$\bar{g}$ =6
31.49	9.6	0.0054	0.34	7.40	85.02	626.77	3302.69
33.25	6.2	0.0049	0.29	5.92	64.20	446.61	2219.32
34.99	5.2	0.0044	0.25	4.80	49.31	324.74	1526.76
36.71	5	0.0035	0.18	3.40	33.21	207.62	926.22
38.42	3.2	0.0037	0.19	3.27	30.39	180.86	767.52
40.11	2.8	0.0027	0.13	2.21	19.63	111.49	451.16
41.79	2.8	0.0031	0.14	2.32	19.66	106.74	412.72
ε	0	6.99	6.68	1.08	51.86	368.76	1722.21

Table 4.5 A comparison of the calculated ε for various $\bar{g}$ with the power input of 36.6W

S	Calculated induction time(s)						
	$t_{ind,\exp}(s)$	$\bar{g}$=1	$\bar{g}$=2	$\bar{g}$=3	$\bar{g}$=4	$\bar{g}$=5	$\bar{g}$=6
31.49	6.4	0.0035	0.22	4.77	54.80	404.03	2128.96
32.204	4.8	0.0034	0.20	4.35	48.87	351.89	1810.52
33.25	4.4	0.0031	0.19	3.82	41.38	287.89	1430.61
33.95	4	0.0030	0.17	3.50	37.17	252.86	1228.53
34.99	3.6	0.0028	0.16	3.09	31.79	209.33	984.17
35.68	3	0.0027	0.15	2.86	28.73	185.23	852.48
36.71	2.8	0.0026	0.14	2.54	24.78	154.97	691.32
ε	0	6.99	6.69	0.89	57.70	433.32	2139.56

Table 4.6 A comparison of the calculated ε for various $\bar{g}$ with the power input of 46.0W

S	Calculated induction time(s)						
	$t_{ind,\exp}(s)$	$\bar{g}$=1	$\bar{g}$=2	$\bar{g}$=3	$\bar{g}$=4	$\bar{g}$=5	$\bar{g}$=6
31.49437	3	0.00174	0.109	2.36	27.15	200.16	1054.75
32.19848	1.8	0.00166	0.10172	2.16	24.21	174.34	896.98
33.2496	2.6	0.00156	0.0922	1.89	20.50	142.63	708.76
34.98834	2	0.00141	0.0789	1.53	15.75	103.71	487.59
35.67937	1.6	0.00136	0.0744	1.41	14.23	91.77	422.34
36.36791	1.4	0.00130	0.0702	1.31	12.89	81.42	366.99
ε	0	5.99	5.74	1.099	50.36	379.80	1886.40

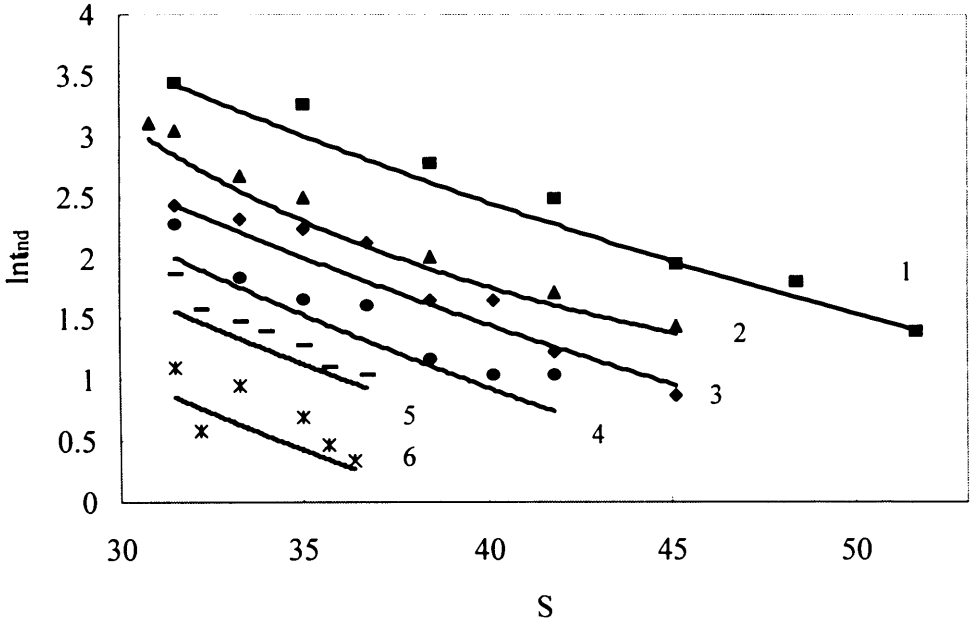

Figure 4.3 Induction time as a function of supersaturation with various power inputs

(■) The experimental data without ultrasound
(▲) The experimental data with the power input of 8.62W
(◆) the experimental data with the power input of 18.0W
(●) the experimental data with the power input of 27.3W
(*) the experimental data with the power input of 36.6W
(–) The experimental data with the power input of 46.0W
(curve1) theoretical curve by using $\bar{g}$ =3 without ultrasound
(curve2) theoretical curve by using $\bar{g}$ =3 with the power input of 8.62W
(curve3) theoretical curve by using $\bar{g}$ =3 with the power input of 18.0W
(curve4) theoretical curve by using $\bar{g}$ =3 with the power input of 27.3W
(curve5) theoretical curve by using $\bar{g}$ =3 with the power input of 36.6W
(curve6) theoretical curve by using $\bar{g}$ =3 with the power input of 46.0W

And Figure 4.3 shows that the experimental and theoretical induction time as the function of supersaturation at six different levels of ultrasonic power inputs. It is found that the total absolute deviation (ε) has a smallest value for $\bar{g}$ =3 at different power input

values. Therefore, the best value of $\bar{g}$ for calculating all induction times is 3. It is found that although ε has smallest value at $\bar{g}$=3, the experimental results of induction time are higher than theoretical curves when the power inputs are 18.0W, 27.3W, 36.6W, and 46.0W. The reason for above phenomenon is that only the value of dominating clusters is considered in the model. In reality, however, clusters with different monomer numbers may exist in real solution. So the dominating clusters can only be a proportion of all clusters. That is the increase of clusters with other monomer numbers will cause the deviation between the experimental results and the predicted curve obtained when only dominating clusters is considered. From the model, when the number of monomers in clusters increases, the induction time also increases. So it can be concluded that although the number of monomers in dominating clusters ($\bar{g}$) is 3 in different power inputs, the number concentrations of bigger clusters increase when the power input increases. But the increase of the concentration of bigger clusters is not as significant as the increase of diffusion coefficient. Clusters with 3 monomers are predominant in the solution.

4.4 Conclusion

When nucleation is predominantly homogeneous, the interfacial tension is estimated as 61.89 mJ/m^2 by employing the classical nucleation theory. The ultrasonic effect on the clusters in solution is analyzed by a cluster coagulation model. It is found that the number of monomers in dominating clusters ($\bar{g}$) is 3 for different power inputs. A theoretical analysis of the total absolute deviation (ε) shows that the number concentration of largest clusters increases slowly with the increase of power input. But compared to the increase of diffusion coefficient (D_{AB}), this effect is very small. In this experimental condition, analysis of the induction time is consistent with clusters having 3 monomers being predominant in the solution.

CHAPTER 5

THE EFFECT OF ULTRASOUND ON THE DIFFUSION COEFFICIENT

5.1 Introduction

The rate coefficient or resistance for primary nucleation is a function of the cluster-liquid interfacial tension and diffusion coefficient. The diffusion coefficient (D_{AB}) increases with ultrasonic power applied to the crystallization system (Sivakumar & Rao, 2003; Mitragotri, 2001; Moholkar & Warmoeskerken, 2004).

When ultrasound propagates through a liquid medium, its power not only is a driving force for mass transfer, but also initiates an important phenomenon known as cavitation. Cavitational bubbles forms during the negative-pressure period of the sound wave. When a cavitational bubble implodes, high pressure with a powerful shock wave will be released to fluid medium. The relationship between power input and diffusion coefficient is established in this chapter.

5.2 Theory

Assuming the molecule of solute is spherical, when it moves slowly in solution, the resistance can be obtained from Stokes' law (Hines, Maddox, 1985; Cussler, 1997):

$$-F_r = 6\pi\mu_B r_A u_A \tag{5.1}$$

where r_A is the radius of solute molecule, μ_B is the viscosity of solvent, u_A is the net velocity of solute molecule in the stagnant film between the bulk of the fluid phase and the solid surface, and F_r is the resistance of diffusion due to fluid viscosity. This force was taken by Einstein (Cussler, 1997) to be opposed by the chemical potential gradient. The chemical potential gradient defined per molecule is often described as a "virtual force", a thermodynamic parallel to mechanical or electrostatic forces. Because the solution is dilute, it is assumed that it is ideal.

$$\mu_A = \mu_A^0 + kT \ln x_A$$

$$= \mu_A^0 + kT \ln \frac{C_A}{C_A + C_B} = \mu_A^0 + kT \ln C_A - kT \ln C_B \qquad (5.2)$$

where μ_A is the chemical potential and x_A is the mole fraction of solute. Since the solvent concentration C_B far exceeds the solute concentration C_A, then C_B is approximately constant. Differentiating each side of equation (5.2) gives:

$$d\mu_A = kTd \ln C_A \qquad (5.3)$$

Dividing each side of the equation by dz, the chemical potential gradient, the impetus for diffusion (F_c), is obtained (Cussler, 1997).

$$F_c = \frac{d\mu_A}{dz} = \frac{kT}{C_A} \frac{dC_A}{dz} \qquad (5.4)$$

After ultrasound is applied to the crystallization system, its power will be a further impetus for diffusion in the stagnant film. Assuming each solute molecule gains energy E_{0A} from ultrasound and the velocity of molecule at the solid surface is zero, then E_{0A} is all consumed in the diffusion process from the bulk of the fluid phase to crystal surface. Thus the amount of energy dE_{0A} that is consumed to move molecule a distance (dz) will be product of impetus (F_u) and distance (dz).

$$dE_{0A} = F_u dz \qquad (5.5)$$

In the diffusion process, the resistance from Stokes' law will have an equilibrium relationship with the impetus from the chemical potential gradient and ultrasonic energy.

$$-F_r = F_u + F_c \qquad (5.6)$$

Inserting equations (5.1), (5.4), (5.5) into equation (5.6) gives:

$$u_A = -\frac{\frac{kT}{C_A}\frac{dC_A}{dz} + \frac{dE_{0A}}{dz}}{6\pi\mu_B r_A} \qquad (5.7)$$

Equation (5.7) can be transformed to following equation:

$$u_A = -\frac{\left(kT + C_A \frac{dE_{0A}}{dC_A}\right)}{6\pi\mu_B r_A C_A} \frac{dC_A}{dz} \tag{5.8}$$

Thus the diffusive flux of solute can be expressed as:

$$N'_A = u_A C_A = -\frac{\left(kT + C_A \frac{dE_{0A}}{dC_A}\right)}{6\pi\mu_B r_A} \frac{dC_A}{dz} \tag{5.9}$$

which has a similar form as Fick's Law. So D_{AB} in an ultrasonic field can be expressed in following equation.

$$D_{AB} = \frac{\left(kT + C_A \frac{dE_{0A}}{dC_A}\right)}{6\pi\mu_B r_A} \tag{5.10}$$

The energy that is consumed by resistance during the mass transfer from the bulk of the liquid to crystal surface is taken as the energy barrier, because only if the molecular energy is higher than the energy consumed can the mass transfer rate be maintained. So the relationship between energy, temperature and concentration is given by Arrhenius equation (Mersmann, 2001).

$$E_{Ab} = -R\frac{d(\ln C_A)}{d(1/T)} \tag{5.11}$$

where E_{Ab} is the energy barrier for mass transfer and R is ideal gas constant.

Integrating equation (5.11) gives:

$$\frac{E_{Ab}}{R}\frac{T - T_0}{T_0 T} = \ln\frac{C_A}{C_{A0}} \tag{5.12}$$

where T_0 is the initial solution temperature and C_{A0} is the initial concentration of solute.

$$C_{Ao} e^{\frac{E_{Ab}}{RT}\left(\frac{T-T_0}{T_0}\right)} = C_A \tag{5.13}$$

Differentiating:

$$\frac{dE_{Ab}}{dC_{A0}} = \frac{RTT_0}{C_{A0}(T - T_0)} e^{-\frac{E_{Ab}}{RT}\left(\frac{T-T_0}{T_0}\right)} \tag{5.14}$$

Assuming that the system is in equilibrium, the value of dE_{0A}/dC_A should be

equal to the value of dE_{Ab} / dC_A. And

$$E_{Ab} = -E_{A0} \tag{5.15}$$

That is all the kinetic energy of molecule (E_{A0}) will be consumed to overcome the energy barrier (E_{Ab}) during mass transfer. So

$$\frac{dE_{A0}}{dC_{A0}} = \frac{RTT_0}{C_{A0}(T-T_0)} e^{\frac{E_{A0}}{RT}(\frac{T-T_0}{T_0})} \tag{5.16}$$

In a solution, the solute and solvent molecules can only absorb a part of energy from ultrasound. That is the solute and solvent molecules will receive an amount of energy k_1E, where k_1 is a coefficient of proportionality and E is the ultrasonic power input. Further, assuming that all the solute molecules receive the same amount of energy and all the solvent molecules get the same amount of energy, respectively, then, since there are only two kinds of molecules in the system, the molecular energy of solute from ultrasound can be expressed as:

$$E_{0B} = k_2 E_{0A} \tag{5.17}$$

where k_2 is a coefficient of proportionality. And the solute concentration (C_A) and the solvent concentration (C_B) are related by:

$$C_B = k_3 C_A \tag{5.18}$$

where k_3 is another coefficient of proportionality. By conservation, the energy absorbed by solute and solvent molecules (k_1E) is equal to the sum of energy gained by solute molecules ($N_A C_A V E_{0A}$) and energy gained by solute molecules ($N_A k_2 E_{0A} k_3 C_A V$).

$$k_1 E = N_A C_A V E_{0A} + N_A k_2 E_{0A} k_3 C_A V \tag{5.19}$$

Then

$$E_{0A} = \frac{k_1}{N_A C_A V(1+k_2 k_3)} E \tag{5.20}$$

Since the volume of solution will not change during crystallization, $\frac{k_1}{N_A V(1+k_2 k_3)}$

will be constant during the diffusion process.

$$k_4 = \frac{k_1}{N_A V(1+k_2 k_3)} \tag{5.21}$$

and equation (5.10) can be expressed as:

$$D_{AB} = \frac{kT + k_4 \dfrac{RTT_0}{C_{A0}(T-T_0)} e^{\frac{K_4 E}{RT}\left(\frac{T-T_0}{T_0}\right)}}{6\pi\mu_B r_A} \tag{5.22}$$

This equation can be transformed to enable calculation of the diffusity in the presence of ultrasound.

$$D_{AB} = \frac{kT + k_5 e^{k_6 E}}{6\pi\mu_B r_A} \tag{5.23}$$

where k_5 and k_6 are also coefficients of proportionality.

From equation (5.23), it can be seen that the diffusion coefficient (D_{AB}) is also determined by the gradient of solute molecular energy with solute concentration distribution in the stagnant film (dE_{0A}/dC_A).

The Stokes-Einstein model of diffusion processes in liquids neglects some factors, such as the viscosity change of the solution after solute is added and the association effect in solution, and is thus liable to error. Nevertheless, it is popularly used as the basic model to predict liquid diffusion coefficients (Skelland, 1974; Bennett and Myers, 1983). Normally, the basic form to predict the diffusion coefficient in real systems without extra power input is (Skelland, 1974; Hines and Maddox, 1985):

$$D_{AB} = K' \frac{T}{\mu V_A^{1/3}} \tag{5.24}$$

So the corresponding equation for diffusion with ultrasonic power input is:

$$D_{AB} = K' \frac{\left(T + k_7 e^{k_6 E}\right)}{\mu V_A^{1/3}} \tag{5.25}$$

where k_7 is also a coefficient of proportionality. And by an Arrhenius-type equation (Hines and Maddox, 1985):

$$D_{AB} = D_{AB0} e^{(-E_{Ab}/RT)} \tag{5.26}$$

where D_{AB0} is the initial diffusion coefficient.

5.3 Experimental

The influence of ultrasonic power input on diffusion coefficient can be obtained from the experiment of induction time with barium sulphate as the working substance precipitated by mixing aqueous $BaCl_2$ and Na_2SO_4 solutions. The influence of solution viscosity on diffusion coefficient is studied by the experiments with the organic materials spectinomycin hydrochloride, roxithromycin and sucrose as substances. The solutions with above substances have different viscosity.

5.3.1 Materials

Induction period experiments were carried out at 25℃. Three typical organic substances viz. spectinomycin hydrochloride, roxithromycin and sucrose having high purity were used as working substances to study the ultrasonic effect on primary nucleation in anti-solvent processes. For spectinomycin hydrochloride, water is used as solvent and acetone is used as anti-solvent. For roxithromycin, acetone is used as solvent and water is used as anti-solvent. While for sucrose, water is used as solvent and ethanol is used as anti-solvent. Acetone and ethanol were used without further purification and the water was de-ionized, distilled, and filtered (0.2 μ m). The solubility of spectinomycin hydrochloride, roxithromycin and sucrose were measured by a dynamic method modeled using the following equations, respectively.

$$C_{SH/W} = 0.17 e^{-1.40 C_{A/W}} \tag{5.27}$$

where $C_{SH/W}$ is the ratio of the weight of spectinomycin hydrochloride and the volume of water (g/ml), $C_{A/W}$ is the ratio of the volume of acetone and the volume of water

(ml/ml).

$$C_{R/A} = 0.20e^{-3.15C_{W/A}} \tag{5.28}$$

where $C_{R/A}$ is the ratio of the weight of roxithromycin and the volume of water (g/ml), $C_{W/A}$ is the ratio of the volume of acetone and the volume of water (ml/ml).

$$C_{S/W} = 0.42e^{-1.48C_{E/W}} \tag{5.29}$$

where $C_{S/W}$ is the ratio of the weight of sucrose and the volume of water (g/ml), $C_{E/W}$ is the ratio of the volume of ethanol and the volume of water (ml/ml).

5.3.2 Apparatus

The experiments were performed in a round-bottomed tube of 40mm diameter. The experimental apparatus is show in Figure 5.1. A jacketed vessel controls the temperature in the tube with an electric contact thermometer inserted in the tube. The water-bath temperature is accurate to ±0.1K. The temperature in the vessel was measured from the mercury thermometer at the top of vessel. The estimated accuracy is about ± 0.05K. Mixing was achieved with the use of a magnetic stirrer with an agitation rate of 750 rpm. The induction time was detected by a beam of He–Ne laser with a wavelength of 531nm continuously throughout the solution. A detector, which is located on the opposite side of the vessel and connects an X–Y recorder, measures the transmitted laser light intensity versus time. The crystal nuclei will cause the changes of light intensity and the detector will transfer this change to electric signal, which will be printed out by recorder.

The ultrasonic equipment with 20kHz and 500W (Ningbo Scientz Technology Co. Ltd., China) functions by emitting vibration waves and induces cavitation voids throughout a defined volume of liquid in our experiment. The ultrasound was produced by a transducer made up of a piezoelectric sandwich and was delivered from a titanium

probe with a tip of 8mm in diameter. During insonation, the probe was immersed in the liquid with the wave traveling downwards and reflecting upwards.

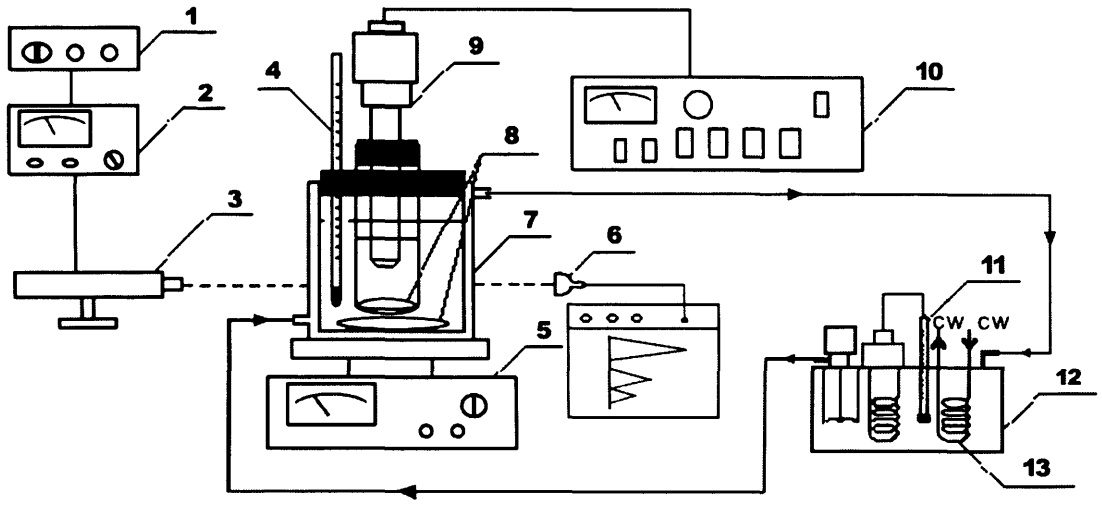

Figure 5.1 Sketch of the apparatus for measuring induction time

1. Voltage stablizer	**2. Power supply**	**3. He–Ne laser emitter**
4. Mercury thermometer	**5. Magnetic stirrer**	**6. X–Y recorder**
7. Jacketed vessel	**8. Magnetic bar**	**9. Ultrasonic probe**
10. Ultrasonic Power supply	**11. Mercury thermometer**	**12. Water-bath**
13. Coiled pipe for cooling	**cw: cooling refrigeration fluid**	

5.3.3 Procedure

To study the induction time, a precision electric analytical balance accurate to 1×10^{-4} g is used to measure 15g spectinomycin hydrochloride and the spectinomycin hydrochloride is solved in 100ml water. In each experiment, precise 15ml solution is measured and transferred into a tube. The magnetic stirrer is switched on. Then, a required quantity of acetone used as the anti-solvent is immediately injected into the

solution. Simultaneously, the power ultrasound is run until the laser recorder shows the induction time. The electrical power to produce the ultrasound is fixed at 400W. During the process, the temperature is kept at 25℃. The transmitted intensity is set at zero to represent no crystal nuclei initially being present in the solution. The light intensity remains constant during the initial period of the experiment, which is recorded as Section AB and shows that no nuclei are formed during this period. Section AB is followed by a sudden decrease indicating the onset of nucleation (Section BC) since the laser beam is scattered by the nuclei in solution. The light intensity continues to decrease as more nuclei are born (Section CD). From point E (intersection), the time when nuclei appear can be obtained. Therefore, the time from point A (when anti-solvent is injected) and point E (intersection) is the induction time. The vessel is sealed during the experiment to prevent evaporation. The process is shown in Figure 5.2.

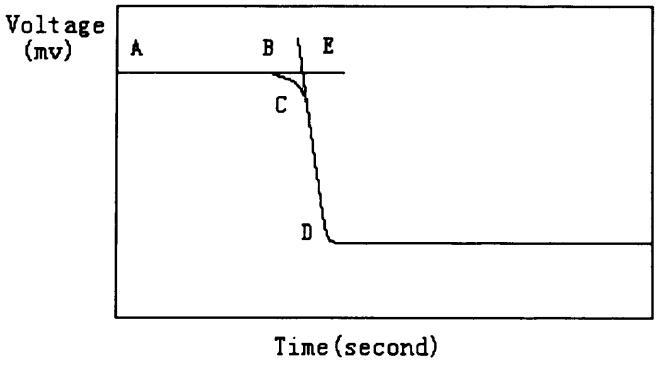

Figure 5.2 Change curve of output voltage of recorder with time for induction time measurement

To study the induction time of sucrose, 150g sucrose is solved in 100ml water and 15ml solution is used in every experiment. Ethanol is used as anti-solvent. To study the induction time of roxithromycin, 2g roxithromycin was measured and dissolved in 25ml

acetone in every experiment. The required quantity of water is used as the anti-solvent. The other steps of procedure are similar to the experiments with spectinomycin hydrochloride as the working substance.

5.4 Results and discussion

The diffusion coefficients (D_{AB}) of barium sulphate are obtained with different power input. They are: $3.65\times10^{-10}m^2/s$ without ultrasound; $6.90\times10^{-10}m^2/s$ with 8.62W; $9.93\times10^{-10}m^2/s$ with 18.0W, $1.52\times10^{-9}m^2/s$ with 27.3W, $2.37\times10^{-9}m^2/s$ with 36.6W, and 4.19×10^{-9} m^2/s with 46.0W.

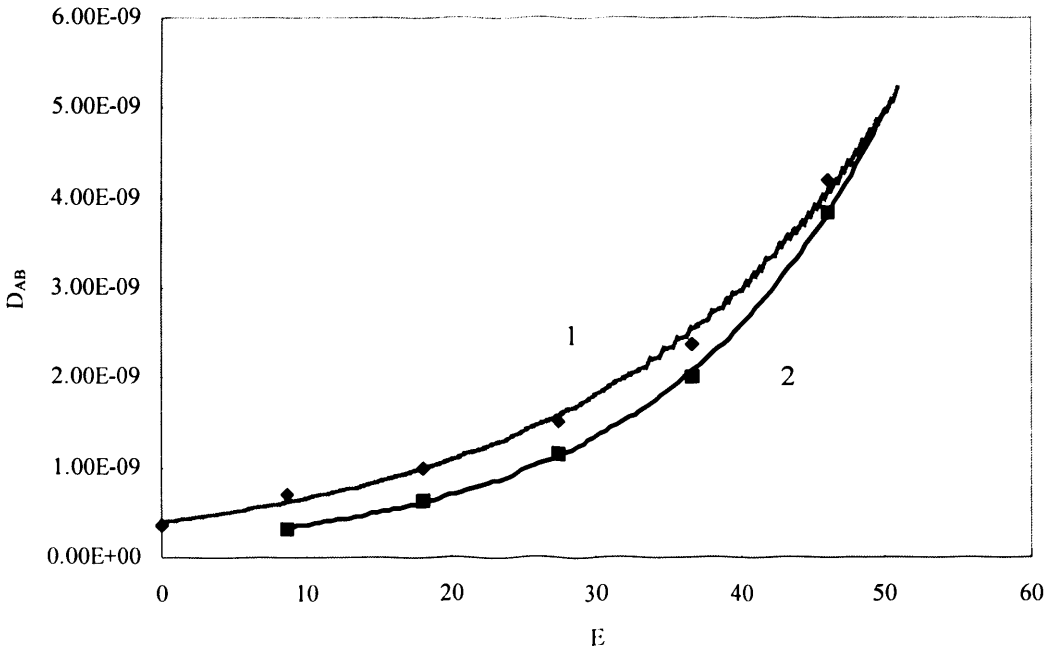

Figure 5.3 The variation of the diffusion coefficient (D_{AB}) vs power input (E)
(◆) D_{AB} vs E with the simulation result of curve 1
(■)D_{AB} - D_{AB0} vs E with the simulation result of curve 2

The plots of D_{AB} and (D_{AB} - D_{AB0}) versus power input (E) for experiments are shown in Figure 5.3. From Figure 5.3, D_{AB} has an exponential relationship with the

power input of ultrasound, which can be expressed by:

$$D_{AB} = 4\times10^{-10} e^{0.0505E} \tag{5.30}$$

In equation (5.26), E_b is the activation energy, the energy necessary to raise a molecule over a barrier to maintain mass transfer rate. Since the energy from ultrasound is the energy obtained by molecule and the activation energy is energy consumed by molecule during mass transfer, they have an opposite value. It is not possible to determine energy gained by $BaSO_4$ molecules from ultrasound, but this amount of energy should have a direct proportional relationship with total power input. So the total power input of ultrasound can work in the exponential term of equation (5.26) as the substitute of molecular energy of $BaSO_4$, as shown in equation (5.30). Thus, although equation (5.26) is an empirical equation, it has some physical meaning. The above analysis indicates the mechanism how ultrasonic power input influences the diffusion coefficient.

From Figure 5.3, as the power input to the system increases, the model prediction of diffusivity of equation (5.26) deviates from the experimental result. A better fit is obtained from equation (5.25). Curve 2 in Figure 5.3 shows the plots of (D_{AB} - D_{AB0}) versus power input (E), the simulation result of equation (5.25) fit the experimental result much better than equation (5.26), especially when power input is increased. The corresponding equation is

$$D_{AB} - D_{AB0} = 2\times10^{-10} e^{0.0652E} \tag{5.31}$$

From these results, it can be concluded that when the temperature is kept constant, the diffusion coefficient will increase exponentially with increasing ultrasonic power input. The effect on diffusivity becomes more significant with the increasing power input.

From equation (5.16), for a given system, the gradient of solute molecular energy with solute concentration distribution in stagnant film (dE_{0A}/dC_A) only depends on temperature and power input. So, when these two parameters are fixed dE_{0A}/dC_A is

also fixed. That is, the molecular energy of $BaSO_4$ has a linear relationship with solute concentration change in the stagnant film between the bulk of the fluid phase and the solid surface. In the solution bulk, the molecule has the highest energy. When a $BaSO_4$ molecule enters stagnant film, its speed is highest. Because the resistance has a direct proportional relationship with speed of molecule, the molecule will be decelerated faster at the beginning of diffusion process. When the molecular speed becomes slower, its speed change will also become slower. Since dE_{0A}/dC_A has a fixed value, the concentration change of $BaSO_4$ is higher in the solution bulk and becomes smaller near the crystal surface. Thus the distribution curve of solute concentration with position in the stagnant film should be concave, which is consistent with the description by Cussler (1997).

The solutions with the organic materials spectinomycin hydrochloride, roxithromycin and sucrose have different viscosities. The solubility of spectinomycin hydrochloride, roxithromycin, and sucrose can be obtained from equations (5.27), (5.28), (5.29), respectively. The supersaturation ratio (S) can be calculated consequently. The experimental results of spectinomycin hydrochloride are shown in Figure 5.4 where the plots of $\ln(t_{ind})$ and $\ln^{-2}(S)$ consist of two linear segments. For high supersaturation levels, the nucleation is predominantly homogeneous and for low supersaturation levels, the nucleation is predominantly heterogeneous (Söhnel & Mullin, 1988).

As can be seen in Figure 5.4, the induction time decreases as supersaturation increases both with and without ultrasound. However, from the experiments, it can be observed that ultrasound has a significant effect in reducing the induction time. The slope and intercept of the straight line 1 are 9.15 and 2.56, respectively, while the corresponding values for the straight line 3 are 9.59 and 0.41. Thus, the slope of straight line 1 is very close to the slope of straight line 3, but the intercepts of two straight lines are different.

From Figure 5.4, when nucleation is consistent with a predominantly heterogeneous model, the straight line without ultrasound (straight line 2) is not parallel

to the straight line with ultrasound (straight line 4). This phenomenon shows that besides D_{AB}, ultrasound will change other parameters of nucleation rate.

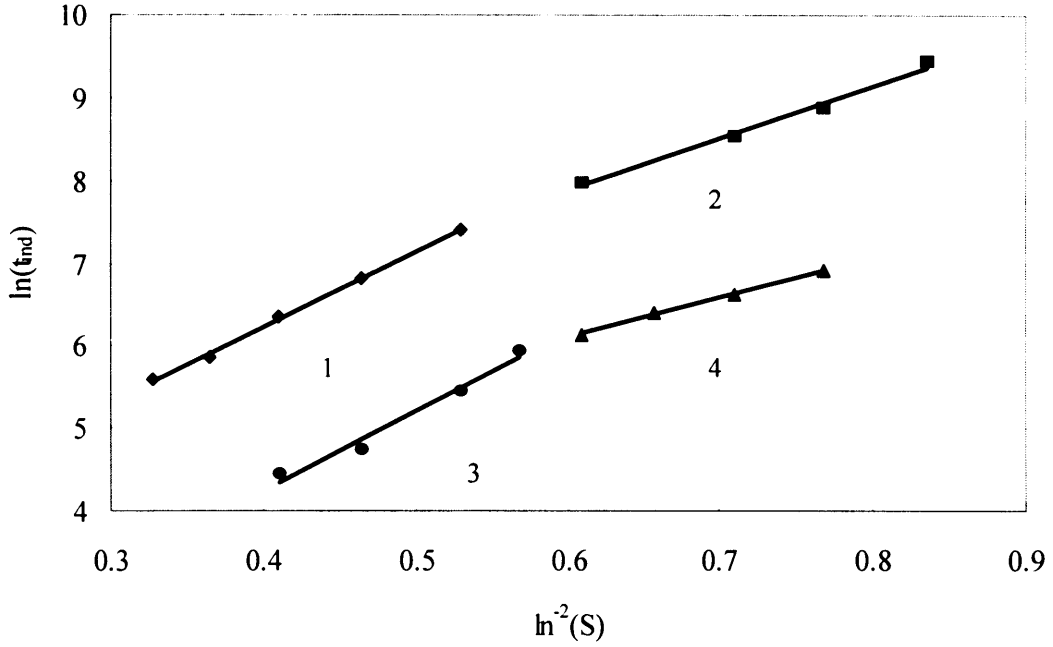

Figure 5.4 Induction time as a function of supersaturation ratio with spectinomycin hydrochloride as the substance:
(◆)homogeneous nucleation without ultrasound
(■)heterogeneous nucleation without ultrasound
(●)homogeneous nucleation with ultrasound
(▲)heterogeneous nucleation with ultrasound

From the equation (3.17), because the straight lines of $\ln^{-2}(S)$ versus $\ln(t_{ind})$ with different power input have approximately similar slopes (B_1), the phenomenon shows the ultrasound has no or little influence on temperature, surface tension (γ_{CL}), or the solubility. From equation (3.20), the value of γ_{CL} is mainly influenced by temperature and will not be influenced by ultrasound. If the heat can be removed immediately and the temperature is constant, γ_{CL} will remain constant in ultrasonic field. No temperature change higher than 0.1K is observed in this experiment, so it can

be concluded that the majority of heat released by hot point can be removed immediately. The slight difference in the gradient of slopes may be the result of the small temperature increase by a hot point. Additionally, no solubility change with ultrasound is observed in this experiment.

From equations (3.18) and (3.19), the main influence of ultrasound will be D_{AB}. This is the reason why the intercept of straight line 1 is different from straight line 3. From above observation, it can be inferred that ultrasound enhances diffusion and significantly shortens induction time. In this experiment, D_{AB} was increased about 8.58 fold by using 400W ultrasound. This shows that ultrasound has a significant influence on the diffusion process.

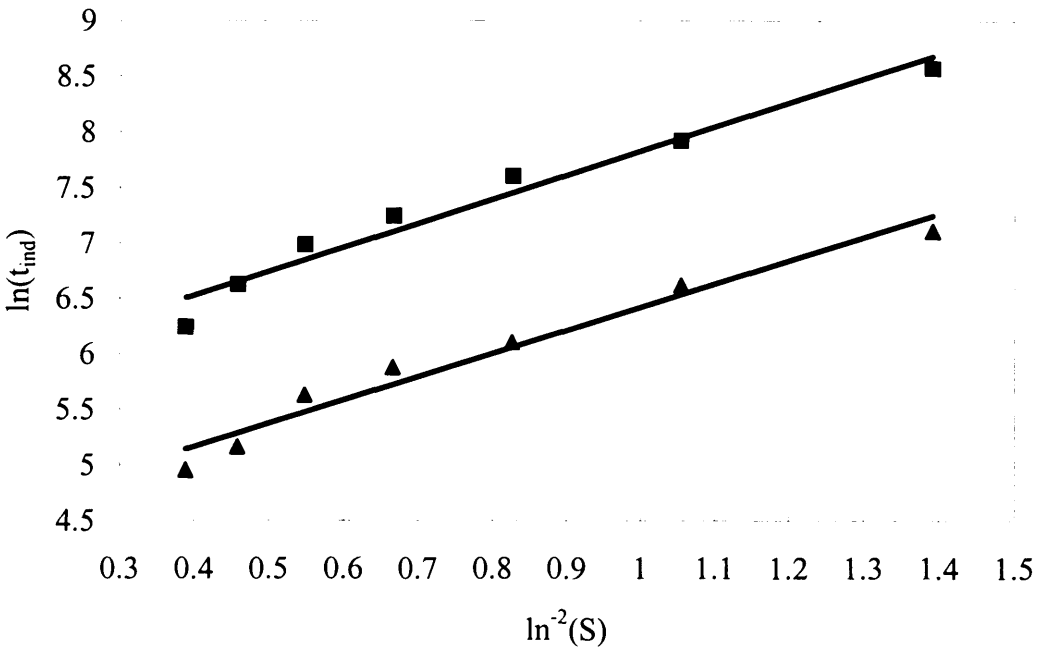

Figure 5.5 Induction time as a function of supersaturation ratio with roxithromycin as the substance, when nucleation is consistent with a predominantly homogeneous model.
(▲)with ultrasound, (■) without ultrasound

To validate above conclusion, roxithromycin and sucrose were used as the working

substances to determine the ultrasonic effect on homogeneous nucleation in organic anti-solvent crystallization systems. The experimental results of roxithromycin are shown in Figure 5.5. When nucleation is consistent with a predominantly homogeneous mechanism, the plots of $\ln^{-2}(S)$ and $\ln(t_{ind})$ consist of two straight lines. The slope and intercept of the straight line without ultrasound are 2.16 and 5.67, respectively, while the corresponding values for the straight line with ultrasound are 2.09 and 4.33. Thus, the slopes of two straight lines are again very close. D_{AB} increases by 3.82 fold by using 400W ultrasound.

The experimental results for sucrose are shown in Figure 5.6. The slope and intercept of the straight line without ultrasound are 38.99 and 3.94, respectively, while the corresponding values for the straight line with ultrasound are 39.94 and 3.28. Figure 5.6 again shows that the slopes of two straight lines are very close. D_{AB} increases by 1.93 fold by using 400W ultrasound.

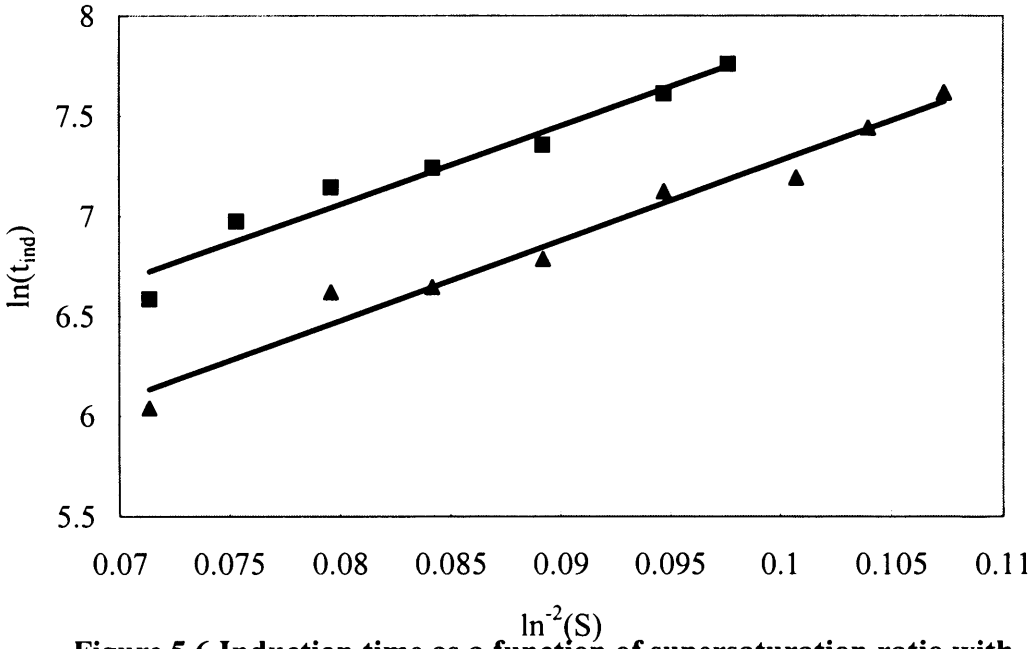

Figure 5.6 Induction time as a function of supersaturation ratio with sucrose as the substance, when nucleation is consistent with a predominantly homogeneous model: (▲)with ultrasound, (■) without ultrasound

From above observations, the experimental results show that when nucleation is consistent with a predominantly homogeneous model, the main effect of ultrasound is an increase in the diffusion coefficient (D_{AB}). Other parameters change only slightly or remain constant in the ultrasonic field. This suggests that diffusion enhancement is the main reason for the reduction in the induction time.

All the experiments were carried with the same power input (400W and 20kHz). Through experiments, it is observed that the ultrasonic effect to increase the diffusion coefficient is different in different systems. The diffusion coefficient (D_{AB}) is increased much more significantly in the spectinomycin hydrochloride crystallization system than in the roxithromycin crystallization system. While in the sucrose crystallization system, the ultrasonic effect on diffusion coefficient (D_{AB}) is smallest of the three systems.

Equation (5.25) can be used for real systems with multi-component solutions. If the temperature remains constant, the value of diffusion coefficient (D_{AB}) will be enhanced when the gradient of solute molecular energy with solute concentration distribution in stagnant film (dE_{0A}/dC_A) increases. dE_{0A}/dC_A will increase with the value of ultrasonic power input since the molecules can receive more energy from ultrasound before moving into the stagnant film between the bulk of the solution and the crystal surface. On the other hand, the diffusion coefficient (D_{AB}) will decrease with the solute molecular radius and viscosity of solution.

In solution, the solute molecular radius will be determined by both the association effect of solvent and the solute molecular volume before dissolution. The molecular formulae of spectinomycin hydrochloride, roxithromycin, sucrose are $C_{14}H_{24}N_2O_7 \cdot 2HCl \cdot 5H_2O$, $C_{41}H_{76}N_2O_{15}$ and $C_{12}H_{22}O_{11}$, respectively. This implies that the roxithromycin molecule has largest radius. If the molecular radiuses of three substances have large differences in the solution, ultrasound should have maximal effect on diffusion coefficient change of roxithromycin. So, from the experimental result, it can be concluded that the solute molecular radiuses of three substances are very close to each other in the solution. The main reason for the change of ultrasonic effect is the

difference in viscosity of the three crystallization systems. Since the spectinomycin hydrochloride solution has lowest viscosity and the sucrose solution has highest, the ultrasonic influence on diffusion coefficient (D_{AB}) is highest for spectinomycin hydrochloride solution and lowest for sucrose solution. So at the same power input, the ultrasonic effect on D_{AB} decreases with increased solution viscosity.

5.5 Conclusion

The mechanism of the ultrasonic effect on homogeneous nucleation is analyzed. It is found that when temperature is kept constant, the main effect of ultrasound is to increase the diffusion coefficient (D_{AB}). Other parameters change only slightly or remain constant within the ultrasonic field. This suggests that diffusion acceleration is the main reason for the reduction of the induction time. The relationship of D_{AB} and power input is also discussed. A mathematical model of power input and diffusion coefficient is presented, from which it is predicted that diffusivity enhancement (D_{AB}- D_{AB0}) has an exponential relationship with power input. The above relationship is consistent with the results of the experiments. From the mathematical model and experimental results, it can be concluded that the molecular energy of $BaSO_4$ has a direct proportional relationship with its concentration in the stagnant film between the bulk of the fluid phase and the solid surface during mass transfer process, and the distribution curve of solute concentration with position in this stagnant film should be concave.

Induction times have also been measured with and without ultrasound to investigate its effect on induction time of spectinomycin hydrochloride, roxithromycin and sucrose during anti-solvent crystallization. The diffusion coefficient increases about 8.58 fold by using 400W ultrasound for spectinomycin hydrochloride. And D_{AB} of roxithromycin and sucrose are increased about 3.82 fold and 1.93 fold by using 400W ultrasound, respectively.

The relationship between ultrasonic power input and diffusion coefficient is also

investigated. It is found that at the same power input, the ultrasonic effect on D_{AB} decreases with increased solution viscosity.

CHAPTER 6

HIGH-SPEED OBSERVATION OF THE EFFECT OF ULTRASOUND ON THE NUCLEATION PROCESS

6.1 Introduction

In industrial crystallization, primary nucleation is difficult to control because it occurs in a thermodynamically unstable region. Primary nucleation commonly requires very high levels of supersaturation, which brings difficulties in controlling the crystallization process. When operating crystallization in a controlled way, crystal products with a large mean size and narrow size distribution can be obtained. In industrial crystallization processes, this is frequently done by seeding (Teipel & Mikonsaari, 2002). Grinding processes are often employed to produce crystal seeds, but the mean size and size distribution of seeds are commonly unsatisfactory, while grinding processes may introduce impurities into seeds and may create dust, which pollutes the environment. When added into solution, seed particles often agglomerate and are difficult to disperse. These undesirable phenomena do not appear in the seeds that are formed by insonated nucleation (AEA Technol, 2001; Guo & Zhang, 2005). Because of the above benefit, ultrasound is used principally to influence nucleation, which is the initial stage of crystallization. The metastable zone width can be reduced by ultrasound and the nucleation can commence at lower supersaturation ratio (McCausland & Cains, 2002; AEA Technol, 2005). Although ultrasound has been used to replace seeding processes in some systems to accelerate nucleation rate and has also been proved to facilitate downstream processes, it is still difficult to scale up a sonocrystallization process from the laboratory to an industrial process owing to the lack of understanding of sonocrystallization mechanism and scale-up strategies.

Although it is reported that ultrasound can accelerate the nucleation rate during crystallization processes with different substances, the mechanism of the phenomenon is still under debate. Two possible reasons have been proposed to explain why ultrasound can accelerate nucleation rate. The first is that cavitation can increase nucleation rate directly. McClements (1995) mentioned that the small cavitation bubbles produced by ultrasound can act as nuclei for crystal growth. While Mzahul supposed that the

cavitation gives rise to electric fields at the boundaries, which make nuclei forms at the cavitation sites (See Kapustin, 1963). Second explanation is that ultrasound can increase mass transfer rate and increase the rate of collision between the clusters of solute. This effect increases nucleation rate indirectly.

In this chapter, barium sulphate is used as the working substance precipitated by mixing aqueous solutions of $BaCl_2$ and Na_2SO_4. The mixing processes with stirring and with ultrasound are investigated by the dispersion of ink in water. The vessel is divided into several sections to investigate the mixing processes by recording the movement of small silicon carbide crystals. The cavitation distribution in different sections is also recorded. The nucleation processes in different sections are also observed by the lens with high magnification. The mechanism of nucleation by ultrasound is analyzed using the above information. Then the induction times, having an inverse ratio relationship with nucleation rate, are measured at different temperatures and the relationships between the cavitation distribution and both the solution temperature and viscosity are also investigated.

6.2 Experimental

The first experiment is the investigation of the dispersion of ink with ultrasound and with stirring respectively in a jacketed vessel of diameter 55mm at 25℃. 200 ml water is used as liquid medium. 100 μl ink is injected into the water by Finnpipette and the dispersion processes are recorded by a Kodak Ektapro Hs motion analyzer, which can take 4500 full frames per second (fps). 3 amplitudes of ultrasonic processor (41%, 51% and 61%) are selected to study the influence of ultrasonic energy on the dispersion process. Three stirring rates (200, 400 and 800 rpm) are selected to investigate the influence of stirring energy on dispersion process. When the stirring rate is 800rpm, only 150 ml water is used to avoid water overflowing from the vessel.

A 750 W ultrasonic processor with 20 kHz was used (Cole-Parmer Instruments,

Illinois, USA), which functions by emitting vibration waves and inducing cavitational voids throughout a defined volume of liquid in each experiment. The ultrasound is produced by a transducer made up of a piezoelectric sandwich and is delivered from a titanium probe with a tip of 8mm in diameter. During insonation, the probe is immersed in the liquid, resulting in the wave traveling downwards and reflecting from the base.

The Kodak Ektapro Hs motion analyzer is also used to record the cavitation distribution, the turbidity change, the dispersion of the ink and the particle movement in the vessel. Two lenses with different magnifications were applied. The lens with low magnification is used to record the change and flows of whole vessel, while the one with high magnification is used to record the local change and flows. Since the magnification of these two lenses is adjustable, the magnification is obtained from the images of the probe of ultrasonic processor and the pole of stirring impeller. The proportion between corresponding dimensions, which are shown on the monitor of Kodak analyzer, and the real dimension of reference substances are used as the magnification.

The relationship between the power input and amplitude has already been established in chapter 3. And the power input from stirring can be obtained from:

$$P = P_0 \rho N^3 d_s^5 \tag{6.1}$$

where P_0 is the power number, P is the power drawn by the stirrer, ρ is the solution density, N is the stirrer speed and d_s is the diameter of stirrer. In the turbulent regime the power number is a constant. The above relationship can be developed to produce a power curve, which is a plot of Po versus Re for different geometrical set-ups (Harnby & Edwards, 1992). In the turbulent regime, when Re > 6000 the power number becomes constant. For a 45° pitch blade, 4-blade impeller, which is the stirrer used in this experiment, P_o is 1.27 (Kougoulos, 2003).

In the second experiment, which is also carried at 25℃, the vessel is divided into 6 sections to study the local mixing process and hydraulic flows, when ultrasound is applied to the system. The division is shown in Figure 6.1A. The experiments are

carried at the amplitudes of 41%, 51% and 61% of the maximum power. Silicon carbide is used as indicator since it is inert in water. The lens with high magnification is used to record the movement of particles in different sections. In every section, 10 particles are randomly chosen from the monitor of Kodak analyzer to indicate the energy and hydraulic flows. Their moving directions and velocities are recorded.

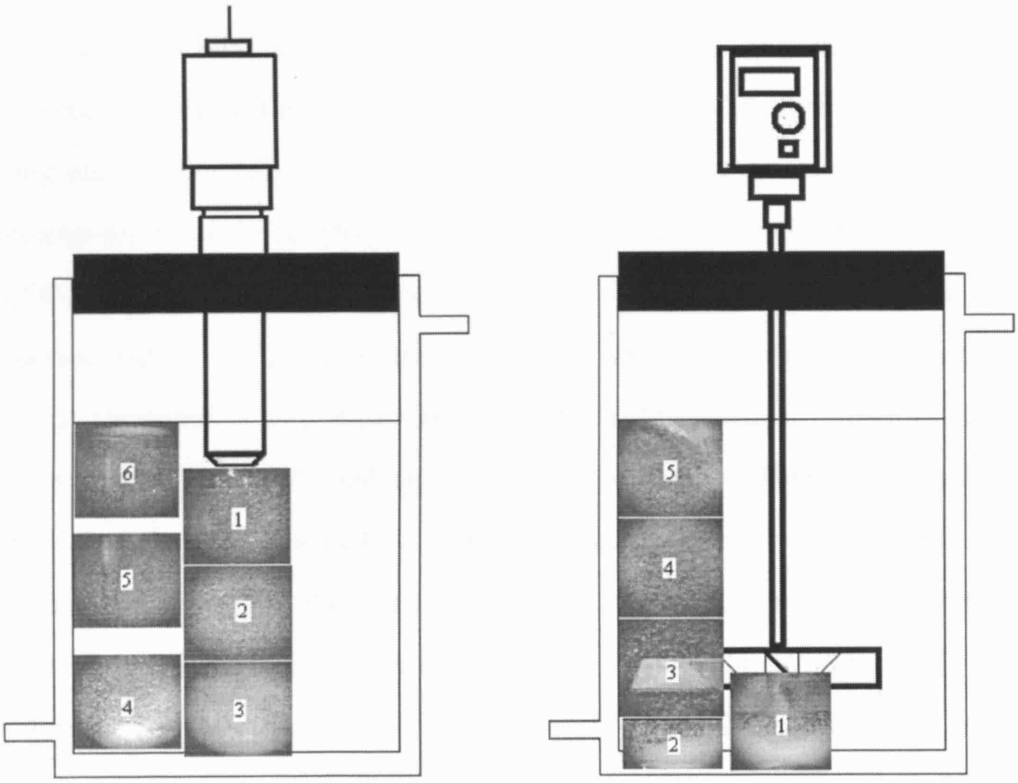

Figure 6.1 The division of the vessel for the experiments of local mixing processes

A:The division when ultrasound is applied with 41% amplitude

B:The division when stirring is applied with the stirring rate of 400rpm

For the experiment with stirring, the vessel is divided into 5 sections, which is

shown in Figure 6.1B. Silicon carbide crystals are also used as indicators and the experimental procedures are similar as the experiment when ultrasound is applied to the system. But in this experiment, only a stirring rate of 400rpm is investigated, because the mixing experiments with ink already indicated the similarity of mixing processes with different stirring rates. The movement and the velocity of indicators in above two experiments are compared to investigate the energy distribution and the movement of flows in the vessel.

The nucleation experiments are also carried in above vessel with ultrasound and stirring at 25℃. Barium sulphate, precipitated by mixing aqueous $BaCl_2$ and Na_2SO_4 solutions, was used as the working substance to study the ultrasonic effect on nucleation during reactive crystallization processes. The 100 ml aqueous $BaCl_2$ solution with the concentration of $1.5\times10^{-3}mol\cdot L^{-1}$ is added into the vessel. Then, 100 ml aqueous Na_2SO_4 solution of the same concentration is also added into the vessel. The ultrasonic processor and Kodak analyzer are switched on immediately to detect the nucleation process. The solution with supersuturation ratio of 54.76 can be formed by the mixing of above two solutions. The induction time, which is the time between the initial mixing and the first observed change of turbidity, is about 3 seconds without ultrasound. After ultrasound is applied to the system, the nuclei precipitate immediately. Because the supersuturation is high, the nuclei should become visible almost immediately after they are formed. And the dispersion of nuclei is observed with high-speed Kodak analyzer.

Firstly, the lens with low magnification is used to observe the time difference of turbidity changes in different sections in the vessel. Then, the lens with high magnification is used to detect the mass transfer flow in section 3, 4, 5, 6. Because the cavitation flow from the probe of ultrasonic processor concentrates in section 1 and 2, it is not possible to identify when nuclei appear in these two sections since the appearance of cavitations is very similar to that of nuclei in the solution. And the cavitation flow also interferes the identification of mass transfer flow. So section 1 and 2 were not investigated by the lens with high magnification.

The cavitation number is obtained from the monitor to calculate the cavitation density in different sections at various amplitudes at 25℃. 200ml pure water is used as medium. The area of each section is obtained from the magnification which is calculated from the comparison with the reference substance. Then, the cavitation density in different sections can be obtained. Thus, the influence of cavitation on nucleation can be analyzed.

The final examination investigates the influence of viscosity on cavitation density and ultrasonic power input to the system at similar amplitudes. Ethanol and acetone are used to compare with water, at 25℃. The cavitation density and ultrasonic power input are also compared when water is used as medium at 5, 25, 50 and 90℃ with the similar amplitudes. Then, the induction times of barium sulphate are compared at different temperatures (5, 25, 50 and 90℃) to investigate the influence of temperature, cavitation and the power input on the nucleation process. The induction time is measured by a nephelometer (He & Oddo, 1995). Ultrasound with 41%, 51% and 61% amplitude is used. The other experimental procedures are similar to the above nucleation experiments but the concentrations of the solutions are $0.8\times10^{-4}mol\cdot L^{-1}$, because the induction times in this situation are long and the experimental errors are minimal.

6.3 Results and discussion

From above experiments, the mechanism of ultrasound on nucleation can be determined.

To investigate the mechanism of ultrasound on the increase of nucleation rate, the flows, mixing effect of stirring and ultrasound are compared in the experiments carried in a 200ml vessel. The dispersion of ink in the vessel with ultrasound and with stirring are shown in Figure 6.2A and Figure 6.2B, respectively. The dispersion process and hydraulic flow pattern can be observed. It is found that the ink disperses from center to the edge during its dispersing from the top to the bottom of the vessel. Some hydraulic

flows are observed during the process, but the flows only move in a small area and their turbulent movements are not strong. When ultrasound is applied to the system, the ink is dispersed and mixed much quicker than the process with stirring. The flows can disperse the ink to majority of the vessel in a very short time and the mixing process is very turbulent. The dispersion of ink is also observed in the lens with high magnification, it is found the ink moves to different directions with high velocity, which shows the high turbulence in the vessel in microscopic scale.

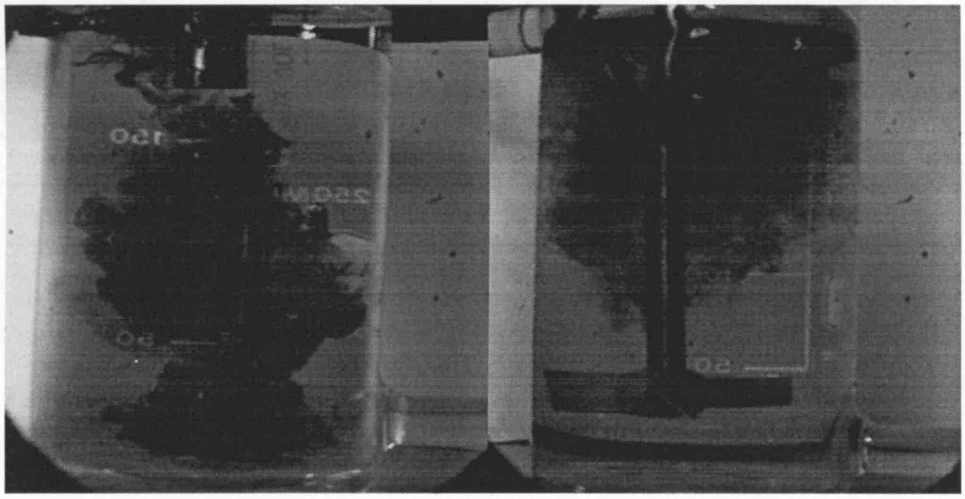

A **B**

Figure 6.2 The dispersion of ink in water
A: dispersion with 41%ultrasound
B: dispersion with 400rpm stirring rate

The vessel is divided into 6 sections to study the local mixing process and hydraulic flows. As mentioned before, silicon carbide crystals are used as indicators. The mixing process in the whole vessel is also observed and recorded from the Kodak camera. The particle movements in the vessel with ultrasound and with stirring are shown in Figure 6.3 A and Figure 6.3 B respectively. It is found that, in general, the

particles move orderly in the vessel with stirring, but erratically in the vessel with ultrasound.

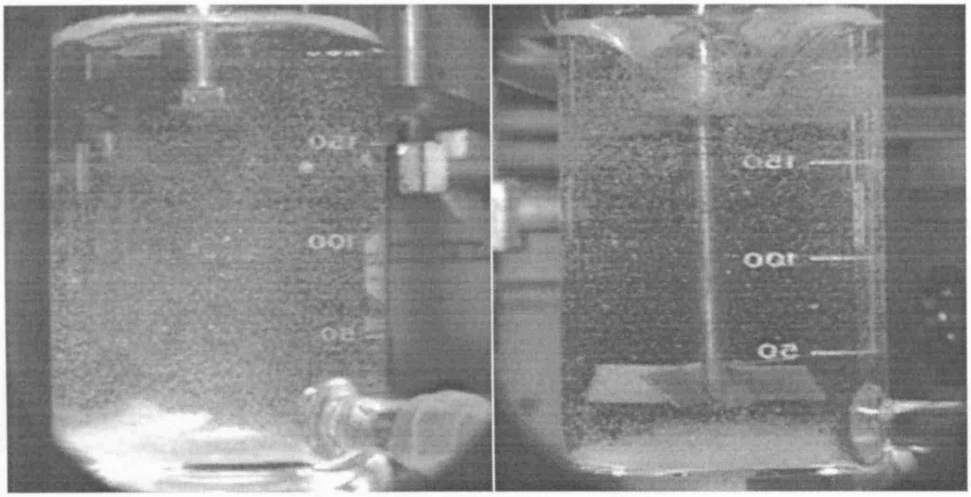

A **B**

Figure 6.3 The distribution and movement of sugar crystals in the vessel
A: with ultrasound
B: with stirring

As described above, ten particles are chosen randomly from every section and their velocities are recorded. The variance of velocity (σ^2) between crystals is used to indicate the local mixing and hydraulic flows. σ^2 can be obtained from equation (6.2) (Zhou, 1993).

$$\sigma^2 = \sum \left(v_c - v_{average}\right)^2 / n \qquad (6.2)$$

where v_c is the velocity of particle, $v_{average}$ is the velocity of average particle and n is the number of crystals. Since the velocity is a vector, it is defined that the particles moving upwards have a positive velocity and those moving downwards have negative velocities, while those move to right have positive velocities and those move to left have negative

velocities. The particle's velocity is divided into horizontal velocity and vertical velocity to calculate σ^2. The mixing process becomes quicker and the difference of velocity between hydraulic flows becomes higher with the increase of σ^2 value.

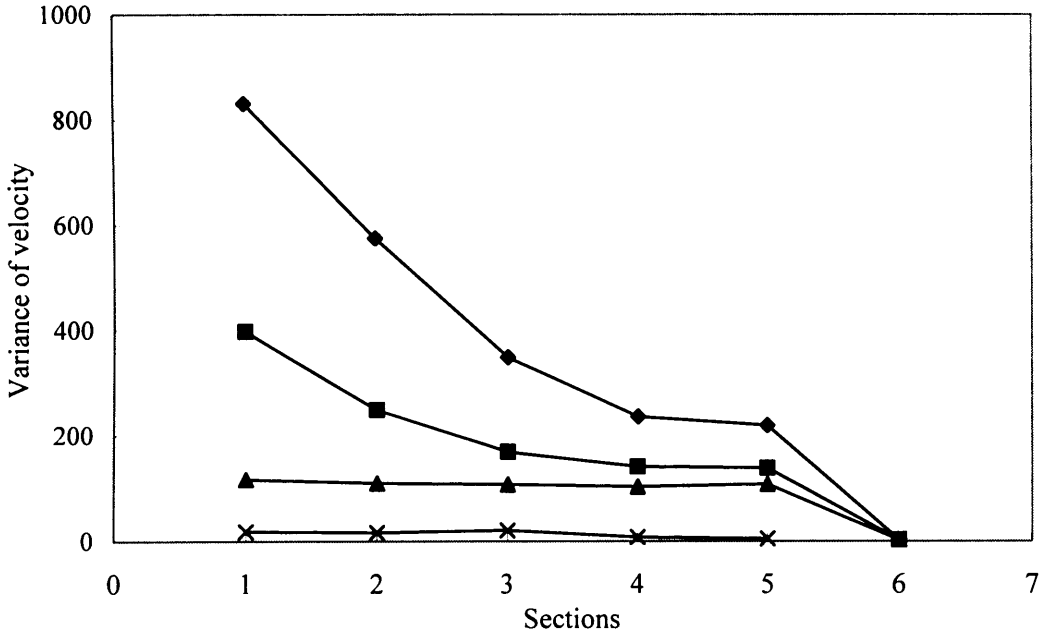

Figure 6.4 The change of variance of velocity with sections
(◆) with the amplitude of 61%
(■) with the amplitude of 51%
(▲) with the amplitude of 41%
(×) with stirring rate of 400rpm

It is found that the amplitude of ultrasonic processor has a direct proportional relationship with power input from the experiment to determine the real power input to the system. The change of σ^2 with the amplitude of ultrasonic processor in different

sections is shown in Figure 6.4. When the amplitude of ultrasonic processor is 41%, variances of crystal velocity are close to each other in different sections. This means that the ultrasonic energy distribution is uniform in the system, so the difference of velocity between hydraulic flows and the mixing time are similar in different sections. When the amplitude is improved, the energy distribution becomes uneven in each section. The difference increases with the increase of amplitude. But section 6 is still a dead zone, where the influence of mixing is insignificant. At 61% and 51% of amplitude, the mixing in section 1 is highest since it is the nearest section to ultrasonic processor while the values of variance in section 4 and 5 are very close to each other.

The variances of crystal velocity with stirring and with ultrasound are also obtained. When stirring is used, it is found the variance in section 2 and 3 is higher than section 4 and 5, because they are near the impeller. From the lens with high magnification, it is observed that when ultrasound is applied to the system, the flows become turbulent, the particles can move to any direction in each section. The above phenomenon is on account of both the vibration and implosion of cavitations, and the hydraulic flow directly caused by ultrasonic energy. Because the crystals move orderly in the system with stirring, the variance between crystal velocities is much lower compared to the system with ultrasound. So it can be concluded that the turbulence of hydraulic flows in a system with ultrasound is better than the system with stirring.

The reason why turbulence of liquid flows is much higher in the system with ultrasound is on account of high power input. From Figure 3.1, it is obtained that the power inputs to the system is 41%: 27.3W; 51%: 36.6W; 61%: 46.0W. And the energy from stirring can be calculated from equation (6.1). The results are 200rpm: 0.073W, 400rpm: 0.59W and 800rpm: 4.7W.

The cavitation distribution is shown in Figure 6.5 at the amplitudes 41%, 51%, 61%. It is found the density and the velocity of cavitations in water increases with the increase of amplitude. At high amplitude, it takes short time for cavitations to move from the ultrasonic probe to the bottom of the vessel. And the density of cavitations

under the ultrasonic probe is higher than the density at low amplitudes.

The cavitation densities in different sections are compared. At the same amplitude, the density of cavitations in section 5 is much lower than section 3 and 4, while the mixing effects are very close. So it can be concluded that the vibration and implosion of cavitations is one reason for mixing improvement in the vessel. The mixing is also improved by the ultrasonic energy, which is transferred directly to the molecules and flows in the system.

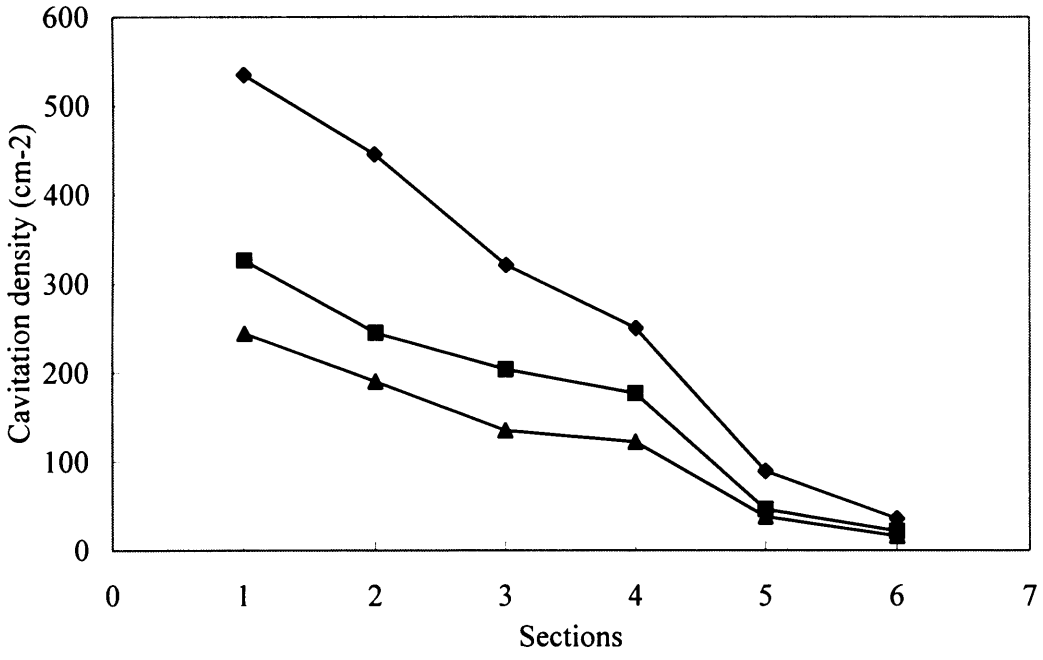

Figure 6.5 The distribution of cavitation in different sections
(◆) with the amplitude of 61%
(■) with the amplitude of 51%
(▲) with the amplitude of 41%

In the vessel with stirring, it is found the turbidity changes isochronously in different sections. The difference of turbidity in different sections in the middle of

nucleation process is shown in Figure 6.6 A. Because the dispersion of ink can be recorded easily by this high-speed camera, the dispersion of nuclei in the system should also be able to be observed. Since the dispersion of nuclei in the system was not observed, it can be concluded that the nuclei are formed at the similar rate in the vessel and the concentrations of nuclei are approximately similar in different sections in the vessel. From the mixing experiment, the difference of mixing effects is very small between different sections, so the chance of monomers to collide with other monomers is also very close in different sections. This is the reason why turbidity changes isochronously in different sections.

After ultrasound is applied to the system, at 41% amplitudes, it is also found the turbidity changes isochronously in section 3, 4, 5. The cavitation stream from ultrasonic probe exists in section 1 and 2. And because the appearances of cavitation stream and the crystal nuclei are very close in the black and white frames, it is not possible to identify when the nuclei formed in section 1 and 2.

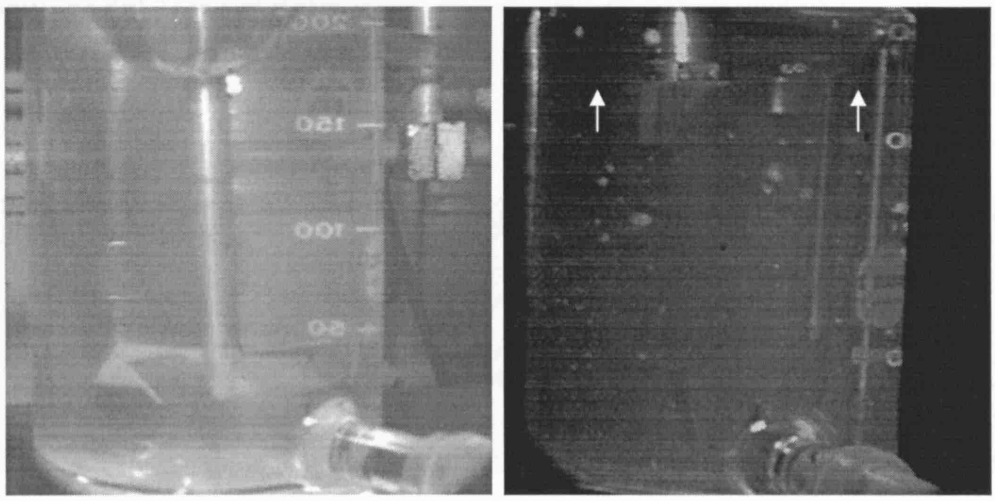

A **B**

Figure 6.6 The difference of turbidity in different sections in the middle of nucleation process
A: with stirring
B: with ultrasound
***Arrows direct area with low turbidity compared to other sections**

The difference of turbidity in different sections in the middle of nucleation process is shown in Figure 6.6 B, when ultrasound is applied. It is found except section 6, the turbidity in other sections changes isochronously. To find the dispersion of nuclei flow, the lens with high magnification is used to catch the dispersion flow and turbidity change in section 3, 4 and 5. The dispersion of nuclei flow is not found in section 3, 4, and 5 at 41% amplitude, so it can be concluded that the nuclei are formed locally. Because the turbidity changes isochronously in section 3, 4, and 5 with different cavitation density, it shows that the reason for acceleration of nucleation rate in ultrasonic fields is on account of increase of mixing, which increases the collision between solute monomers. The change of turbidity in section 6 is shown in Figure 6.7 C, D, where the nebulous flow of nuclei dispersion can be observed easily. Above nebulous flow is not found in Figure 6.7 A, B, which shows the change of turbidity in section 5. The reason for above phenomenon is that the mixing in section 6 is not as quick and turbulent as other sections. So the nucleation rate in this section is lower than the nucleation rate in other sections. The similar phenomena are also observed when amplitudes are 51% and 61%.

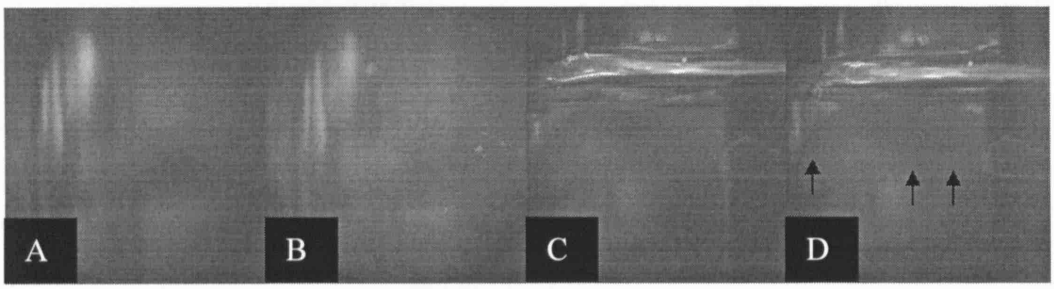

Figure 6.7 The change of turbidity in sections 5 and 6
A: the beginning of nucleation process in section 5
B: the middle of nucleation process in section 5
C: the beginning of nucleation process in section 6
D: the end of nucleation process in section 6
***Arrows direct nuclei dispersion flows**

The variance of velocity in different sections increases with amplitude. This is the reason why nucleation rate increases with the increase of ultrasound amplitude. The induction time (t_{ind}), which is believed to have an inverse ratio relationship with the nucleation rate, is used to indicate the change of nucleation rate with ultrasound. The influence of ultrasound on t_{ind} is shown in Figure 3.5. The induction time decreases with the increase of amplitude and this phenomenon is distinct when supersturation ratio is low.

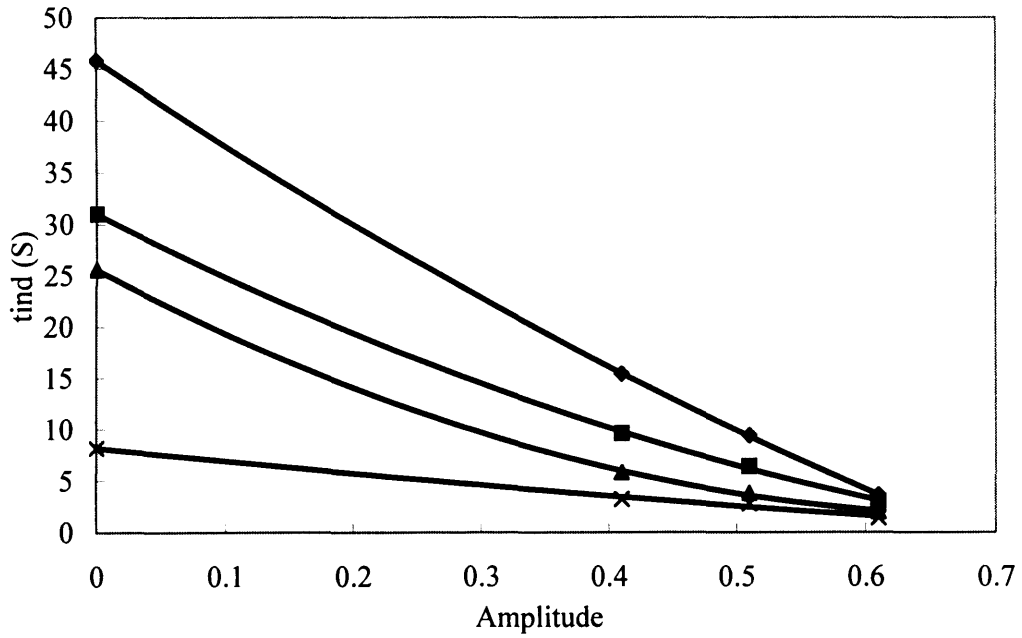

Figure 6.8 Influence of ultrasound on induction time at different temperatures
(◆) at 5^{0}C
(■) at 25^{0}C
(▲) at 50^{0}C
(×) at 90^{0}C

The temperature influence on induction time (t_{ind}) is shown in Figure 6.8. It is

found that t_{ind} decreases with the increase of temperature at various amplitudes. But at high temperature, the increase of amplitude has a low influence on induction time. The change of t_{ind} with amplitude is minimal at 90 ^{0}C.

The influence of temperature on cavitation density in the vessel is also investigated. It is found that at the same amplitude, the cavitation density increases with the increase of temperature, as shown in Figure 6.9 A, B, C and D. The reason why similar amplitude can generate more cavitation is on account of decrease of viscosity with increase of temperature. The viscosity of water at 5 ^{0}C is 1.52cp; 25 ^{0}C is 0.89cp, 50^{0}C is 0.55cp, 90 ^{0}C is 0.32cp (Mullin, 2000). The similar phenomena can be observed when ultrasound is applied to ethanol and acetone at 25 ^{0}C, as shown in Figure 6.9 E and F. The viscosity of ethanol is 1.15cp and acetone is 0.325cp (Hines & Maddox, 1985).

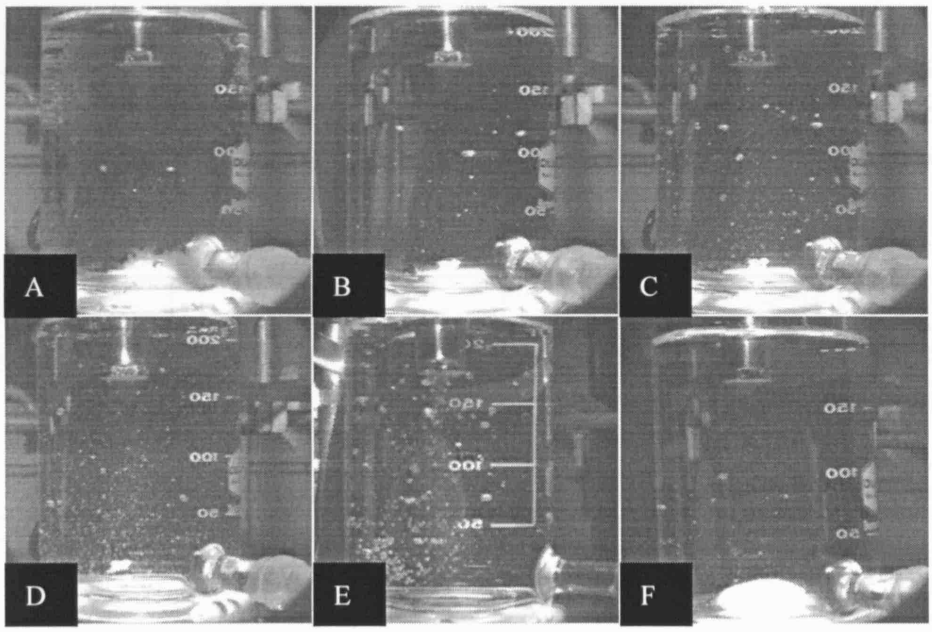

Figure 6.9 The change of cavitation density with viscosity of liquid medium

A: water at 5 ^{0}C **B: water at 25^{0}C**
C: water at 50 ^{0}C **D: water at 90 ^{0}C**
E: acetone at 25 ^{0}C **F: ethanol at 25 ^{0}C**

It is found that at the similar amplitude, the cavitation density is high in the solution with lower viscosity. The power inputs to the water, ethanol and acetone at various amplitudes and temperatures are shown in Table 6.1. At the similar amplitude, the power input to the system decreases with the decrease of viscosity. The low power input can cause worse mixing. This is the reason why the ultrasonic influence on t_{ind} decreases when temperature increases, although the cavitation density becomes higher at high temperature. This phenomenon shows that the cavitation has no direct relationship with homogeneous nucleation rate increase. Ultrasound and its cavitational effect can increase homogeneous nucleation rate through increase mixing and dispersion processes.

Table 6.1 The power inputs (W) to 200ml fluid medium at different temperatures

Amplitude	water (5℃)	water(25℃)	water(50℃)	water(90℃)	acetone(25℃)	ethanol(25℃)
0.41	33.4	27.3	23.1	16.2	17.3	29.3
0.51	43.5	36.6	33.4	25.9	27.1	39.6
0.61	55.2	46.0	41.8	32.4	34.1	49.7

6.4 Conclusion

A Kodak motion analyzer is used to observe the mixing process and nucleation process. The dispersion processes of ink with ultrasound and stirring are respectively used to compare the difference of mixing processes and hydraulic flows. It is found that ultrasound can make flows much more turbulent in the vessel. The vessel is divided into several sections to investigate the local mixing process by recording the movement of

small silicon carbide crystals. It is found at 41% amplitude, the energy distribution is uniform in the vessel. But at 51% and 61% amplitudes, it is uneven. The velocity variances of crystals, which indicate the mixing process, are close in sections 3, 4, which are at the bottom of the vessel, and section 5, which is at the middle part of the vessel. But in the section 6, which is at the top of the vessel, the mixing process is much worse. However, the cavitaion distributions in sections 5 and 6 are much lower than other sections. The velocity variance of crystals in the stirred vessel is much lower than the vessel with ultrasound.

The effect of ultrasound on nucleation is also studied in different sections. Barium sulphate is used as the working substance precipitated by mixing aqueous solutions of $BaCl_2$ and Na_2SO_4. It is found the nuclei appear isochronously in sections 3, 4 and 5. The mechanism of nucleation by ultrasound is analyzed.

Then, the induction times at different temperatures are measured with different power inputs at a given supersaturation level. It is found the ultrasonic effect on nucleation decreases with increase of temperature. But the cavitation density increases with temperature increase. This phenomenon shows that the cavitation has no direct relationship with homogeneous nucleation rate increase. Ultrasound and its cavitational effect can increase homogeneous nucleation rate through the increase of mixing and dispersion processes. The relationship between the cavitation distribution and temperature is established. Ethanol and acetone are used to verify this relationship. It is found the cavitation density decreases with increase of viscosity of the fluid medium.

CHAPTER 7

THE EFFECT OF ULTRASOUND ON HETEROGENEOUS NUCLEATION

7.1 Introduction

Primary nucleation encompasses both homogeneous nucleation and heterogeneous nucleation. Mere traces of impurities can act as a nucleation accelerator in the system. Compared to homogeneous nucleation, during heterogeneous nucleation nuclei are induced by foreign particles in a solution (Mullin, 2000).

The mechanism of heterogeneous nucleation is more complex than homogeneous nucleation, since the nucleation rate will be influenced by both the properties of solute and the properties of foreign impurities. In notionally clean and particle-free solutions, it is believed to be associated with spurious traces of suspended material or with imperfections in the container vessel surfaces that can function as nucleation sites. So in practice, nucleation almost always occurs heterogeneously. Homogeneous nucleation predominantly occurs at very high supersaturation ratios. And heterogeneous nucleation predominantly occurs at low supersaturation ratios. In addition to the diffusion coefficient (D_{AB}), ultrasound may change other parameters which will influence nucleation rate.

Because of the "catalytic effect" of foreign particles to nucleation process, nucleation mechanism of heterogeneous nucleation is more complex compared with homogeneous nucleation. If the nucleus forms on the surface of the foreign phase, the energy barrier to nucleation can be reduced significantly. And ultrasound may influence this effect by changing the contact angle (θ) and geometric factor (f) between the foreign solid phase and crystalline phase. So to understand the mechanism of ultrasonic effect on heterogeneous nucleation, it is necessary to investigate the influence of ultrasound on these factors which influence heterogeneous nucleation rate.

In this chapter, the mechanism of the ultrasonic effect on heterogeneous nucleation is investigated by measuring the induction time. Barium sulphate is also used as the working substance precipitated by mixing aqueous solutions of $BaCl_2$ and Na_2SO_4 with relatively low concentrations compared to the experiments of homogeneous nucleation.

Based on the conclusion obtained from homogeneous nucleation experiment, the ultrasonic effects on other factors in classic heterogeneous nucleation model, which do not appear in classic homogeneous nucleation model, are obtained and the reasons for these effects are also analyzed. The ultrasonic effect on critical supersaturation ratio (S_{crit}), where the predominant nucleation mechanism will change from homogeneous nucleation to heterogeneous nucleation, is also investigated. And the ultrasonic effects on homogeneous nucleation and heterogeneous nucleation are compared.

In addition, the effect of ultrasound on nucleation order (n) and the nucleation coefficient (k_N) are also investigated during heterogeneous nucleation. And the ultrasonic effects on these factors during heterogeneous nucleation are compared with the corresponding effects during homogeneous nucleation.

7.2 Theory

The rate of nucleation of a solution or melt can be affected considerably by the presence of mere traces of impurities in the system. In reality, it is impossible to remove completely all solid matter from a solvent or solution. When carrying out nucleation experiments, there exists a critical supersaturation level. When this is exceeded, the rate of homogeneous nucleation is higher than the rate of heterogeneous nucleation. But below this critical supersaturation, heterogeneous nucleation is the predominant mechanism of nucleation (Mersmann, 2001); the new phase therefore appears as a result of heterogeneous nucleation. The rate of heterogeneous nucleation is proportional to the volumetric surface area (a_{for}) of foreign particles. So the rate of heterogeneous nucleation (B_{het}) is the product of the volumetric surface area (a_{for}) and heterogeneous nucleation rate based on the surface of foreign particles ($B_{het,surf}$) (Mersmann, 2001).

$$B_{het} = a_{for} B_{het,surf} \tag{7.1}$$

The heterogeneous nucleation rate ($B_{het,surf}$) can be described in the same form of

homogeneous nucleation.

$$B_{het,surf} = k' n_c' Z \tag{7.2}$$

where k' is the rate which clusters cross the barrier, n'_c the number concentration of critical clusters, when nucleation is predominantly heterogeneous and Z is the imbalance factor.

According to the Boltzmann distribution, the number of critical cluster (n'_c) depends on the number of molecules adsorbed on the foreign surface ($C_{ad}N_A$), where C_{ad} is the concentration based on the area of foreign surface, and the free energy of critical cluster, when nucleation is predominantly heterogeneous ($\Delta G_{c,het}$).

$$n_c' = C_{ad} N_A \exp(-\frac{\Delta G_{c,het}}{kT}) \tag{7.3}$$

The thickness of the adsorption layer cannot exceed the diameter of the molecule (d_m), C_{ad} can be expressed in terms of the volume-related concentration ($C_{ad,v}$), which is

$$C_{ad} = C_{ad,v}\, d_m \tag{7.4}$$

At low concentrations, there is a linear relationship between $C_{ad,v}$ and bulk concentration (C). It is

$$C_{ad,v} = He_{ad} C \tag{7.5}$$

The free energy of critical cluster during heterogeneous nucleation ($\Delta G_{c,het}$), is smaller than the free energy needed for homogeneous nucleation and is given by (Mersmann, 2001),

$$\Delta G_{c,het} = f \Delta G_{c,\mathrm{hom}} = f\left(\frac{16}{3}\right)\pi\left(\frac{\gamma_{CL}}{kT}\right)^3 V_m^2 \left(\frac{1}{\nu \ln S}\right)^2 kT \tag{7.6}$$

and

$$f = \frac{(2+\cos\theta)(1-\cos\theta)^2}{4} \tag{7.7}$$

Here, f is a geometric correction factor depending on the contact angle (θ), which is the angle between crystalline deposit and the foreign solid surface (Mullin, 2000).

The coefficient k' in heterogeneous nucleation is influenced by the surface area of a nucleus (A) and the circumference of the nucleus (U_{surf}) (Mersmann, 2001).

$$k' = U_{surf}\dot{n}_{surf} + A\dot{n}_{\upsilon} \tag{7.8}$$

where the impact rate of units from the volume ($\dot{n}_{\upsilon}$) and the impact rate of units from the surface ($\dot{n}_{Surf}$) is given by:

$$\dot{n}_{\upsilon} = \frac{3}{4} D_{AB} (CN_A)^{4/3} \tag{7.9}$$

$$\dot{n}_{Surf} = \frac{D_{surf}}{2\pi} (C_{ad} N_A)^{3/2} \tag{7.10}$$

while
$$D_{surf} = \frac{1}{4 d_m C_{ad} N_A} \sqrt{\frac{\pi k T N_A}{2\tilde{M}}} \tag{7.11}$$

A_c and U_c can be calculated from the radius of critical nucleus (r_c) and the contact angle (θ).

$$A_c = 2\pi r_c^2 (1 - \cos\theta) = 2\pi \left(\frac{2\tilde{M}\gamma_{CL}}{\rho_c \nu R T \ln S} \right)^2 (1 - \cos\theta) \tag{7.12}$$

$$U_c = 2\pi r_c \sin\theta = 2\pi \left(\frac{2\tilde{M}\gamma_{CL}}{\rho_c \nu R T \ln S} \right) \sin\theta \tag{7.13}$$

Combining equations (7.1) -(7.13), the rate of heterogeneous nucleation can be obtained.

$$B_{het} = \frac{1}{2\pi} a_{for} d_m He_{ad} (CN_A)^{7/3} \sqrt{\frac{f\gamma_{CL}}{kT}} V_m$$
$$\times \left(\frac{(\sin\theta) D_{surf}}{r_c} He_{ad} d_m^{3/2} (CN_A)^{1/6} + 3\pi D_{AB} (1 - \cos\theta) \right)$$
$$\times \exp\left[-f \left(\frac{4}{3} \right) \pi \frac{\gamma_{CL}}{kT} \left(\frac{2\tilde{M}\gamma_{CL}}{\rho_c \nu R T \ln S} \right)^2 \right] \tag{7.14}$$

The induction time is normally found to have an inverse ratio relationship with nucleation rate. It can be expressed by (Mullin, 2000; Myerson, 2002):

$$t_{ind}^{-1} = KB \tag{7.15}$$

where K is a coefficient of proportionality.

Combining equation (7.14) and (7.15), the following equation is obtained:

$$t_{ind}^{-1} = \frac{1}{2\pi} Ka_{for} d_m He_{ad} (CN_A)^{7/3} \sqrt{\frac{f\gamma_{CL}}{kT}} V_m$$

$$\times \left[\frac{(\sin\theta) D_{surf}}{\left(\frac{2\tilde{M}\gamma_{CL}}{\rho_c \nu RT \ln S} \right)} He_{ad} d_m^{3/2} (CN_A)^{1/6} + 3\pi D_{AB} (1 - \cos\theta) \right]$$

$$\times \exp\left[-f\left(\frac{4}{3}\right)\pi \frac{\gamma_{CL}}{kT} \left(\frac{2\tilde{M}\gamma_{CL}}{\rho_c \nu RT \ln S} \right)^2 \right] \tag{7.16}$$

When the heat of ultrasound can be removed instantly, K, a_{for}, d_m, He_{ad}, N_A, C, T, V_m, k, $\tilde{M}$, ν, R will be constant at the same concentration. D_{AB}, and D_{surf} will both increase with ultrasound. To investigate the effect of ultrasound on f and θ, natural logarithm is taken on both sides of equation (7.16).

$$\ln t_{ind} = A_1 + B_1 + C_1 \ln^{-2} S \tag{7.17}$$

where

$$A_1 = -\ln\left[\frac{1}{2\pi} Ka_{for} d_m He_{ad} (CN_A)^{7/3} V_m \sqrt{\frac{f\gamma_{CL}}{kT}} \right] \tag{7.18}$$

$$B_1 = -\ln\left[\frac{(\sin\theta) D_{surf}}{\left(\frac{2\tilde{M}\gamma_{CL}}{\rho_c \nu RT \ln S} \right)} He_{ad} d_m^{3/2} (CN_A)^{1/6} + 3\pi D_{AB} (1 - \cos\theta) \right] \tag{7.19}$$

$$C_1 = f\left(\frac{4}{3}\right)\pi \frac{\gamma_{CL}}{kT} \left(\frac{2\tilde{M}\gamma_{CL}}{\rho_c \nu RT} \right)^2 \tag{7.20}$$

The second term B_1 can be divided into the contribution of the impacts coming from the volume and the contribution of the impacts from the surface of the foreign particle on the circumference of the nucleus. When concentration is high or when He_{ad} or D_{surf} is small, the dominant contribution is from the volume. In normal conditions, the contribution of the surface is much smaller than the contribution from the volume. Therefore B_1 can be simplified to the form of equation (7.21) (Mersmann, 2001).

$$B_1 = -\ln[3\pi D_{AB} (1 - \cos\theta)] \tag{7.21}$$

Thus, in normal conditions there is a linear relationship between $\ln^{-2}(S)$ and $\ln(t_{ind})$. By comparing the slope of equation (7.17), the effect of ultrasound on geometric correction factor (f) and the contact angle (θ) can be determined.

At the critical supersaturation ratio (S_{crit}), the rate of heterogeneous nucleation is equal to the rate of homogeneous nucleation. Since the rate of heterogeneous nucleation depends on the volumetric surface (a_{for}), contact angle (θ) or geometric correction factor (f) and adsorption constant (He_{ad}), all these above parameters can influence the value of S_{crit}.

The homogeneous nucleation can be expressed by equation (3.14) (Mersmann, 2001). And the relationship of induction time and supersaturation ratio can be expressed as following equations (3.17)-(3.19), when nucleation is predominantly homogeneous.

From equations (7.17) and (3.17),

$$\frac{3}{2}a_{for}d_m He_{ad}(CN_A)^{7/3}\sqrt{\frac{f\gamma_{CL}}{kT}}V_m D_{AB}(1-\cos\theta)$$

$$\times\exp\left[-f\left(\frac{16}{3}\right)\pi\left(\frac{\gamma_{CL}}{kT}\right)^3\left(\frac{1}{C_C N_A}\right)^2\frac{1}{(\nu\ln S_{crit})^2}\right]=$$

$$1.5D_{AB}(CN_A)^{7/3}\sqrt{\frac{\gamma_{CL}}{kT}}\frac{1}{C_C N_A}\exp\left[-\frac{16}{3}\pi\left(\frac{\gamma_{CL}}{kT}\right)^3\left(\frac{1}{C_C N_A}\right)^2\frac{1}{(\nu\ln S_{crit})^2}\right] \quad (7.22)$$

Simplifying above equation, following equation can be obtained.

$$a_{for}d_m He_{ad}\sqrt{f}(1-\cos\theta)\exp\left[\frac{16}{3}\pi\left(\frac{\gamma_{CL}}{kT}\right)^3\left(\frac{1}{C_C N_A}\right)^2\frac{1-f}{(\nu\ln S_{crit})^2}\right]=1 \quad (7.23)$$

Taking natural logarithm on both sides of equation (7.23).

$$\ln\left[a_{for}d_m He_{ad}\sqrt{f}(1-\cos\theta)\right]=-\frac{16}{3}\pi\left(\frac{\gamma_{CL}}{kT}\right)^3\left(\frac{1}{C_C N_A}\right)^2\left[\frac{1-f}{(\nu\ln S_{crit})^2}\right] \quad (7.24)$$

Solving for critical supersaturation ratio (S_{crit}),

$$\frac{1}{(\ln S_{crit})^2}=\frac{\ln\left[\frac{1}{2}a_{for}d_m He_{ad}(1-\cos\theta)^2\sqrt{2+\cos\theta}\right]}{-\frac{16}{3}\pi\left(\frac{\gamma_{CL}}{kT}\right)^3\left(\frac{1}{C_C N_A\nu}\right)^2\left(\frac{2+3\cos\theta-\cos^3\theta}{4}\right)} \quad (7.25)$$

where the value of $\frac{16}{3}\pi\left(\frac{\gamma_{CL}}{kT}\right)^3\left(\frac{1}{C_C N_A \nu}\right)^2$ can be obtained from the straight line plots of $\ln^{-2}(S)$ versus $\ln(t_{ind})$ basing on equation (3.17), and the relationship between S_{crit} and θ can be determined from equation (7.25).

And the relationship between the induction time (t_{ind}) and the relative supersolubility (σ) can be expressed by equation (3.5):

$$\ln(t_{ind}) = \ln\left(\frac{K_1}{k_N C_s^n}\right) - n\ln(\sigma) \tag{3.5}$$

From the relationship between $\ln(t_{ind})$ and $\ln(\sigma)$, the apparent nucleation order can be determined.

7.3 Experimental

The experimental apparatus is shown in Figure 7.1. The experimental instruments and procedures are very close to induction time experiments when nucleation is predominantly homogeneous. That is: the experiments were also carried out at 25℃ in the jacketed glass vessel (55mm diameter). Barium sulphate was precipitated by mixing aqueous $BaCl_2$ solution and Na_2SO_4 solutions. The 750 W ultrasonic processor with the frequency of 20 kHz (Cole-Parmer Instruments, Illinois, USA) was also used and the ultrasound is delivered from the similar titanium probe with a tip of 8mm in diameter. The ultrasonic wave travels downwards and reflects from the vessel base.

The difference of homogeneous experiments and heterogeneous experiments is the temperature control process. The temperature in heterogeneous experiments is controlled by both a water-bath and a temperature controller. Because the working time of ultrasonic processor in the heterogeneous nucleation experiment is much longer than its working time in homogeneous nucleation experiments, the heat produced by power input cannot be eliminated quickly enough. So the temperature of solution will continue to increase. It is found that if a water-bath only is used to control temperature, temperature can increase

by even 7.8 degrees with the highest power input, if the working time is long enough. So a temperature controller is required in this experiment.

The temperature of water-bath is adjusted to 17.2 ℃ to make sure all the heat generated can be removed quickly. The temperate controller is connected with a 70W heater, which is higher than the highest ultrasonic power input in this experiment. The reason why the heater power needs to be higher than power input is in order to maintain the constant temperature at 25℃ at the initial stage of experiment. At this time, the ultrasound does not work on solution and temperature is lower than 25℃. Only a heater with power higher than the power input can make sure the temperature is kept at 25℃, since the heat input can be kept equal to the heat removed.

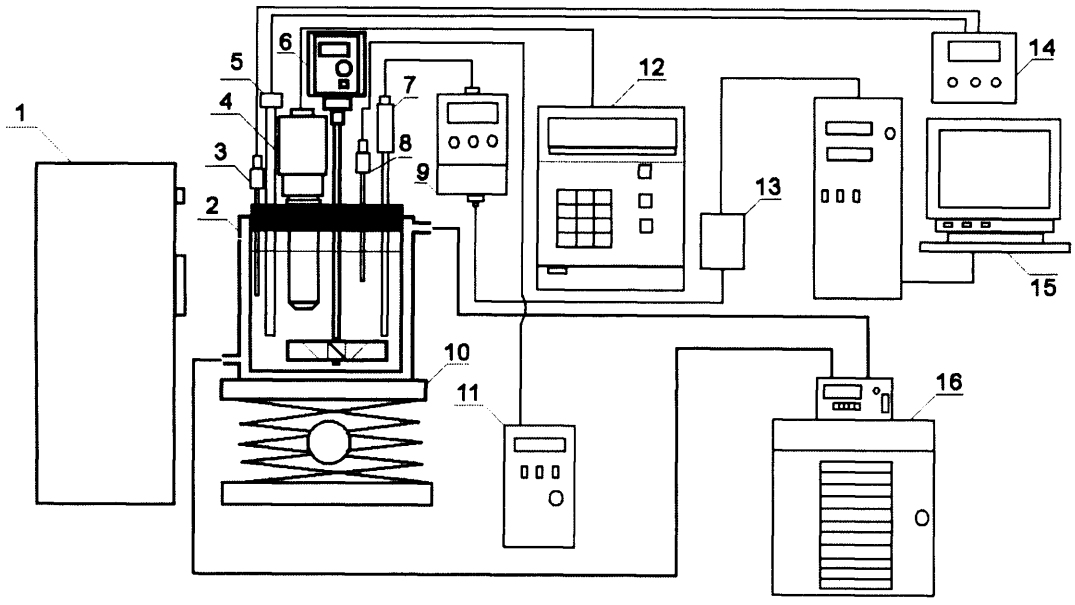

Fig 7.1 Sketch of the apparatus for measuring induction time

1. Focus lamp
2. Jacketed vessel
3. Thermoelectric couple
4. Ultrasonic probe
5. Heater
6. Agitation motor
7. The probe of nephelometer
8. The probe of temperature meter
9. Nephelometer
10. Iron shelf
11. Temperature meter
12. Ultrasonic processor
13. Cable hub
14. Temperature controller
15. Computer
16. Water-bath

Through a thermocouple, the temperature controller can detect temperature change in the solution. If the temperature in solution is lower than 25℃, the controller will switch on the heater. Because the power of heater is higher than the rate of heat removing, temperature will come back to 25℃ quickly. And if the solution temperature is higher than 25℃, the controller will switch off the heater to let redundant heat be removed. From experiment, it is found that the temperature can be controlled in the range of ±0.3K. Thus, the influence of temperature on induction time can be ignored.

The mixing in the experiment is also achieved with the use of a pitch blade impeller with an agitation rate of 400rpm. The appearance of nuclei is also detected by a nephelometer (Guo et al., 2006). A computer is connected to the instrument. The change of turbidity, which is recorded as the change of input voltage, is collected automatically by software (SP 1300- PD from Data Translation Ltd). It has been demonstrated that measuring induction time by nephelometer is reliable and reproducible in the existing literature (Guo et al., 2006). The time between initial mixing and the first observed change of turbidity, which is reflected as the change of voltage, is defined as induction time in this experiment. Since the induction time can be obtained from change of voltage, there is no need to calibrate voltage and turbidity.

The supersaturation level of barium sulphate can be determined from equations (3.22) and (3.23) (Mullin, 2000). And the activity coefficient of $BaSO_4$ can be obtained from Bromley correlation, which is expressed as equation (3.24) (Söhnel and Garside, 1992). From the above equations, the supersaturation ratio (S) can be calculated.

The relationship between power input into the system and amplitude of maximal energy output is expressed in Figure 3.1.

5 amplitudes of ultrasonic processor, 21%, 31%, 41%, 51% and 61% of maximum power, are also selected to determine the influence of energy value on nucleation. From former calculation, when the amplitude is 21% of maximum power, the power input value is 8.62W, 31%: 18.0W, 41%: 27.3W, 51%: 36.6W, 61%: 46.0W.

$BaCl_2$ and Na_2SO_4 solutions with the concentration as 0.01M are also used in the experiments when nucleation is predominantly heterogeneous. In each experiment, required amounts of $BaCl_2$ and Na_2SO solutions are precisely measured and transferred by Finnpipettes to smaller volumetric flasks. The solutions with required concentrations are made. After the $BaCl_2$ solution is transferred into the vessel, the nephelometer, the impeller and the temperature controller are switched on. After the signal of voltage and the temperature become stable, Na_2SO_4 solution is immediately injected into the vessel. Simultaneously, the power ultrasound is run until the computer shows the induction time. During the process, the temperature is kept at 25℃ and the agitation rate is maintained at 400 rpm. These procedures are very close to the experiment to measure induction time when nucleation is predominantly homogeneous (Guo et al., 2006).

7.4 Results and discussion

The result of the induction time experiments with and without ultrasound, when nucleation is consistent with a predominantly heterogeneous model, is shown in Figure 7.2. From this figure, the induction time decreases when supersaturation increases with and without ultrasound. From the experiments, however, it is observed that ultrasound has a significant effect in reducing the induction time. At the same supersaturation level, the induction time reduces with increasing ultrasonic energy. This phenomenon is similar to the ultrasonic effect on nucleation, when nucleation is consistent with a predominantly homogeneous model (Guo et al., 2006).

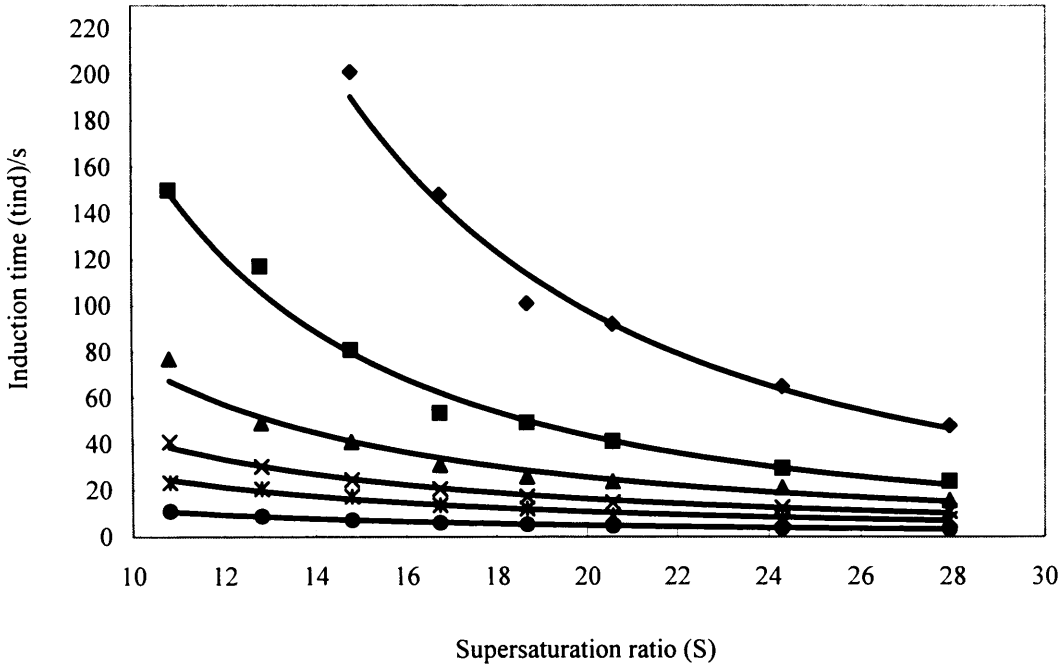

Fig 7.2 Induction time as a function of supersaturation ratio
(◆) The experimental data without ultrasound
(■) The experimental data with the power input of 8.62W
(▲) The experimental data with the power input of 18.0W
(╳) The experimental data with the power input of 27.3W
(*) The experimental data with the power input of 36.6W
(●) The experimental data with the power input of 46.0W

Plots of $\ln(t_{ind})$ versus $\ln^{-2}(S)$ are shown in Figure 7.3. The data in Figure 7.3 shows two distinct regions with similar power inputs. This phenomenon is consistent with the experimental results without ultrasound. The linear portion with a lower slope at high $\ln^{-2}(S)$ values is due to the dominance of heterogeneous nucleation in the low supersaturation range, while the linear portion at low $\ln^{-2}(S)$ values is due to dominance of homogeneous nucleation in the high supersaturation range (Mullin, 2000). When

nucleation is consistent with a predominantly heterogeneous model, $\ln(t_{ind})$ and $\ln^{-2}(S)$ exhibits a linear relationship in Figure 7.3. This observation demonstrated that the contribution of the impacts from the surface to k' can be ignored. The relationships of $\ln(t_{ind})$ and $\ln^{-2}(S)$ represent equation (7.17) and (7.21) well.

From Figure 7.3, the values of slope and intercept of the straight line without ultrasound are 29.828 and 1.205 respectively. When ultrasound is applied to the system, the corresponding values for the straight line with 8.62W are 21.955 and 1.273; 18.0W: 17.490 and 1.249; 27.3W: 15.448 and 1.032; 36.6W: 14.466 and 0.736; 46.0W: 13.939 and 0.007. The slopes and the intercepts of straight lines with different power inputs are different to each other. Similar non-parallel straight lines of $\ln(t_{ind})$ versus $\ln^{-2}(S)$ with different power inputs are observed in cooling crystallization experiments with potassium sulphate (Lyczko et al., 2002).

The mechanism of ultrasonic radiation on homogeneous nucleation has already been analyzed. From the experiment of ultrasonic effect on homogeneous nucleation, it is found that when temperature is kept constant, the main effect of ultrasound is to increase the diffusion coefficient (D_{AB}). Other parameters change only slightly or remain constant within the ultrasonic field.

When nucleation is predominantly heterogeneous, the influence from foreign particles to nucleation rate becomes significant by its catalytic effect, which results decrease in the energy barrier to nucleation (Söhnel and Garside, 1992). This effect is determined by the contact angle (θ), which will change geometric correction factor (f) subsequently. The unparallel straight lines in Figure 7.3 show that in addition to D_{AB}, ultrasound will change other parameters in equation (7.17). If γ_{CL} is kept constant, the only parameter that could be changed is geometric correction factor (f).This effect causes the slopes of the straight lines of $\ln(t_{ind})$ versus $\ln^{-2}(S)$ change.

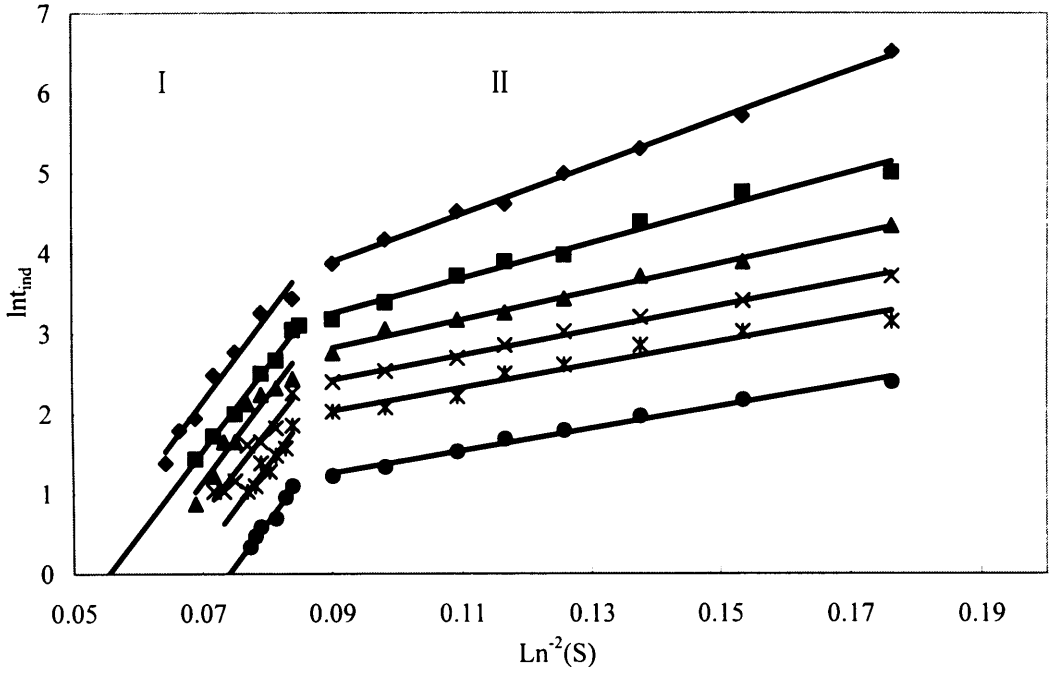

Fig 7.3 The plots of $ln^{-2}(S)$ versus $ln(t_{ind})$

At Zone I , when nucleation is consistent with a predominantly homogeneous model

(◆) The experimental data without ultrasound
(■) The experimental data with the power input of 8.62W
(▲) The experimental data with the power input of 18.0W
(×) The experimental data with the power input of 27.3W
(*) The experimental data with the power input of 36.6W
(●) The experimental data with the power input of 46.0W

At Zone II , when nucleation is consistent with a predominantly heterogeneous model

(◆) The experimental data without ultrasound
(■) The experimental data with the power input of 8.62W
(▲) The experimental data with the power input of 18.0W
(×) The experimental data with the power input of 27.3W
(*) The experimental data with the power input of 36.6W
(●) The experimental data with the power input of 46.0W

When nucleation is consistent with a predominantly homogeneous model, it is found that the straight lines of $\ln(t_{ind})$ versus $\ln^{-2}(S)$ are parallel with each other and the average slope can be obtained as 105.56. From the ration of the slope of the straight line during heterogeneous nucleation to the slope of the straight line during homogeneous nucleation, the value of f with different ultrasonic power inputs can be obtained. They are: 0.283 without ultrasound; 0.208 with 8.62W; 0.166 with 18.0W; 0.146 with 27.3W; 0.137 with 36.6W; 0.132 with 46.0W. The relationship between f and power input values is shown in Figure 7.4. It is found that f decreases with the increase of power input, but the gradient of f with power input decreases with the increase of power input. That is: when the power input is high, a given increase in ultrasonic energy, does not bring about as significant an effect on f as when the power input is low.

A similar phenomenon was also observed in the experiments of Lyczko et al. (2002). It is found that when nucleation is predominantly heterogeneous with potassium sulphate as the substance, the slopes of the straight lines of $\ln(t_{ind})$ versus $\ln^{-2}(S)$ are 3.69×10^{-2} without ultrasound; 2.35×10^{-2} with 0.05W g^{-1} solution; and 0.91×10^{-2} with 0.12W g^{-1} solution. This experiment did not measure the induction time data during homogeneous nucleation, so f values cannot be obtained because of the lack of the slope value of $\ln(t_{ind})$ versus $\ln^{-2}(S)$ during homogeneous nucleation. But since this slope value does not change at different power inputs during homogeneous nucleation, the trend of power input to f can be evaluated. It is also found that when potassium sulphate is used as the working substance, f decreases with the increase of power input and the gradient of f with power input decreases with the increase of power input.

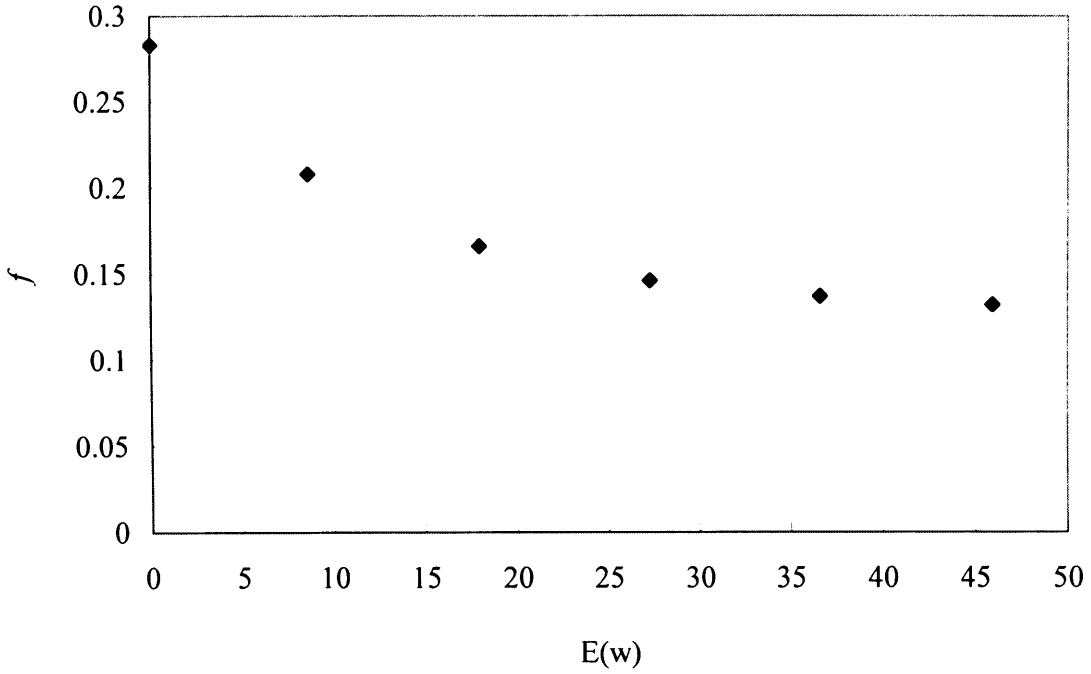

Fig 7.4 The plots of geometric correction factor (*f*) versus ultrasonic power input (*E*)

From equation (7.7), the contact angle (θ) can be obtained from the value of f. They are: 72.61° without ultrasound; 65.61° with 8.62W; 61.08° with 18.0W; 58.81° with 27.3W; 57.65° with 36.6W; 57.01° with 46.0W. The ultrasonic effect on θ is shown in Figure 7.5. Because θ increases with f, the relationship between θ and power input are very close to the relationship between f and energy. Thus θ decreases with the increase of power input and the gradient of θ with power input decreases with the increase of power input.

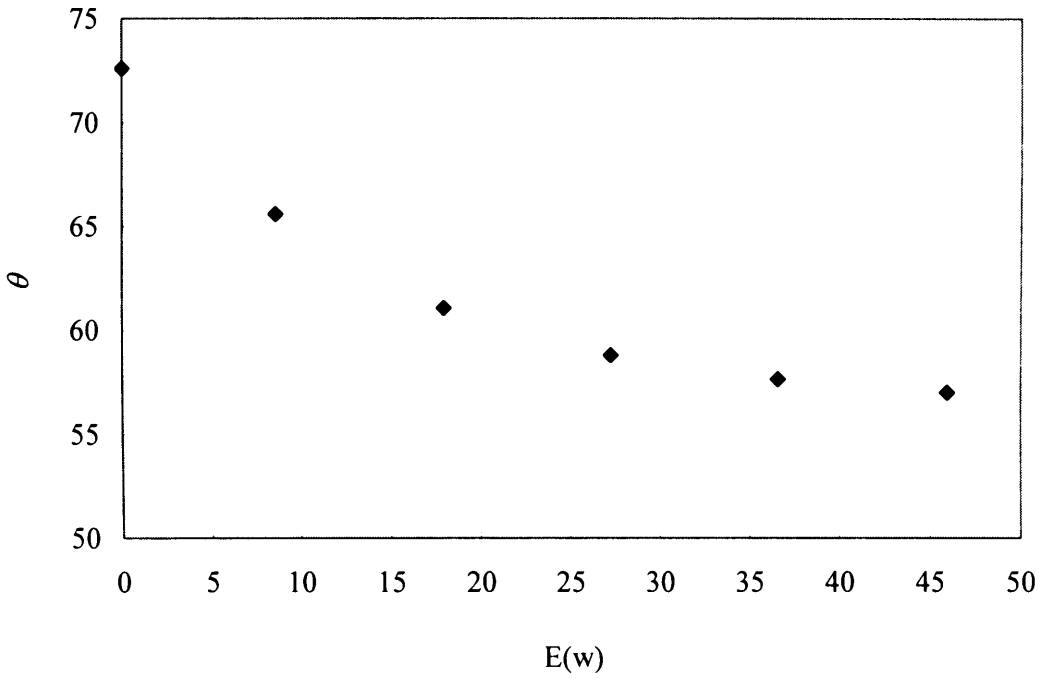

Fig 7.5 The plots of contact angle (θ) versus ultrasonic power input (*E*)

There are three possible reasons why the contact angle (θ) should change with power input:

a)- The shock wave caused by the cavitational bubble implosion may bring force (F in Figure 7.6) to nuclei. The force can compress the crystal and change the crystal shape. This will consequently reduce the contact angles (θ). From Figure 7.6, the three interfacial tensions are denoted by contact angles (θ) can be explained by γ_{CL} (between the solid and the liquid), γ_{CS} (between the solid crystalline phase and the foreign solid surface) and γ_{SL} (between another foreign solid surface and the liquid). Resolving these forces in a horizontal direction can obtain following equation (Mullin, 2000).

$$\gamma_{SL} = \gamma_{CS} + \gamma_{CL} \cos\theta \tag{37}$$

The force in the crystal, which is caused by crystal habit change, will work with the

interfacial tension to balance force F to reach a new equilibrium.

b)-Another reason why ultrasound can decrease the geometric correction factor (f) and the contact angles (θ) is on account of the cavitation bubbles. From Aquilano et al. (2003), in a heterogeneous system nucleation can occur in the solution bulk (homogeneous nucleation); on the foreign solid surface; at the cavitation bubble/solution interface and at the bubble/solution/foreign solid interface.

With the increase of power input, the density of cavitation bubbles in the solution also increases. Thus, more useful sites for crystal nucleation will form in the solution. The increase of energy can also increase vibration intensity of cavitation. And to maintain vibration of cavitation, ultrasound needs to overcome more resistance, which is composed of interfacial tension and the force between solvent molecules. When nucleation process occurs at the cavitation bubble/solution interface, both the interfacial tension between the solid crystalline phase and cavitation bubble surface and the interfacial tension between the liquid and cavitation bubble may be increased with the increase of energy. This effect may change the contact angles (θ) consequently.

c)-The nucleation process occurring at bubble/solution/foreign solid interface, which is also shown in Figure 7.6, is more complex. In this case, both the change of bubble diameters and the change of interfacial tensions can influence θ. And the increase of cavitation density may also make more nuclei growing at bubble/solution/foreign solid interface.

It is also observed that the gradient of θ with power input decreases with the increasing power input. One reason for above phenomenon is that the deformation of nuclei may generate another force to counteract the force from ultrasound. And this force may increase with the increase of ultrasonic energy, when the deformation of nuclei becomes bigger. This makes the gradient of θ with power input decrease with the increase of power input.

Another reason why the gradient of θ with power input decreases with the increasing power input may be the increase of ultrasonic energy absorption by solution.

The higher the power input, the higher part of ultrasonic energy may be transferred into heat after absorption by the solution. And this part of energy is not available kinetic energy to bring any influence to clusters.

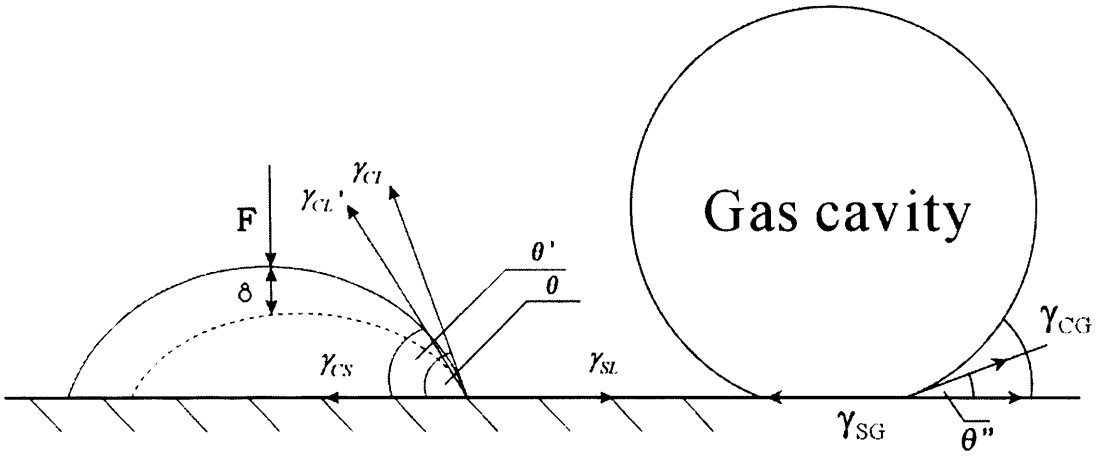

Fig 7.6 The influence of ultrasound on contact angle(θ)

The force can compressing the crystal and the nucleation process occurring at bubble/solution / foreign solid interface is another predominant reason why contact angle (θ) decreases with the increase of power input.

To determine which reason in a), b), c), mentioned above, has more contribution to the change of the contact angles (θ), the ultrasonic effect on critical supersaturation ratio (S_{crit}) is also investigated. S_{crit} determines the mechanism of nucleation process at certain supersaturation. Its value can be experimentally determined from the point of intersection between the straight line of $\ln(t_{ind})$ versus $\ln^{-2}(S)$ during heterogeneous nucleation and the corresponding straight line during homogeneous nucleation. From Figure 7.3, the values of S_{crit} are: 30.2 without ultrasound, 30.5 with 8.62W, 30.8 with 18.0W, 30.6 with 27.3W; and 30.2 with 36.6W, and 30.7 with 46.0W. The value of S_{crit} changes with different power inputs, but the variance is not significant.

At critical supersaturation ratio, the rate of heterogeneous nucleation is equal to the rate of homogeneous nucleation. Without considering the nucleation process occurring at the cavitation bubble/solution interface and at bubble/solution/foreign solid interface, the critical supersaturation ratio (S_{crit}) can be simulated by equation (7.25). From equation (7.25), the value of volumetric surface of foreign particles (a_{for}) can influence S_{crit}. In reality, it is impossible to remove completely all solid matter from a solvent or solution (Mersmann, 2001) and even in ultrapure water, many SiO_2 particles in the size range of only a few nanometers can be found. Schubert estimated that the volumetric surface of foreign particles (a_{for}) in ultrapure water is approximately $2.5\times 10^3 m^2/m^3$, which is used in the simulation of S_{crit} in this experiment since it is very difficult to determine the value of a_{for} directly. The adsorption constant of $BaSO_4$ and SiO_2 was also estimated by Mersmann (2001) to be $He_{ad}=1.1\times 10^{-8}$ at 25℃. While the value of interfacial tension (γ_{CL}), obtained from homogeneous nucleation experiment, 61.89 mJ/m^2, is used in this simulation. The value of γ_{CL} is not constant at different Na^+ concentrations (He et al., 1995), but because the change of Na^+ concentration during homogeneous nucleation experiments is not significant, it is believed that the deviance of γ_{CL} at S_{crit} and at homogeneous nucleation section is not significant. The relationship between S_{crit} and contact angle (θ) is shown in Figure 7.7.

The comparison between simulated results and the experimental results are shown in Figure 7.8. It is found that from the simulation, the critical supersaturation ratio (S_{crit}) increases with the decrease of contact angle (θ), but, the simulation result is not consistent with the experimental results. As mentioned above, some parameters in equation (7.25), such as volumetric surface of foreign particles (a_{for}) and interfacial tension (γ_{CL}), cannot be determined precisely, but the influence of these parameters to the simulated values is significant. This is the reason why simulated value of S_{crit} is different from experimental value. But it is found that the trend that S_{crit} increases with the decrease of θ does not change at different a_{for} and γ_{CL}. So from the deviation of the simulation

result and the experimental results, it can be concluded that in addition to reason a), reason b) and c) may also have influence on the contact angle (θ) change.

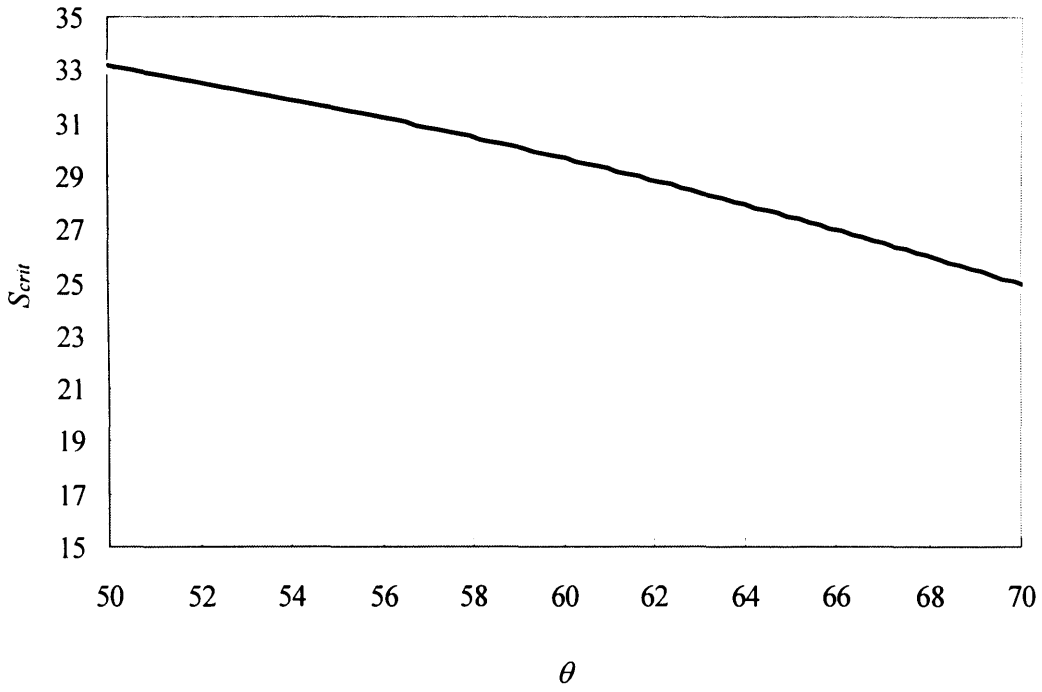

Fig 7.7 The simulated relationship between critical supersaturation ratio (S_{crit}) and contact angle (θ)

Talanquer (2002) mentioned that the interfacial tension for a liquid-liquid interface always tends to be smaller than that for a gas-liquid interface. Thus the barrier to nucleation should be lower for liquid-like clusters than for gas-like nuclei and the formation of the former will be favored. This means that the nucleation rate at the cavitation bubble/solution interface should be much lower than homogeneous nucleation rate, when nucleation is predominantly heterogeneous. Thus, it can be concluded that reason b) should not be the main reason of the contact angle decrease since very few nuclei forming at the cavitation bubble/solution interface.

From Figure 7.8, it is also observed that S_{crit} keeps increasing with power input when

it is low. The reason of this phenomenon is the cavitaiton density is not so high as when power input is high. The trend of S_{crit} changing with θ is consistent with equation (7.25). So Both a) and c) are the predominant reasons why the contact angle (θ) decreases with increasing power input.

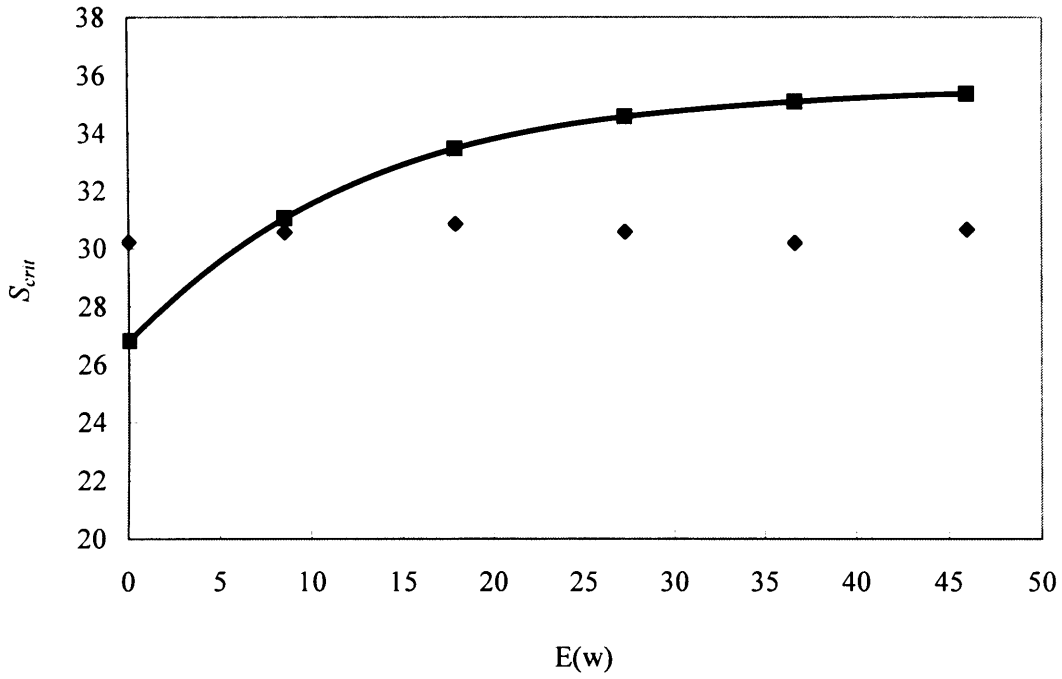

Fig 7.8 The comparison of simulated values of critical supersaturation ratio (S_{crit}) and its experimental results
(◆) The experimental results of S_{crit}
(■) The simulated results of S_{crit}

Compared to homogeneous nucleation, when nucleation is consistent with a predominantly heterogeneous model, in addition to the increase of diffusion coefficient (D_{AB}), the reduction of contact angles (θ) and geometric correction factor (f) can further increase the nucleation rate. If the temperature keeps constant during experiments, and if the input energy of ultrasound does not change at different supersturation levels, D_{AB} will keep constant during both heterogeneous nucleation and homogeneous nucleation

processes at the same amplitude of ultrasonic processor. Thus the effect of ultrasound on the rate of heterogeneous nucleation is more significant than its effect during homogeneous nucleation.

Conventionally, the relationship of t_{ind} as a function of the relative supersolubility is also expressed by equation (3.5). The plots of $\ln(t_{ind})$ versus $\ln(\sigma)$ for experiments are shown in Figure 7.9. From this figure, three zones are observed. Zone I corresponds to heterogeneous nucleation, Zone II corresponds to mixed mechanisms and Zone III corresponds to homogeneous nucleation respectively (Söhnel and Garside, 1992). In Zone I , it is observed that the induction time decreases when supersaturation increases and that ultrasound has a significant effect in reducing the induction time. At a given supersaturation level, the induction time decreases with increasing ultrasonic energy. The slope and intercept of the straight line without ultrasound are –2.51 and 12.00 respectively. When ultrasound is applied to the system, the corresponding values for the straight line with the power input of 8.62W are –1.88 and 9.30, 18.0W: –1.48 and 7.59, 27.3W: –1.31 and 6.66, 36.6W: –1.25 and 6.05, 46.0W: –1.19 and 5.11. The values of apparent nucleation order (n) are 2.51 without ultrasound, 1.88 with the power input of 8.62W; 1.48 with 18.0W; 1.31 with 27.3W; 1.25 with 36.6W; 1.19 with 46.0W. It is found that that when nucleation is consistent with a predominantly heterogeneous model, ultrasound can change the apparent nucleation orders (n). n decreases with the increase of ultrasonic power input.

When nucleation is predominantly heterogeneous, the ultrasonic effect on nucleation coefficient (k_N) can also be evaluated from equation (3.5). As shown in Figure 7.10, compared to k_N without power input, the k_N value with the power input of 8.62W is increased by 1.29 fold; 1.58 fold with the power input of 18.0W; 1.80 fold with 27.3W; 1.98 fold with 36.6W; 2.35 fold with 46.0W. Thus, the ultrasound increases the nucleation coefficient (k_N).

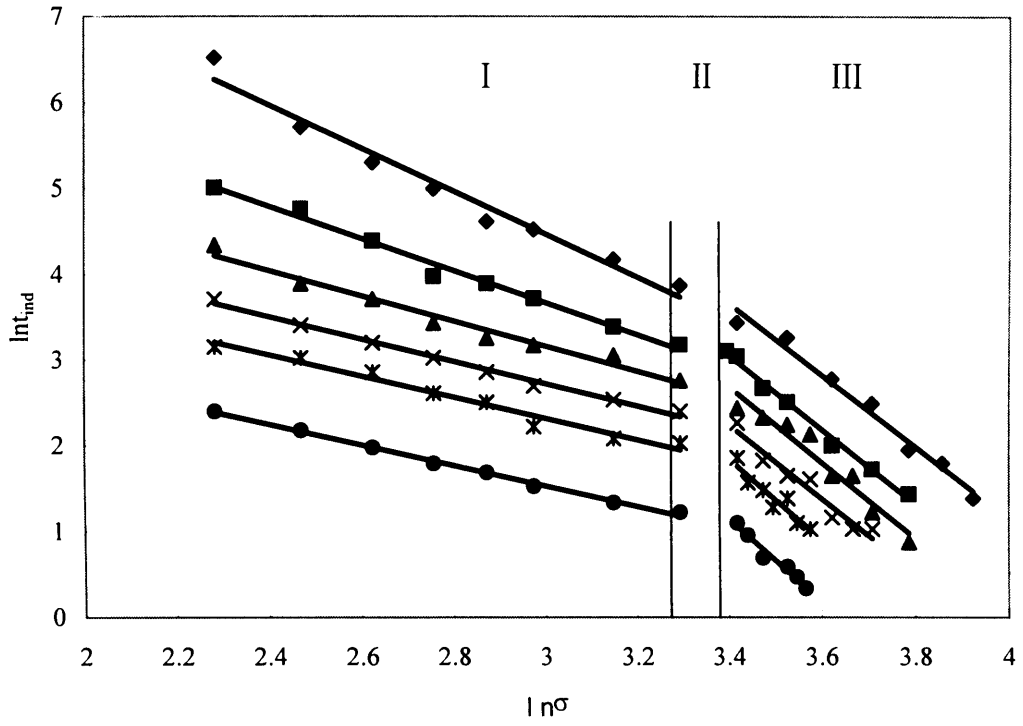

Fig 7.9 Induction time as a function of relative supersolubility
(◆) The experimental data without ultrasound
(■) The experimental data with the power input of 8.62W
(▲) The experimental data with the power input of 18.0W
(×) The experimental data with the power input of 27.3W
(*) The experimental data with the power input of 36.6W
(●) The experimental data with the power input of 46.0W

From Guo et al. (2006), when nucleation is consistent with a predominantly homogeneous model, ultrasound does not increase the apparent nucleation order (n) significantly, but increases nucleation coefficient (k_N) markedly. However, when nucleation is consistent with a predominantly heterogeneous model, both n and k_N are increased significantly, but the increase fold of k_N is not so significant during heterogeneous nucleation. From Figure 7.10, k_N has an exponential relationship with power input. It is consistent with equation (3.2).

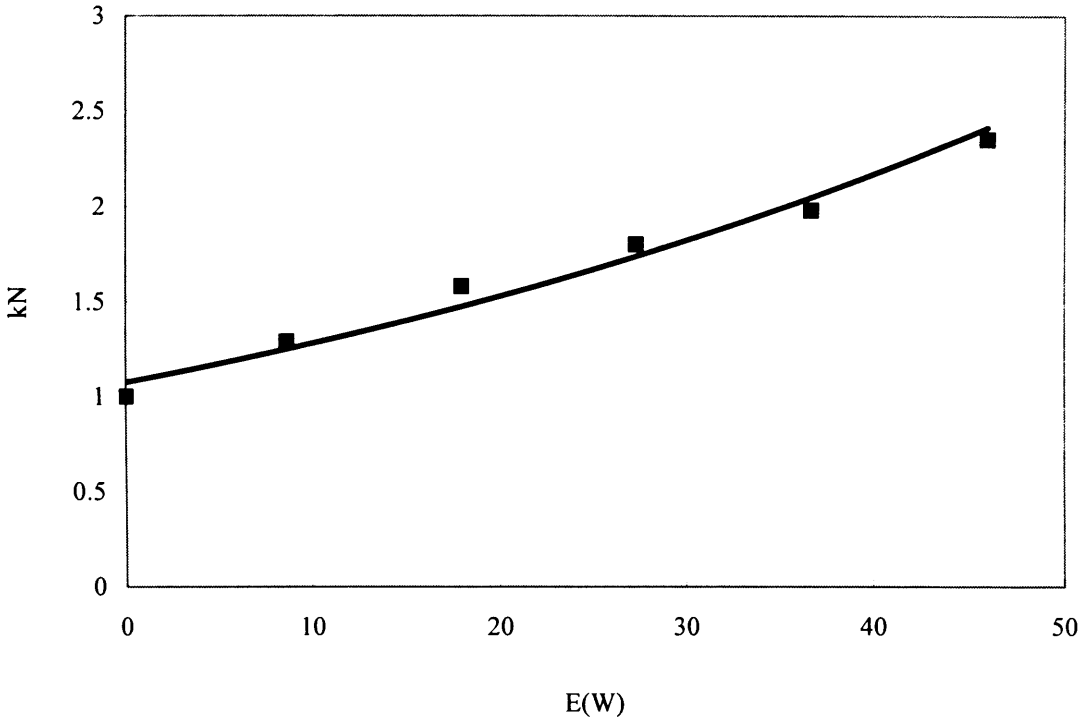

Fig 7.10 The variation of power input vs the nucleation coefficient (k_N), compared to k_N without power input

7.5 Conclusion

The effect of ultrasound on reactive crystallization when nucleation is consistent with a predominantly heterogeneous model is studied by measuring the induction time. Barium sulphate is used as the working substance precipitated by mixing aqueous $BaCl_2$ and Na_2SO_4 solutions with relatively low concentrations compared to experiments for homogeneous nucleation. The experiments were carried with ultrasonic power input at 0, 8.62, 18.0, 27.3, 36.6 and 46.0W. It is observed that ultrasound has a significant effect in reducing the induction time.

The mechanism of the effect of ultrasound on heterogeneous nucleation is determined. Compared to homogeneous nucleation, the mechanism of ultrasonic effect

on heterogeneous nucleation is more complex. From the non-parallel straight lines of plots of $\ln(t_{ind})$ versus $\ln^{-2}(S)$, it is found that geometric correction factor (f) and the contact angles (θ) decrease with increasing power input, but both the gradient of f with power input and the gradient of θ with power input decrease with increasing power input. That is: when the power input is high, a given increase in ultrasonic energy, does not bring about as significant effects on f and θ as when the power input is low.

The ultrasonic effect on critical supersaturation ratio (S_{crit}) is also investigated to determine the mechanism of the effect of ultrasound on f and θ. From the simulation of S_{crit}, it is found that the critical supersaturation ratio (S_{crit}) increases with the decrease of contact angle (θ). The values of S_{crit} are: 30.2 without ultrasound, 30.5 with 8.62W, 30.8 with 18.0W, 30.6 with 27.3W; and 30.2 with 36.6W, and 30.7 with 46.0W. S_{crit} changes with different power input, but the variance is not significant. The simulation result is not consistent with the experimental results, which means the force from the cavitational bubble implosion cannot be the only reason for the change of f and θ in the ultrasonic field. After analysis of other possible reasons for ultrasonic effect on f and θ, it is found that the nucleation process occurring at bubble/solution/foreign solid interface may also contribute to the decrease of f and θ in the ultrasonic field.

The ultrasonic effects on nucleation order (n) and the nucleation coefficient (k_N) are investigated as well. It is found that unlike homogeneous nucleation, ultrasound can decrease the apparent nucleation order (n) significantly, when nucleation is consistent with a predominantly heterogeneous model. The nucleation coefficient (k_N) is also changed substantially and increases exponentially with the power input.

CHAPTER 8

THE EFFECT OF ULTRASOUND ON CLUSTER COAGULATION DURING HETEROGENEOUS NUCLEATION

8.1 Introduction

In chapter 4, the ultrasonic effect on the clusters in solution was analyzed by a cluster coagulation model, when nucleation is consistent with a predominantly homogeneous model. It is found that the analysis of the induction time is consistent with clusters having 3 monomers being predominant in the solution for different power inputs. The number concentration of largest clusters increases slowly with the increase of power input. But compared to the increase of diffusion coefficient (D_{AB}), this effect is very small.

Ultrasound does not change the size of dominant cluster significantly when nucleation is consistent with a predominantly homogeneous model (Guo et al., 2006). But, because of the "catalytic effect" of foreign particles to nucleation process, however, nucleation mechanism of heterogeneous nucleation is more complex compared with homogeneous nucleation. With the influence of foreign particles, ultrasound may change the number of monomers in dominating clusters significantly and this effect may consequently change the heterogeneous nucleation rate. Since the heterogeneous nucleation commonly happens during industrial crystallization processes, the research on ultrasonic effect is very important for the laboratory-scale development and industrial scale-up of sonocrystallization technology.

In this chapter, the cluster coagulation model is used to calculate the induction time at different levels of supersaturation, when nucleation is consistent with a predominantly heterogeneous model. Barium sulphate is used as the working substance precipitated by mixing aqueous $BaCl_2$ and Na_2SO_4 solutions with relatively low concentrations compared to the experiments of homogeneous nucleation. A theoretical analysis of the total absolute deviation (ε) is used to evaluate the number of monomers in dominating clusters. Using this method, the ultrasonic effect on the cluster size in the solution is investigated with different power inputs, when nucleation is consistent with a predominantly heterogeneous model. The ultrasonic effect on dominant cluster size during heterogeneous nucleation is compared with its effect during homogeneous nucleation.

8.2 Theory

Particles of a foreign solid phase can act as a "catalyst " of nucleation. The catalytic effect of a foreign solid phase on nucleation is explained by the resulting decrease in the energy barrier to nucleation if the nucleus forms on the surface of the foreign phase (Söhnel and Garside, 1992). Heterogeneous nucleation has frequently been treated in terms of a spherical cap nucleus, as shown in Figure 8.1.

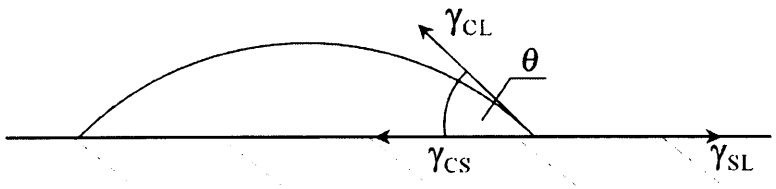

Fig 8.1 The nucleus forms on the surface of the foreign phase during heterogeneous nucleation

Solute monomers coagulate and form clusters after the solution is supersaturated. If the cluster size exceeds a critical value, a nucleus forms and the subsequent growth of nucleus leads to a crystal. The steady-state distribution of these molecular clusters can be calculated using equation (4.2) (Mullin, 2000):

Compared with homogeneous nucleation, when the nucleation is predominantly heterogeneous, foreign particles in solution will decrease the overall excess free energy of formation of a g-mer (ΔG_g) significantly and influence the nucleation rate consequently. From Figure 8.1, the three interfacial tensions are denoted by γ_{CL} (between the solid and the liquid), γ_{CS} (between the solid crystalline phase and the foreign solid surface) and γ_{SL} (between another foreign solid surface and the liquid). Resolving these forces in a horizontal direction can obtain following equation (Granberg et al., 2001; Mullin, 2000).

$$\gamma_{SL} = \gamma_{CS} + \gamma_{CL}\cos\theta \tag{8.1}$$

where θ is the contact angle between nuclear and foreign particle surface. Considering the "catalyst effect" of foreign particles, the overall excess free energy (ΔG_g) of the cluster, which is the sum of the surface excess free energy (ΔG_s) and the volume excess free energy (ΔG_v), can be expressed as (Zettlemoyer, 1969):

$$\Delta G_{g,het} = \pi(r\sin\theta)^2\gamma_{CS} - \pi(r\sin\theta)^2\gamma_{SL} + 2\pi r^2(1-\cos\theta)\gamma_{CL} + \frac{1}{3}\pi r^3(1-\cos\theta)^2(2+\cos\theta)\Delta G_{v,unit} \tag{8.2}$$

where r is the radius of curvature of the nucleus and $\Delta G_{v,unit}$ is the free energy change of the transformation per unit volume. Combining equations (8.1) and (8.2) leads the following equation for overall excess free energy:

$$\Delta G_{g,het} = \pi\gamma_{CL}r^2(-\sin^2\theta\cos\theta + 2 - 2\cos\theta) + \frac{1}{3}\pi r^3(1-\cos\theta)^2(2+\cos\theta)\Delta G_v \tag{8.3}$$

And equation (8.4) can be obtained from equation (8.3):

$$\Delta G_{g,het} = \pi\gamma_{CL}r^2(1-\cos\theta)^2(2+\cos\theta) + \frac{1}{3}\pi r^3(1-\cos\theta)^2(2+\cos\theta)\Delta G_v \tag{8.4}$$

The basic Gibbs-Thomson relationship can be written as:

$$\ln\frac{C}{C_s} = \ln S = \frac{2\gamma_{CL}V_m}{kTr} \tag{8.5}$$

where V_m is the monomer volume; this gives:

$$-\Delta G_{v,unit} = \frac{2\gamma_{CL}}{r} = \frac{kT\ln S}{V_m} \tag{8.6}$$

where k is the Boltzmann constant and T is the temperature (Mullin, 2000).

As mentioned in chapter 4, we consider that in the bulk solution, a single monomer has the smallest radius and is the fundamental unit of nuclei, so its excess free energy can be considered as zero (Guo et al., 2006). Using the above assumption and introducing the number of monomers in a cluster (g) into equation (8.4) leads to equation (8.7):

$$\Delta G_{g,het} = \pi\gamma_{CL}\left(\frac{3gV_m}{4\pi}\right)^{\frac{2}{3}}(1-\cos\theta)^2(2+\cos\theta) - \pi\gamma_{CL}\left(\frac{3V_m}{4\pi}\right)^{\frac{2}{3}}(1-\cos\theta)^2(2+\cos\theta)$$

$$-\frac{1}{4}(g-1)(1-\cos\theta)^2(2+\cos\theta)kT\ln S \tag{8.7}$$

A thermodynamically stable nucleus exists when the total enthalpy ΔG_g does not change when elementary units are added or removed, that is:

$$\frac{\partial \Delta G_g}{\partial g} = 0 \tag{4.5}$$

So the critical cluster size can be derived from the classical nucleation theory by differentiating equation (8.7).

$$g_c = \frac{32\pi V_m^2 \gamma_{CL}^3}{3(kT\ln S)^3} \tag{8.8}$$

which is similar as the critical cluster size model when nucleation is predominantly homogeneous.

$n_{\bar{g}}$ can be obtained by equation (4.7). And the induction time (t_{ind}) can be evaluated by equation (4.4). The values of the contact angle (θ) and geometric factor (f) have already been obtained from Figure 7.4 and Figure 7.5 in chapter 7.

Substituting equations (4.2), (8.7), (8.8), and (4.7) into equation (4.4) gives:

$$t_{ind} = \left(\frac{1}{8\pi D_{AB} r_{\bar{g}}}\right)\left[\frac{32\pi V_m^2\gamma_{CL}^3}{3\bar{g}(kT\ln S)^3} - 1\right]\left\{n_1^{-1}\exp\left[-\frac{\pi\gamma_{CL}\left(\frac{3gV_m}{4\pi}\right)^{\frac{2}{3}}(1-\cos\theta)^2(2+\cos\theta)}{kT}\right.\right.$$

$$\left.\left.\frac{-\pi\gamma_{CL}\left(\frac{3V_m}{4\pi}\right)^{\frac{2}{3}}(1-\cos\theta)^2(2+\cos\theta) - \frac{1}{4}(g-1)(1-\cos\theta)^2(2+\cos\theta)kT\ln S}{}\right]\right\} \tag{8.9}$$

From equation (8.9) the induction time (t_{ind}) can be evaluated by the contributions from diffusion, coagulation concentration and critical nuclei size. Because of "catalytic effect" of foreign particles, above model is much more complex than the model of

homogeneous nucleation.

8.3 Results and discussion

The supersaturation level of barium sulphate can be determined from equations (3.22) and (3.23) (Mullin, 2000). And the activity coefficient of $BaSO_4$ can be obtained from Bromley correlation, which is expressed as equation (3.24) (Söhnel and Garside, 1992). From the above equations, the supersaturation ratio (S) can be calculated.

Diffusion coefficient (D_{AB}) exhibits only a weak relationship with concentration of the solution. So if the temperature keeps constant during experiments, and if the power input of ultrasound does not change at different supersturation levels, D_{AB} will keep approximately constant during both heterogeneous nucleation and homogeneous nucleation processes at the same amplitude of ultrasonic processor. Here, from chapter 4, D_{AB} is: $3.65\times10^{-10}m^2/s$ without ultrasound, $6.90\times10^{-10}m^2/s$ with 8.62W, $9.93\times10^{-10}m^2/s$ with 18.0W, $1.52\times10^{-9}m^2/s$ with 27.3W, $2.37\times10^{-9}m^2/s$ with 36.6W, and 4.19×10^{-9} m^2/s with 46.0W (Guo et al., 2006).

The value of interfacial tension (γ_{CL}) varies with sodium chloride concentration. From He et al. (1995), γ_{CL} is $93.4mJ/m^2$ when NaCl concentration is lower than 0.03mol/L. When nucleation is consistent with a predominantly heterogeneous model, the concentration of solution added into system is relatively low. So the concentration of NaCl, one product of reaction, is also low. Thus, $93.4mJ/m^2$ is used here as the value of interfacial tension.

The change of overall excess free energy (ΔG_g) with the number of monomers in clusters (g) in solution, when nucleation is consistent with a predominantly heterogeneous model, is shown in Figure 8.2. The maximum value, where $d\Delta G/dg = 0$, corresponds to the critical nucleus.

It is found that when supersaturation ratio range is 31.49 to 51.59 with predominantly homogeneous nucleation, the number of monomers in critical nuclei varies between 14 and 21 (Guo et al., 2006). But when supersaturation ratio range is between 10.81 and 27.93

with predominantly heterogeneous nucleation, the number of monomers in critical nuclei varies between 79 and 216. Compared to homogeneous nucleation, the size of critical nuclei increases significantly, when nucleation is consistent with a predominantly heterogeneous model.

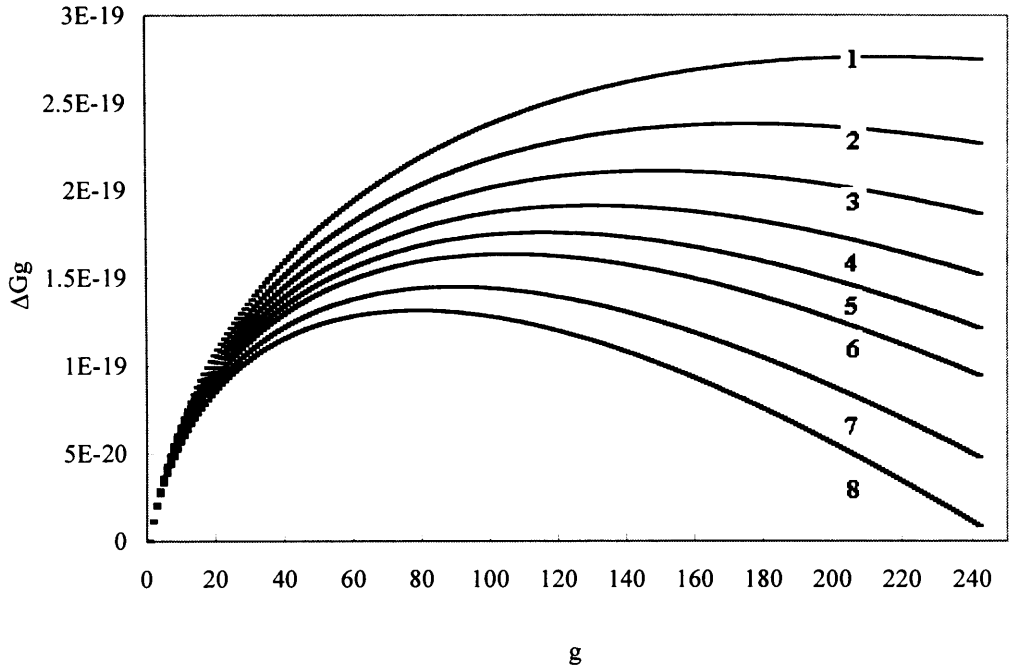

Fig 8.2 ΔG_g versus g in the solution, when nucleation is predominantly heterogeneous
Curve 1: with the supersaturation ratio of 10.81
Curve 2: with the supersaturation ratio of 12.82
Curve 3: with the supersaturation ratio of 14.80
Curve 4: with the supersaturation ratio of 16.75
Curve 5: with the supersaturation ratio of 18.67
Curve 6: with the supersaturation ratio of 20.57
Curve 7: with the supersaturation ratio of 24.29
Curve 8: with the supersaturation ratio of 27.93

From Figure 8.2, it is also observed that the requirement of ΔG_g to form a critical nuclei also increases. But because of catalytic effect of foreign particles, its increase is not

as significant as critical nuclei size. ΔG_g of critical nuclei increases from 6.97×10^{-20} J/molecule to 9.39×10^{-20}J/molecule, when supersaturation ratio decreases from 51.59 to 31.49 (Guo et al., 2006). But when nucleation is consistent with a predominantly heterogeneous model, ΔG_g of critical nuclei increases from 1.31×10^{-19} J/molecule to 2.76×10^{-19} J/molecule, when supersaturation ratio decreases from 27.93 to 10.81. This is the reason why nucleation rate decreases during heterogeneous nucleation process, when supersaturation is much lower compared with homogeneous nucleation. But, without catalytic effect of foreign particles, however, the nucleation rate can decrease even more significantly.

Figure 8.3 illustrates the experimental data of induction time obtained from experiments and the theoretical curves calculated from equation (8.9) using assumed values of parameter $\bar{g}$. Both the experimental and theoretical results show that the induction time decreases with increasing supersaturation ratio at constant temperature. The total absolute deviation between the theoretical and experimental induction times (ε) is used to choose the best values for $\bar{g}$. ε can be obtained from equation (4.11).

The experimental data with theoretical curves of induction time are also shown in Figure 8.3. The experimental points situate in the zone between theoretical curves plotted by the parameter $\bar{g}$ = 4 and 5. The reason for above phenomenon is that only the value of dominating clusters is considered in the model. In reality, however, clusters with different monomer numbers may exist in real solution. In this case, the clusters with 4 monomers and 5 monomers have highest concentration in the solution and the concentration difference of these two clusters is not significant. So both of them are dominant clusters in the solution. Compared with $\bar{g}=3$ when nucleation is consistent with a predominantly homogeneous model (Guo et al., 2006), the size of dominant cluster increases on account of catalytic effect of foreign particles. This is the reason in microcosmic scale why heterogeneous nucleation rate is higher than homogeneous nucleation rate at similar supersaturation level, since fewer collisions between clusters are required to form critical nuclei due to the larger cluster size. Collision between clusters is the first step for nucleation process since they can coagulate together. The coagulation of large clusters can make the formation of critical

nuclei faster, because the new clusters, formed from the coagulation of large clusters, have larger sizes than the new clusters formed from the coagulation of small clusters. Thus, few collisions between clusters are required to form a critical nucleus. This effect increases nucleation rate consequently.

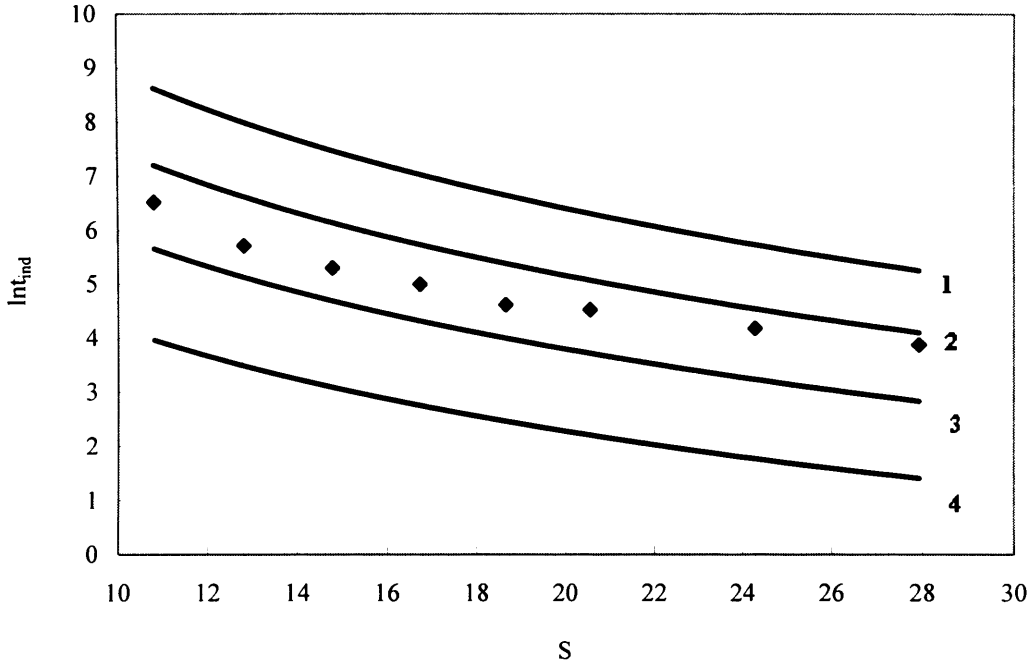

Fig 8.3 Induction time as a function of supersaturation without ultrasound

(◆) The experimental data

(curve1) theoretical curve by using $\bar{g}$ =6

(curve2) theoretical curve by using $\bar{g}$ =5

(curve3) theoretical curve by using $\bar{g}$ =4

(curve4) theoretical curve by using $\bar{g}$ =3

After ultrasound is applied to the system, induction times decrease experimentally with energy increase at constant supersaturation. Figure 8.4 shows that the experimental and theoretical induction time as the function of supersaturation with the power input of 8.62W. At high supersaturation level, clusters with 7 monomers are dominant, while at low

supersaturation level, clusters with 6 monomers are dominant. Unlike homogeneous nucleation and heterogeneous nucleation without ultrasound, the size of dominant cluster changes at a different supersaturation levels after ultrasound is applied to the system.

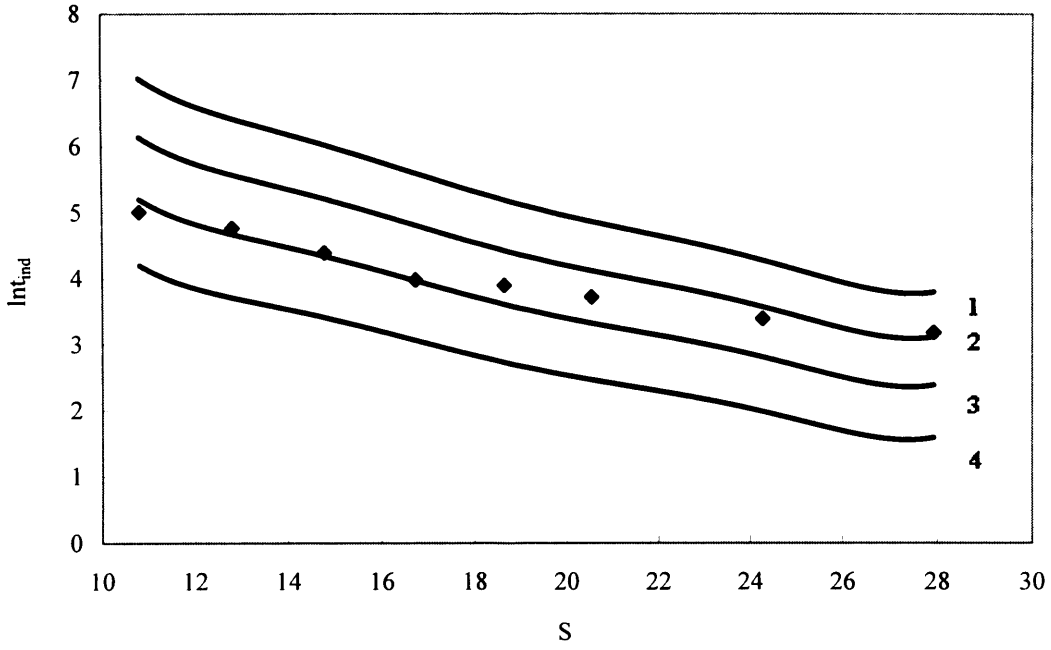

Fig 8.4 Induction time as a function of supersaturation with the power input of 8.62W
(◆) The experimental data
(curve1) theoretical curve by using $\bar{g}$ =8
(curve2) theoretical curve by using $\bar{g}$ =7
(curve3) theoretical curve by using $\bar{g}$ =6
(curve4) theoretical curve by using $\bar{g}$ =5

Figures 8.5, 8.6, 8.7, and 8.8, show the experimental and theoretical induction times as the function of supersaturation with the power inputs of 18.0W, 27.3W, 36.6W, and 46.0W, respectively. From these figures, it is also observed that the dominant cluster size changes with supersaturation level at different power inputs. And the difference of dominant cluster

sizes at different supersaturation levels increases with the increase of power input.

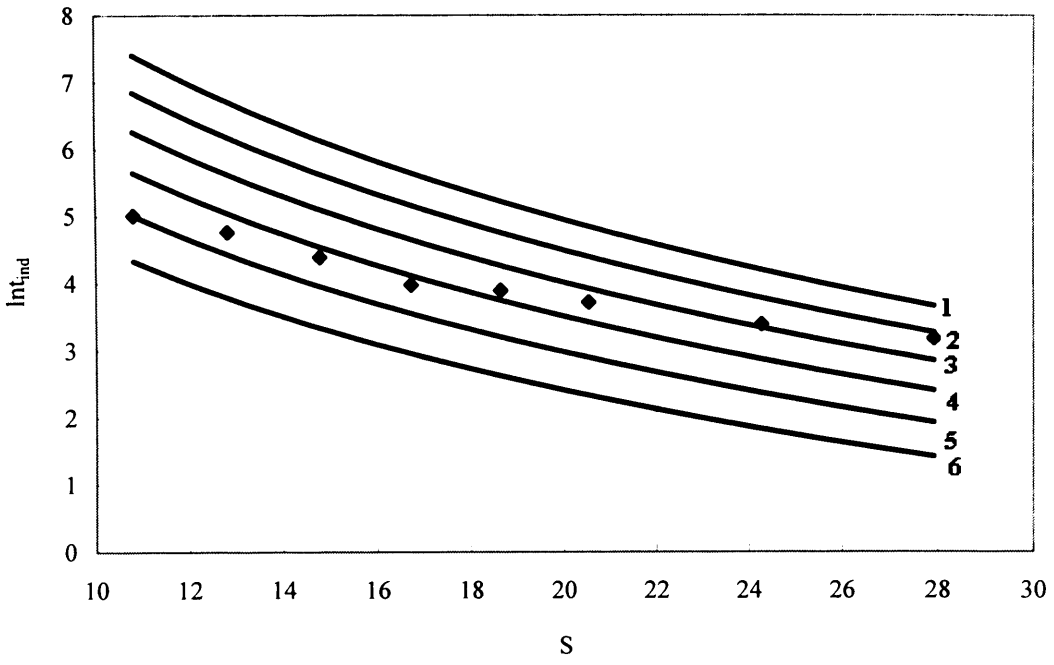

Fig 8.5 Induction time as a function of supersaturation with the power input of 18.0W

(◆) The experimental data

(curve1) theoretical curve by using $\bar{g}$ =12

(curve2) theoretical curve by using $\bar{g}$ =11

(curve3) theoretical curve by using $\bar{g}$ =10

(curve4) theoretical curve by using $\bar{g}$ =9

(curve5) theoretical curve by using $\bar{g}$ =8

(curve6) theoretical curve by using $\bar{g}$ =7

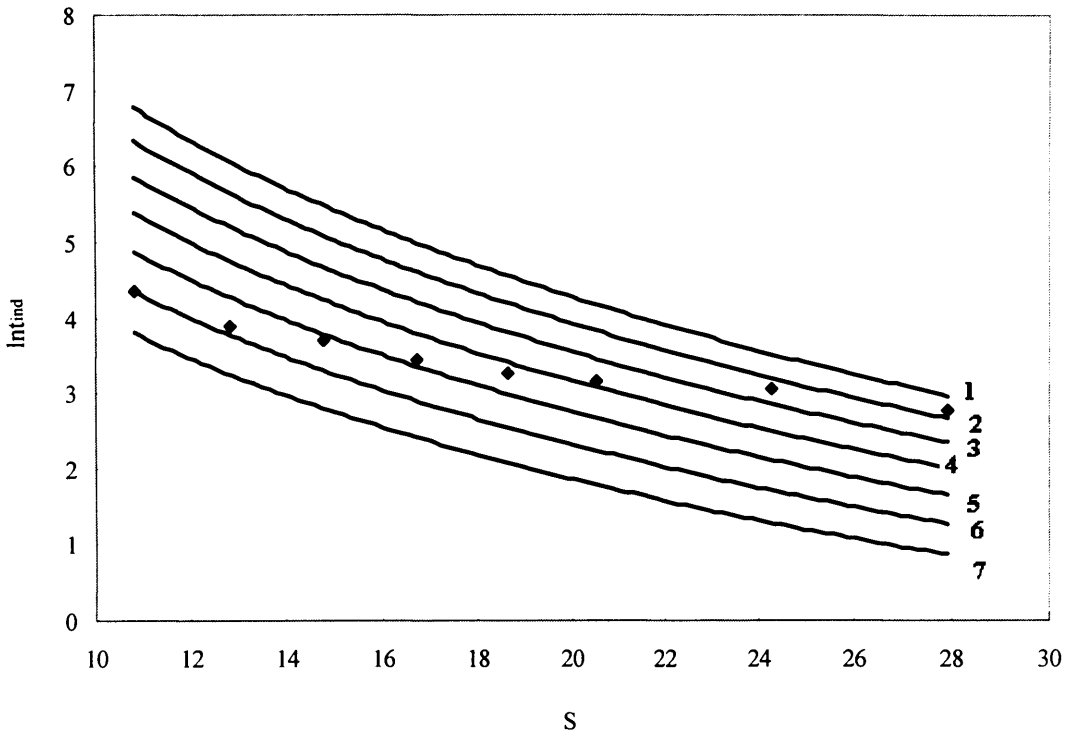

Fig 8.6 Induction time as a function of supersaturation with the power input of 27.3W

(◆) The experimental data

(curve1) theoretical curve by using $\bar{g}$ =14

(curve2) theoretical curve by using $\bar{g}$ =13

(curve3) theoretical curve by using $\bar{g}$ =12

(curve4) theoretical curve by using $\bar{g}$ =11

(curve5) theoretical curve by using $\bar{g}$ =10

(curve6) theoretical curve by using $\bar{g}$ =9

(curve7) theoretical curve by using $\bar{g}$ =8

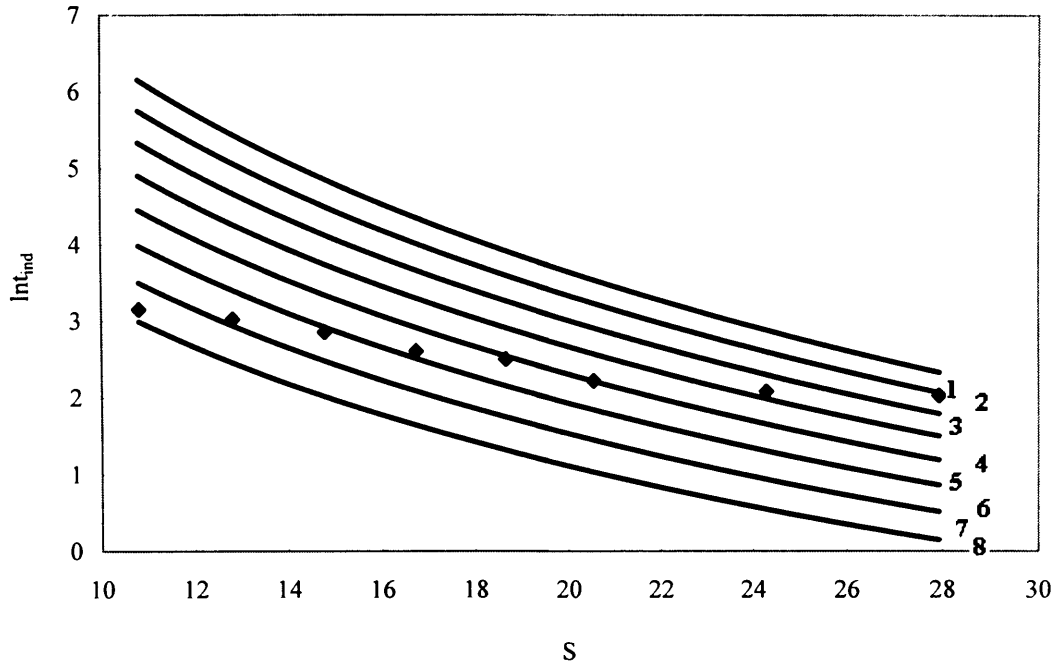

Fig 8.7 Induction time as a function of supersaturation with the power input of 36.6W

(◆) The experimental data

(curve1) theoretical curve by using $\bar{g}$ =15

(curve2) theoretical curve by using $\bar{g}$ =14

(curve3) theoretical curve by using $\bar{g}$ =13

(curve4) theoretical curve by using $\bar{g}$ =12

(curve5) theoretical curve by using $\bar{g}$ =11

(curve6) theoretical curve by using $\bar{g}$ =10

(curve7) theoretical curve by using $\bar{g}$ =9

(curve8) theoretical curve by using $\bar{g}$ =8

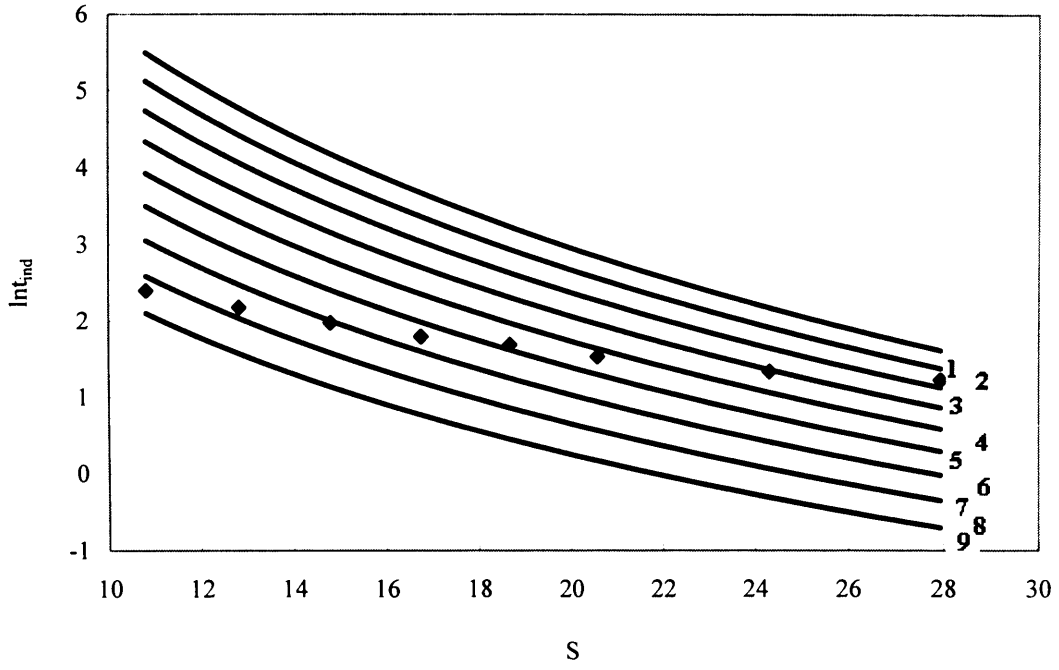

Fig 8.8 Induction time as a function of supersaturation with the power input of 46.0W

(◆) The experimental data

(curve1) theoretical curve by using $\bar{g}$ =16

(curve2) theoretical curve by using $\bar{g}$ =15

(curve3) theoretical curve by using $\bar{g}$ =14

(curve4) theoretical curve by using $\bar{g}$ =13

(curve5) theoretical curve by using $\bar{g}$ =12

(curve6) theoretical curve by using $\bar{g}$ =11

(curve7) theoretical curve by using $\bar{g}$ =10

(curve8) theoretical curve by using $\bar{g}$ =9

(curve9) theoretical curve by using $\bar{g}$ =8

It is found that when nucleation is consistent with a predominantly homogeneous model, the number of monomers in dominating clusters ($\bar{g}$) is 3 for different power inputs. A theoretical analysis of the total absolute deviation (ε) shows that the number concentration of largest clusters increases slowly with the increase of power input. But compared to the increase of diffusion coefficient (D_{AB}), this effect is very small. While the ultrasound can increase the size of dominant cluster significantly when nucleation is

consistent with a predominantly heterogeneous model. The relationship between the number of monomers in dominant clusters ($\bar{g}$) and supersaturation ratio (S) at different power inputs is shown in Figure 8.9. With 8.62W power input, the monomer number in dominant clusters varies between 6 and 7 at different supersaturation levels; with 18.0W: between 8 and 11; with 27.3W: between 9 and 13; with 36.6W: between 8 and 14; and with 46.0W, between 8 and 15. It is found that the dominant cluster size increases when supersaturation increases in the ultrasonic field. However, at the same supersaturation level, the size of dominant cluster increases with increasing ultrasonic energy.

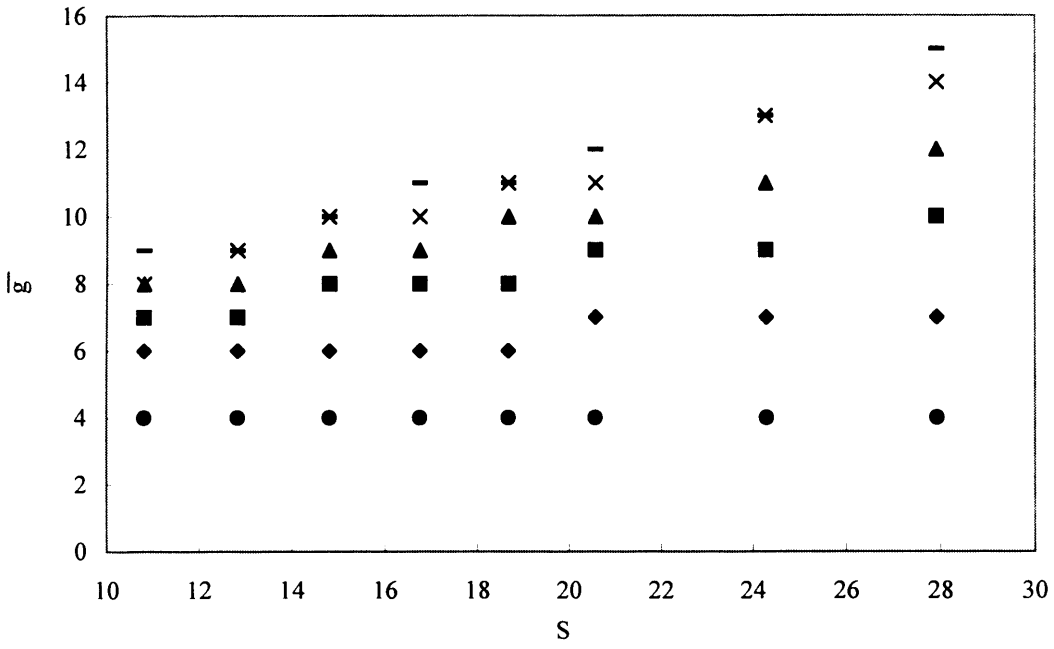

Fig 8.9 The relationship between the number of monomers in dominating clusters ($\bar{g}$) and supersaturation ratio (S) at different power inputs

(●) without ultrasound
(◆) with the power input of 8.62W
(■) with the power input of 18.0W
(▲) with the power input of 27.3W
(×) with the power input of 36.6W
(−) with the power input of 46.0W

So from above analysis, it can be concluded that in addition to the increase of diffusion coefficient (D_{AB}), ultrasound can also increase the dominant cluster size when nucleation is predominantly heterogeneous and this effect increases with increasing power input and supersaturation level. Thus, when nucleation is predominantly heterogeneous, both the two effects above increase nucleation rate after ultrasound is applied to the system.

8.4 Conclusion

The ultrasonic effect on the clusters in solution is analyzed by a cluster coagulation model when nucleation is consistent with a predominantly heterogeneous mechanism. It is found that without ultrasound, the monomer number in dominant clusters is 4 or 5. But, with 8.62W power input, however, the monomer number in dominant clusters varies between 6 and 7 at different supersaturation levels; with 18.0W: between 8 and 11;with 27.3W: between 9 and 13; with 36.6W: between 8 and 14; and with 46.0W, between 8 and 15. Thus the dominant cluster size increases when supersaturation increases with different power inputs. At the same supersaturation level, however, the size of dominant cluster increases with increasing ultrasonic energy. This phenomenon is different from what is observed when nucleation is consistent with a predominantly homogeneous model. In the homogeneous nucleation experiments with barium sulphate as the working substance, nucleation clusters having 3 monomers are predominant in the solution for different power inputs. That is the ultrasound has an insignificant effect on the size of dominant clusters during homogeneous nucleation. When nucleation is consistent with a predominantly heterogeneous model, the increase of cluster size can decrease the induction time further in the ultrasonic field. The coagulation of large clusters can make the formation of critical nuclei quicker, because the new clusters, formed from the coagulation between large clusters, have larger sizes than the new clusters formed from the coagulation of small clusters. Thus, as ultrasonic energy increases, fewer collisions between clusters are required to form a critical nucleus, consequently increasing the heterogeneous nucleation rate.

CHAPTER 9

HIGH-SPEED OBSERVATION OF THE EFFECT OF ULTRASOUND ON BREAKAGE PROCESS

9.1 Introduction

Ultrasound has been reported to accelerate or depress agglomeration (Freitas & Hielscher, 2004; Veličković & Milenović, 2005), break aggregated (Kim & Kim, 2002) and agglomerated crystals (Schaefer & Suryawanshi, 2002). Ciftcioglu and Aoki (See Kusters & Pratsinis, 1993) proposed that agglomerate breakage results from the interaction with cavitation bubbles formed in the liquid. Another mechanism for breakage is on account of velocity increase of particles and rate of collision between particles after ultrasound is applied to the system.

In heterogeneous solid-liquid systems, the interface produces a perturbation in the sonic field which induces an asymmetric collapse of the cavitational bubbles. At extended interfaces several times larger than the resonance cavitation size, the result is a micro-jet of liquid passing through the cavitation which impinges with the solid surface at velocities estimated around 100 $m \cdot s^{-1}$. This phenomenon is the origin of the erosion effect used for ultrasonic pitting and surface cleaning (Cains & Martin, 2005). Ultrasound also has mechanical effects on crystallization system, which increase the collision rate between crystals and between crystals and wall of crystallizer. All of above effects will depress agglomeration and increase breakage rate during crystallization process.

To investigate the mechanism of agglomerate breakage in the present work, a Kodak Ektapro Hs motion analyzer is used to observe the cavitations and particle movement in a 200 ml vessel. In the experiment, cavitational effects on particles with different sizes are investigated. The mixing processes with stirring and with ultrasound are investigated by the dispersion of ink in ethanol. The vessel is divided into several sections to investigate the mixing processes by recording the movement of small sugar crystals. The cavitation distribution in different sections is also recorded. Through above experiments, the relationship between vibration and implosion of cavitations and mixing is established. Then, agglomerated sugar crystals are used as working substance. The

breakage process is observed through a lens with high magnification to determine its mechanism in ultrasonic field. In order to determine the ultrasonic effects on the bond between agglomerated particles, photographs of broken sugar are compared with the agglomerated sugar crystals, sugar crystals without agglomeration and sugar crystals after mechanical grinding.

9.2 Experimental

The first experiment is the investigation of the ultrasonic effect on inert particles of different size suspended in ethanol. The substances are: two kinds of alumina particles, viz. alumina particle 1 with the particle size of 3.30mm and alumina particle 2 of 2.34mm respectively; silica-gel sphere of 3.24mm; agglomerated sugar crystals from 2 to 2.22mm; sugar crystals without agglomeration from 0.30 to 0.40mm; and salt crystals with the particle size from 0.20mm to 0.30mm.

A 750 W ultrasonic processor with 20 kHz was used (Cole-Parmer Instruments, Illinois, USA), which functions by emitting vibration waves and inducing cavitational voids throughout a defined volume of liquid in each experiment. The ultrasound is produced by a transducer made up of a piezoelectric sandwich and is delivered from a titanium probe with a tip of 8mm in diameter. During insonation, the probe is immersed in the liquid, resulting in the wave traveling downwards and reflecting from the base.

A Kodak Ektapro Hs motion analyzer, which can take 4500 full frames per second (fps), is used to observe the cavitation movement on particle surfaces. A lens with high magnification is used in this experiment to observe the cavitations clearly. The experiment is carried out in a small vessel with 15ml ethanol. 5 particles are added into the vessel in each of the experiments with different substances. The amplitude of ultrasonic processor is adjusted to 31% of maximum power, which is the upper limit for stable conditions in this vessel. Then, 5 agglomerated sugar crystals are used to study the breakage process. The cavitational effect on breakage is recorded by the Kodak

analyzer and qualitatively analyzed in the monitor.

The second experiment is the investigation of the dispersion of ink with ultrasound and stirring respectively in a jacketed vessel of diameter 55mm at 25℃. 200 ml ethanol is used as solvent. 100 μl of ink is injected into the ethanol by Finnpipette and the dispersion processes are recorded by the camera with the lenses of high magnification and low magnification respectively. The amplitude of the ultrasonic processor is fixed at 41% of maximum power and the stirring rate is adjusted to 400rpm. The difference of mixing processes and hydraulic flows between ultrasound and stirring are investigated with lens of low magnification, which record changes within the whole vessel. In this experiment, the temperature is kept at 25℃.

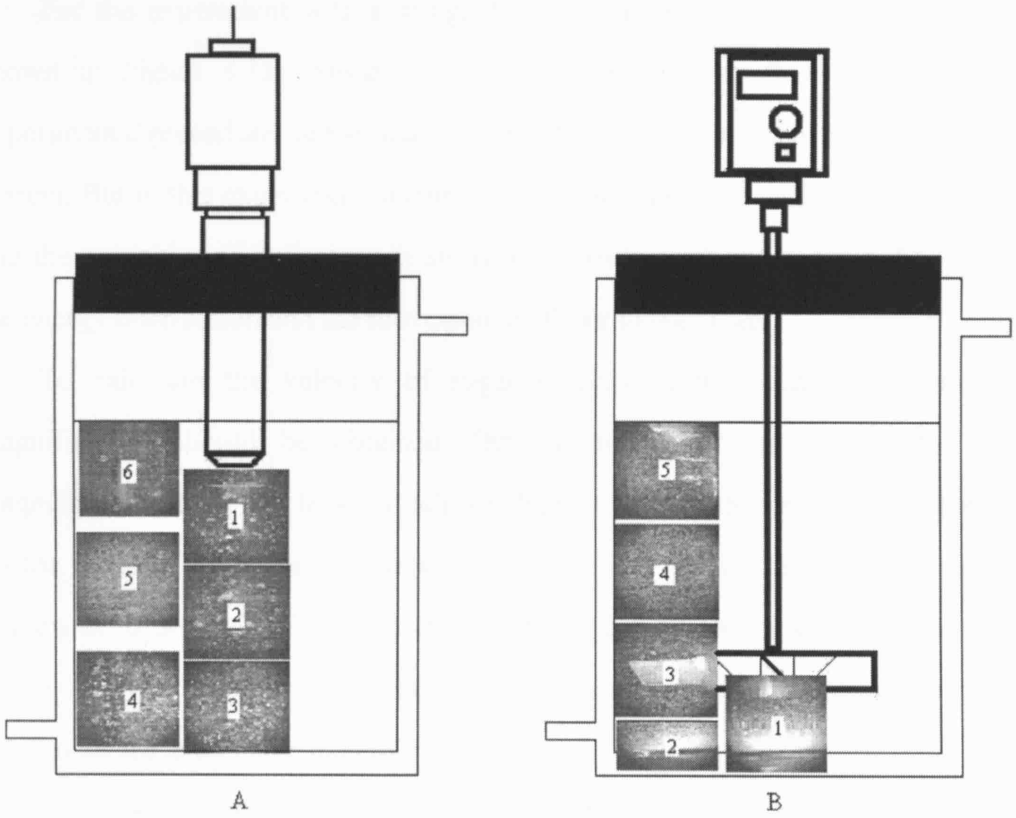

Figure 9.1 The division of the vessel for the experiments of local mixing processes

A: The division when ultrasound is applied with 41% amplitude

B: The division when stirring is applied with the stirring rate of 400rpm

In the third experiment, which is also carried at 25℃, the vessel is divided into 6 sections to study the local mixing process and hydraulic flows when ultrasound is applied to the system. The division is shown in Figure 9.1A. The experiments are carried out at the amplitude of 41%, 51% and 61% of maximum power. Sugar crystals without agglomeration are used as indicators for the movement of hydraulic flows in different sections. The lens with high magnification is used to record the movement of particles in this experiment. In each section, 10 particles are randomly chosen from the monitor of the Kodak analyzer to indicate the energy and hydraulic flows and their velocities are recorded. Afterwards, the vessel is emptied and refilled with 200ml ethanol and the cavitation bubbles in each section is numerated and the cavitation density is calculated.

For the experiment with stirring, the vessel is divided into 5 sections, which is shown in Figure 9.1B. Sugar crystals are also used as flow indicators and the experimental procedures are similar as the experiment when ultrasound is applied to the system. But in this experiment, a stirring rate of 400rpm is investigated. The movement and the velocities of indicators in above two experiments are compared to investigate the energy distribution and the movement of flows in the vessel.

To calculate the velocity of sugar crystals in the vessel, the value of the magnification should be obtained. But, as mentioned in chapter 6, since the magnification of the two lenses is adjustable, it is not possible to get this value directly. So the probe of ultrasonic processor and the pole of stirring impeller are used as the references to obtain it. The proportion between corresponding dimensions, which are shown on the monitor of Kodak analyzer, and the real dimension of reference substances are used as the magnification.

An isolated vessel, which is covered with thermal insulating material, is employed to determine the real power input to the system by continuously applying ultrasound with a given power amplitude to 200ml ethanol (Kim & Lee, 2002). When the change of temperature on heat capacity is ignored, the power input of ultrasonic processor can

be obtained from:

$$E = n_{ethonal} C_p \left(\frac{dT}{dt} \right) \tag{9.1}$$

where the specific heat capacity (C_p) of ethanol is 2.4×10^3 J kg^{-1} K^{-1} at 25°C (G R Delpierre & B T Swell 2002). Thus, from the rate of temperature increase and the heat capacity of ethanol, the relationship between the power input and amplitude can be obtained. And the power input from stirring can be obtained from the method mentioned in chapter 6.

The breakage processes of agglomerated sugar in the above 6 sections are recorded by the Kodak analyzer with lens of high magnification at different amplitudes respectively. 5g of agglomerated sugar is measured by a precise electronic balance and added into 200ml ethanol. Ultrasound is applied to the solution to break the crystals. The amplitudes of ultrasound are 41%, 51% and 61% of maximum power and the temperature is kept at 25℃ during all the experiments. After 5 minutes, the sugar crystals are filtered and washed by ethanol. The product is observed under an Olympus BX60 microscope with magnifications of ×10 and ×20. Then some new agglomerated crystals are mechanically stirred at 400rpm for 5 minutes. The process is recorded and the product is also filtered out. Additionally some agglomerated crystals are ground in a mortar to get single crystals. The above two products are also observed by microscope and the photographs are compared with the product of the ultrasonic breakage process.

The final experiment is to study the upper limit of power input to the system, which is an important factor affecting the breakage rate of crystals, by ultrasound and by stirring. The amplitude of the ultrasonic processor and the stirring rate are adjusted to the highest values until liquid overflows from the vessel. The power inputs are calculated by equations (9.1) and (6.1).

9.3 Results and discussion

The ultrasonic effects on particles with different sizes are shown in Figure 9.2 (A, B, C, D, E, F). Since all the substances are insoluble and inert in ethanol, the only reason for the change of ultrasonic effect on particles is the difference in particle size. It is observed that after ultrasound is applied to the system, cavitation bubbles are formed in the system. The vibration of cavitation can cause powerful shock wave, which can also cause erratic flow in the solution. This flow and the hydraulic flow directly caused by ultrasound drives the particles to move erratically in the solution. Particles collide frequently with each other and the wall of the vessel. It is also found that the particle size has a significant influence on the ultrasonic effect on particles. Some cavities attach to the surface of large particles and the larger the particles, the easier it is for cavitation bubbles to attach to their surface. This phenomenon is observed in the experiments with alumina particle 1, alumina particle 2, silica-gel spheres and agglomerated sugar crystals.

After the cavitation bubble attaches to the particles, it moves with the particle and releases a shock wave during the compression and rarefaction of phases. Collisions and erratic movements of particles are only observed, however, in the experiments with sugar crystals without agglomeration and with sodium chloride crystals. Cavitation bubbles do not attach to the surfaces of small particles. Particularly, the bubble adhesion on agglomerated sugar crystals but not on single sugar crystals further proves that the size of particles is predominant reason for adhesion. That is, cavitaion bubbles have a higher influence on particles with larger particle size, since they are attached to the particle surface. Because the size of agglomerated particles is larger than particles without agglomeration, the effect of cavitation is more significant on agglomerated particles. The shock wave caused by cavitation can break the bond between agglomerated particles and prevent the reattachment of discrete particles. This ultrasonic effect can increase the breakage rate and prevent agglomeration in

crystallization process.

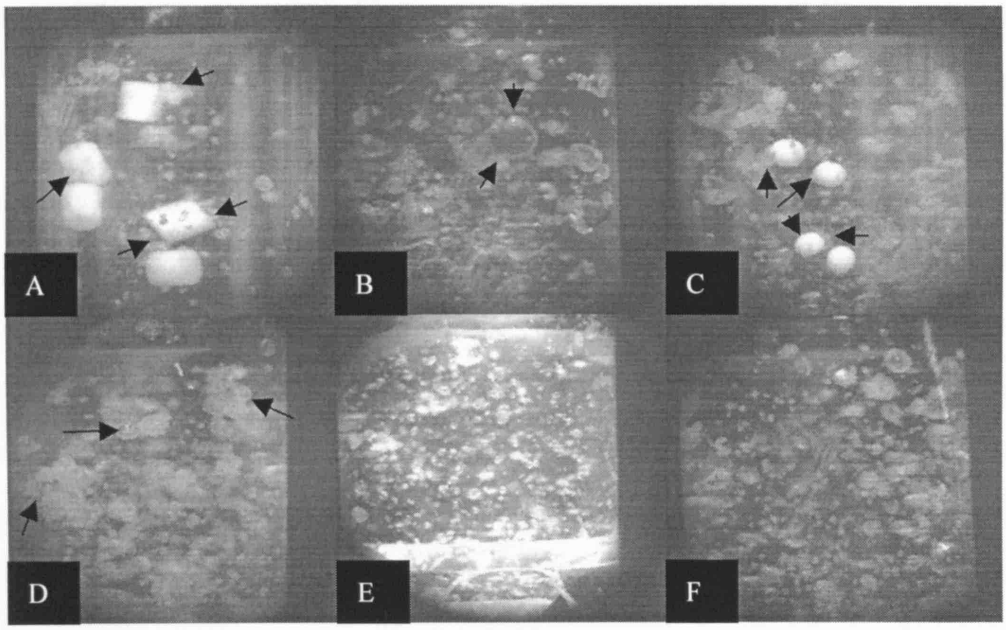

Figure 9.2 Cavitation effect on particles with different particle sizes
A: large alumina supporter 1 B: silica-gel sphere
C: small alumina supporter 2 D: agglomerated sugar crystals
E: single sugar crystals F: salt crystals
Arrows indicate cavitations attached on particle surface

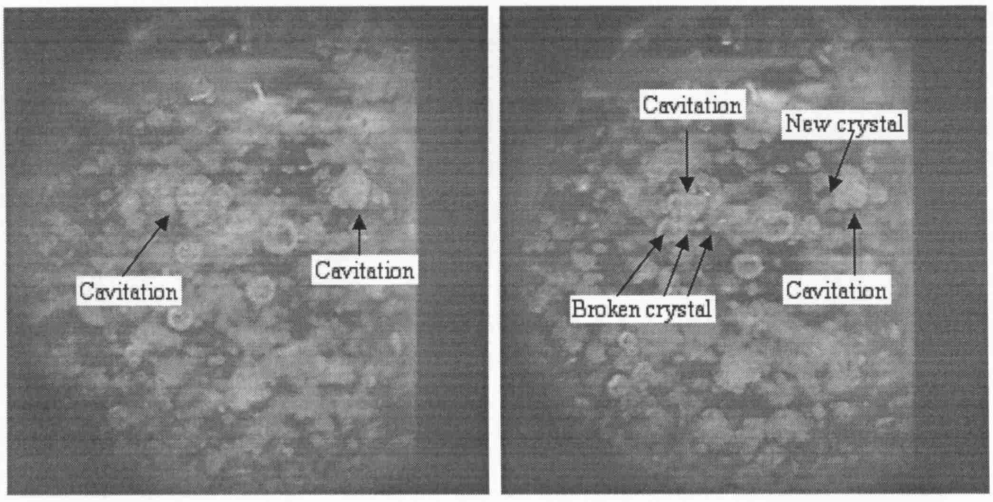

Figure 9.3 The breakage process of agglomerated sugar crystals
A: before breakage B: after breakage

Figure 9.2D shows the effect of ultrasound on breakage of agglomerated sugar crystals. When the sugar crystal is moving in the system (Figure 9.2D), it collides with the wall of vessel and other crystals. Because of the hydraulic flows caused by vibration and implosion of cavitation, the movements of crystals are erratic, which increase the possibility of collision between crystals significantly. It is also observed, however, that the cavitation vibration and implosion at the surface of agglomerated crystals are important for their breakage. Since cavitation bubbles attach to the agglomerated crystals of large size, their effect in breaking the agglomerated crystals is distinct. The breakage of agglomerated crystals by cavitation bubble attaching the surface of agglomerated crystals is shown in Figure 9.3, where the agglomerated crystals are broken by the implosion of cavitation and the separated crystals move in different directions.

From equation (9.1), the power input to the system is 41%: 29.3W; 51%: 39.6W; 61%: 49.7W. The energy from stirring can be calculated from equation (6.1). When the stirring rate is 400rpm, the power input is 0.46W.

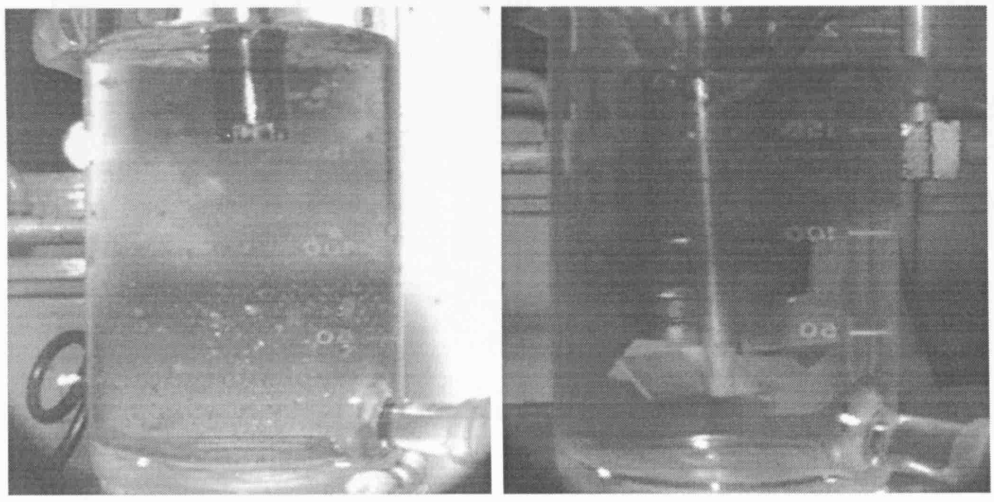

A **B**

Figure 9.4 The dispersion of ink in the vessel
A: dispersion with ultrasound after 0.52s of ink addition
B: dispersion with stirring after 0.72s of ink addition

The flows, mixing effect and the breakage effect of stirring and ultrasound are compared in the experiments carried out in the 200ml vessel. The dispersion of ink in the vessel with stirring and with ultrasound are shown in Figures 9.4 A and B, respectively, where Figure 9.4A is taken at 0.52s after ink is added into the vessel with the amplitude of 41% of maximum power and Figure 9.4B is taken at 0.72s after ink is added into the vessel with the stirring rate of 400rpm. Thus, the dispersion process and hydraulic flow pattern can be observed. It is found that the ink disperses from vessel center to the wall during its motion from the top to the bottom of the vessel. Some hydraulic flows are observed during the process, but the flows are only moved in a small area and their turbulent movements are not great. When ultrasound is applied to the system, however, the ink is dispersed and mixed much quicker than the process with stirring. The flows disperse the ink to majority of the vessel in a very short time and the mixing process is very strong. Thus, the rate of collision between crystals in the system with ultrasound is higher than the system with stirring.

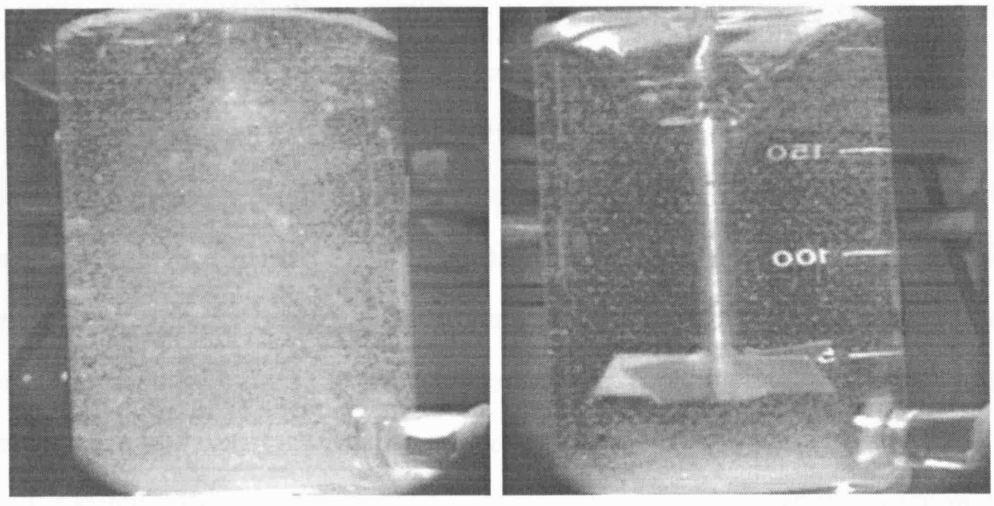

A **B**

Figure 9.5 The distribution and movement of sugar crystals in the vessel
A: with ultrasound
B: with stirring

The vessel is divided into 6 sections to study the local mixing process and hydraulic flows. Small sugar crystals are used as indicators as mentioned before. The whole vessel is also observed using the Kodak motion analyzer. The particle movements in the vessel with stirring and with ultrasound are shown in Figure 9.5A with the amplitude of 41% and Figure 9.5B with the stirring rate of 400rpm, respectively. It is found that, in general, the particles move orderly in the vessel with stirring, but erratically in the vessel with ultrasound. And in Figure 9.5A, majority of particles are dispersed in the whole vessel. While, in Figure 9.5B, majority of particles are precipitated in the bottom of the vessel.

As described, ten particles are chosen randomly from every section and their velocities are recorded. The variance of velocity (σ^2) between crystals is used to indicate the local mixing and hydraulic flows. σ^2 can be obtained from equation (6.2).

The change of σ^2 with the amplitude of ultrasonic processor in different sections is shown in Figure 9.6. When the amplitude of ultrasonic processor is 41%, variances of crystal velocity are close to each other in different sections. This means that the ultrasonic energy distribution is uniform in the system, so the difference of velocity between hydraulic flows and the mixing time are similar in different sections. When the amplitude is improved, the energy distribution becomes uneven in each section. The difference increases with the increase of amplitude. But section 6 is still a dead zone, where the influence of mixing from ultrasound is insignificant. At 61% and 51% of amplitude, the mixing in section 1 is highest since it is the nearest section to ultrasonic processor, while the values of variance in section 3, 4 and 5 are very close to each other. The densities of cavitations in different sections are also counted and shown in Figure 9.7. It is found the density of cavitations in section 5 is much lower than section 3 and 4, while the mixing effects are very close. So it can be concluded that the vibration and implosion of cavitations is one reason for mixing improvement in the vessel. The mixing is also improved by the ultrasonic power input, which is transferred directly to

the molecules and flows in the system.

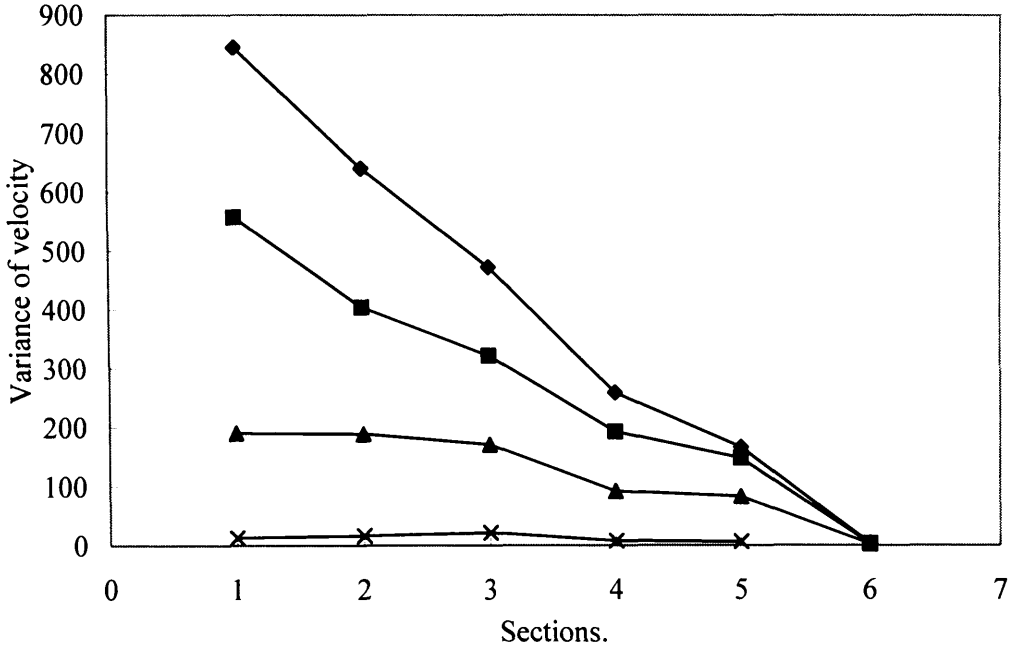

Figure 9.6 The change of variance of velocity with sections
(◆) with the amplitude of 61%
(■) with the amplitude of 51%
(▲) with the amplitude of 41%
(×) with stirring rate of 400rpm

The variance of crystal velocity in sections 1, 2 and 3 is higher than in sections 4 and 5, because they are near impeller. From the lens with high magnification, it is observed that when ultrasound is applied to the system, the flows are turbulent, the particles can move to any direction in each section. The reasons for above phenomenon are the vibration and implosion of cavitations and the hydraulic flows directly caused by ultrasonic energy. Because the crystals move orderly in the system with stirring, the variance between crystal velocities is much lower compared to the system with

ultrasound. Obviously, the chance for collision between crystals is much higher in the system with ultrasound.

Since the agglomerated crystals have larger particle size, it is very difficult for them to be distributed uniformly in the vessel. So normally majority of agglomerated sugar crystals stay at the bottom of the vessel with stirring. Their chance to collide with other crystals and the wall of the vessel is therefore limited, while it is found the agglomerated crystals are distributed uniformly in the vessel with ultrasound, and the crystals have more chance to collide with each other.

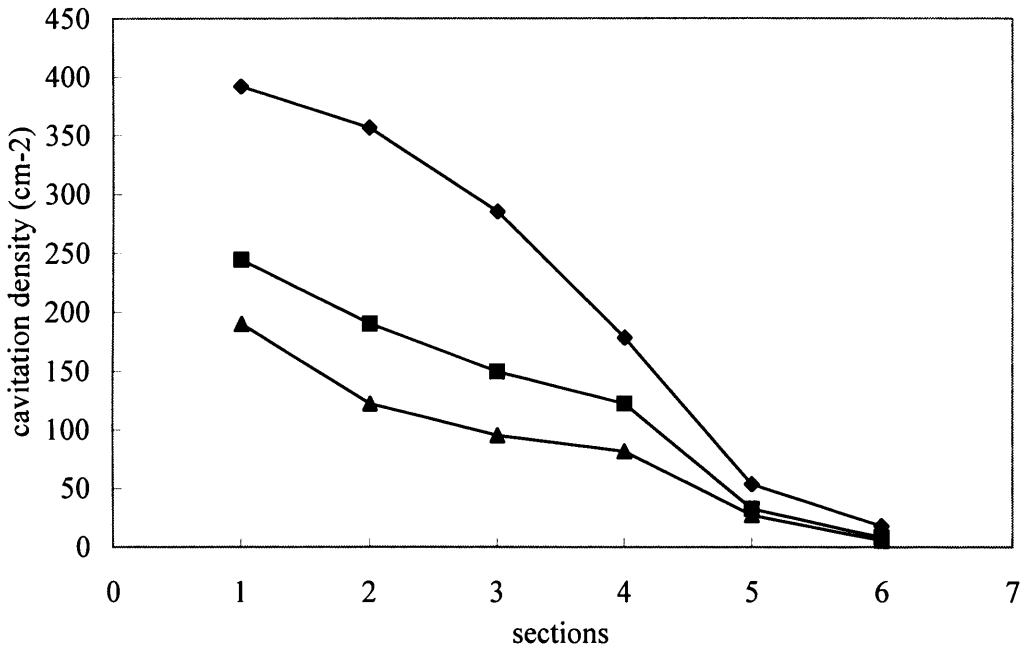

Figure 9.7 The distribution of cavitation in different sections
(◆) with the amplitude of 61%
(■) with the amplitude of 51%
(▲) with the amplitude of 41%

The ultrasonic effect on breakage of agglomerated crystals is observed in different

sections in the 200ml vessel. It is observed that, except section 6, the collision rate between crystals is very high in each section. The cavitation attachment on the agglomerated crystals and their implosion are also observed in different sections. Agglomerates are broken by the implosion of cavitations. Then, the broken crystals move to different directions and have no chance to approach and agglomerate again. This breakage process by implosion of ultrasound is similar to the process that occurs in the vessel with 15ml ethanol.

In these experiments, it is found that the effect of crystal breakage by implosion of cavitations decreases from section 1 to sections 2 and 3. It is observed that the chance of crystal breakage by cavitations in section 3 is very close to the chance in section 4. In section 5, collision is the dominant mechanism for breakage, while breakage by cavitations is seldom observed, since the density of cavitation in section 5 is much lower than other sections. In section 6, the chance of collision becomes low and the breakage by cavitations is not observed.

In the next experiment, 5g agglomerated sugar crystal is added in the 200ml ethanol and ultrasound with 3 different amplitudes is applied to the system for 5 minutes. It is found when 41% amplitude is used, although the majority of agglomerated crystals is broken, some agglomerated crystals still can be found in the crystal product. And when 51% amplitude is used, there are almost no agglomerated crystals in the product. When 61% amplitude is used, in addition to disappearance of agglomerated crystals, many fine crystals are formed and make solution become cloudy, as shown in Figure 9.8B. The similar experiment was also carried with 400rpm stirring. It is found that agglomerated crystals have almost no change after 5 minutes stirring. The comparison between the beginning and the end of breakage process with 61% ultrasonic amplitude and 400rpm stirring rate is shown in Figure 9.8.

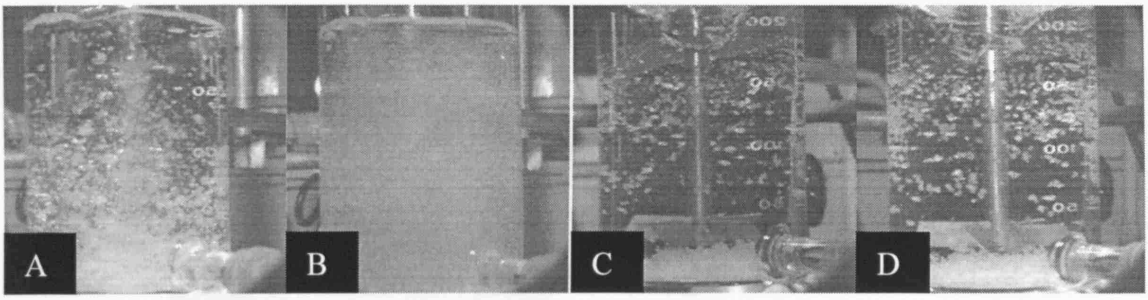

Figure 9.8 The comparison between the beginning and the end of breakage process
A: beginning of process with 61% amplitude
B: end of process with 61% amplitude
C: beginning of process with the stirring rate of 400rpm
D: end of process with the stirring rate of 400rpm

Photographs of sugar crystals without agglomeration and those of agglomerated crystals are shown in Figure 9.9A and Figure 9.9B respectively. It is found that the agglomerated crystals are connected by the solid bridges between crystal surfaces. Unlike the crystals sticking together, the bonds between crystals are very difficult to break. The crystals after ultrasonic treatment are shown in Figure 9.9C. From the figure, the surfaces of crystals are eroded by cavitations and the collision, and become damaged. The agglomeration is thoroughly eliminated by ultrasound. When compared with the crystals in Figure 9.9A, it is observed that the crystal size is not reduced significantly by ultrasound. Finally, the agglomerated crystals are also ground gently in a mortar to eliminate the agglomeration and the product is shown in Figure 9.9D. A few agglomerated crystals still exist in the product after grinding treatment. And some crystals are broken before the bonds are broken, while the surfaces of crystals are much damaged compared to the crystals treated by ultrasound. The erosion of grinding process to the surface of crystals is higher than ultrasonic process. Compared to grinding process, ultrasound has a selective effect on solid bonds between crystals. This effect may be useful in precipitating large crystals without agglomeration. A similar phenomenon is also observed during the anti-solvent crystallization process of roxithromycin with and without ultrasound (Guo & Zhang, 2005).

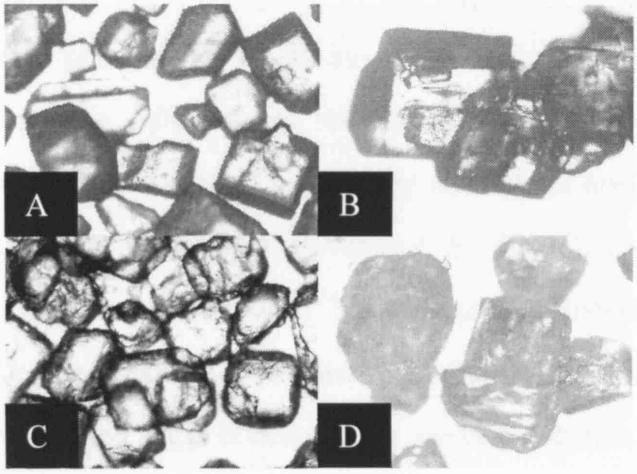

Figure 9.9 The photographs of crystals observed by microscope
A: single sugar crystals
B: agglomerated sugar crystal and the bond between crystals
C: sugar crystals after ultrasonic treatment
D: sugar crystals after grinding

One reason why ultrasound has such a significant effect on breakage is its power input. When the power input from ultrasound to the system is 100.4W, the system can remain stable. But when the power input from stirring to the system is only 3.7W, the system has already become unstable and liquid overflows from the vessel. Thus, the value of the energy transfer from ultrasound to liquid can be much higher than the energy transfer from stirring.

9.4 Conclusion

A Kodak motion analyzer is applied to observe the effect of ultrasound on the breakage process of agglomerated crystals. The cavitation effects on the particles with different sizes are investigated. It is found that the influence on particles with large size

is stronger than its effect on particles with small size. The mixing processes with stirring and with ultrasound are investigated by the dispersion of ink in ethanol. Small sugar crystals are used as indicators for the movement of hydraulic flows. Velocity variance is used to indicate the difference of turbulence when ultrasound is applied and when stirring is applied respectively. The velocity variance of crystals in the stirred vessel is much lower than the vessel with ultrasound. So the collision rate between crystals is higher in the vessel with ultrasound. The cavitation distribution in different sections is also recorded. The breakage mechanism in different sections is observed respectively with the agglomerated sugar crystals as the working substance. It is found that both the collision between crystals and the vibration and implosion of cavitation bubbles contribute to the breakage process of agglomerated crystals. The agglomerated sugar crystals are added into vessel with ultrasound and stirring treatment for 5 minutes. The product is observed by microscope and compared with the product after grinding. The surfaces of crystals after grinding are much more damaged compared to the crystals treated by ultrasound. The reason of high breakage rate in the vessel with ultrasound is on account of high power input. The fluid medium is more stable with high ultrasonic power input than with impeller stirring power input.

CHAPTER 10

THE COMMERCIAL EVALUATION OF SONOCRYSTALLIZATION TECHNOLOGY

10.1 Executive summary

This chapter details the commercial evaluation to apply sonocrystallization technology into industry. In essence, the drafts of two possible new crystallizer designs are presented in this chapter. It is proposed that these technologies can help to develop a new market which does not exist at present and a potential company based on these technologies will become the leading provider of process designs, sonocrystallizer optimization and advice to industry needing crystallization technology.

10.2 The business opportunity

The current business opportunity is supported by optimal market condition and the advantages of sonocrystallization technology.

10.2.1 A dramatic awareness of the importance of industrial crystallization processes

Crystallization is a solid-liquid interfacial process aimed at obtaining solid particles and purifying products. Today there are few sections of the chemical industry that do not, at some stage, utilize crystallization as a method of production, purification or recovery of solid material. Apart from being one of the best and cheapest methods available for the production of pure solids from impure solutions, crystallization has the additional advantage of giving an end product many desirable properties. Uniform crystals have good flow, handling and packaging properties: they also have an attractive appearance and this latter property alone can be a very important sales factor.

In the pharmaceutical industry, crystallization is widely used for manufacturing bioactive drug substances and formulation of excipients during final and intermediate stages of purification and separation. Over 90% of all pharmaceutical products contain

drugs in particulate, generally crystalline form. It comprises a market for more than $273 billion per year. Over the course of the last 20 years in the US, pharmaceutical sales have increased by around 12% per year. China, the world's seventh largest pharmaceutical market with sales of $9.3 billion in 2000, is also growing at an annual rate of 11%, according to McKinsey & Company. But, the growing demands for safer, more effective and higher quality medicines, increasing regulation, and greater competition are bringing challenges to pharmaceutical manufacturers. So, as one of the most important processes in pharmaceutical manufacture, crystallization technology gets increasing attention nowadays.

10.2.2 The advantages using ultrasound to optimize crystallization processes

Pharmaceutical crystallizations frequently produce crystals, that do not satisfy the defined quality and crystal size distribution. Another problem is the inclusion of mother liquor during subsequent re-crystallization may cause particulate agglomerate formation; a process referred to caking of particles. Operational problems also constitute a large portion of the problems encountered in crystallization processes. The application of power ultrasound to crystallizing systems appears to offer significant potential for modifying and improving both processes and products.

Generally, after ultrasound is applied to crystallization system properly, it may bring following advantages to operation process:

1. Narrowing of the metastable zone width and controlling initiation of nucleation.
2. Improving crystal shape and habit.
3. Reducing polymorphs.
4. Reducing processing time.
5. Improving product properties including, handling, bulk density and appearance.
6. Reducing agglomeration crystals with fewer imperfections.

7. Making small crystals.

The improvement of crystal product by sonocrystallization technology can be easily observed from Figure 10.1, where agglomeration is depressed and the purity is improved.

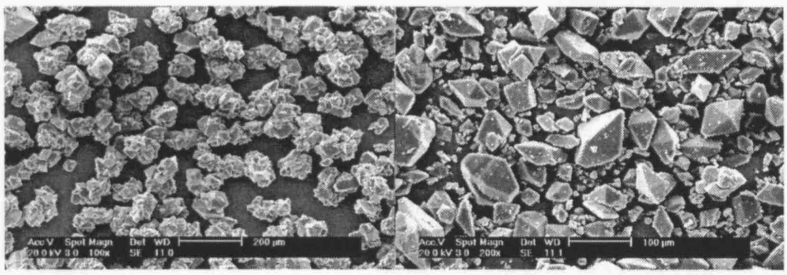

a **b**

Figure 10.1 The ultrasonic effect to depress the agglomeration of roxithromycin crystals (Guo et al., 2005)
a: without ultrasound b: with ultrasound

Ultrasound can provide multiple controls to crystallization processes and bring promising solutions to the industrial problems, which cannot be solved by using conventional crystallization technology. The result of this research can provide the essential directions to both laboratory-scale development of sonocrystallization technology and its industrial application. So using ultrasound to optimize the crystallizer will facilitate the improvement of the quality for crystal product.

10.2.3 The existing technology

Accentus plc developed flow cell and in situ seeding cell to control crystallization processes in traditional crystallizer (AEA Technol, 2001). The sketch of crystallization processes with flow cell and in situ seeding cell is shown in Figure 10.2. In the in situ

seeding cell, ultrasound is applied to the solution, and after seeds are formed, the solution will be injected into crystallizer. This technology can be used to substitute traditional seeding process, where seeds are formed by grinding. In the flow cell, ultrasound is applied on recirculated solution continuously. Through this cell, both nucleation process and crystal growth process can be controlled partially.

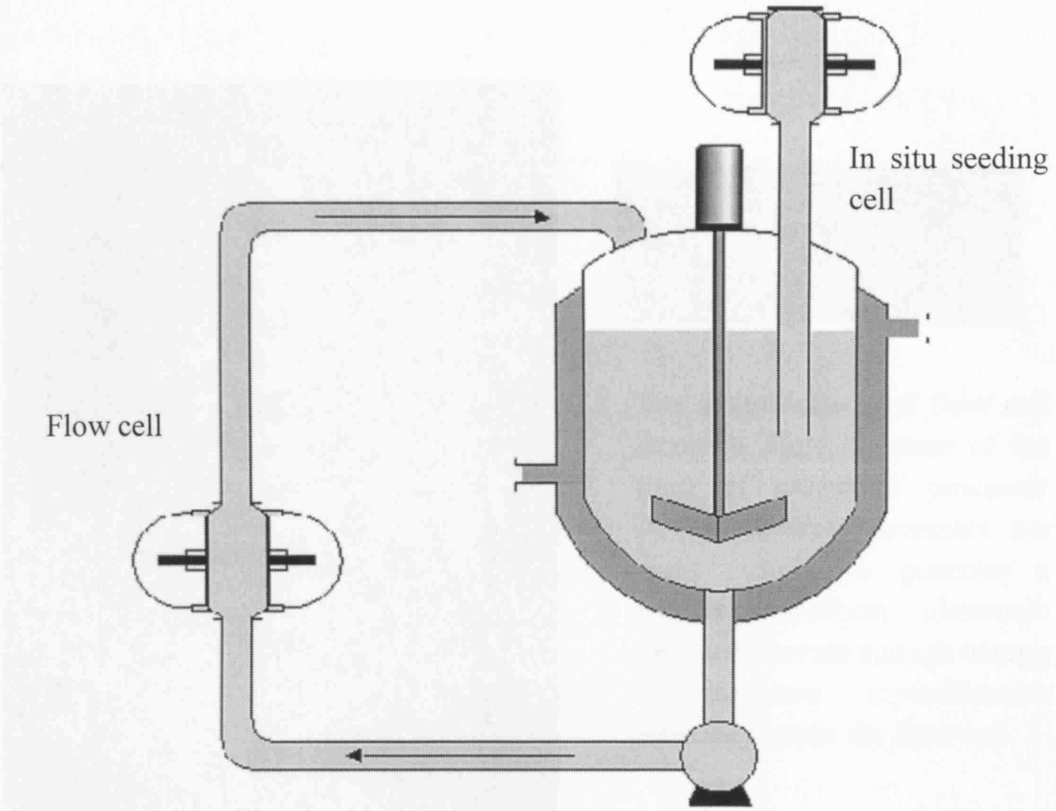

Figure 10.2 The sketch of crystallization processes with flow cell and in situ seeding cell developed by Accentus plc

The details of flow cell design are shown in Figure 10.3. But there are some problems with the above technologies. The main problem of this technology is on mixing. During nucleation processes, nuclei are quite small after formed. Because of the high surface tension, it is very easy for nuclei to agglomerate together without ultrasound. When in situ seeding cell or flow cell is used, nuclei will pass the pipe

connecting cells with crystallizer. There exists no ultrasonic field in this pipe. So after nuclei arrive in crystallizer, they should already agglomerate. This effect will bring significant negative influence to the following crystallization process. Moreover, the poor mixing condition may cause amorphous material precipitated from high supersaturation solution.

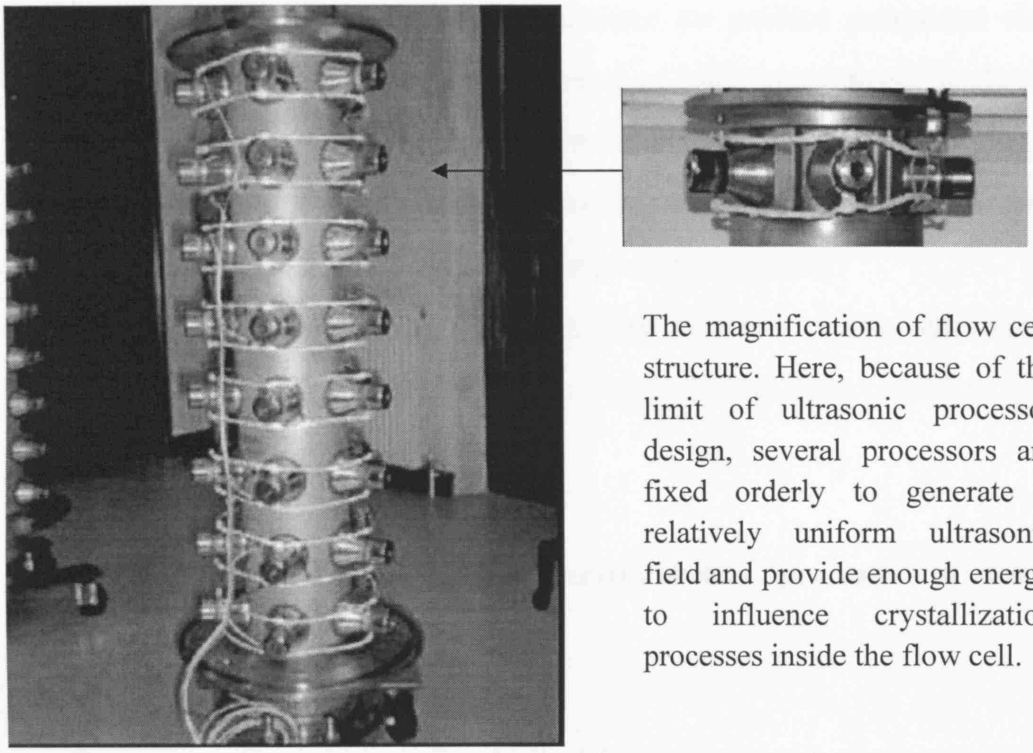

The magnification of flow cell structure. Here, because of the limit of ultrasonic processor design, several processors are fixed orderly to generate a relatively uniform ultrasonic field and provide enough energy to influence crystallization processes inside the flow cell.

Figure 10.3 The details of flow cell design

The second problem is the non-uniformity of ultrasonic treatment to crystals in crystallizer, when flow cell is used. Because the crystal size is not similar in crystallizer, their dispersion will not be uniform either. So only crystals with certain sizes can be injected into flow cell by pump. The bigger or smaller crystals cannot be treated because they are far away from the entrance of the pump. It is also difficult to make sure

all the crystals with similar sizes to be pumped into flow cell with similar times, because of mixing problem. Thus, it is not possible to obtain product with stable quality from this technology.

The third problem is that it is difficult to determine power input value in flow cell to obtain required product. Because each flow cell can only treat a small part of solution in crystallizer, the energy value used in the laboratory-scale experiments cannot be applied in flow cell directly. Even using energy value considering flow cell volume, it is still difficult to determine the energy influence on product parameters since the laboratory-scale experiments are always carried as batch experiments, while the flow cell method can be considered as a continuous process. Because of conflicting and unknown parameters, it is also difficult to carry batch laboratory-scale experiments to simulate the process before industrial application of the flow cell.

Because of above problems, it is not easy to obtain product developed from laboratory-scale experiments, where well-mixing and other ideal conditions are much more easily to be obtained.

10.2.4 Using ultrasound to control crystallization processes in traditional crystallizers

Two new technologies can be obtained from the research results of this project, which investigates the ultrasonic effect on crystallization processes. One is using sonocrystallization technology to control crystallization processes in traditional crystallizers (normally of volume more than 2000L). When sonocrystallization technology is used to control crystallization processes in traditional crystallizer, it is much better to apply ultrasound on solution directly than using flow cell. From mixing analysis and design experience of crystallizer, the most turbulent zone in crystallizer is the zone near impeller. Here, the mixing condition is best inside the crystallizer. So the best way to use sonocrystallization technology on traditional crystallizers is applying

ultrasound on this zone. In practice, there are two kinds of ultrasound generators commonly used in industry. One is the ultrasonic horn. The other is the ultrasonic amplifier. The former one can provide high intensive energy in relatively small zone. This kind of generator is especially suitable for the design of using ultrasound to initiate and control nucleation process. The second one can provide relatively low intensive energy to big zone. It is especially suitable for the design of using ultrasound to control crystal growth process. Since it can generate low intensive energy uniformly for big zone, it can depress agglomeration between crystals while keep majority of crystals perfect. Thus, different generators can be used to fit different purposes in crystallizer design.

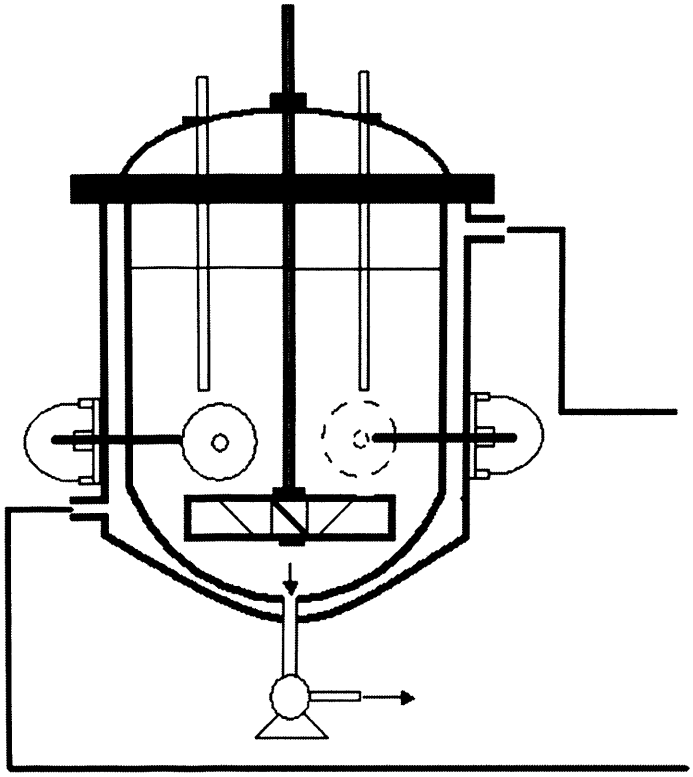

Figure 10.4 The sketch of a traditional crystallizer using ultrasound to control crystallization processes, where ultrasound works on solution directly

There are several advantages for this design over the designs of flow cell and in situ seeding cell. First of all, because the mixing condition is good here, nuclei can be

dispersed in the main solution system immediately after their formation. Thus, the agglomeration among nuclei will be reduced significantly. Secondly, because the ultrasound generator is close to impeller and almost all crystals with different sizes will pass impeller during their moving, ultrasound can work on crystal with different sizes uniformly. Third, ultrasound can be applied to system continuously. Thus, it is easy to calculate the energy value to the system based on laboratory-scale experiments. The ratio of crystallizer volume to the volume of vessel used in laboratory-scale experiments can be used for energy scale-up directly. The sketch of traditional crystallizer using ultrasound to control crystallization processes inside is shown in Figure 10.4. In this figure, several ultrasound generators are fixed on the crystallizer and the generators are close to the impeller. The zone where ultrasound will work is the zone with best mixing condition in the crystallizer.

10.2.5 Using sonocrystallization technology to scale-out the crystallization processes

Another technology is using ultrasound to initiate a new technology, names scale-out of crystallization processes, which can be used to substitute industrial scale-up of crystallization processes from laboratory-scale. This is a totally new technology and it is anticipated that its commercialization will initiate a new business in future.

The sketch of production unit designed by scale-out method is shown in Figure 10.5. Here, instead of using one traditional crystallizer with large volume, new production unit is composed of many small crystallizers (1 or 2 L) linked by parallel connection method to provide enough productive capacity. The designs of every small crystallizers are similar and the operational parameters such as temperature, feeding rates, cooling rate, agitation rate and mass output rate will be kept similar for different small crystallizers in the production unit. Ultrasound is used to initiate crystallization process and control primary nucleation rate.

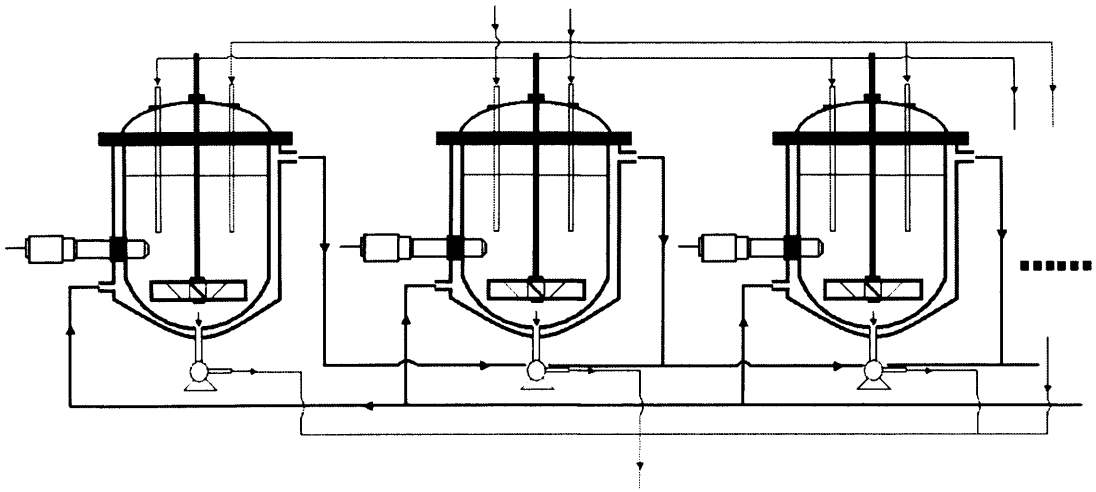

Figure 10.5 The sketch of production unit designed by scale-out method

The sketch of the details of one single small crystallizer (Model 1) is shown in Figure 10.6. The single crystallizer can be used for both batch and continuous production. So the whole production unit can be used for both batch and continuous production as well.

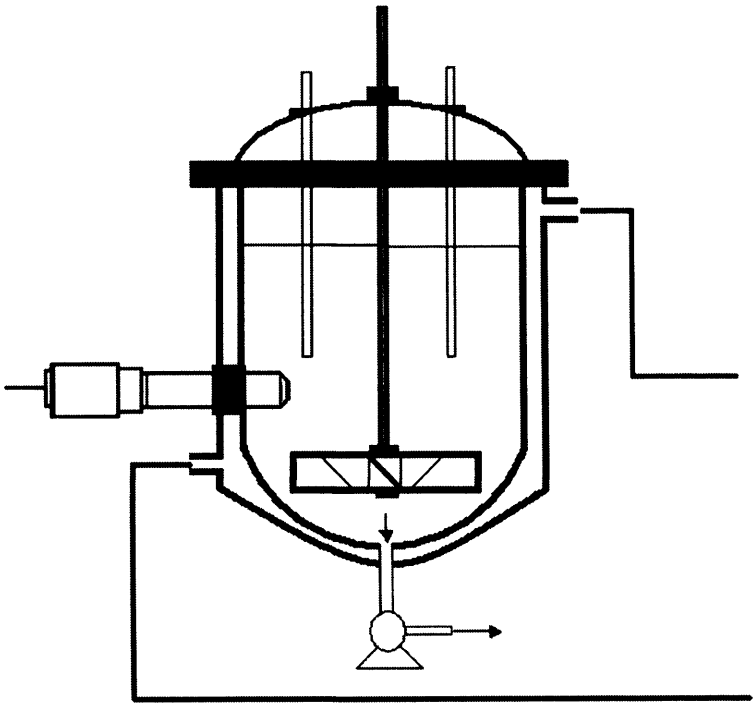

Figure 10.6 The sketch of single small crystallizer model 1

The result and conclusion of this research provide the necessary knowledge to actualize scale-out design. Since the initiation of nucleation depends on some casual factors, such as foreign particles, rough surfaces of impeller and crystallizer, nucleation will not begin at the same time in different crystallizers. Thus, the products from different crystallizers will be different and the quality cannot be controlled. Using ultrasound, nucleation will begin at the same time and the nucleation process can be controlled. This brings a uniform quality to products from different small crystallizers. The comparison of spontaneous nucleation and controlled nucleation processes with cooling crystallization as example is shown in Figure 10.7. Without control, crystallization processes may follow curve 1, curve 2 or curve 3 and so on. This will bring differences in product quality. But with control, nucleation will happened in metastable zone and crystallization processes in different crystallizers can only follow curve 4.

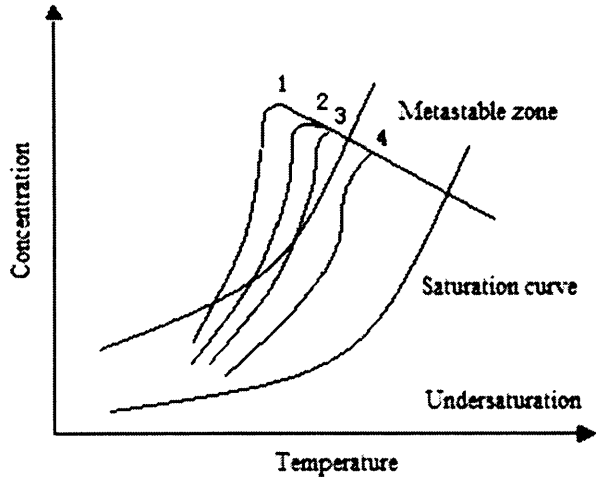

Figure 10.7 The comparison of spontaneous nucleation and controlled nucleation processes with cooling crystallization as example

There are many advantages in scale-out method of crystallization process. The

most important advantage of the scale-out design is that it can be used to substitute crystallization scale-up, which is possibly the most difficult task in industrial technological development. Scale-up of crystallization process is frequently a very difficult task, however, as a variety of factors can influence the quantity and quality of the final product of a process. Even more complications occur with crystallization processes as the reaction and precipitation rates are likely to be mixing-limited. This mixing limitation can occur on the macroscale (macromixing limitation), mesoscale (mesomixing limitation) or microscale (micromixing limitation), or any combination of these. There is a lack of understanding as to what role certain physical and chemical processes play in scale-up, and so they are scaled up empirically or by trial and error. Both technical and economic aspects have to be taken into account. Time and money can thus restrict the scale-up procedure, while calculated risks have to be taken in design and construction. The financial uncertainties resulting from the risks have to be compared with the additional expense necessary for a deeper insight into the process. Thus, scale–up not only needs time-consuming and costly large-scale precipitation experiments but often fails.

There are many advantages to the scale-out method. When scale-out is used, since the crystallizer in production unit is similar to the crystallizer which is used in laboratory, the optimized operational parameters obtained from laboratory-scale experiments can be used directly in industrial production. There is no need to do any simulation, any pilot tests or any experiments on production unit. And there is also no need to design the structure of crystallizer with big volume. The only requirement to increase productive capacity is increase the number of small crystallizers in parallel connection. If customers want to increase or decrease the productive capacity, some small crystallizers can be added or removed to satisfy the requirements. Thus, the scale-out method will save significant time and money in the development process.

And because of the problems in material and design, it is not possible to manufacture single ultrasound generator, which can generate uniform ultrasonic field

with big scale. But since the volume of crystallizers in scale-out production unit is small, the limitation of ultrasound generator will not bring any problem to the design of scale-out crystallizers. And the mixing limitation will not be a problem for small crystallizers as well.

Another advantage is that it is very easy to install both ultrasonic horns and ultrasonic amplifiers on crystallizers. Thus, ultrasonic horns can be used to control primary nucleation process and ultrasonic amplifiers can be used to control crystal growth process. Since in small crystallizers, ultrasonic amplifiers can generate uniform ultrasonic field in the solution, the crystallization processes can be controlled properly. And this kind of crystallizers can be especially used to depress agglomeration. The sketch of small crystallizer design with both ultrasonic horn and ultrasonic amplifier is shown in Figure 10.8.

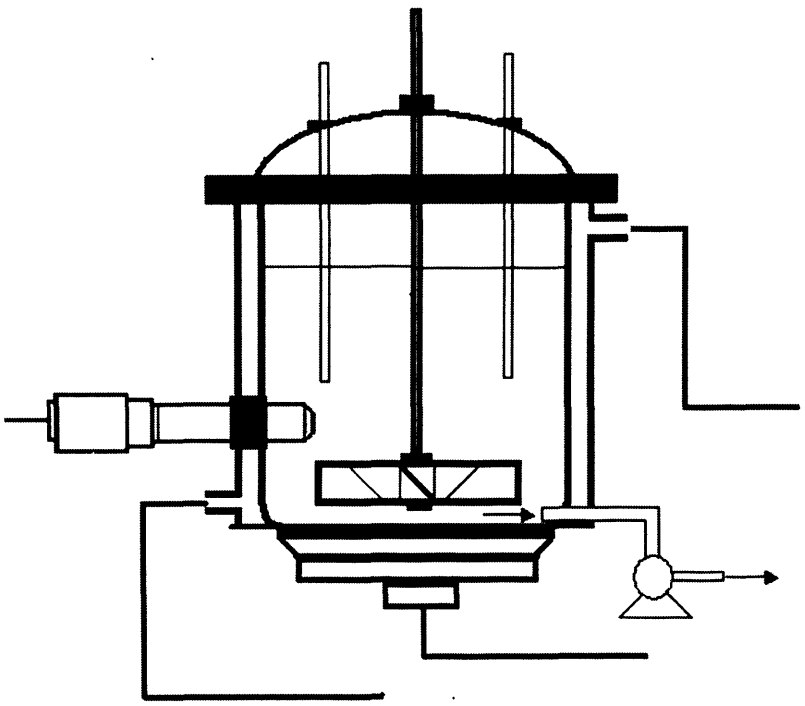

Figure 10.8 The sketch of small crystallizer design with both ultrasonic horn and ultrasonic amplifier

The technology of scale-out will be the most important commercialization of sonocrystallization technology in future business.

10.2.6 The shortage of experts in crystallization scale-up in pharmaceutical companies

Presently, scale-up is the only method to industrialize crystallization processes after its laboratory-scale technological development is finished. But a successful scale-up requires comprehensive understanding in crystallization, good knowledge in fluid dynamics and many years' experience in different scale-up projects. Normally, pharmaceutical companies do not have many experts in scale-up in their crystallization group, since the requirement for an engineer who can carry scale-up is even much higher than the engineer who can do laboratory-scale technological development. There exist some companies focusing on crystallization scale-up service. These companies have enough engineers and experience to do crystallization scale-up. But, however, since the secrecy requirement in whole pharmaceutical industry, no pharmaceutical company is willing to seek outside help. Thus, in many pharmaceutical companies, even they can develop laboratory-scale crystallization processes successfully, the failure of scale-up will cause the significant decrease of product quality.

10.3 The approach to this opportunity

10.3.1 The characteristics of the technologies and their applications

The two technologies using ultrasound to control crystallization processes can be used in different chemical industrial fields. The technology, which uses sonocrystallization technology to control crystallization processes in traditional crystallizers, can be used to purify and crystallize heavy chemicals and mineral products.

These processes are always used to produce intermediate products, which will be used as raw material for further treatment. Compared to fine chemicals industry, the high productive capacity and the low operational cost are most important factors for these processes, since the requirements of the products are quite high but the prices are relatively low. The crystallization technologies of this kind of materials are relatively mature and the requirements of secrecy in these industrial fields are not as strict as fine chemicals industry. There exist some companies with business of crystallization design providing services to these industries. Thus, although the quality improvement of chemical product can increase their sales, the change of production unit will be controlled by cost. The scale-out technology is not suitable for this industry because of its relatively high cost. But the technology, which uses sonocrystallization technology to control crystallization processes in traditional crystallizers, is much more suitable for these fields because of their low cost and acceptable effect on crystallization processes. The installation of several ultrasonic generators will not bring significant financial problem but will increase the product quality significantly.

The scale-out technology is especially suitable for fine chemicals industry, such as pharmaceutical industry, food industry and cosmetic industry and so on, because no company in these fields is willing to let other companies know what they are doing. The productive capacity is relatively low and the product quality is much more important than the cost of technological progress. The increase of product quality can increase the producer's market share and profit significantly. So the scale-out technology is particularly suitable for these industries.

Thus, the technologies based on the research results and conclusions of this research will meet the requirements of crystallization processes in different industries.

10.3.2 Future research and development in scale-out technology

There is not a lot can be done to improve the technology, which uses

sonocrystallization technology to control crystallization processes in traditional crystallizers. The only thing needed is to do some experiments in a large crystallizer to test the result of sonocrystallization and choose a suitable ultrasound generator.

But to apply scale-out method into industrial design, more research and development need to be carried. The first R&D task is to test whether two similar small crystallizers can precipitate crystals with similar quality, if the operational parameters are similar. Through experiments, the reproducibility and stability of the scale-out technology can be obtained. Another R&D task is to design a system which can make the operational parameters, such as, temperature, cooling rates, feeding rates, and so on, uniform in different small crystallizers. Thus, good controllers and distributors need to be developed and chosen to satisfy the requirement of the new production unit. Then after assembly, experiments are still need to be carried to test reproducibility and stability. After the development of first generation of scale-out production unit, further optimization of production unit can be drafted.

10.3.3 Testing service

To help future customers understand and adopt the sonocrystallization technology in their production processes, some testing services are necessary to be provided.

For the companies producing heavy chemicals and mineral products, some researches should be carried to determine the ultrasonic effects, such as the ultrasonic effect on nuclei amount, the energetic influence to crystal size and so on. The results will be used to determine the operational parameters for new cystallizer.

To the fine chemicals industry, since secrecy requirement is strict, other people cannot attend their R&D directly. So single small crystallizers will be provided to these companies for experiments. Only the optimized operational parameters will be provided to the company producing scale-out production unit. Followed these parameters, the crystallization processes can be run and controlled in scale-out production unit. The

production unit by scale-out can act as a black box, which will not show any secret of customers, such as substances, solutions, quality requirements and so on.

10.3.4 Long term growth

The sonocrystallization technology can offer excellent growth opportunity for a potential company. After the promotion of both the technologies, which uses sonocrystallization technology to control crystallization processes in traditional crystallizers, and scale-out technology. Further development can be carried to improve the sonocrystallization technology.

More studies can be carried to solve the problems in crystallization such as, how to depress agglomeration, how to increase crystal growth rate and how to change crystal habits and so on. From these results, other new crystallizers can be designed and promoted to market. Some simulation models can also be developed and included into software to help factories predict the ultrasonic effect on their product.

The business can also be expanded to other fields. Because design and optimization of crystallization processes are based on the methods obtained from chemical reaction processes. They have many similarities. Many problems existing in crystallization processes may also exist in chemical reaction processes. Thus, some technologies developed to solve crystallization problems may also be used to solve chemical reaction problems. So it is highly likely that the new chemical reactors with ultrasonic control will be developed in future. The market for the design and installation of chemical reactors is an existing market, which is much bigger than the market of crystallization.

10.4 Marketing

The business will depend on two new technologies, which are not totally mature at

present and the designs can be copied. Thus, the IP is most important issue for this company and the further R&D for technological progresses will become a source of sustainable competitive advantage.

10.4.1 Target customers

The analysis of the features of two different technologies and their application has identified two discrete customer segments: Those companies who need to purify and precipitate heavy chemicals and mineral products. And those companies who need to produce solid fine chemicals with high value, such as pharmaceutical, food, cosmetic and so on.

Initially, the business should target on the companies who need to purify and precipitate heavy chemicals and mineral products, because the installation and reconstruction of a traditional crystallizer are much cheaper than building a new production unit for crystallization with scale-out design. So the threshold of this market is relatively lower compared to the second segment. But because there already exist some companies with sonocrystallization technologies in this segment, and the margin is relatively low. Thus, after the initial stage, the concentration of the business should be transferred to the second segment.

The second segment does not exist at present. It requires some time to be developed. The pharmaceutical companies can be considered as the first and main niche in the second segment. Because of their secrecy requirement, it is not possible for them to get help from companies specializing in crystallizer design. As mentioned above, over 90% of all pharmaceutical products contain drugs in particulate, generally crystalline form. The requirement of crystallization process design is quite high in this field, but not all the pharmaceutical companies have financial capability to support a R&D group to do all the work from laboratory-scale technological development to industrial scale-up. Thus, scale-out technology should attract enough customers because

of its convenience and stability. The company can try to attract some small pharmaceutical companies initially since these companies do not have enough technological resource to do their industrial scale-up. The scale-out technology can solve their problems with relatively low cost.

Another factor which may promote scale-out technology is that it has become more and more expensive to develop a new pharmaceutical nowadays. The cost may easily reach billions of US dollars. Thus, to maintain their profit, many small pharmaceutical companies, and even large pharmaceutical companies begin to find ways to decrease their production cost and increase the quality of their existing products. Because of this trend, crystallization processes are receiving increasingly attention. So a technology which can apply the R&D result directly to production will definitely be welcomed by pharmaceutical industry.

Then, after the launch campaign of scale-out technology in pharmaceutical industry, the technology can also be promoted in other fine chemical industries, such as, food industry and cosmetic industry. The companies in these fields also need to use crystallization processes to manufacture solid products.

10.4.2 The IP appraisal

Patentable elements of this technology will lie in uniqueness of the research and the technology.

There has been so far no literature available to elucidate the relationship of crystallization nucleation parameters with ultrasonic power, because of the difficulties of conducting the experiments directly to measure crystallization parameters in ultrasonic field. All the existing literatures and reports of sonocrystallization are "phenomenon description", which obviously cannot provide any prediction for the technological development with new substance. And there is also no report about the concept of the scale-out of crystallization processes. Without the thorough

understanding of ultrasonic effect on primary nucleation during crystallization processes, it is not possible to design the scale-out crystallization production unit.

This research not only offers numerical results of ultrasonic effects on crystallization parameters, but also provides mechanism of these effects, that can be used for the laboratory-scale experiments and the scale-out of sonocrystallization technology.

The most important patents should include the idea of scale-out method, the design and the structure of production unit, and the control parts for temperature, feeding rate, and so on. The operational conditions in crystallization processes and the control software are essential to sonocrystallization technology. These factors can also be included into patent. The patent of these innovations and their further improvements can exclude other competitors from the market segment of the producers of solid fine chemicals.

The design of small crystallizers with ultrasonic generators should also be included into patent. This patent will forbid the copy of this design into other technology.

The designs and subsequent revisions of traditional crystallizers with ultrasound are also expected to be patentable. These are all expected to produce the opportunities for several patents to emerge.

10.4.3 Building brand awareness and credibility

The launch campaign will focus primarily on exploiting PR opportunity. The technologies can be reported on academic journals. The advertisement should be made both on journals and conferences. Some exhibitions can be held on conferences to introduce sonocrystallization technology to industry.

At the launch stage of sonocrystallization, the company can find some collaboration partners in industry. The success of one or two projects to apply ultrasound on crystallization processes will help more companies take notice of

sonocrystallization technology and build credibility. In these several projects, the company can ask small amount of reward or even no payment but to concentrate on the process of collaboration. This collaboration will also make company understand the needs of industry and satisfy these needs properly.

Credibility will be built over time through the professional nature of company's technology and service. IP is quite important in credibility establishment since it can provide uniquity of the company. The company should pay enough attention to its R&D since the stability and improvement of sonocrystallization technology are essential for company's future credibility.

10.4.4 Possible competitive landscape

Accentus plc developed flow cell and in situ seeding cell, which targets on the companies need to purify and precipitate heavy chemicals and mineral products. Their design and technology are different from that proposed here. So the result and cost of the services from Accentus plc and our plan will be different. Currently, it is found that Accentus plc is still in the stage of launch campaign for its technology. Not many companies have adopted its technology. So it is still possible to enter into this market segment.

The market of scale-out design currently does not exist. So there is no direct competition in this market segment at present. The competition in this market segment is from two aspects: one is the companies specializing in crystallizer design and installation. But normally, because of secrecy reason, the companies producing fine chemicals are not willing to let them know many important operational parameters, which are important for crystallizer design. And their service is totally different from our plan. Thus, in the market segment, their threatening to scale-out business will not be serious. Another competition is from pharmaceutical companies, which are our customer targets. Since sonocrystallization technology has got more and more attention

in recent years, many pharmaceutical companies have their own research group to do R&D in this field. After the investigation, it is found that their R&D concentrates on using ultrasound to control polymorphism of crystal product and crystallization process. So their technologies will not overlap with ours. Thus, if IP is kept properly, the competition capacity can be maintained in this segment.

10.4.5 Pricing

At the beginning of launch campaign of the new business, the company's has two tasks. One is entering the market of crystallizers for heavy chemicals and mineral products. In this market, the price of every project should be attractive to the companies in this segment. Thus, assuming this technology is better than the technologies from other companies, the price charged should be similar or only a little bit higher.

At the launch campaign stage of scale-out technology, collaboration with pharmaceutical companies will be most important thing. At this stage, the main task is letting future customers understand the advantages of scale-out technology. Thus, the price charged should be low enough to attract the collaborators. Then, the price can be increased after scale-out technology is accepted.

10.5 Technology risk

Since the technology using ultrasound in traditional crystallizers concerns hydrodynamic condition inside the crystallizer, the ultrasonic effect may be influenced by the hydrodynamic condition. Although it can be predicted that ultrasound will definitely bring favorable influence to crystallization processes, it is hard to predict how much the influence is. Thus, to some crystallization processes, adoption of ultrasound in traditional crystallizers may not be a good choice. Some further experiments on crystallizers may help to solve this problem.

The development of distributors and controllers is a "technology venture" in scale-out method. These controllers and distributors are important since they will provide uniform operational parameters in different small crystallizers inside the production unit. The small difference of these parameters in different small crystallizers may cause the unqualified product. But the existing technologies and methods should be already advanced enough to provide required distributors and controllers

10.6 Estimated cost for a potential company

The cost for a scale-out production unit should be around £500,000, which comprises 1000 small crystallizers. It is estimated that each crystallizer is roughly worth £500, with £100 for ultrasonic generator and £400 for other parts. Large-scale manufacture may make costs lower. One ultrasonic generator used on traditional crystallizer may cost £ 4,000, since it should be bigger and more powerful. Their installation will also carry a large cost. Assuming one traditional crystallizer needs 8 ultrasonic generators, the total cost to reconstruct a crystallizer will be £ 32,000. Thus the initial investment to the business should be more than £2,000,000, which include the research cost, some stock, the cost of launch, and the cost to cover employees' salary for 2 years.

10.7 Progress so far

The development of mathematic models for nucleation during crystallization process using ultrasound in this research has been finished. It is essential for the industrialization of sonocrystallization technology. Particularly, it is the theoretical foundation for the scale-out method of crystallization processes. And the experiment to investigate the ultrasonic effect on breakage during crystallization processes has also been finished. It is demonstrated that there should exist an energy value, where

ultrasound can depress agglomeration while does not breaking the majority of crystal product. This conclusion can be used to develop technology, which can control agglomeration using ultrasound during crystallization processes.

The mathematic models and mechanism have been developed. More particularly, commercially this present research offers:

1. The directions to laboratory-scale development of sonocrystallization technology. With the aid of the result from our research, the experimental cost can be reduced efficiently and the possibility of success can be increased significantly.
2. The directions to industrial scale-out of sonocrystallization processes. The operational conditions can be transferred directly to production unit whose theoretical foundation has been finished in this research.
3. The design and optimization of crystallizers with ultrasonic control of crystallization process. Especially, when ultrasound is used to reconstruct traditional crystallizers, using the theory and knowledge obtained from this research, it will be very easy to determine the number of ultrasound generators and their positions on crystallizers.

CHAPTER 11

CONCLUSIONS AND FUTURE WORK

11.1 Conclusions

Crystallization is a technique which involves the formation of an ordered solid phase from a homogeneous gas, liquid or amorphous phase. Ultrasound may bring a significant influence on the crystallization process. The application of power ultrasound to crystallizing systems appears to offer significant potential for modifying and improving both processes and products. The main reason why ultrasound can bring such a significant influence to crystallization process is on account of its effects on crystallization kinetics. Ultrasound can influence nucleation, crystal growth, agglomeration and breakage during crystallization processes.

This thesis has focused on studying the ultrasonic effect on nucleation and crystal breakage during crystallization processes.

The effect of ultrasound on reactive crystallization when nucleation is consistent with a predominantly homogeneous model is studied by measuring the induction time. Barium sulphate is used as the working substance precipitated by mixing aqueous $BaCl_2$ and Na_2SO_4 solutions. The relationship between amplitude of ultrasonic processor and power input was determined. The experiments were carried with ultrasonic power inputs at 0, 8.62, 18.0, 27.3, 36.6 and 46.0W. It is observed that ultrasound has a significant effect in reducing the induction time. At a given supersaturation level, the induction time decreases with increasing ultrasonic energy.

The relationship with power input (E) and the activation energy of nucleation (E_N) is discussed. And the equation between total power input and the nucleation rate coefficient (k_N) is obtained. When applying ultrasound to the system, the change in the apparent nucleation order (n) is small, however, k_N increases significantly. From the experiments, it is observed that k_N has an exponential relationship with total power input. The above relationship fits the equation between total power input and k_N well.

The mechanism of the ultrasonic effect on homogeneous nucleation is analyzed. It is found that when temperature is kept constant, the main effect of ultrasound is to increase the diffusion coefficient (D_{AB}). Other parameters change only slightly or

remain constant within the ultrasonic field. This suggests that diffusion acceleration is the main reason for the reduction of the induction time.

When nucleation is consistent with a predominantly homogeneous model, the interfacial tension is estimated as 61.89 mJ/m^2 by employing the classical nucleation theory. The ultrasonic effect on the clusters in solution is analyzed by a cluster coagulation model. It is found that the number of monomers in dominating clusters ($\bar{g}$) is 3 for different power inputs. A theoretical analysis of the total absolute deviation (ε) shows that the number concentration of largest clusters increases slowly with the increase of power input. But compared to the increase of diffusion coefficient (D_{AB}), this effect is very small. In this experimental condition, analysis of the induction time is consistent with clusters having 3 monomers being predominant in the solution.

The mechanism of the ultrasonic effect on homogeneous nucleation is analyzed. The relationship of D_{AB} and power input is also discussed. A mathematical model of power input and diffusion coefficient is presented, from which it is predicted that diffusivity enhancement (D_{AB}- D_{AB0}) has an exponential relationship with power input. The above relationship is consistent with the results of the experiments. From the mathematical model and experimental results, it can be concluded that the molecular energy of $BaSO_4$ has a direct proportional relationship with its concentration in the stagnant film between the bulk of the fluid phase and the solid surface during mass transfer process, and the distribution curve of solute concentration with position in this stagnant film should be concave.

Induction times have also been measured with and without ultrasound to investigate its effect on induction time of spectinomycin hydrochloride, roxithromycin and sucrose during anti-solvent crystallization. The diffusion coefficient increases about 8.58 fold by using 400W ultrasound for spectinomycin hydrochloride. And D_{AB} of roxithromycin and sucrose were increased about 3.82 fold and 1.93 fold by using 400W ultrasound, respectively.

The relationship between ultrasonic power input and diffusion coefficient is also

investigated. It is found that at the same power input, the ultrasonic effect on D_{AB} decreases with increased solution viscosity.

The effect of ultrasound on nucleation of $BaSO_4$ is also studied by a Kodak motion analyzer. The dispersion processes of ink with ultrasound and stirring are used to compare the difference of the mixing processes and hydraulic flows. It is found that ultrasound can make flows much more turbulent in the vessel. The vessel is divided into several sections to investigate the local mixing process by recording the movement of small silicon carbide crystals. It is found at 41% amplitude, the energy distribution is even in the vessel. But at 51% and 61% amplitudes, it is uneven. The velocity variances of crystals, which indicate the mixing process, are close in section 3, 4 and 5. But in the section 6, the mixing process is much worse. However, the cavitation distributions in section 5 and 6 are much lower than other sections. The velocity variance of crystals in the agitated vessel is much lower than the vessel with ultrasound.

$BaSO_4$ is precipitated by mixing aqueous solutions of $BaCl_2$ and Na_2SO_4. The nucleation processes are also observed by Kodak motion analyzer in different sections. It is found the nuclei will appear isochronously in sections 3, 4 and 5. The mechanism of nucleation by ultrasound is analyzed.

Then, the induction times at different temperatures are measured with different power inputs at a given supersaturation level. It is found the ultrasonic effect on nucleation will decrease with increase of temperature. But the cavitation density will increase with temperature increase. This phenomenon shows that the cavitation has no direct relationship with the increase of homogeneous nucleation rate. Ultrasound and its cavitational effect can increase homogeneous nucleation rate through the increases of mixing and diffusion processes. The relationship between the cavitation distribution and temperature is established. Ethanol and acetone are used to verify this relationship. It is found the cavitation density will decrease with increase of viscosity of fluid medium.

After the investigation of ultrasonic effect on homogeneous nucleation, the effect of ultrasound on reactive crystallization when nucleation is consistent with a

predominantly heterogeneous model is studied by measuring the induction time. Barium sulphate is used as the working substance precipitated by mixing aqueous $BaCl_2$ and Na_2SO_4 solutions with relatively low concentrations compared to the experiments of homogeneous nucleation. The experiments were also carried with ultrasonic power input at 0, 8.62, 18.0, 27.3, 36.6 and 46.0W. It is observed that ultrasound has a significant effect in reducing the induction time, when nucleation is consistent with a predominantly heterogeneous model as well.

The mechanism of the effect of ultrasound on heterogeneous nucleation is determined. Compared to homogeneous nucleation, the mechanism of ultrasonic effect on heterogeneous nucleation is more complex. From the non-parallel straight lines of plots of $\ln(t_{ind})$ versus $\ln^{-2}(S)$, it is found that geometric correction factor (f) and the contact angles (θ) decrease with increasing power input, but both the gradient of f with power input and the gradient of θ with power input decrease with increasing power input. That is: when the power input is high, a given increase in ultrasonic energy, does not bring about as significant effects on f and θ as when the power input is low.

The ultrasonic effect on critical supersaturation ratio (S_{crit}) is also investigated to determine the mechanism of the effect of ultrasound on f and θ. From the simulation of S_{crit}, it is found that the critical supersaturation ratio (S_{crit}) increases with the decrease of contact angle (θ). The values of S_{crit} are: 30.2 without ultrasound, 30.5 with 8.62W, 30.8 with 18.0W, 30.6 with 27.3W, and 30.2 with 36.6W, and 30.7 with 46.0W. S_{crit} changes with different power inputs, but the variance is not significant. The simulation result is not consistent with the experimental results, which means the force from the cavitational bubble implosion cannot be the only reason for the change of f and θ in the ultrasonic field. After analysis of other possible reasons for ultrasonic effect on f and θ, it is found that the nucleation process occurring at bubble/solution/foreign solid interface may also contribute to the decrease of f and θ in the ultrasonic field.

The ultrasonic effects on nucleation order (n) and the nucleation coefficient (k_N) are investigated, when nucleation is consistent with a predominantly heterogeneous

model as well. It is found that unlike homogeneous nucleation, ultrasound can decrease the apparent nucleation order significantly, when nucleation is consistent with a predominantly heterogeneous model. The nucleation coefficient (k_N) is also changed substantially and increases exponentially with power input.

The ultrasonic effect on the clusters in solution is analyzed by a cluster coagulation model, when nucleation is consistent with a predominantly heterogeneous model. It is found that without ultrasound, the monomer number in dominant clusters is 4 or 5. But, however, with 8.62W power input, the monomer number in dominant clusters varies between 6 and 7 at different supersaturation levels; with 18.0W: between 8 and 11;with 27.3W: between 9 and 13; with 36.6W: between 8 and 14; and with 46.0W, between 8 and 15. Thus the dominant cluster size increases when supersaturation increases with different power inputs. At the same supersaturation level, however, the size of dominant cluster increases with increasing ultrasonic energy. This phenomenon is different from what is observed when nucleation is consistent with a predominantly homogeneous model. In the homogeneous nucleation experiments with barium sulphate as the working substance, nucleation clusters having 3 monomers are predominant in the solution for different power inputs. That is the ultrasound has insignificant effect on the size of dominant clusters during homogeneous nucleation. When nucleation is consistent with a predominantly heterogeneous model, the increase of cluster size can decrease the induction time further in the ultrasonic field. The coagulation of large clusters can make the formation of critical nuclei quicker, because the new clusters, formed from the coagulation of large clusters, have larger size than the new clusters formed from the coagulation of small clusters. Thus, as ultrasonic energy increases, fewer collisions between clusters are required to form a critical nucleus, consequently increasing the nucleation rate.

A Kodak motion analyzer is applied to observe the ultrasonic effect on breakage process of agglomerated crystals after the studying of ultrasonic effect on primary nucleation. The cavitation effects on the particles with different sizes are investigated. It

is found that the influence on particles with big sizes is stronger than its effect on particles with small sizes. The mixing processes with stirring and with ultrasound are investigated by the dispersion of ink in the ethanol. Small sugar crystals are used as indicators for the movement of hydraulic flows. Velocity variance is used to indicate the difference of turbulence when ultrasound is applied and when stirring is applied respectively. The velocity variance of crystals in the agitated vessel is much lower than the vessel with ultrasound. So the collision rate between crystals is higher in the vessel with ultrasound. The cavitation distribution in different sections is also recorded. The breakage mechanism in different sections is observed respectively with the agglomerated sugar crystals as the working substance. It is found that both the collision between crystals and the vibration and implosion of cavitation bubbles contribute to breakage process of agglomerated crystals. The agglomerated sugar crystals are added into vessel with ultrasound and stirring treatment for 5 minutes. The product is observed by microscope and compared with the product after grinding. The surfaces of crystals after grinding are much damaged compared to the crystals treated by ultrasound. The reason of high breakage rate in the vessel with ultrasound is on account of high power input. The fluid medium will be more stable with high ultrasonic power input than with stirring power input.

The thesis also details the commercial evaluation to apply sonocrystallization technology into industry. In essence, the drafts of two possible new crystallizer designs are displayed. One is using sonocrystallization technology to control crystallization processes in traditional crystallizers (normally of volume more than 2000L). Another technology is using ultrasound to initiate a new technology, namely scale-out of crystallization processes, which can be used to substitute industrial scale-up of crystallization processes from laboratory-scale. Here, instead of using one traditional crystallizer with large volume, the new unit is composed of many small crystallizers (1 or 2 L) linked by parallel connection method to provide enough productive capacity. The business opportunity is analyzed and the plans to approach this business market are

also evaluated. The potential customers are separated into different segments. Then, the PR and advertisement plans to approach different segments are formulated. The technology risk and the financial cost of the business are estimated as well. It is found that the research result has a good chance to be commercialized.

11.2 Future work

11.2.1 The future research on crystal growth and secondary nucleation

From the existing literatures which are reviewed in the second chapter, ultrasound can influence secondary nucleation, crystal growth rate, agglomeration and breakage significantly during crystallization processes. So in addition to primary nucleation, ultrasound can also be used to control other operational parameters and product quality of crystallization processes. But successful application of ultrasound on crystallization processes is difficult, however, as there is a lack of understanding that physical and chemical processes play in the ultrasonic field. Thus, the mechanisms of ultrasonic effect on secondary nucleation, crystal growth rate, agglomeration and breakage have to be clearly researched and the related mathematic models need to established for the industrialization of sonocrystallization.

Because of the underdevelopment of mathematic analytical methods, it has not been possible to obtain the crystallization parameters of nucleation, crystal growth, agglomeration and breakage from a population balance equation directly. But during crystallization processes in ultrasonic field, primary nucleation, secondary nucleation crystal growth, agglomeration and breakage will occur simultaneously, thus, it is difficult to determine the ultrasonic effects on above parameters directly from population balance equation. So these parameters can only be determined separately by different experiments.

In this thesis, the ultrasonic effect on primary nucleation is determined. But

because it is not easy to design the separate experiments to determine ultrasonic effect on the crystal growth rate, agglomeration kernel and breakage kernel, these parameters could not be studied quantitatively in this thesis.

From the qualitative research of ultrasonic effect on agglomeration and breakage during crystallization process, it is found that ultrasound will decrease agglomeration kernel and increase breakage kernel, while the ultrasonic energy and frequency may also influence its effect on agglomeration and breakage processes. The ultrasonic effect on crystal growth may be much more complicated. Generally, ultrasound should have significant influence on the diffusion-controlled crystal growth process, since ultrasound can increase diffusion processes significantly. But it is hard to predict the ultrasonic effect on reaction-controlled crystal growth process. Similarly to agglomeration and breakage processes, the change of energy and frequency may also change ultrasonic effect on crystal growth rate.

To determine the mechanism of these complicated phenomena, new mathematic analytical methods are required to be developed to solve population balance equation, when primary nucleation, secondary nucleation crystal growth, agglomeration and breakage occur simultaneously. And the new experimental methods and new equipment need to be designed and set up as well.

11.2.2 The further research on scale-out method of crystallization processes

To apply scale-out method into industrial design, more research and development need to be carried. The first experiment is to test the reproducibility of products from different small crystallizers. The experiment can be carried out in two similar small crystallizers. The quality of crystals from different crystallizers will be measured to determine whether the parameters of products from different crystallizers are similar, if the operational parameters are similar. Through experiments, the reproducibility and stability of the scale-out technology can be obtained and the further optimization of

production unit can be drafted. The second R&D task is to design a system which can make the operational parameters, such as, temperature, cooling rates, feeding rates, and so on, uniform in different small crystallizers. Thus, good controllers and distributors need to be developed and chosen to satisfy the requirement of the new production unit. These controllers and distributors are important since they will provide uniform operational parameters in different small crystallizers inside the production unit. The small difference of these parameters in different small crystallizers may cause the unqualified product. But the existing technologies and methods should be already advanced enough to provide required distributors and controllers. Then after assembly, experiments are still need to be carried to test reproducibility and stability. These experiments will facilitate the application of scale-out method into industrial design.

Therefore, possible future works would advance the theoretical foundation of sonocrystallization technologies and initiate its industrialization processes.

NOMENCLATURE

a	the slope of the straight line
a_{for}	the volumetric surface
A	monomer of solute
A	the surface of nucleus
A_c	the surface area of cluster
A_1	the intercept of equation (3.17)
A'	a frequency factor
B	nucleation rate
B_1	the slope of equation (3.17)
B_{hom}	homogeneous nucleation rate
B_{het}	heterogeneous nucleation rate
$B_{het,surf}$	heterogeneous nucleation rate based on the surface of foreign particles
C	the actual concentration
C_{ad}	the adsorption-related concentration
$C_{ad,v}$	the volume-related concentration
C_A	solute concentration
C_B	solvent concentration
C_p	the heat capacity of water
C_s	the saturated concentration of solute
C^*	the equilibrium concentration
C_C	molecular density of solid
C_0	initial concentration
d_m	the diameter of the molecule
d_s	the diameter of stirrer
D_{AB}	the diffusion coefficient
D_{AB0}	the initial diffusion coefficient
D_{surf}	the surface-diffusion coefficient of units

E	the ultrasonic power input
E_0	the energy per molecule from ultrasound
E_b	the energy barrier per molecule
E_N	activation energy of nucleation
f	geometric correction factor
F_c	the impetus of diffusion from the chemical potential gradient
F_r	the resistance of diffusion from Stokes' law
F_u	the impetus of diffusion from ultrasound
g	the exponent for crystal growth
g	number of monomers in a cluster
g'	exponent for crystal growth
g_c	the number of monomers in a critical cluster
$\overline{g}$	the number of monomers in dominating clusters
ΔG_C	the free energy of critical cluster
$\Delta G_{C,\text{hom}}$	the free energy of critical cluster, when nucleation is predominantly homogeneous
$\Delta G_{C,heter}$	the free energy of critical cluster, when nucleation is predominantly heterogeneous
ΔG_g	overall excess free energy of formation of a g-mer
ΔG_s	the surface excess free energy

ΔG_v	the volume excess free energy
$\Delta G_{v,unit}$	the free energy change of the transformation per unit volume
He_{ad}	absorption constant
i_c	the critical cluster number
I	ionic strength
k	Boltzmann constant
K	the coefficient of proportionality
k_N	the nucleation coefficient
k_1 , k_2 , k_3 , k_4 , k_5, k_6, k_7	the coefficients of proportionality
k'	the rate which clusters cross the barrier
K_{sp}	solubility product
K'	constant in diffusion coefficient model
K_1	factor in surface tension model
K_1	a proportion constant
L_c	the cluster diameter
$\widetilde{M}$	molar mass
n	the apparent nucleation order
n	the number of crystals.
n'	true nucleation order
n_g	the number concentrations of g-mers
$n_{\bar{g}}$	the number concentrations of dominating clusters
n_0	the initial number concentration of monomers
n_1	the number concentrations of monomers
n_c	the number concentration of critical

	clusters, when nucleation is predominantly homogeneous
n'_c	the number concentration of critical clusters, when nucleation is predominantly heterogeneous
n_0	the number concentration of molecules in the supersaturated solution
n_{water}	the mole of water
$\dot{n}_{Surf}$	the impact rate of units from the surface
$\dot{n}_{\upsilon}$	the impact rate of units from the volume
N	the stirrer speed
N_A	Avogadro's number
N'_A	Diffusion flux of solute A
P	the power drawn by the agitator,
P_0	the power number,
Q	quantity of heat
r	radius of curvature of the nuclear
r_A	the radius of solute molecule
r_c	the radius of critical nucleus
r_g	the radius of $\overline{g}$ -mer
R	ideal gas constant
S	supersaturation ratio
S_{crit}	critical supersaturation ratio
t	time
t_{ind}	induction time
T	absolute temperature
T_0	initial temperature

u_A	the net velocity of solute molecule in stagnant film
U_{surf}	circumference of nucleus
v	the number of moles of ions produced by one mole of electrolyte
$v_{average}$	the velocity of average particle
v_c	the velocity of particle
V	the volume of solution
V_A	the volume of solute molecule
V_B	the volume of solvent molecule
V_m	the molecular volume
x_A	mole fraction of solute
z	the moving distance of solute molecules in the stagnant film
Z	the imbalance factor
z_+, z_-	ionic charge of positive ion and negative ion
σ	the relative supersolubility
σ^2	variance of velocity
ρ	the solution density
ρ_c	density
γ_{CL}	the surface tension
γ_{CS}	the interfacial tension between the solid crystalline phase and the foreign solid surface
γ_{SL}	the interfacial tension between another foreign solid surface and the liquid

$\gamma_{\pm}$	the activity coefficient
ν	the number of moles of ions formed from one mole of electrolyte
θ	contact angle
μ_A	the chemical potential
μ	the viscosity of solution
μ_B	the viscosity of solvent
ε	the total absolute deviation

REFERENCES

AEA Technol (2001) Sonocrystallization, FAQ Sonocrystallization, available at http://www.aeat.com/sono/.

AEA Technol (2005) Ultrasound to make crystals, available at http://www.accentus.co.uk/articles.htm.

AEA Technol (2005) Complete crystallization control, available at http://www.accentus.co.uk/c3_brochures.htm.

Amara, N., Ratsimba, B., Wilhelm, A. and Delmas, H. (2001) Crystallization of potash alum: effect of power ultrasound, Ultrasonics Sonochemistry 8, 265-270.

Aquilano, D., Costa, E., Genovese, A., Massaro, F.R. and Rubbo, M. (2003) Heterogeneous nucleation and growth of crystalline micro-bubbles around gas cavities formed in solution, Progress in Crystal Growth and Characterization of Materials, 46, 59-84.

Baldyga, J. and Bourne, J. R. (1992) Interactions between mixing on various scales in stirred tank reactors. Chemical Engineering Science, 47, 1839-1848.

Baldyga, J., Podgorska, W. and Pohorecki, R. (1995) Mixing-precipitation model with application to double feed semibatch precipitation. Chemical Engineering Science, 50, 1281-1300.

Baldyga, J. and Poherecki, R. (1995) Turbulent micromixing in chemical reactors - a review. Chemical engineering Journal, 58, 183-195.

Baldyga, J., Bourne, J. R. and Hearn, S. J. (1997) Interaction between chemical

reactions and mixing on different scales. Chemical Engineering Science, 52, 457-466.

Balibar, S., Chavanne, X., and Caupin, F., (2003) Very fast growth and melting of ^{4}He crystals, Physica B: Condensed Matter, 329-333(Part 1), 380-381.

Behrend, O., and Schubert, H., (2001) Influence of hydrostatic pressure and gas content on continuous ultrasound emulsification, Ultrasonics Sonochemistry, 8, 271-276.

Bennett, C. O. and Myers, J. E., (1983) Momentum, Heat and Mass Transfer, International edition, McGraw-Hill Book Company.

Biscans, B. (2004) Impact attrition in crystallization processes. Analysis of repeated impacts events of individual crystals, Powder Technology, 143-144, 264-272.

Buckley, H.E. (1952) Crystal growth, Chapman and Hall, London.

Cains, P. W., Martin, P. D. and Price, C. J., (1998) The use of ultrasound in industrial chemical synthesis and crystallization. 1. Application to synthetic Chemistry. Organic Process Research & Development, 2(1), 34-48.

Carosso, P. A., Pelizzetti, E., (1984) A stopped-flow technique in fast precipitation kinetics — The case of barium sulphate, Journal of Crystal Growth, 68, 532-536.

Chavanne, X., Balibar, S., and Caupin, F., (2001) Acoustic crystallization and heterogeneous nucleation Physical review letters, 86(24), 5506-5509.

Chemat, F., Grondin, I., Shum Cheong Sing, A. and Smadja J., (2004) Deterioration of edible oils during food processing by ultrasound, Ultrasonics Sonochemistry, 11, 13-15.

Chen, C. and Yu, C., (2004) Two-dimensional image characterization of powder mixing and its effects on the solid-state reactions, Materials Chemistry and Physics, 85(1), 227-237.

Chernov, A.A (1989) Formation of crystals in solution. Contemporary Physics, 30, 251-276.

Chew, C. M., Ristic, R. I., Reynolds, G. K. and Ooi, R. C, (2004) Characterisation of impeller driven and oscillatory mixing by spatial and temporal shear rate distributions, Chemical Engineering Science, 59, 1557-1568.

Chow, R., Blindt, R., Chivers, R. and Povey, M., (2003) The sonocrystallisation of ice in sucrose solutions: primary and secondary nucleation, Ultrasonics, 41(8), 595-604.

Chow, R., Blindt, R., Kamp, A., Grocutt, P. and Chivers, R., (2004) The microscopic visualisation of the sonocrystallisation of ice using a novel ultrasonic cold stage, Ultrasonics Sonochemistry, 11(3-4), 245-250.

Chow, R., Blindt, R., Chivers, R. and Povey, M., (2005) A study on the primary and secondary nucleation of ice by power ultrasound, Ultrasonics, 43, (4), 227-230.

Contamine, F., Faid, F., Wilhelm, A.M. Berlan, J. and Delmas, H., (1994) Chemical reactions under ultrasound: discrimination of chemical and physical effects, Chemical Engineering Science, 49, 5865-5873.

Cussler, E. L., (1997) Diffusion: Mass Transfer in Fluid Systems, 2nd edition, Cambridge University Press.

Dahlem, O., Demaiffe, V., Halloin, V. and Reisse, J., (1998) Direct Sonication System Suitable for Medium-Scale Sonochemical Reactors, AIChE Journal, 44, 2724-2730.

Dalas, E., (2001) The ultrasonic field on calcium carbonate scale formation, Journal of Crystal Growth, 222, 289-292.

Danckwerts, P.V. (1958) The effect of incomplete mixing on homogeneous reactions, Chemical Engineering Science, 8, 93-99.

Delpierre, G. R. and Swell, B. T. (2002) Specific heat capacity, available at http://www. physchem.co.za/Heat/Specific.htm.

Dirnstorfer, I., Burkhardt, W., Meyer, B.K., Ostapenko, S. and Karg, F., (2000) Effect of ultrasound treatment on $CuInSe_2$ solar cells, Solid State Communications, 116, 87-91.

Doktycz, S.J. and Suslick, K.S. (1990) Interparticle Collisions Driven by Ultrasound, Science, 247, 1067-1069.

Dunn, F. and Pond, J.B. (1978) Selected non-thermal mechanisms of interaction of ultrasound and biological media. In: Fry, F.J., ed. Ultrasound: Its application in medicine and biology, Part II, Amsterdam, Oxford, and New York, Elsevier Science Publish Co., 539-559.

Enomoto, N., Maruyama, S. and Nakagawa, Z. (1996) Sonochemical power processing of iron hydroxides, Ultrasonics Sonochemistry 3, S97-S103.

Enomoto, N., Maruyama, S. and Nakagawa, Z. (1997) Agglomeration of silica spheres under ultrasonication, Journal of materials research, 12, 1410-1415.

Entezari, M.H., and Keshavarzi, A., (2001) Phase-transfer catalysis and ultrasonic waves II: saponification of vegetable oil, Ultrasonics Sonochemistry, 8(3), 213-216.

Feng, R., Zhao, Y. and Bao, C. (1997) Sonochemistry in China, Ultrasonics Sonochemistry, 4(2), 183-187.

Fini, A., Holgado, M.A., Rodriguez, L. and Cavallari, C. (2002) Ultrasound-compacted Indomethacin/Polyvinylpyrrolidone systems Effect of compaction process on particle morphology and dissolution behaviour, Journal of pharmaceutical sciences, 91(8), 1880-1890.

Finnie, S. D., Ristic, R. I., Sherwood, J. N. and Zikic, A. M. (1999) Morphological and growth rate distributions of small self-nucleated paracetamol crystals grown from pure aqueous solutions, Journal of Crystal Growth, 207(4), 308-318.

Floros, J.D. and Liang, H. (1994) Acoustically assisted diffusion through membranes and biomaterials. Food technology, 48(12), 79-84.

Ford, I. J. (1996) Thermodynamic properties of critical clusters from measurements of vapour–liquid homogeneous nucleation rates, Journal of Chemical Physics, 105 (18), 8324-8332.

Ford, I. J. (1997) Cluster energies and nucleation theorems, Journal of Aerosol Science, 28(Supplement 1), S359-S360.

Freitas, S., Hielscher, G., Merkle, H.P. and Gander, B., (2004) Continuous contact- and contamination-free ultrasonic emulsification—a useful tool for pharmaceutical development and production, Ultrasonics Sonochemistry, In Press, Corrected Proof,

Available online.

Gahn C. and Mersmann A., (1999) Brittle fracture in crystallization processes Part A. Attrition and abrasion of brittle solids, Chemical Engineering Science, 54, (9), 1273-1282.

Gahn, C. and Mersmann, A. (1999) Brittle fracture in crystallization processes Part B. Growth of fragments and scale-up of suspension crystallizers, Chemical Engineering Science, 54(9), 1283-1292.

Gao, D. and Zhao, Q., (1998) Investigation of the methods to improve the quality of antibiotics during anti-solvent crystallization process, Huanan Ligong Daxue Xuebao, Ziran Kexueban, 26(11):16-23.

Glasgow, I. and Aubry, N. (2003) Enhancement of micro.uidic mixing using time pulsing. Lab on a chip, 3, 114-120.

Granberg, R. A., Ducreux, C., Gracin, S. and Rasmuson, A. C., (2001) Primary nucleation of paracetamol in a acetone-water mixtures, Chemical Engineering Science, 56, 2305-2313.

Guo, Z., (2003) Study on Crystallization of Roxithromycin, Master Thesis, Tianjin University.

Guo, Z., Zhang, M., Li, H., Wang, J. and Kougoulos, E. (2005) Effect of ultrasound on anti-solvent crystallization process, Journal of crystal growth, 273, 555-563.

Guo, Z., Jones, A.G., and Li, N. (2006) Interpretation of the ultrasonic effect on

induction time during $BaSO_4$ homogeneous nucleation by a cluster coagulation model, Journal of Colloid and Interface Science, 297(1), 190-198.

Harnby, N., Edwards, M.F. and Nienow, A.W., (1992) Mixing in the Process Industries. 2nd Edition. Butterworth-Heinemann.

He, S., Oddo, J. E. and Tomson, M. B. (1995) The nucleation kinetics of barium sulfate in NaCl solutions up to 6m and 90°C, Journal of colloid and interface science, 174, 319-326.

Hibberd, D., Holmes, A., Garrood, M., Fillery-Travis, A., Robins, M. and Challis, R., (1997) Ultrasonic Monitoring of Oil-in-Water Emulsions Undergoing Depletion Flocculation, Journal of Colloid and Interface Science, 193, 77-87.

Hines, A. L. and Maddox, R. N., (1985) Mass transfer: fundamentals and applications, Prentice-Hall, Inc..

Ichitsubo, T., Matsubara, E., Kai, S. and Hirao, M., (2004) Ultrasound-induced crystallization about the glass transition temperature for $Pd_{40}Ni_{40}P_{40}$ metallic glass, Acta Materialia, 52, 423-429.

Ince, N.H., Tezcanli, G., Belen, R. K. and Apikyan, I.G. (2001) Ultrasound as a catalyzer of aqueous reaction systems: the state of the art and environmental applications, Applied Catalysis B: Environmental, 29, 167-176.

Ito, Y., Nagata, K. and Komoria S., (2002) The effects of high-frequency ultrasound on turbulent liquid mixing with a rapid chemical reaction, Physics of Fluids, 14(12), 4362-4371.

Javier Del Campo, F., Neudeck, A., Compton, R.G. and Marken, F., (1999) Low-temperature sonoelectrochemical processes: Part 1. Mass transport and cavitation effects of 20 kHz ultrasound in liquid ammonia, Journal of Electroanalytical Chemistry, 477(1), 71-78.

Jones, A.G., Budz, J. and Mullin, J.W., (1986) Crystallization kinetics of potassium sulfate in an MSMPR agitated vessel, AICHE Journal 32, 2002-2009.

Kakinouchi, K., Adachi, H., Matsumura, H., Inoue, T., Murakami, S., Mori, Y., Yuichi K., Takano, K., and Kanaya, S., (2006) Effect of ultrasonic irradiation on protein crystallization, Journal of Crystal Growth, In Press, Available online.

Kapustin, A.P., (1963) The effects of ultrasound on the kinetics of crystallization / authorized translation from the Russian. New York: Consultants Bureau.

Kawahara, N., Yarin, A.L., Brenn, G., Kastner, O. and Durst, F., (2000) Effect of acoustic streaming on the mass transfer from a sublimating sphere, Physics of Fluids, 12(4), 912-923.

Kim, J., Kim, S. and Yoon, H. (2002) Ultrasonic effect on aggregation and agglomeration in crystallization of cerium carbonate in semi-batch reactor, 15th International Symposium on Industrial Crystallization, 215-220.

Kim, J., Kim, S. and Yoon, H., Lee, J.Y., Shin, D.M., Chung, M.K. and Kim, W., (2002) Ultrasonic effect on aggregation and agglomeration in crystallization of cerium carbonate in semi-batch reactor, 15th International Symposium on Industrial Crystallization, 239-244.

Kim, H., and Lee, J.W., (2002) Effect of ultrasonic wave on the degradation of polypropylene melt and morphology of its blend with polystyrene, Polymer, 43(8), 2585-2589.

Kim, Y. H., Lee, K., Koo, K. K., Shul, Y. G. and Haam, S. (2002) Comparison study of mixing effect on batch cooling crystallization of 3-Nitro-1,2,4-triazol-5-one(NTO) using mechanical stirrer and ultrasound irradiation, Crystal research technology, 37, 928-944.

Kosaka, S., Takahashi, Y., Benino, Y., Fujiwara T., and Komatsu T., (2006) Crystallization of langasite-type phases in gallium germanate glasses and optical properties of crystallized glasses, Optical Materials, 28(10), 1129-1135.

Kougoulos, E., (2003) Scale-up of Organic Crystallization Processes, Transfer Thesis, University College London.

Kusters, K. A., Pratsinis, S. E., Thoma, S. G. and Smith, D. M. (1993) Ultrasonic fragmentation of agglomeration powders, Chemical engineering science, 48, 4119-4127.

Lee, J., Kim, N. and Park, B. (2001) Effect of ultrasound on crystallization behavior and ferroelectric properties of sol-gel-derived Pb(Zr, Ti)O_3 thin film, Journal of Crystal Growth, 222, 289-292.

Lee, J., Kim, N. and Park, B., (2003) Effects of ultrasound on crystallization behavior and ferroelectric properties of sol–gel-derived Pb(Zr, Ti)O_3 thin films, Journal of Crystal Growth, 249, (3-4), 531-537.

Lenart, I. and Ausländer, D. (1980) The effect of ultrasound on diffusion through membranes, Ultrasonics, 18(5), 216-218.

Lewis, B. (1980) Nucleation and growth theory. In Crystal growth, 2nd edition., B.R. Pamplin (ed). Pergamon Press, Oxford, 23-63.

Li., D., Wang, Y., Liu, P., Wang, W. and Shi, D., (2005) Preparation of Nanosized γ-MnO_2 by presipitation under ultrasound radiation, Chinese Journal of inorganic chemistry, 21(2), 202-206.

Li, S. and Lin, Q., (1995) Sonochemistry. Beijing Scientific publishing company.

Li, H., Wang, J., Bao, Y., Guo, Z. and Zhang, M. (2003) Rapid sonocrystallization in the salting-out process, Journal of Crystal Growth, 247, 192-198.

Li, H., Li, H., Guo, Z. and Liu, Y., (2006) The application of power ultrasound to reaction crystallization, Ultrasonics Sonochemistry, 13(4), 359-363.

Liu, R.H., Yang, J., Pindera M.Z., Athavale, M. and Grodzinski, P. (2002). Bubble-induced acoustic micromixing. Lab on a chip, 2, 151 - 157.

Liu, R.H., Lenigk, R., Druyor-Sanchez, L.R., Yang, J. and Grodzinski, P. (2003) Hybridization enhancement using cavitation microstreaming. Analytical chemistry, 75 (8), 1911 - 1917.

Liu, C., Wu, C. Weng, Y., and Tseng, C., (2005) Ultrasound-assisted extraction methodology as a tool to improve the antioxidant properties of herbal drug Xiao-chia-hu-tang, Journal of Ethnopharmacology, In Press, Corrected Proof.

Louhi-Kultanen, M., Karjalainen, M., Rantanen, J., Huhtanen, M. and Kallas, J., (2006) Crystallization of glycine with ultrasound, International Journal of Pharmaceutics, In

Press, Corrected Proof, Available online.

Lu, L.-H., Ryu, K.S. and Liu, C. (Eds.) (2001) A novel microstirrer and arrays for micro.uidic mixing. In: Ramsey, J.M., van den Berg, A. (Eds.) Micro Total Analysis Systems. Kluwer Academic Publishers, Dordrecht.

Lyczko, N., Espitalier, F., Louisnard, O. and Schwartzentruber, J. (2002) Effect of ultrasound on the induction time and the metastable zone widths of potassium sulphate, Chemical Engineering Journal, 86, 233-241.

Manish, M, Harshal, J. and Anant, P., (2005) Melt sonocrystallization of ibuprofen: Effect on crystal properties, European Journal of Pharmaceutical Sciences, 25(1), 41-48.

Mason, T. (1991) Practical sonochemistry : user's guide to applications in chemistry and chemical engineering, New York ; London : E. Horwood.

McCausland, L.J. and Cains, P.W., (2002) Sonocrystallization-ultrasonically promoted crystallization for the optimal isolation of drug active. ATA Technol., Available at http://www. accentus.co.uk/articles.htm.

McCausland L. J., Cains, P.W. and Martin, P.D., (2005) Sonocrystallization– Using Power Ultrasound to Improve Crystallization Processes and Products, ATA Technol, available at http://www. accentus.co.uk/articles.htm.

McClements, D.J., (1995) Advances in the application of ultrasound in food analysis and processing, Trends in food science & technology, 6 (9), 293-299.

Mersmann, A., (1990) Calculation of interfacial tensions, Journal of Crystal Growth,

102, 841-847.

Mersmann, A. (2001) Crystallization Technology Handbook, 2nd edition. Marcel Dekker, Inc..

Mersmann, A., Braun, B. and Loffelmann, M. (2002) Prediction of crystallization on the population balance, Chemical Engineering Science, 57, 4267-4275.

Miao, J., Wang, H., Li, Y., Zhu, J. and Zhu, J. (2005) Ultrasonic-induced synthesis of CeO_2 nanotubes, Journal of Crystal Growth, 281(2-4), 525-529.

Mitragotri, S. (2001) Effect of therapeutic ultrasound on partition and diffusion coefficient in human stratum corneum, Journal of controlled release, 71, 23-29.

Mitome, H., Kozuka, T. and Tuziuti, T., (1996) Measurement of the establishment process of acoustic streaming using laser Doppler velocimetry, Ultrasonics, 34(2-5), 527-530.

Miyasaka, E, Kato, Y, Hagisawa, M. and Hirasawa, I., (2006) Effect of ultrasonic irradiation on the number of acetylsalicylic acid crystals produced under the supersaturated condition and the ability of controlling the final crystal size via primary nucleation, Journal of Crystal Growth, 289(1), 324-330.

Miyasaka, E., Takai, M., Hidaka, H., Kakimoto, Y. and Hirasawa, I., (2006) Effect of ultrasonic irradiation on nucleation phenomena in a $Na_2HPO_4 \cdot 12H_2O$ melt being used as a heat storage material, Ultrasonics Sonochemistry, 13(4), 308-312.

Moholkar, V.S., Nierstrasz, V.A. and Warmoeskerken, M.M.C.G., (2003) Intensification

of Mass Transfer in Wet Textile Processes By Power Ultrasound, AUTEX Research Journal, 3(3), 129-138.

Moholkar, V. S. and Warmoeskerken, M. M. C. G. (2004) Investigation in mass transfer enhancement in textiles with ultrasound, Chemical engineering science, 59, 299-311.

Monnier, H., Wilhelm, A.M., and Delmas, H., (1999) The influence of ultrasound on micromixing in a semi-batch reactor, Chemical Engineering Science, 54(13-14), 2953-2961.

Monnier, H., Wilhelm, A.M. and Delmas, H., (1999) Influence of ultrasound on mixing on the molecular scale for water and viscous liquids, Ultrasonics Sonochemistry, 6(1-2), March, Pages 67-74.

Monnier, H., Wilhelm, A.M. and Delmas, H., (2000) Effects of ultrasound on micromixing in flow cell, Chemical Engineering Science, 55, 4009-4020.

Monnier, H., Wilhelm, A.M. and Delmas, H., (2000) Effects of ultrasound on micromixing in flow cell, Chemical Engineering Science, 55(19), 4009-4020.

Mougin, P., Wilkinson, D., Roberts, K.J., Jack, R. and Kippax, P., (2003) Sensitivity of particle sizing by ultrasonic attenuation spectroscopy to material properties, Powder Technology, 134, 243-248.

Mullin, J. W. (2000) Crystallization, Paperback edition, Butterworths London.

Myerson, A. (2002) Handbook of Indusrial Crystallization, 2nd edition, Butterworth –Heinemann.

National Institute of Standards and Technology (accessed 19 January 2001) A gateway to the data collections. Available at http://webbook.nist.gov.

Nishida, I. (2004) Precipitation of calcium carbonate by ultrasonic irradiation, Ultrasonics Sonochemistry, 11, 423-428.

Niu, X. and Lee, Y.-K. (2003) Efficient spatial-temporal chaotic mixing in micro-channels. Journal of micromechanics and microengineering 13, 454 - 462.

Nyborg, W.L. (1978) Physical principles of ultrasound. In: Fry, F.J., ed. Methods and phenomena 3, Ultrasound: Its applications in medicine and biology, Part I, Amsterdam, Elsevier Scientific Publishing Co..

Nyvlt, J. (1985) The Kinetics of Industry Crystallization, Elsevier.

Oddy, M.H., Santiago, J.G. and Mikkelsen, J.C. (2001) Electrokinetic instability micromixing. Analytical Chemistry, 73 (24), 5822 - 5832.

Palk, P., Pamula, V.K. and Fair, R.B. (2003) Rapid droplet mixers for digital microfluidic systems. Lab on a chip, 3, 253 - 259.

Patrick, M., Blindt, R. and Zeqiri, B. (2004) The effect of ultrasonic intensity on crystal structure of palm oil, Ultrasonics Sonochemistry, 11, 251-255.

Patwardhan, A.W., Pandit, A.B. and Joshi J.B., (2003)The role of convection and turbulent dispersion in blending, Chemical Engineering Science, 58(13), 2951-2962.

Paul, E. L., Tung, H. and Midler, M. (2005) Organic crystallization processes, Powder

Technology, 150, 133-143.

Peña, R.M., Barciela, J., Herrero C. and García-Martín, S., (2005) Comparison of ultrasound-assisted extraction and direct immersion solid-phase microextraction methods for the analysis of monoterpenoids in wine, In Press, Corrected Proof, Available online.

Pétrier, C., and Francony, A., (1997) Ultrasonic waste-water treatment: incidence of ultrasonic frequency on the rate of phenol and carbon tetrachloride degradation, Ultrasonics Sonochemistry, 4, 295-300.

Pokrovsky, O. S., (1998) Precipitation of calcium and magnesium carbonates from homogeneous supersaturated solutions, Journal of Crystal Growth, 186, 233-239.

Pollet, B.G., Lorimer, J.P., Hihn, J.-Y., Phull, S.S., Mason, T.J. and Walton, D.J., (2002) The effect of ultrasound upon the oxidation of thiosulphate on stainless steel and platinum electrodes, Ultrasonics Sonochemistry, 9(5), 267-274.

Portenlänger, G. and Heusinger, H., (1992) Chemical reactions induced by ultrasound and γ-rays in aqueous solutions of L-ascorbic acid, Carbohydrate Research, 232, 291-301.

Povey, M.J.W. (1997) Ultrasonic techniques for fluids characterization, San Diego, Calif : Academic Press.

Povey, M.J.W., Golding, M., Higgs, D. and Wang, Y., (1999) Ultrasonic spectroscopy studies of casein in water, International Dairy Journal, 9, 299-303.

Povey, M.J.W. and Mason, T.J., (1998) Ultrasound in food processing, Blackie Academic & Professional.

Preston, R.C., (1986) Measurement and characterisation of bio-medical ultrasonic fields: Summary of the London Meeting on Ultrasound Standards, 5 July 1985, Ultrasound in Medicine & Biology, 12, 706-707.

Priego-Capote, F. and Luque de Castro, M. D., (2004) Analytical uses of ultrasound: II. Detectors and detection techniques, TrAC Trends in Analytical Chemistry, 23, 829-838.

Qian, S. and Bau, H.H. (2002) A chaotic electroosmotic stirrer. Analytical chemistry 74 (15), 3616-3625.

Qian, R., Botsaris, G. D., (1997) A new mechanism for nuclei formation in suspension crystallizers: the role of interparticle forces, Chemical engineering science, 52, 3429-3440.

Repacholi, M. H. and Grandolifo, M. (1987) Ultrasound. Plenum Press New York and London.

Rusanov, A.I. (1999) Thermodynamics of dispergation: development of Rehbinder's ideas, Colloids and Surfaces A: Physicochemical and Engineering Aspects, 160(2), 79-87.

Ristic, R. I., Shekunov, B. and Shewood, J. N., (1996) Long and short period growth rate variations in potash alum crystals, Journal of Crystal Growth, 160(3-4), 330-336.

Sajas, J.F. and Gorbatow, W.M. (1978) Use of ultrasound in meat technology,

Fleischwirtschaft, 58(6), 1009-1021.

Samsonov, V.M., Sdobnyakov, N.Yu. and Bazulev, A.N., (2003) On thermodynamic stability conditions for nanosized particles, Surface Science, 532-535, 526-530.

Schläfer, O., Sievers, M., Klotzbücher H., and Onyeche, T. I., (2000) Improvement of biological activity by low energy ultrasound assisted bioreactors, Ultrasonics, 38(1-8), 711-716.

Seader, J.D. and Henley, E.J., (1998) Separation process principles, John Wiley& Sons, Inc..

Shekunov, B.Yu. and York, P., (2000) Crystallization processes in pharmaceutical technology and drug delivery design, Journal of Crystal Growth 211, 122-136.

Simal, S., Benedito, J., Sánchez E.S. and Rosselló C., (1998) Use of ultrasound to increase mass transport rates during osmotic dehydration, Journal of Food Engineering, 36(3), 323-336.

Sivakumar, V. and Rao, P. G. (2003) Studies on the use of power ultrasound in leather dyeing, Ultrasonics Sonochemistry, 10, 89-94.

Skelland, A. H. P. (1974) Diffusional Mass Transfer, John Wiley& Sons, Inc..

Smoluchowski, V. M. (1916) Three lectures on diffusion, brownian movement and coagulation of colloid particles. Physik. Z., 17, 585-599.

Söhnel, O., Garside, J. (1992) Precipitation, Basic principles and industrial applications,

Butterworth-Heinemann Ltd.

Söhnel, O., Mullin, J. W., (1988) Interpretation of crystallization induction periods. Journal of Colloid and Interface Science, 123(1), 43-50.

Tai, C. Y. and Chien, W. C. (2003) Interpreting the effects of operating variables on the induction period of $CaCl_2$-Na_2CO_3 system by a cluster coagulation model, Chemical Engineering Science, 58, 3233-3241.

Tai-Quin, Q. (1993) Nucleation of sucrose solution by sound field, Int. Sugar Journal, 95(1140), 513–519.

Takeda, S. and Goetz, P.J., (1998) Dispersed/flocculated size characterization of alumina particles in highly concentrated slurries by ultrasonic attenuation spectroscopy , Colloid and Surface A: Physicochemical and Engineering Aspect, 143, 35-39.

Talanquer, V. (2002) Nucleation in Gas–Liquid Transitions, Journal of Chemical Education, 79, 877-883.

Teipel, U., Mikonsaari, I. and Ulrich, J. (2002) Ultrasonic crystallization of potassium alum, 15th International Symposium on Industrial Crystallization, 239-244.

Thompson, L. H. and Doraiswamy, L. K. (2000) The rate enhancing effect of ultrasound by inducing supersaturation in a solid–liquid system. Chemical Engineering Science, 55(16), 3085-3090.

Torbacke, M., and Rasmuson, Å.C., (2001) Influence of different scales of mixing in reaction crystallization, Chemical Engineering Science, 56(7), 2459-2473.

Trabelsi, F., Aït-Lyazidi, H., Ratsimba, B., Wilhelm, A.M., Delmas, H., Fabre, P-L. and Berlan J., (1996) Oxidation of phenol in wastewater by sonoelectrochemistry, Chemical Engineering Science, 51(10), 1857-1865.

Ueno, S., Ristic, R.I., Higaki, K. and Sato, K., (2003) In-situ studies of ultrasound-stimulated fat crystallization using synchrotron radiation, Journal of Physical Chemistry B, 107, 4927-4935.

Ueno, S., Sakata, J., Takeuchi, M. and Sato, K., (2003) Study for ultrasonic stimulation effect on promotion of crystallization of triacylglycerols, Materials science, Photon factory activity report, 182.

Ueno, S., Takeuchi, M., Sakata, J., Nozue, Y., Amemiya, Y. and Sato, K., (2003) Ultrasonic effect for the acceleration of polymorphic crystallization on fats, Materials science, available at http://pfwww.kek.jp/acr2001pdf/PartB/PF01UR136.pdf.

Veličković, D.T., Milenović, D.M., Ristić, M.S. and Veljković, V.B., (2005) Kinetics of ultrasonic extraction of extractive substances from garden (Salvia officinalis L.) and glutinous (Salvia glutinosa L.) sage, Ultrasonics Sonochemistry, In Press, Corrected Proof, Available online.

Verduranda, E., Bebonb, C., Colsonb, D., Kleinb, J.-P., Blandinc, A.-F., Bossoutrotc, J.-M., (2005) Secondary nucleation and growth of organic crystals in industrial crystallization, Journal of Crystal Growth 275, e1363– e1367.

Vichare, N.P., Gogate, P.R., Dindore, V.Y., and Pandit, A.B., (2001) Mixing time analysis of a sonochemical reactor, Ultrasonics Sonochemistry, 8(1), 23-33.

Voldman, J., Gray, M.L., Schmidt, M.A., 1998. Liquid mixing studies with an integrated mixer/valve. In: Harrison, J., van den Berg, A. (Eds.) Micro Total Analysis Systems. Kluwer Academic Publishers, Dordrecht.

Wadhawan, J.D., Marken, F. and Compton, R.G., (2001) Biphasic sonoelectrosynthesis. A review, Pure Applied Chemestry, 73(12), 1947-1955.

Wang, L., Zhu, C. and Mi. Z., (2005) Effect of ultrasonic wave on crystallization in solution), available at http://hxtb.icas.ac. cn/col/2001/c01047.htm.

Wells, A.F. (1946) Crystal growth. Annual reports on the progress of Chemistry. The Chemical society, London, 43, 62-87.

West, J., Karamata, B. Lillis, B., Gleeson, J.P., Alderman, J., Collins, J.K., Lane, W., Mathewson, A., and Berney, H. (2002) Application of magnetohydrodynamic actuation to continuous flow chemistry. Lab on a chip, 2, 224-230.

Woias, P., Hauser, K. and Yacoub-George, E. (Eds.) (2000) An active silicon micromixer for _TAS applications. In: van den Berg, A., Olthuis, W., Bergveld, P. (Eds.) Micro Total Analysis Systems. Kluwer Academic Publishers, Dordrecht.

Yang, Z., Matsumoto, S., Goto, H., Matsumoto, M. and Maeda, R. (2001) Ultrasonic micromixer for microfluidic systems, Sensors and Actuators A: Physical, 93(3), 266-272.

Zauner, R., and Jones, A.G., (2000) Determination of nucleation, growth, agglomeration and disruption kinetics from experimental precipitation data: the calcium oxalate system.

Chemical Engineering Science, 55, 4219-4232.

Zettlemoyer, A.C. (1969) Nucleation, Marcel Dekker, Inc. New York.

Zhang, G. and Hua, I., (2000) Ultrasonic degradation of trichloroacetonitrile, chloropicrin and bromobenzene: design factors and matrix effects, Advances in Environmental Research, 4(3), 219-224.

Zhang I., Shung K.K. and Edwards D.A., (1996) Hydrogels with Enhanced Mass Transfer for Transdermal Drug Delivery, Journal of Pharmaceutical Science, 85(12), 1312-1316.

Zhao, L., Li, J., Guo, S., and Du, Q., (2006) Ultrasonic oscillations induced morphology and property development of polypropylene/montmorillonite nanocomposites, Polymer, 47(7), 2460-2469.

Zhou, A., (1993) Mathematics of chemical engineering, Chemical industry publisher, Beijing.

APPENDIX

A3.1 The temperatures at different time with 21% amplitude of ultrasound (determination of power input and ultrasonic amplitude)

T(s)	0	30	60	90	120	150	180	210	240	270	300
T(^{0}C)	22.3	22.7	23.1	23.4	23.7	24.1	24.4	24.7	25	25.3	25.7

A3.2 The temperatures at different time with 31% amplitude of ultrasound (determination of power input and ultrasonic amplitude)

T(s)	0	30	60	90	120	150	180	210	240	270	300
T(^{0}C)	22.1	22.9	23.6	24.2	25	25.6	26.3	27	27.6	28.3	29

A3.3 The temperatures at different time with 41% amplitude of ultrasound (determination of power input and ultrasonic amplitude)

T(s)	0	30	60	90	120	150	180	210	240	270	300
T(^{0}C)	22.8	23.8	24.6	25.6	26.6	27.5	28.3	29.3	30.3	31.1	32.1

A3.4 The temperatures at different time with 51% amplitude of ultrasound (determination of power input and ultrasonic amplitude)

T(s)	0	30	60	90	120	150	180	210	240	270	300
T(^{0}C)	22.2	23.6	24.7	25.9	27.2	28.4	29.7	30.8	32	33.1	34.5

A3.5 The temperatures at different time with 61% amplitude of ultrasound (determination of power input and ultrasonic amplitude)

T(s)	0	30	60	90	120	150	180	210	240	270	300
T(^{0}C)	22.3	24	25.5	27.1	28.8	30.3	32	33.5	35	36.6	38.3

A3.6 The temperatures at different time with 71% amplitude of ultrasound (determination of power input and ultrasonic amplitude)

T(s)	0	30	60	90	120	150	180	210	240	270	300
T(^{0}C)	22.4	24.4	26.2	28.1	30	32	33.9	35.7	37.6	39.5	41.5

A3.7 The temperatures at different time with 81% amplitude of ultrasound (determination of power input and ultrasonic amplitude)

T(s)	0	30	60	90	120	150	180	210	240	270	300
T(^{0}C)	22.5	24.7	26.9	29.2	31.5	33.8	36.2	38.5	40.6	42.9	45.2

A3.8 The temperatures at different time with 91% amplitude of ultrasound (determination of power input and ultrasonic amplitude)

T(s)	0	30	60	90	120	150	180	210	240	270	300
T(^{0}C)	22.2	24.8	27.3	30.1	32.7	35.4	38.1	40.6	43.3	45.8	48.6

A3.9 The temperatures at different time with 100% amplitude of ultrasound (determination of power input and ultrasonic amplitude)

T(s)	0	45	60	90	120	150	180	210	240	270	300
T(^{0}C)	22.2	26.6	28.2	31.2	34.2	37.2	40.3	43.3	46.3	49	52.2

A3.10 Induction time without ultrasound when nucleation is consistent with a predominantly heterogeneous model

S	10.80993	12.82261	14.80213	16.75159	18.6735	20.5699	24.29281	27.93146
t_{ind}(s)	679	303	201	148	101	92	65	48

A3.11 Induction time without ultrasound when nucleation is consistent with a predominantly homogeneous model

S	31.49437	34.98834	38.41895	41.79086	45.10807	48.37401	51.59169
t_{ind}(s)	31	26	16	12	7	6	4

A3.12 Induction time with 21% amplitude of ultrasound when nucleation is consistent with a predominantly homogeneous model

S	31.49437	34.98834	38.41895	41.79086	45.10807	30.7875	33.2496
t_{ind}(s)	21	12.2	7.4	5.6	4.2	22.3	14.4

A3.13 Induction time with 31% amplitude of ultrasound when nucleation is consistent with a predominantly homogeneous model

S	31.49437	34.98834	38.41895	41.79086	45.10807	33.2496	36.71125	40.11198
t_{ind}(s)	11.4	9.4	5.2	3.4	2.4	10.2	8.4	5.2

A3.14 Induction time with 41% amplitude of ultrasound when nucleation is consistent with a predominantly homogeneous model

S	31.49437	34.98834	33.2496	36.71125	38.41895	40.11198	41.79086
t_{ind}(s)	9.6	5.2	6.2	5	3.2	2.8	2.8

A3.15 Induction time with 51% amplitude of ultrasound when nucleation is consistent with a predominantly homogeneous model

S	31.49437	34.98834	33.2496	36.71125	32.19848	35.67937	33.94704
t_{ind}(s)	6.4	4	4.4	2.8	4.8	3	3.6

A3.16 Induction time with 61% amplitude of ultrasound when nucleation is consistent with a predominantly homogeneous model

S	31.49437	34.98834	32.19848	33.2496	35.67937	36.36791
t_{ind}(s)	3	1.8	2.6	2	1.6	1.4

A5.1 Induction time of spectinomycin hydrochloride without ultrasound

S	2.9854	3.1281	3.2775	3.5982	3.9503	4.3369	4.76122	5.2271	5.7386
t_{ind}(s)	12600	7100	5120	2920	1650	905	575	350	265

A5.2 Induction time of spectinomycin hydrochloride with ultrasound

S	3.12807	3.27754	3.43415	3.59824	3.77018	3.95033	4.33686	4.76122
t_{ind}(s)	1005	750	605	465	380	230	115	85

A5.3 Induction time of roxithromycin without ultrasound

S	2.334	2.648	3.004	3.407	3.865	4.384	4.974
t_{ind}(s)	5276	2751	2005	1405	1083	757	514

A5.4 Induction time of roxithromycin with ultrasound

S	2.334	2.648	3.004	3.407	3.865	4.384	4.974
t_{ind}(s)	1221	750	448	358	278	175	142

A5.5 Induction time of sucrose without ultrasound

S	24.53568	25.77793	28.45428	31.4085	34.66944	38.26894	42.24215
t_{ind}(s)	2340	2020	1565	1395	1265	1068	725

A5.6 Induction time of sucrose with ultrasound

S	21.15674	22.22791	23.3533	25.77793	28.45428	31.4085	34.66944	42.24215
t_{ind}(s)	2030	1705	1330	1242	885	770	750	420

A6.1 The variance of velocity in different sections in water

Section	1	2	3	4	5	6
61%	830.9569	575.8245	348.6846	236.0406	219.368	2.543492
51%	398.1138	248.8051	168.6067	140.7201	138.3861	2.399514
41%	116.5525	109.4289	106.9221	102.874	107.5846	1.857813
Agitation	18.13664	16.23298	20.49372	7.743765	4.676448	

A6.2 Cavitation density in different sections in water (cm^{-2})

Section	1	2	3	4	5	6
41%	244	190	135	122	38	16
51%	326	244	204	176	46	22
61%	535	446	321	250	89	36

A7.1 Induction time with 21% amplitude of ultrasound when nucleation is consistent with a predominantly heterogeneous model

S	10.80993	12.82261	14.80213	16.75159	18.6735	20.5699	24.29281	27.93146
t_{ind}(s)	150	117	80.8	53.4	49.2	41.2	29.6	24

A7.2 Induction time with 31% amplitude of ultrasound when nucleation is consistent with a predominantly heterogeneous model

S	10.80993	12.82261	14.80213	16.75159	18.6735	20.5699	24.29281	27.93146
t_{ind}(s)	77	49	41	31	26	23.8	21.2	15.8

A7.3 Induction time with 41% amplitude of ultrasound when nucleation is consistent with a predominantly heterogeneous model

S	10.80993	12.82261	14.80213	16.75159	18.6735	20.5699	24.29281	27.93146
t_{ind}(s)	41	30.2	24.6	20.6	17.4	14.8	12.6	11

A7.4 Induction time with 51% amplitude of ultrasound when nucleation is consistent with a predominantly heterogeneous model

S	10.80993	12.82261	14.80213	16.75159	18.6735	20.5699	24.29281	27.93146
t_{ind}(s)	23.4	20.6	17.4	13.6	12.2	9.2	8	7.6

A7.5 Induction time with 61% amplitude of ultrasound when nucleation is consistent with a predominantly heterogeneous model

S	10.80993	12.82261	14.80213	16.75159	18.6735	20.5699	24.29281	27.93146
t_{ind}(s)	11	8.8	7.2	6	5.4	4.6	3.8	3.4

A9.1 The variance of velocity in different sections in ethanol

Section	1	2	3	4	5	6
61%	845.0731	639.9937	472.1432	258.77	166.2666	3.848937
51%	557.9867	404.0526	321.6806	192.6728	147.5514	3.399092
41%	190.357	188.8596	170.9632	92.02707	82.85508	2.49076
Agitation	13.41736	16.6472	21.86889	7.918288	6.612201	

A9.2 Cavitation density in different sections in ethanol (cm^{-2})

Section	1	2	3	4	5	6
41%	190	122	95	81	27	5
51%	244	190	149	122	32	8
61%	392	356	285	178	53	18

1. Z. Guo, M. Zhang, H. Li, J. Wang and E. Kougoulos, "Effect of ultrasound on anti-solvent crystallization process" Journal of Crystal Growth, Volume 273, Issue 3-4, January 2005, Pages 555-563.
2. Z. Guo, A.G. Jones and N. Li, "The effect of ultrasound on the homogeneous nucleation of $BaSO_4$ during reactive crystallization" Chemical Engineering Science, Volume 61, Issue 5, March 2006, Pages 1617-1626.
3. Z. Guo, A.G. Jones and N. Li, "Interpretation of the ultrasonic effect on induction time during $BaSO_4$ homogeneous nucleation by a cluster coagulation model" Journal of Colloid and Interface Science, Volume 297, Issue 1, May 2006, Pages 190-198.
4. Z. Guo, A.G. Jones and N. Li, "The effect of ultrasound on homogeneous nucleation in reactive crystallization", 16 International Symposium on Industrial Crystallization, September 2005, Pages 241-246.
5. Z. Guo, A.G. Jones and N. Li, "A study of the ultrasonic effect on $BaSO_4$ homogeneous nucleation during reactive crystallization", Particle System Analysis 2005, available at http://www.psa2005.com/downloads/posters/012.doc.
6. Z. Guo, A.G. Jones and N. Li, "A study of the effect of ultrasound on $BaSO_4$ heterogeneous nucleation during reactive crystallization", 5th World Congress on Particle Technology, April 2005, 70w.
7. Z. Guo, A.G. Jones, N. Li and S. Germana "High-speed observation of the effect of ultrasound on the nucleation of $BaSO_4$ during reactive crystallization", Powder Technology, In Press, Available online, 5 December 2006.
8. Z. Guo, A.G. Jones, H. Hao, B. Patel and N. Li, "The effect of ultrasound on the heterogeneous nucleation of $BaSO_4$ during reactive crystallization", (Accepted by Journal of Applied Physics).
9. Z. Guo, A.G. Jones and N.Li, "Investigation of ultrasonic effects on primary nucleation during anti-solvent crystallization" (Submitted).
10. Z. Guo, A.G. Jones, N. Li, N. Shao and B.Wang, "High-speed observation of the ultrasonic effect on the breakage process of agglomerated sugar crystals", (Submitted).
11. Z. Guo, A.G. Jones, H. Hao, B. Patel and N. Li, "Interpretation of the ultrasonic effect on induction time during $BaSO_4$ heterogeneous nucleation by a cluster coagulation model", (Submitted).